

C



- ▶ [Ethyne Radical](#)



- ▶ [Ethylene Oxide](#)



- ▶ [Propynylidyne](#)



- ▶ [Cyclopropenylidene](#)



- ▶ [Cyanoethynyl Radical](#)



- ▶ [Butadiynyl Radical](#)



- ▶ [Diacetylene](#)



- ▶ [4-Cyano-1,3-Butadiynyl](#)



- ▶ [Benzene](#)



- ▶ [Cyanoacetylene](#)
- ▶ [N-Carbamoyl-Amino Acid](#)

CAB (Centro de Astrobiología, Spain)

Definition

The Spanish Centro de Astrobiología (CAB) was created as a Joint Center between CSIC (Consejo Superior de Investigaciones Científicas) and the Spanish space agency INTA (Instituto Nacional de Técnica Aeroespacial) with the support of the Comunidad Autónoma de Madrid (CAM). The main goal of the CAB is to provide a truly transdisciplinary research environment for the development of the new science of Astrobiology. The CAB operates with the specific new contribution of a common methodology based on complexity theory and the application of the scientific method to understanding the origin of life by exploring the habitability conditions on Earth and beyond, within the Solar System, or in extrasolar planets. CAB scientific activities started in late 1999 at temporary buildings, while awaiting a new building to be constructed and equipped. The new CAB premises were inaugurated in January 2003.

CAB is located within the campus of INTA and, in addition, has one astronomical facility with a robotic

telescope at the Observatorio Astronómico Hispano-Alemán de Calar Alto (CAHA). CAB's scientists and engineers are deeply involved in space missions such as ► [MSL](#), ► [ExoMars](#), INTEGRAL, Bepi Colombo, ► [PLATO](#), ► [HERSCHEL](#), and SPICA.

History

The origin of the CAB goes back to a proposal presented to NASA in 1998 by a group of Spanish and American scientists, led in Spain by Juan Pérez-Mercader, to join the newly created NASA Astrobiology Institute (NAI). The group was integrated within the ► [NAI](#) as a full Associate Member in 2000. Following an exchange of letters at Government level, CAB became the first Associate Member of NAI outside the US. The other NAI Associate Member since 2003 is the Australian Centre of Astrobiology.

See also

- [Evolution \(Biological\)](#)
- [ExoMars](#)
- [Extremophiles](#)
- [Geomicrobiology](#)
- [Genetics](#)
- [HERSCHEL](#)
- [Mars Science Laboratory](#)
- [NAI](#)
- [Origin of Life](#)
- [PLATO](#)
- [Terrestrial Analog](#)

Cahn Ingold Prelog Rules

Synonyms

[CIP Rules](#)

Definition

In chemistry, these are a set of rules for determining the stereochemistry of a molecule. For molecules with double bonds, stereoisomerism can be E (entgegen, German for opposed) or Z (zusammen, German for together), also referred to in English as trans and cis, respectively. For stereocenters, molecules are denoted as S or R (for *sinister* or *rectus*) indicating whether the sequence of groups follows a left or right direction of viewing, with priority of substituents assigned on the basis of molecular weight.

See also

- [Stereoisomers](#)

CAI

- [Extinct Radioactivity](#)

CAIs

MATTHIEU GOUNELLE

Laboratoire de Minéralogie et Cosmochimie du Muséum (LMCM) MNHN USM 0205 - CNRS UMR 7202, Muséum National d'Histoire Naturelle, Paris, France

Synonyms

[Calcium-Aluminium-rich Inclusions](#)

Keywords

Chondrites, chronology, inclusions

Definition

CAIs (Calcium-, Aluminum-rich Inclusions) are white inclusions found in carbonaceous chondrites. They are made of calcium- and aluminum-rich oxides and silicates. They are among the oldest solids of the solar system. They provide clues on the immediate environment of the nascent solar system and on its earliest phases.

Overview

CAIs were discovered in the Vigarano chondrite by M. Christophe in 1968. They are an assemblage of calcium- and aluminum- oxides and silicates, i.e., spinel, hibonite, grossite, melilite, anorthite and calcium-, aluminum-rich pyroxenes. CAIs are enriched in refractory elements by a factor of 10–100 relative to bulk chondrites. They have variable textures: irregular, fluffy, round, compact... Some CAIs show evidence of melting, probably during chondrule formation. Others exhibit evidence of reprocessing in the chondrite parent-bodies (see entry ► [Allende](#)). CAIs are enriched in oxygen-16 relative to chondrules. Some of them are enriched in the heavy isotopes of magnesium and silicon. They often are isotopically anomalous relatively to the bulk solar system. These anomalies, at the level of a few hundred ppm, were found mostly in neutron-rich isotopes, such as ⁴⁸Ca or ⁵⁰Ti. They contain a high abundance of short-lived radionuclides (see entry ► [cosmochemistry](#)). Their Pb-Pb absolute ages (4567–4568 Ma) are older than those of chondrules or differentiated meteorites.



CAIs are very abundant in carbon-rich carbonaceous chondrites, while they are virtually absent from other chondrites. Studies of CAIs during the last 30 years are heavily biased towards CAIs found in the CV3 chondrites epitomized by the Allende meteorite which fell in Mexico in 1969. The reason for that bias is that CAIs in CV3 chondrites are large (up to a cm) and abundant (~10% volume). It is, however, important to note that CAIs in CV3 chondrites are quite peculiar when compared to CAIs in other chondrites' groups and may record specific events in the solar protoplanetary disk. More studies should and will be dedicated to CAIs in other chondrites groups. Two CAIs were found among the dust brought back by the Stardust spacecraft from comet Wild 2.

CAIs probably formed by condensation. Some of them endured severe evaporation. Because of their old age, the extent of the isotopic anomalies they bear, and their richness in short-lived radionuclides, they are believed to be the first solids to have formed in the solar protoplanetary disk. As such, they record the earliest phases of solar system formation. Short-lived radionuclides as well as isotopic anomalies record nucleosynthesis processes in generation of stars prior to the solar system. Some short-lived radionuclides also record irradiation processes in the early solar system. Because they formed at high temperature, in a gas-poor region, they are believed to have formed close (0.1 AU) to the protoSun. They were transported to chondrite formation distances either by winds powered by the magnetic interaction between the Sun and the disk, or by turbulence.

See also

- ▶ [Chronology, Cratering and Stratigraphy](#)
- ▶ [Cosmochemistry](#)
- ▶ [Meteorite \(Allende\)](#)
- ▶ [Meteorites](#)
- ▶ [Parent Body](#)
- ▶ [Protoplanetary Disk](#)

References and Further Reading

- Christophe Michel-Lévy M (1968) Un chondre exceptionnel dans la météorite de Vigarano. *Bull Soc Fr Minéral Cristallogr* 91:212–214
- MacPherson GJ, Simon SB et al (2005) Calcium- Aluminium-rich inclusions: major unanswered questions. In: Krot AN, Scott ERD, Reipurth B (eds) *Chondrites and the protoplanetary disk*, vol 341. ASP Conference Series, San Francisco, pp 225–250
- Shu FH, Shang H et al (1996) Toward an astrophysical theory of chondrites. *Science* 271:1545–1552
- Wadhwa M, Amelin Y et al (2007) From dust to planetesimals: implications for the solar protoplanetary disk from short-lived radionuclides. In: Reipurth VB, Jewitt D, Keil K (eds) *Protostars and Planets*. University of Arizona Press, Tucson, pp 835–848

Calcareous Sediment

- ▶ [Carbonate](#)

Calcium-Aluminium-rich Inclusions

- ▶ [CAIs](#)

Caldophile

- ▶ [Thermophile](#)

Callisto

Definition

Callisto is a satellite of Jupiter discovered by ▶ [Galileo Galilei](#) in January 1610; it is the outermost of the Galilean satellites. With a radius of 2,410 km, Callisto is, after Ganymede and Titan, the third biggest satellite in the solar system. Its distance to ▶ [Jupiter](#) is 1,882,700 km or 26 Jovian radii. Its density is 1.8 g/cm³, typical of icy objects. Callisto has been investigated by the Voyager 1 and 2 spacecrafts in 1979, then by the Galileo orbiter between 1995 and 2003. The surface of Callisto is heavily cratered and consists of a mixture of ice and dust. A great basin, Valhalla, over 500 km in diameter, is the signature of a large major impact.

See also

- ▶ [Galileo Galilei](#)
- ▶ [Jupiter](#)

Calvin's Conception of Origins of Life

History

Melvin Calvin (1911–1997) was an American biochemist, who discovered, with Benson, the cycle of reactions in the obscure phase of photosynthesis during the 1940s (Calvin–Benson cycle). Calvin obtained the Nobel Prize in 1961 for this discovery.

In 1951, Calvin published one of the first works in prebiotic chemistry. He reduced carbon dioxide in aqueous solution, by ionizing radiation, to formic acid.

In 1953, Harold Urey rejected this result because of the presence of CO_2 . Urey was in favor of a reductive primitive atmosphere without CO_2 . However, Calvin maintained his interest for origins of life during the rest of his career, and published his main book on this topic in 1969 (*Molecular Evolution towards the Origin of Living Systems on Earth and Elsewhere*).

See also

- ▶ [Calvin–Benson Cycle](#)
- ▶ [Miller, Stanley](#)
- ▶ [Urey's Conception of Origins of Life](#)

Calvin–Benson Cycle

JULI PERETÓ

Cavanilles Institute for Biodiversity and Evolutionary Biology and Department of Biochemistry and Molecular Biology, University of València, València, Spain

Synonyms

[Dark reactions](#); [Reductive pentose phosphate cycle](#)

Keywords

Biosynthesis, autotrophy, carboxylation, carbon dioxide

Definition

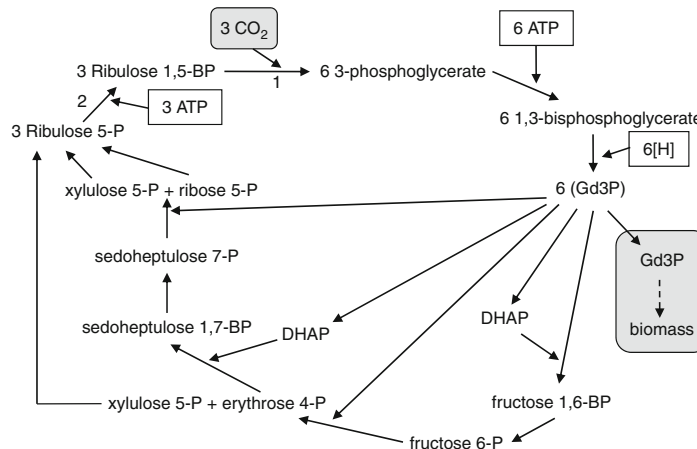
A carbon dioxide fixation pathway where a molecule of CO_2 condenses with a 5-C compound (ribulose 1,5-bisphosphate) to yield two molecules of a 3-C compound (3-phosphoglycerate). These 3-C molecules serve both as precursors for biosynthesis and, through a cyclic series of enzymatic reactions, to regenerate the 5-C molecule necessary for the first carboxylating step (Fig. 1). The pathway is present in several bacterial lineages (e.g., cyanobacteria) and its acquisition by eukaryotic cells (chloroplast in algae and plants) was through the endosymbiotic association with ancient cyanobacteria.

History

Melvin Calvin (1911–1997) and coworkers established this autotrophic path of carbon in phototrophic organisms using ^{14}C labelled carbon dioxide and *Chlorella* (a green algae) cultures (Benson & Calvin 1950). Calvin was awarded with the Nobel Prize in Chemistry in 1961 “for his research on the carbon dioxide assimilation in plants.”

Overview

The Calvin–Benson cycle allows the synthesis of one triose from three molecules of carbon dioxide (Fig. 1):



Calvin–Benson Cycle. Figure 1 The Calvin–Benson cycle. The stoichiometry of the cycle allows the net synthesis of one molecule of triose from three molecules of carbon dioxide (gray boxes). Other five trioses (5 C_3) are converted into three pentoses (3 C_5) necessary to initiate the cycle again. The energetic cost for the synthesis of one triose is nine ATP molecules and six reducing equivalents (NADH or NADPH). These energetic requirements could be satisfied by a photosynthetic apparatus or a chemolithotrophic metabolism. Except for two key enzymatic steps (1 and 2), all the transformations are a combination of enzymes participating in the Embden–Meyerhof–Parnas pathway and the non-oxidative pentosephosphate pathway. Key enzymatic steps: (1) Rubisco; (2) phosphoribulokinase. Abbreviations: Gd3P, glyceraldehyde 3-phosphate; DHAP, dihydroxyacetonephosphate

12 electrons (provided by redox coenzymes like NADH or NADPH) and 9 ATP equivalents are required for bringing CO₂ to the oxidation level of the triose glyceraldehyde 3-phosphate. These fueling requirements are supplied by either a phototrophic or a chemolithotroph metabolism. The cycle can be divided into two stages: a reductive carboxylation of the pentose ribulose 1,5-bisphosphate (RuBP) up to glyceraldehyde 3-phosphate and a series of rearrangements of carbon skeletons from trioses to regenerate RuBP throughout 4-, 6-, and 7-C sugar intermediates (Fig. 1). The first step is catalyzed by the key carboxylating enzyme ► **Rubisco**. As other carboxylases, Rubisco also shows a preference for lighter stable isotopes and thus CO₂ fixation results in the depletion of ¹³C (δ¹³C) in the biosynthesized organic matter ranging from –20‰ to –30‰. The second stage of the cycle occurs by the combination of several enzymatic activities from the ► **Embden–Meyerhof–Parnas pathway** and the non-oxidative branch of the pentose phosphate pathway.

The Calvin–Benson cycle was originally described in green plant (i.e., chloroplast) photosynthesis (Benson & Calvin 1950). It is also active in endosymbiotic chemolithotrophic proteobacteria of invertebrates living in close proximity to hydrothermal vents. In free-living prokaryotes, this pathway has been demonstrated in cyanobacteria (the group to which the ancestors of plastids belonged), some aerobic or facultative anaerobic proteobacteria, CO-oxidizing mycobacteria, diverse iron-sulfur-oxidizing firmicutes and in some green sulfur bacteria. Although Rubisco has been isolated from some Archaea, there is no evidence for the operation of the full cycle in autotrophic species from this domain (Berg et al. 2010).

See also

- [Autotrophy](#)
- [Embden-Meyerhof-Parnas Pathway](#)
- [Isotopic Fractionation \(Planetary Process\)](#)
- [Rubisco](#)

References and Further Reading

- Benson AA, Calvin M (1950) Carbon dioxide fixation by green plants. *Annu Rev Plant Physiol* 1:25–42
- Berg IA, Kockelkorn D, Ramos-Vera WH, Say RF, Zarzycki J, Hügler M, Alber BE, Fuchs G (2010) Autotrophic carbon fixation in archaea. *Nat Rev Microbiol* 8:447–460
- Berg JM, Tymoczko JL, Stryer L (2007) *Biochemistry*, 6th edn. Freeman, New York, ch 20
- Kim BH, Gadd GM (2008) *Bacterial physiology and metabolism*. Cambridge University Press, Cambridge, ch 10

Cambrian Explosion

Synonyms

[Cambrian radiation](#)

Definition

The Cambrian explosion was a major evolutionary radiation of organisms, notably multicellular animals (metazoans), that occurred during the Cambrian period (542–588 Ma). Pre-Cambrian fossils reveal a mainly microbial biota, with complex, large-bodied organisms only becoming conspicuous during the latest Proterozoic Eon (the Ediacaran biota). In contrast, Cambrian fossils include abundant evidence for macroscopic motile organisms, and unambiguous examples of most major animal lineages. Exactly what determined the timing of the Cambrian explosion is not clear, and current research aims to disentangle the effects of physical environment, ecological context, and factors related to development and genetics.

See also

- [Burgess Shale Biota](#)
- [Chengjiang Biota, China](#)

Cambrian Radiation

- [Cambrian Explosion](#)

Campbellrand–Malmani Platform, South Africa

Definition

The Campbellrand–Malmani ► **carbonate** platform was deposited in the Kaapval craton, South Africa between 2,588 and 2,520 Ma (Neoproterozoic). This 1.9-km-thick carbonate platform is preserved over at least 190,000 km² and probably originally covered the entire remaining extent of the Kaapvaal craton (600,000 km²). The Campbellrand–Malmani is the first extended carbonate deposit in the Neoproterozoic ocean, prior of the buildup of the oxygen in the ocean and atmosphere, 2.35 Ga ago. Abundant of aragonite in its deposits suggests a neutral to

slightly alkaline ocean, which may indicate a very low CO₂ concentration in the atmosphere.

See also

- ▶ Carbonate
- ▶ Earth's Atmosphere, Origin and Evolution of
- ▶ Great Oxidation Event
- ▶ Ocean, Chemical Evolution of
- ▶ Oxygenation of the Earth's Atmosphere
- ▶ Sedimentary Rock

Canadian Precambrian Shield

PHIL THURSTON

Laurentian University, Sudbury, ON, Canada

Synonyms

Canadian shield; North American shield

Keywords

Accreted terrane, accretion, craton, geological province, magmatic arc, supercontinent cycle

Definition

The Canadian ▶ **Shield** is the region of North America underlain by Precambrian rocks (>542 Ma), extending from the Arctic Ocean to the Great Lakes and further south and west in the subsurface (Fig. 1).

Overview

The Canadian Precambrian Shield is subdivided into geological provinces (regions of similar age). The major ▶ **Archean** (>2.5 Ga) provinces are: the Slave (S), Superior (Sup), Rae (R), and Hearne (H). All of them have a similar architecture: linear sub-provinces or belts of fine-grained subaqueously erupted volcanic rocks which are surrounded and cut by granites (Hoffman 1989). In detail, the Superior Province consists of an old (~3 Ga) core (NCT) surrounded by linear belts of volcanic rocks that alternate with granites and belts of sedimentary rocks which become younger (2.9 Ga to ~2.7 Ga) north and south of the core (Percival 2007). This architecture suggests the Archean Provinces (pink on Fig. 1) grew as successively younger belts of volcanic rocks were added to the continental margin by plate tectonic processes. This was followed by intrusion of much granitic rock during the interval 2.7–2.6 Ga, transforming the Archean

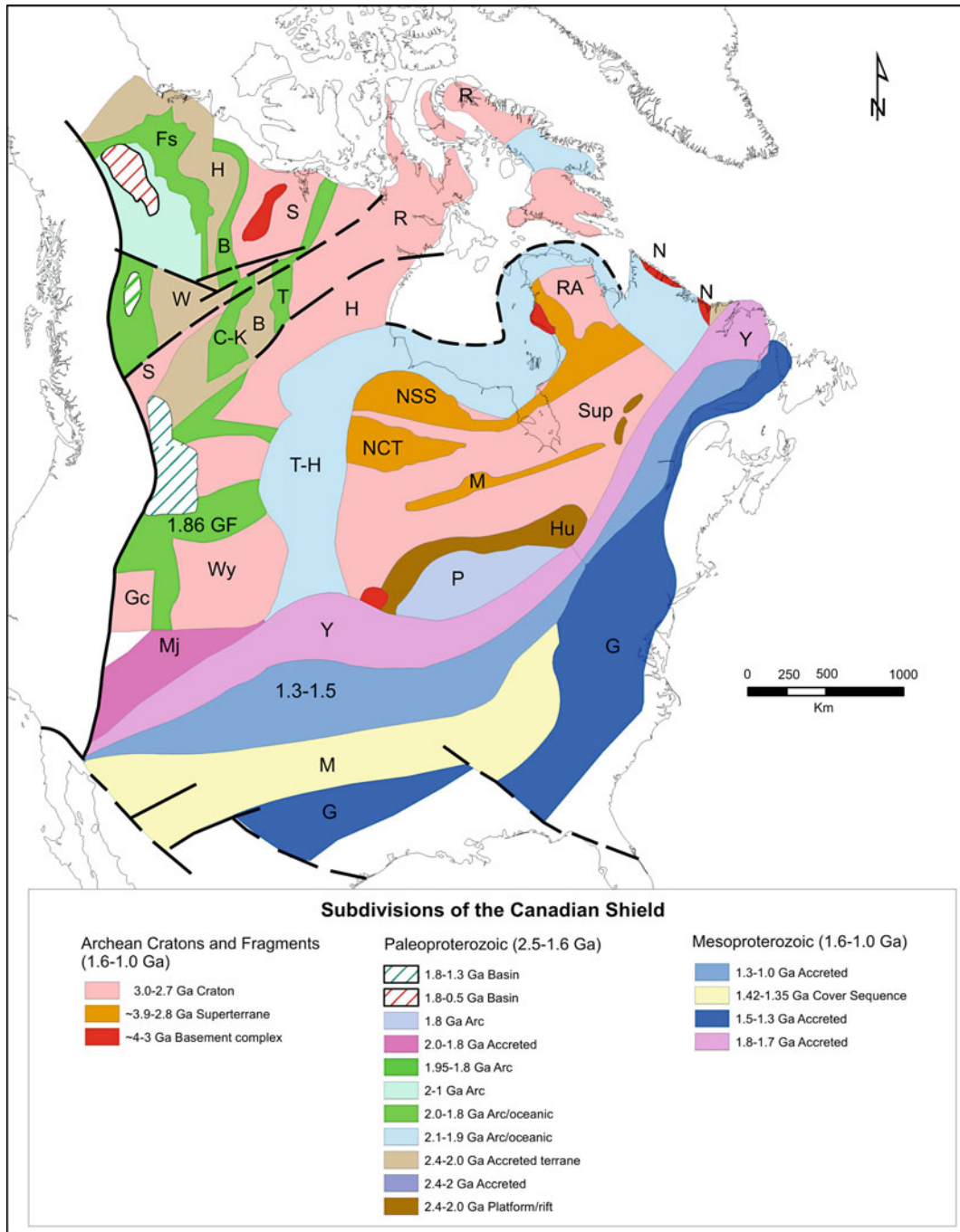
provinces into light, buoyant ▶ **craton**. The cratons typically are ~40 km thick. The cratonization processes involved development of large-scale faults that brought gold-bearing fluids from deep in the Earth to the near-surface environment. Several cratons of this age (2.7 Ga) joined to form a ▶ **supercontinent** “Kenorland” (Aspler and Chiarenzelli 1998). The edges of Kenorland include some much older (~3.8 Ga) fragments (red units on Fig. 1) that were accreted onto the margin of the supercontinent. Kenorland broke apart by development of 2.48–2.10 Ga old rifts containing dykes and volcanic rocks followed by development of uranium-bearing sandy continental margin sedimentary units [e.g., Hu in brown on Fig. 1, on the south edge of the Superior craton]. The various Archean cratons then drifted apart and became separated by ocean basins and island arcs. The oceans later closed and the various accreted terranes and 2.0–1.8 Ga volcanic arcs accreted onto the margins of the Archean cratons to form the “Columbia” supercontinent (Zhao et al. 2004). During the interval 1.8–1.2 Ga, Columbia grew by accretion of multiple belts, again consisting mostly of volcanic and granitic rocks along its southern and eastern margins, e.g., the Yavapai-Central Plains belt [Y on Fig. 1, (1.8–1.7 Ga)], the Mazatzal (M) (1.7–1.5 Ga) belt in the USA and the Labradorian belt of Quebec and Labrador and the 1.3–1.0 Ga Grenville Province (G on Fig. 1) (Karlstrom et al. 1999).

See also

- ▶ Archea
- ▶ Craton
- ▶ Proterozoic (Aeon)
- ▶ Shield
- ▶ Supercontinent

References and Further Reading

- Aspler LB, Chiarenzelli JR (1998) Two Neoproterozoic supercontinents? evidence from the paleoproterozoic. *Sed Geol* 120:75–104
- Aspler LB, Pilkington M, Miles WF (2003) Interpretations of Precambrian basement based on recent aeromagnetic data, Mackenzie Valley, Northwest Territories, Geological Survey of Canada, Current Research 2003-C2, Ottawa, ON, Canada, pp 11
- Hoffman PF (1989) Precambrian geology and tectonic history of North America. In: Bally AW, Palmer AR (eds) *The geology of North America; an overview. A decade of North American geology*. Geological Society of America, Boulder, pp 447–512
- Karlstrom KE, Harlan SS, Williams ML, McLelland J, Geissman JW, Ahall K-I (1999) Refining Rodinia; geologic evidence for the Australia-Western U.S. connection in the Proterozoic, *GSA Today*, Vol 9, pp 1–7
- Percival JA (2007) Geology and metallogeny of the superior province, Canada. In: Goodfellow W (ed) *Mineral deposits of Canada: a synthesis of major deposit types, District metallogeny, the evolution*



Canadian Precambrian Shield. Figure 1 Subdivisions of the Canadian Shield of North America based on the age of the rock unit. Archean cratons and subdivisions within: Sup = Superior craton, NSS = Northern Superior superterrane and Hudson Bay terrane, RA = Riviere Arnaud terrane, NCT = North Caribou terrane, M = Marmion terrane; N = Nain craton; S = Slave craton; R = Rae craton; H = Hearn craton; Wy = Wyoming craton, GC = Grouse Creek block. Paleoproterozoic (2.5–1.6 Ga) tectonic domains after Ross (2002) and Aspler et al. (2003): Hu = Huronian, T = Taltson; B (brown) = Buffalo Head; B (green) = Great Bear; H = Hottah; Fs = Fort Simpson; W = Wabamun; Chinchaga & Ksituan terranes

of geological provinces and exploration methods, Special Publication No. 5, Geological Association of Canada Mineral Deposits Division, pp 903–928

Ross GM (2002) Evolution of precambrian continental lithosphere in western Canada; results from lithoprobe studies in Alberta and beyond. *Can J Earth Sci* 39:413–437

Zhao G, Sun M, Wilde SA, LI S (2004) A Paleo-Mesoproterozoic supercontinent: assembly, growth and breakup. *Earth Sci Rev* 67: 91–123

Canadian Shield

- ▶ [Canadian Precambrian Shield](#)

Canadian Space Agency

- ▶ [CSA](#)

Canyon

- ▶ [Chasma, Chasmata](#)

Cap Carbonates

Definition

Cap ▶ [carbonates](#) are a special type of laminated carbonate rocks (limestone and/or dolostone) associated with glacial deposits in the Neoproterozoic (▶ [Snowball Earth](#)). They sharply overly (“cap”) unsorted glacial sediments called tillites. Their origin is not well understood, but they may be related to a particular ocean and atmosphere chemistry with high CO₂ concentration and alkalinity from silicate weathering or to upwelling of highly alkaline deep waters following deglaciation. They are associated with negative excursions of carbon isotopes that are widespread and can serve for correlation.

See also

- ▶ [Carbonate](#)
- ▶ [Glaciation](#)
- ▶ [Snowball Earth](#)

Capillary Electrophoresis

- ▶ [Electrophoresis](#)

Capsid Encoding Organism

- ▶ [Virus](#)

Carbamide

- ▶ [Urea](#)

Carbamonitrile

- ▶ [Cyanamide](#)

Carbenes

Definition

Carbenes are organic molecules having two electrons available on a carbon atom for chemical bonding. Short-chain and long-chain carbenes are very common in interstellar chemistry, e.g., C₃ and H₂CCCC.

See also

- ▶ [Interstellar Chemical Processes](#)
- ▶ [Interstellar Medium](#)

Carbimide

- ▶ [Cyanamide](#)

Carbodiimide

- ▶ [Cyanamide](#)

Carbohydrate

HESHAN "GRASSHOPPER" ILLANGKON
Department of Chemistry, University of Florida,
Gainesville, FL, USA

Synonyms

Disaccharide; Monosaccharide; Oligosaccharide; Polysaccharide; Saccharide; Sugar

Keywords

Cellulose, formaldehyde, formose, fructose, glucose, glyceraldehyde, glycolaldehyde, origins of life, primordial soup, ribose, sucrose, sugars

Definition

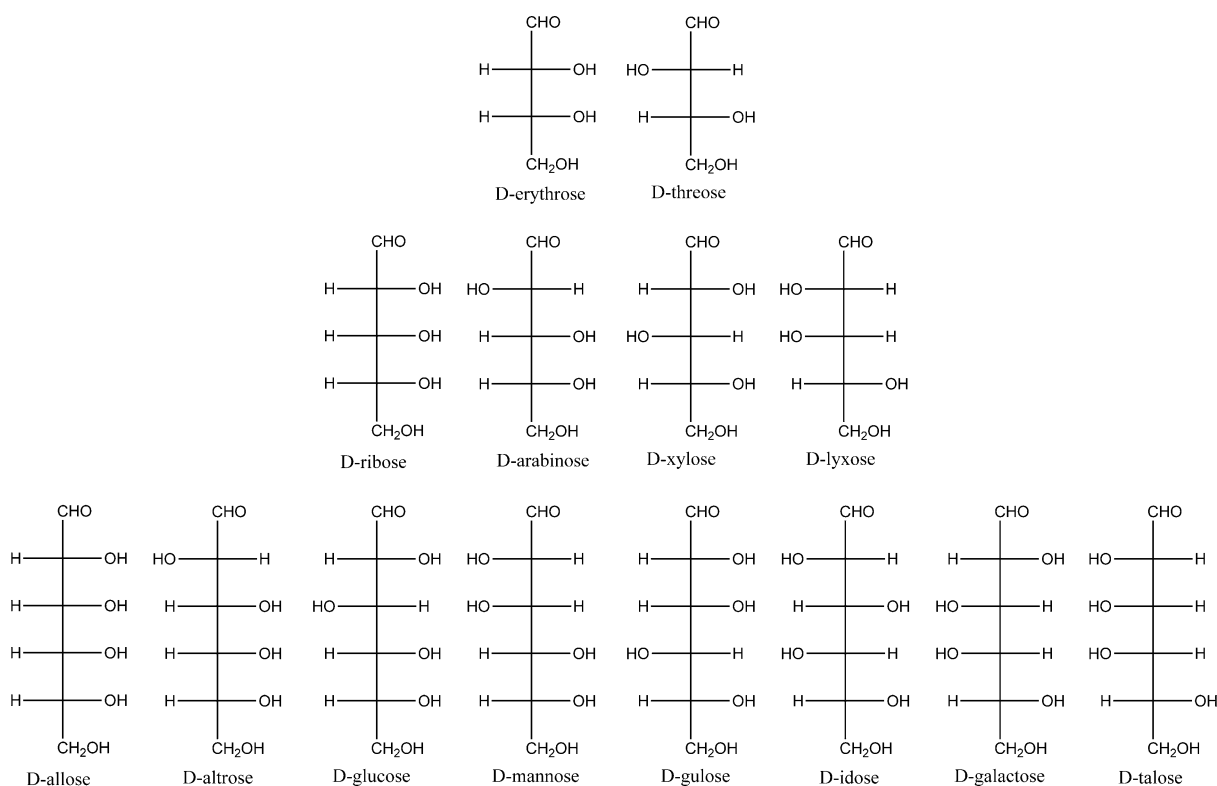
Carbohydrates are composed solely of carbon, oxygen, and hydrogen, and consist of a general formula $C_n(H_2O)_m$. The ratio of carbon to hydrogen to oxygen atoms in a carbohydrate is 1:2:1. Carbohydrates are involved in cell signaling, serve as a source of energy, and

provide structure to cells. Chains that alternate negatively charged phosphates with carbohydrates forms the backbones of the genetic biopolymers RNA and DNA.

Overview

Carbohydrates are an essential component of life on Earth. From ► **ribose** being an integral component of the genetic biopolymers DNA and RNA, to polymers of glucose used for cell wall support in plants, carbohydrates are involved in many varied and crucial biological roles. The complex structures of carbohydrates can be easily visualized using ► **Fischer projections**. Figure 1 depicts Fischer projections of aldoses, a class of carbohydrates that contain an aldehyde group. In the structures below, each line represents a covalent bond and each intersection of lines represents an unwritten carbon (C).

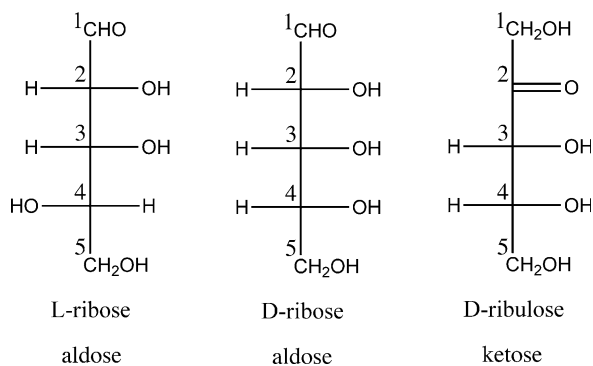
There are 2^n stereoisomers of a given sugar, where n is the number of chiral centers in the molecule. For instance, the aldopentoses contain five carbons, three of which are chiral centers, giving $2^3 = 8$ stereoisomers. These pentoses have the common names of ribose, arabinose, xylose, and lyxose and each come in a D or L enantiomer. The D or L configuration of the sugar is determined by the position of



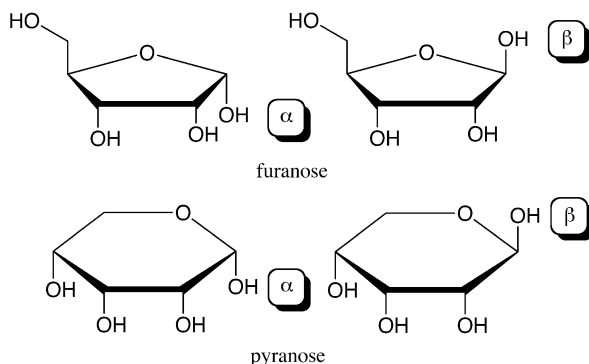
Carbohydrate. Figure 1 The four-, five-, and six-carbon D-aldoses

the alcohol on the chiral center furthest away from the aldehyde carbon. If the alcohol is on the right of the backbone the sugar is classified as *D*, while if it is on the left it is *L*. In the case of aldopentoses, this chiral center is on carbon four (Fig. 2). On Earth, the *D* isomer prevails as the dominant carbohydrate incorporated by nature; however, it has been postulated that *L* sugars could also be used as the predominant isomer in alternate “alien” biochemistries.

Carbohydrates can also form cyclic structures that produce an anomeric center giving the sugar an alpha (alcohol pointing down) or beta (alcohol pointing up) label. Ribose, for example, can be found in a furanose (five-membered) or pyranose (six-membered) form. Figure 3 shows both the alpha and beta configurations of the furanose and pyranose forms of ribose. The ribose



Carbohydrate. Figure 2 Carbohydrates can occur in either *D* or *L* forms. The ketose ribulose has an oxidized center at carbon two



Carbohydrate. Figure 3 The furanose (five-membered) and pyranose (six-membered) forms of *D*-ribose and their alpha (α) and beta (β) anomers

found in DNA is in a furanose configuration whereas ribose in crystalline form is predominantly pyranose (Šišak et al. 2010).

Presence of Carbohydrates in the Universe

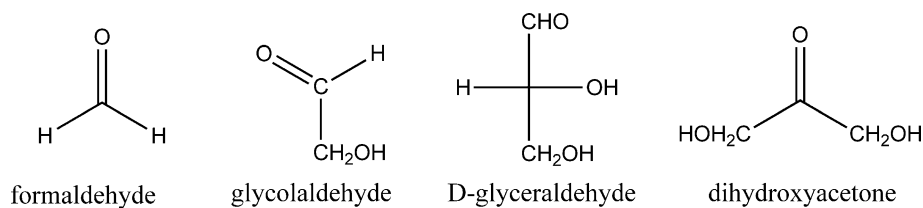
Astrobiologists studying the ► [origins of life](#) seek an answer to seminal questions related to the origins of carbohydrates. Through the use of radio telescopes, scientists have determined the presence of carbohydrates and their building blocks in interstellar gas clouds. Examples of some organic molecules confirmed present in these clouds (Fig. 4) include ► [formaldehyde](#), ► [glycolaldehyde](#), glyceraldehyde, and more recently dihydroxyacetone (Snyder et al. 1969; Hollis et al. 2004; Weaver and Blake 2005). Meteoritic bombardment could have delivered these molecules to the surface of the early Earth (Sephton 2002). Aldol reactions of glycolaldehyde and formaldehyde on a primitive Earth could also have been sources of glyceraldehyde, erythrulose, and higher carbohydrates (Fig. 5).

Prebiotic Synthesis of Carbohydrates

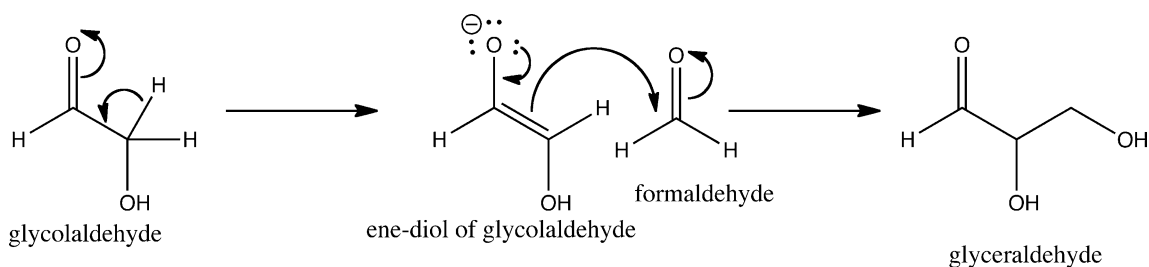
The prebiotic synthesis of carbohydrates is fundamental to astrobiology and origins of life research. The “► [RNA World](#)” hypothesis, which purports that life as we know it evolved from simple RNA molecules, is widely held as offering the most likely scenario for the emergence of life on Earth. This theory presupposes the existence of a prebiotic soup with abundant building blocks including amino acids, carbohydrates, purines, and pyrimidines.

One of the first reported instances of prebiotic carbohydrate synthesis occurred in 1861 when a German scientist, Butlerov, added formaldehyde to hot solutions of barium and calcium hydroxide forming a sweet sugary substance (Butlerov 1861). This became known as the ► [formose](#) reaction. A century later, Breslow discovered that the glycolaldehyde formed in this reaction initiates a series of autocatalytic reaction cycles which, over time, fix more formaldehyde to give higher carbohydrates (Breslow 1959). A side reaction in this experiment is the disproportionation of ► [formaldehyde](#) to form ► [methanol](#) and formic acid in a process now known as the Cannizzaro reaction (Fig. 6).

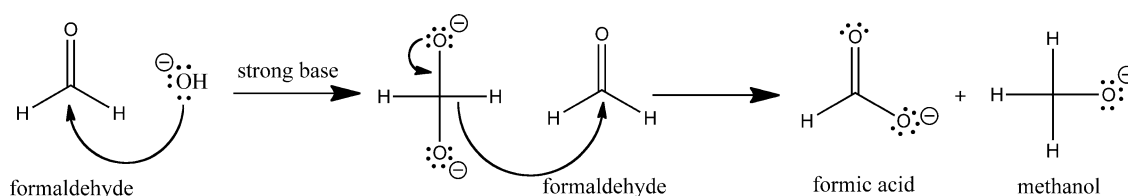
One argument against the RNA world arising from the ► [primordial soup](#) involves the formation of problematic tar, which is a seemingly useless by-product of highly reactive species (Larralde et al. 1995). The propensity of the formose reaction to form tar is an indication of the functionality and reactivity of these building blocks. The tar prevents the accumulation of genetically relevant



Carbohydrate. Figure 4 Formaldehyde and some lower carbohydrates glycolaldehyde, D-glyceraldehyde and dihydroxyacetone, have all been identified in interstellar gas clouds



Carbohydrate. Figure 5 An example of an Aldol addition of formaldehyde to glycolaldehyde



Carbohydrate. Figure 6 In the Cannizzaro reaction, formaldehyde reacts in strong base to give formic acid and methanol (both shown in their deprotonated forms)

carbohydrates and complicates in-depth product analysis. Recently, however, ► [borate](#) minerals have been shown to stabilize and direct the reactivity of carbohydrates, making them a viable participant in prebiotic reactions (Ricardo et al. 2004). Here, borate binds to adjacent alcohols of sugars as they are formed. This in turn reduces their reactivity and improves carbohydrate stability, preventing further uncontrolled tar-forming reactions.

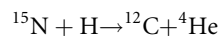
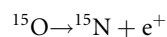
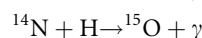
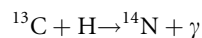
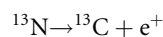
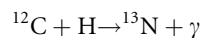
A different approach to prebiotic carbohydrate synthesis assembles activated pyrimidine nucleosides by side-stepping the model of adding a nucleobase to a previously synthesized ribose sugar (Powner et al. 2009). Though this methodology does not yet account for the synthesis of purine nucleosides, it opens new avenues for research toward the prebiotic synthesis of RNA and DNA.

See also

- [Aldose](#)
- [Biopolymer](#)
- [Borate](#)
- [Disproportionation](#)
- [Fischer Projection](#)
- [Formaldehyde](#)
- [Formose Reaction](#)
- [Glycolaldehyde](#)
- [Ketose](#)
- [Methanol](#)
- [Origin of Life](#)
- [Primordial Soup](#)
- [Ribose](#)
- [RNA World](#)

References and Further Reading

- Breslow R (1959) On the mechanism of the formose reaction. *Tetrahedron Lett* 1:22–26
- Butlerov A (1861) Formation synthétique d'une substance sucrée. *Comp Rend Acad Sci* 53:145–147
- Hollis JM et al (2004) Green bank telescope observations of interstellar glycolaldehyde: low temperature sugar. *Astronphys J* 613: L45–L48
- Larralde R, Robertson MP, Miller S (1995) Rates of decomposition of ribose and other sugars: implications for chemical evolution. *Proc Nat Acad Sci USA* 92:8158–8160
- Powner MW, Gerland B, Sutherland JD (2009) Synthesis of activated pyrimidine ribonucleotides in prebiotically plausible conditions. *Nature* 459:239–242
- Ricardo A, Carrigan M, Olcott AN, Benner SA (2004) Borate minerals stabilize ribose. *Science* 303:196
- Sephton M (2002) Organic compounds in carbonaceous meteorites. *Nat Prod Rep* 19:292–311
- Šišak D, McCusker LB, Zandomenighi G, Meier BH, Bläser D, Boese R, Schweizer WB, Gilmour R, Dunitz JD (2010) The crystal structure of D-ribose – at last! *Angew Chem Int Ed* 49:4503–4505
- Snyder LE, Buhl D, Zuckerman B, Palmer P (1969) Microwave Detection of Interstellar Formaldehyde. *Phys Rev Lett* 22:679
- Weaver SLW, Blake GA (2005) 1, 3-Dihydroxyacetone in Sagittarius B2(N-LMH): the first interstellar ketose. *Astronphys J* 624:L33



Carbon Isotopes

Carbon exists on Earth in the form of two stable (^{12}C and ^{13}C) and one unstable isotope (^{14}C). ^{12}C and ^{13}C have abundances of 98.89% and 1.108%, respectively (Wederpohl 1978). The standard atomic weight of carbon on Earth (abridged to five figures) is, therefore, 12.011 (Commission on Isotopic Abundances and Atomic Weights, IUPAC). ^{14}C (six protons and eight neutrons) is produced in the upper atmosphere by the interaction of thermal neutrons (produced from cosmic rays) and nitrogen atoms. The isotope has a half-life for decay (into ^{14}N and a beta particle, β^-) of 5,730 years and is employed in determining the age of objects having a biological origin up to about 50,000 years of age (Arnold and Libby 1949). In addition to the use of ^{14}C decay kinetics to determine the age of objects of archeological and anthropological interest, the ratio of the stable isotopes $^{12}\text{C}/^{13}\text{C}$ is an important indication of the pathway of synthesis of organic compounds. Because of the kinetic isotope effect, both biological and nonbiological synthetic processes can produce organic material containing a distinctive enrichment of the lighter isotope of carbon, ^{12}C . While the isotopic fractionation ratio ($\delta^{13}\text{C}$) was once thought to be a reliable indication of a biological carbon fixation (Schidlowski et al. 1983), this has recently been questioned (McCollom and Seewald 2006).

Carbon

ALAN W. SCHWARTZ

Radboud University Nijmegen, Nijmegen,
The Netherlands

Synonyms

Elemental carbon

Definition

Carbon: The Sixth Element of the Periodic Table

Overview

Carbon is the sixth element in the periodic table. Its stable isotopes include ^{12}C , the nucleus of which contains six protons and six neutrons and ^{13}C , which contains six protons and seven neutrons. Carbon is the fourth most abundant element in the solar atmosphere, after hydrogen, helium, and oxygen. This predominance is largely due to the autocatalytic role of carbon in the stellar nucleosynthesis of elements higher than hydrogen via proton addition (Bethe 1939):

Electronic Structure

The electronic structure of carbon is abbreviated as: $1s^2, 2s^2, 2p^2$ (two electrons in the 1s orbital, two electrons in the 2s orbital and two electrons in the 2p orbital). The element can therefore accept 4 electrons in the outermost (valance) shell to complete an octet and form a neon-like configuration: $1s^2, 2s^2, 2p^6$. It was pointed out by Wald that the prevalence of H, O, N, and C in biochemistry can be rationalized by the fact that these elements are the smallest that can reach stable (filled, i.e., noble gas-like) electronic configurations in the valance shell by adding (i.e., sharing with other atoms) one, two, three and four electrons, respectively, and thereby forming covalent bonds (Wald 1958).

This suggests that the same properties of these elements would similarly be responsible for a central role for organic chemistry (and biochemistry) anywhere in the universe. Wald also argued that silicon's electronic configuration (one period lower in the periodic table; $1s^2, 2s^2, 2p^6, 3s^2, 3p^2$), while potentially also permitting the forming of covalent bonds by accepting four electrons in the outermost shell, is substantially larger than carbon. The larger distance between the nucleus of silicon and the outer electronic orbitals results in differences in bonding energies, as well as the geometry of the orbitals, compared to carbon. The result is that C forms stable covalent bonds (single as well as multiple) with itself and with other atoms, while Si has much less tendency to do so. Thus, CO_2 is a discrete molecule and a stable gas, and C–C bonds produce stable chains of hydrocarbons. SiO_2 , on the other hand, is a crystalline solid (of average composition SiO_2), which exists as an unlimited three-dimensional network, and Si–Si chains are not stable in the presence of water or O_2 . Carbon is thus regarded by most astrobiologists as being central to and probably necessary for life.

Native Forms of Carbon

In spite of its importance to life and its role in the biosphere, elemental carbon is only a trace constituent in most of the Earth's crust, where it is present at an average level of 200 ppm. In sedimentary rocks, carbon is abundant, but usually in compounds such as ► **carbonates** (limestone) or organic matter (petroleum, coal). In the biosphere, hydrosphere and atmosphere, carbonic acid equilibria (carbon dioxide, carbonate and bicarbonate) play major roles in the weathering of crustal rocks and presumably would have similar roles on other, Earth-like planets.

The primary forms of elemental carbon in Earth's crust and mantle are graphite and diamond. Diamond is thought to form under high-pressure and high-temperature conditions in the mantle and to be transported to the surface by magmatic activity. Graphite has a sheet-like network of so-called sp^2 (planar) bonded carbon atoms (see below) and can be hydrogenated to produce hydrocarbons, or oxidized to carboxylic acids. In contrast, diamond, which has a tetrahedral or sp^3 structure, forms face-centered cubic crystals which are difficult to oxidize or reduce. The hexagonal mineral lonsdaleite, another allotrope which is said to be even harder than diamond, is only found in strongly shocked areas such as meteorite craters, where it is thought to have formed from graphite during impact (Wederpohl 1978).

Similarly, fullerenes and related “cage” forms of carbon also require exceptional conditions to form, but have been identified in the unshocked Allende and Murchison meteorites as C_{60} – C_{400} fullerenes (Becker et al. 2000).

Compounds of Carbon and the History of Organic Chemistry

Although the element has been known from ancient times, an understanding of its chemical nature and particularly its role in organic material did not emerge until the development of analytical methods of analysis by Lavoisier and others in the eighteenth century. Thus, Lavoisier demonstrated that carbonic acid or carbon dioxide was formed by the union of carbon and oxygen, or by burning organic substances in air or oxygen (Moore 1918). The terms “organic chemistry” and “organic compound” were historically intended to indicate the nature of biologically derived compounds of carbon, which were thought to be unique to life. Today, organic chemistry is usually described as the chemistry of compounds of carbon, but probably can be more accurately regarded as focusing on the chemistry of hydrocarbons (compounds composed of hydrogen and carbon) and of their derivatives with oxygen and nitrogen.

Modern organic chemistry is generally considered to have started in mid-nineteenth century with the work of Wöhler, who synthesized the well-known animal waste product, urea. The actual story of Wöhler's work is somewhat more complicated than the usual description. The great chemist was attempting to synthesize ammonium cyanate by studying the reaction between cyanogen and (aqueous) ammonia, one of the products of which was a white crystalline substance. The same product was also obtained by the reaction of lead cyanate and ammonia. It was in the course of purifying the latter, that Wöhler obtained urea. His realization of the potential importance of the reaction led him to write to Berzelius, saying that he could make urea without using a kidney or even an animal (McKie 1944). In spite of the enthusiastic nature of this communication to Berzelius, the latter's reaction, as well as those of many of Wöhler's contemporaries, was restrained and ► **vitalism** only gradually died out.

During this same period, chemists became aware of the existence of meteorites containing organic compounds. Berzelius and Wöhler, among others, remarked on the presence of organic material in several carbonaceous meteorites. It is noteworthy, however, that neither Berzelius nor Wöhler thought that the organic compounds present were necessarily biological products (Nagy 1975). Today, the universality of organic chemistry has become

obvious; not only through investigation of meteorites and ► [comets](#), but due to observations of interstellar organic compounds.

Molecular Structure of Carbon Compounds

Bond formation between carbon atoms (or with other elements) occurs by sharing electrons and involves a process known as hybridization of molecular orbitals. In methane and related hydrocarbons, the carbon atom is located in the center of a tetrahedron, with the bonded hydrogen atoms located at the corners. This geometry was explained by Pauling:

- We have thus derived the result that an atom in which only s and p eigenfunctions contribute to bond formation and in which the quantization in polar coordinates is broken can form one, two, three, or four equivalent bonds, which are directed toward the corners of a regular tetrahedron. (Pauling 1931)

The tetrahedral geometry of compounds of carbon thus results from so-called sp³ hybridized orbitals. As a consequence of this symmetry, substitution of other atoms bonded to the central carbon atom (such as substitution of the hydrogen atoms in methane, CH₄ by atoms or groups A, B, and C to produce CHABC), produces an unsymmetrical molecule which displays the phenomenon of ► [chirality](#). Synthesis of such a chiral molecule by a spontaneous chemical reaction produces a mixture of isomers or enantiomers which are chemically but not physically identical. It can readily be seen by inspecting models, that such simple examples of chiral enantiomers are mirror images of each other. The phenomenon of chirality was discovered historically by Pasteur, in the form of “optical activity,” as determined by the property of rotating the plane of polarization of a plane-polarized beam of light. The carbon atom in this simple compound is referred to as an asymmetric center. More complex molecules, such as the biological product tartaric acid, which led Pasteur to his discovery, contain more than one chiral center and can produce even more complicated sets of chiral enantiomers.

See also

- [Carbon Isotopes as a Geochemical Tracer](#)
- [Carbonaceous Chondrite](#)
- [Carbonate](#)
- [Chirality](#)
- [Comet](#)
- [Delta, Isotopic](#)
- [Fischer–Tropsch Effects on Isotopic Fractionation](#)
- [Interstellar Chemical Processes](#)
- [Organic Molecule](#)
- [Vitalism](#)

References and Further Reading

- Arnold JR, Libby WF (1949) Age determinations by radiocarbon content: checks with samples of known age. *Science* 110:678–680
- Becker L, Poreda RJ, Bunch TE (2000) Fullerenes: an extraterrestrial carbon carrier phase for noble gases. *Proc Natl Acad Sci* 97: 2979–2983
- Bethe HA (1939) Energy production in stars. *Phys Rev* 55:434–456
- Henderson LJ (1913) *The fitness of the environment: an inquiry into the biological significance of the properties of matter*. Macmillan, Boston
- McCollom TM, Seewald JS (2006) Carbon isotope composition of organic compounds produced by abiotic synthesis under hydrothermal conditions. *Earth Planet Sci Lett* 243:74–84
- McKie D (1944) Wöhler’s ‘synthetic’ urea and the rejection of vitalism: a chemical legend. *Nature* 153:608–610
- Moore FJ (1918) *A history of chemistry*. McGraw-Hill Books, New York (Reprint by General Books, Memphis, Tennessee, 2009)
- Nagy B (1975) *Carbonaceous meteorites*. Elsevier, Amsterdam, pp 43–78
- Pauling L (1931) The nature of the chemical bond. Applications of results obtained from the quantum mechanics and from a theory of paramagnetic susceptibility to the structure of molecules. *J Am Chem Soc* 53:1367–1400
- Schidlowski M, Hayes JM, Kaplan IR (1983) In: Schopf JW (ed) *Isotopic inferences of ancient biochemistries: carbon, sulfur, hydrogen, and nitrogen in earth’s earliest biosphere*. Princeton University Press, Princeton, pp 149–186
- Wald G (1958) Introduction to the 1958 edition of Henderson, op.cit. Beacon Press, Boston, pp xvii–xxiv
- Wederpohl KH (ed) (1978) *Handbook of geochemistry*, vol III/1(6). Springer, Berlin

Carbon Cycle (Biological)

J. CYNAN ELLIS-EVANS

UK Arctic Office, Strategic Coordination Group, British Antarctic Survey, Cambridge, UK

Keywords

Biogeochemical cycles, carbon source, fermentation, photosynthesis, respiration

Definition

The carbon cycle is one of the most important biogeochemical cycles on Earth and involves all five environmental spheres. Its geological components operate on a scale of millions of years, while biological carbon cycling operates over a scale of days to thousands of years. Every organism on Earth needs carbon either for structure or energy, and the primary biological processes in carbon cycling are ► [photosynthesis](#) and respiration. Incorporation of biological carbon in sedimentary deposits subsequently used as fossil fuels is now also an important process in

biological carbon cycling, notably through influencing the global carbon budget and thus the Earth's climate.

Overview

Carbon is the fourth commonest element in the Universe and is present in all five Earth spheres (► [biosphere](#), geosphere, pedosphere, ► [hydrosphere](#), and atmosphere). The annual rates of biological carbon cycling are several orders of magnitude greater than geological cycling of carbon and very responsive to environmental fluctuations. Carbon is essential to life on Earth, and the biological processes of light-mediated carbon fixation (photosynthesis, chemolithoautotrophy), ► [aerobic respiration](#) of organic carbon to form inorganic CO₂, and (to a lesser extent) ► [anaerobic respiration](#) to form methane (and some CO₂) are important mechanisms for processing carbon within the five spheres. Exchange of carbon between land and atmosphere is driven by the key biological processes, but in the oceans is dominated by physical exchange as the world's oceans hold vast quantities of dissolved inorganic carbon. This reservoir of dissolved inorganic carbon (DIC) is relatively dynamic, but other reservoirs are more stable. In the case of terrestrial carbon cycling, low rates of decomposition can result in accumulation of organic carbon (e.g., peat deposits, bogs) which can under certain geological conditions form substantial coal, oil, and gas (including methane hydrate) deposits. In the oceans, sedimentation of plankton with calcareous skeletons results in burial and limestone formation though this can also form through reaction of carbonate ions with calcium. This range of organic and particularly inorganic carbon deposits represents significant long-term sinks for atmospheric CO₂. Anthropogenic activities significantly contributing to carbon cycling include burning of fossil fuels and agro fuels and industrial processes, such as cement production (limestone decomposition). The observed buildup of CO₂ in the atmosphere since the start of the industrial revolution and associated regional warming has led to warmer ocean surface waters. Warmer waters absorb less CO₂, and so the “braking” effect of the oceans on rising atmospheric CO₂ concentrations is reduced. Warming also allows potential release of methane from temperature sensitive methane hydrate deposits within shallow marine sediments and from thawing permafrost peat deposits on land, as well as extending the active season for soil respiration, further enhancing release of carbon dioxide and methane to the atmosphere.

See also

- [Aerobic Respiration](#)
- [Anaerobic Respiration](#)

- [Biosphere](#)
- [Fermentation](#)
- [Hydrosphere](#)
- [Methanogens](#)
- [Photosynthesis](#)

References and Further Reading

- Knonova MM (1966) Soil organic matter. Pergamon, New York
- Olson JS, Pfuderer HA, Chan Y-H (1978) Changes in the global carbon cycle and the biosphere, ORNL/EIS-109. Oak Ridge National Laboratory, Tennessee
- Sedjo R (1993) The Carbon Cycle and Global Forest Ecosystem. *Water Air Soil Pollut* 70:295–307

Carbon Dioxide

THOMAS MCCOLLOM

Laboratory for Atmospheric and Space Physics, University of Colorado, Boulder, CO, USA

Keywords

Carbon cycle, carbon fixation, carbon-silicate cycle, greenhouse effect

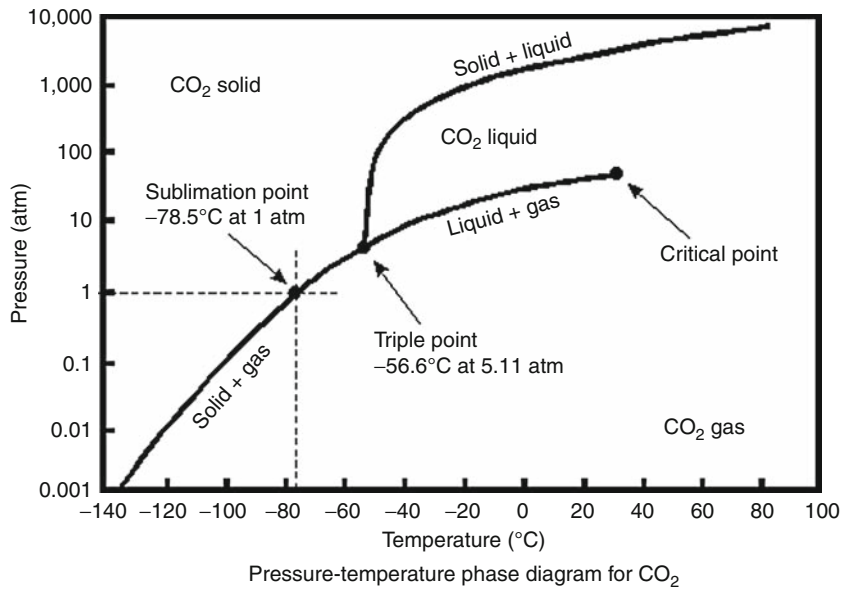
Definition

Carbon dioxide is a triatomic compound with the chemical composition CO₂. The molecule is symmetrical and nonpolar. The triple point of pure CO₂ occurs at -56.6°C and 518 kPa (Fig. 1). As a gas, carbon dioxide is clear, colorless, and odorless.

Overview

Carbon dioxide occurs predominantly as either a gas or a solid ice in the solar system. As a gas, it is the predominant constituent of the atmospheres of Venus and Mars, as well as a minor component of the atmospheres of many other planetary bodies including the Earth. As an ice, CO₂ is a significant component of ► [comets](#) and the Martian polar caps. Liquid carbon dioxide requires temperatures above -56°C and pressures greater than 5 bar (Fig. 1) to exist. Such conditions are not presently known to occur in the solar system, but might have been present on early Mars and may occur on extrasolar planets. Carbon dioxide has been found in interstellar clouds in gas and ice phases by the ► [Infrared Space Observatory \(ISO\)](#).

Carbon dioxide is also present in the interior of the Earth, where it occurs as a trace component within



Carbon Dioxide. Figure 1 Phase diagram for pure carbon dioxide

the crystal structures of minerals or occupies void spaces between minerals. At the oxidation state of the Earth's mantle, carbon dioxide together with the minerals graphite and diamond are the predominant stable forms of carbon. Carbon dioxide dissolves into magmas as they form within the Earth's interior, and is released into the atmosphere when the magmas cool and solidify as volcanic rocks at the surface. As a consequence, carbon dioxide is a major component of volcanic gases, and is the primary form of carbon in those gases. Carbon dioxide that accumulates in the atmosphere contributes to the ► [greenhouse effect](#) that plays a significant role in warming of planetary surfaces.

Carbon dioxide dissolves readily in water, where it hydrates to form carbonic acid ($\text{H}_2\text{CO}_{3(\text{aq})}$), which in turn generates acidity through release of protons ($\text{H}_2\text{CO}_{3(\text{aq})} \rightarrow \text{H}^+ + \text{HCO}_3^- \rightarrow 2\text{H}^+ + \text{CO}_3^{2-}$). The protons released can react with minerals to cause rock weathering, altering the rock's mineralogy and releasing cations such as Ca^{2+} and Mg^{2+} into solution. Under some circumstances, the cations released can react with dissolved CO_2 to precipitate as ► [carbonate](#) minerals including calcite (CaCO_3) and siderite (FeCO_3) as part of the carbon-silicate cycle. The net result is removal of atmospheric CO_2 into carbonate-bearing rock.

Some biological organisms, the photoautotrophs and chemoautotrophs, are capable of transferring electrons to carbon dioxide (CO_2 ► [reduction](#)) to form bioorganic compounds, a process termed carbon fixation. Conversely, heterotrophic organisms consume bioorganic matter and convert much of it back to carbon dioxide in a process known as ► [respiration](#). Transformation of CO_2 through carbon fixation and respiration are primary components of the biological carbon cycle.

See also

- [Carbon Cycle \(Biological\)](#)
- [Carbon Dioxide](#)
- [Carbonate](#)
- [Chemoautotroph](#)
- [Greenhouse Effect](#)
- [Infrared Space Observatory](#)
- [Photoautotroph](#)
- [Reduction](#)
- [Respiration](#)

References and Further Reading

- Archer D (2010) The global carbon cycle. Princeton University Press, Princeton, NJ
- MacKenzie FT, Lerman A (2006) Carbon in the geobiosphere - earth's outer shell. Springer, Dordrecht

Carbon Isotopes as a Geochemical Tracer

NOAH PLANAVSKY¹, CAMILLE PARTIN², ANDREY BEKKER²

¹Department of Earth Sciences, University of California, Riverside, CA, USA

²Department of Geological Sciences, University of Manitoba, Winnipeg, MB, Canada

Keywords

Biosignature, carbon cycle, carbonates, organic carbon burial

Definition

Carbon has two stable isotopes (¹²C and ¹³C) and one radiogenic isotope (¹⁴C). Carbon is the main constituent of the biosphere, and is rapidly recycled in the ocean-atmosphere system, Carbon isotope ratios are easily measured, and therefore stable [carbon isotopes](#) can be widely used to trace the [carbon cycle](#) on Earth. Carbon isotopes may equally have utility in tracing the carbon cycle on other planets. Stable carbon isotopes measured from samples collected in a geological context can be used to differentiate between biotic and abiotic carbon transformations and can, therefore, serve as a biosignature.

Overview

Carbon isotopes are one of the most extensively used geochemical tracers of biological processes on both local and global scales. Carbon isotopes have been essential to the development of our understanding of modern carbon fluxes and the long-term evolution of the global carbon cycle (Schidlowski 1988).

Most of Earth's carbon (~98.89%) occurs as the lighter stable isotope (¹²C). The remaining ~1.1% of Earth's carbon occurs as the heavier (¹³C) stable isotope (de Laeter et al. 2003). There are trace levels (<1 ppt) of radiogenic carbon (¹⁴C), which are generated in the upper atmosphere through interaction between divalent nitrogen and background radiation. The half-life of ¹⁴C is 5,730 ± 40 years (Scott 2003). Variations in carbon isotopes are reported in standard delta notation:

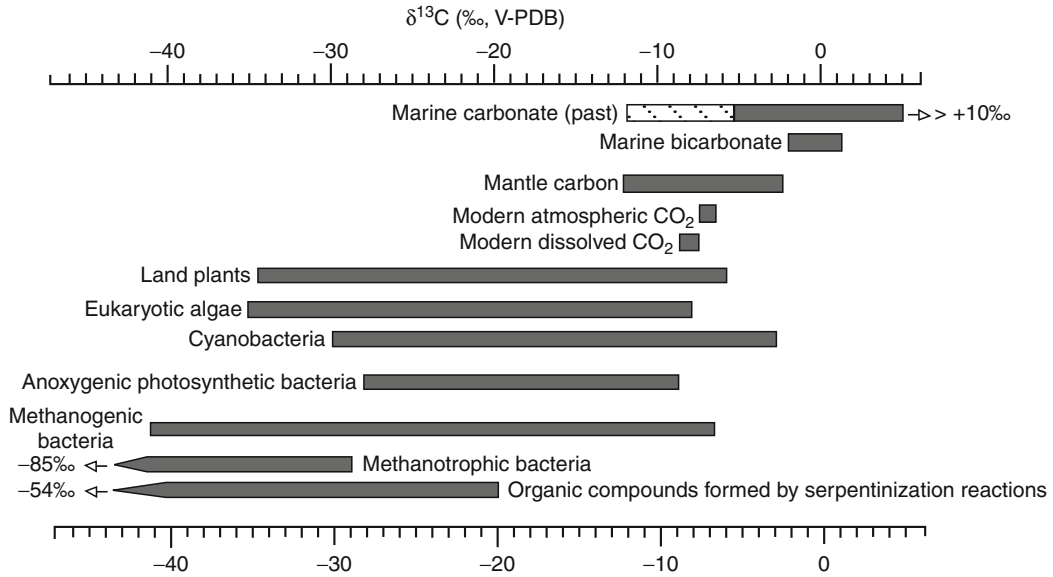
$$\delta^{13}\text{C} = \left[\frac{(^{13}\text{C}/^{12}\text{C})_{\text{sa}}}{(^{13}\text{C}/^{12}\text{C})_{\text{st}}} - 1 \right] \times 1000(\text{‰}, \text{PDB})$$

where the sample (sa) composition is reported with respect to the standard (st) an international reference material

(V-PDB [Vienna Pee Dee Belemnite]). Stable isotope ratios of carbon in natural samples range from about -100‰ to +50‰. However, the majority of natural samples on Earth possess $\delta^{13}\text{C}$ values ranging from -35‰ to +5‰, which reflect the typical kinetic isotope fractionation associated with the enzymatic carboxylation step of carbon assimilation in autotrophic organisms (Fig. 1). This fractionation is the main process responsible for the creation of isotopically light organic matter and a remnant inorganic carbon pool that is isotopically heavy relative to carbon sourced from the Earth's mantle, which has a $\delta^{13}\text{C}$ value of ~-5‰ (e.g., Broecker 1970). However, there is a wide range of abiotic and biotic processes (as discussed below) that cause significant carbon isotope fractionations. Therefore, the presence of an isotopically light or heavy carbon pool is not definitive evidence for autotrophic carbon fixation i.e., life.

Basic Methodology

There are several methods employed to measure carbon isotopes. The most standard technique involves CO₂ analysis on a gas source isotope ratio mass spectrometer (IR-MS), using gas prepared with either combustion of organic carbon or acidification of inorganic carbon. Mass spectrometers equipped with a dual inlet system require offline combustion and provide the highest precision, but standard deviation on continuous flow IR-MS is commonly better than 0.15‰. Accurate carbon isotope measurements can also be made using absorption spectroscopy coupled with a diode laser (tunable diode laser absorption spectroscopy [TDLAS]). In this method the laser is tuned to a specific absorption wavelength, the intensity of the transmitted radiation is measured, and this intensity can be directly related to the concentration of the species (in this case an isotopologue) to which the laser was tuned. TDLAS systems are significantly smaller and more mobile than mass spectrometers and are of particular interest from an astrobiological perspective since a TDLAS system is expected to be one of the joint NASA and ESA Mars Science Lab rover, which may be deployed as soon as 2020. In situ techniques to analyze solid samples include secondary ion mass spectrometry (SIMS) and laser ablation inductively coupled plasma mass spectrometry (LA-ICP-MS). Both techniques offer high spatial resolution, on the order of a few microns, and sub-per mil precision. An alternative non-destructive technique is Raman spectroscopy, but analytical errors can be prohibitively large. Infrared spectroscopy is another emerging non-destructive method to measure carbon isotopes.



Carbon Isotopes as a Geochemical Tracer. Figure 1 Range of carbon isotope values in common inorganic and biological carbon compounds (Modified from Schidlowski 2001 with the data for organic compounds produced by serpentinization reactions from Horita and Berndt 1999 and Foustoukos and Seyfried 2004)

Key Research Findings and Applications

Stable carbon isotopes have been used extensively to trace changes in the global carbon cycle. Use of carbon isotopes to track the evolution of carbon fluxes stems from the assumption that there must be an isotopic balance between the continuous supply of mantle carbon and the burial of organic and carbonate carbon (Schidlowski 2001). The relationship between mantle-derived carbon (C_{prim}) and burial of organic (C_{org}) and carbonate (C_{carb}) carbon on geological time-scales is determined by the relative burial rate of organic carbon (R) and can be expressed mathematically as

$$\delta^{13}\text{C}_{\text{prim}} = R\delta^{13}\text{C}_{\text{org}} + (1 - R)\delta^{13}\text{C}_{\text{carb}}$$

The isotopic composition of the mantle flux of carbon ($\delta^{13}\text{C}_{\text{prim}}$) is, based on the carbon isotope composition of diamonds and carbon dioxide released from volcanoes, generally accepted to be $\sim -5\text{‰}$. However, the carbon isotopic composition of diamonds indicates some heterogeneity in the mantle: eclogites, which represent subducted oceanic crust, commonly possess more negative isotopic values (Deines et al. 1991). Assuming a mantle isotopic composition, the ratio of organic to carbonate carbon burial can be estimated using their isotopic compositions. Open-marine carbonates typically have a $\delta^{13}\text{C}$ value of $\sim 0\text{‰}$ and average organic matter has a $\delta^{13}\text{C}$

value $\sim -25\text{‰}$. It follows that about 20% of carbon today is buried as organic matter (Holland 1978).

This concept is interesting from an astrobiological perspective since carbon stable isotope values can be used to track the evolution of the carbon cycle through Earth's history. The carbon isotope composition of the Earth's mantle is generally assumed to have been essentially constant through time, in contrast to that of marine carbonates and organic matter. However, the composition of both carbonates and organic matter can be measured at almost any point in Earth's history, since both these carbon pools are common in the geologic record. Importantly, the carbon isotope composition of ancient carbonates is roughly equal to that of the dissolved inorganic carbon reservoir, since only a small positive fractionation takes place during mineral precipitation. Therefore, the carbon isotope values of carbonates deposited in open-marine settings usually reflect time-averaged seawater isotope composition. The $\delta^{13}\text{C}$ value of ancient organic matter is, similarly, usually roughly equivalent to that of organic matter when first sedimented (Hayes et al. 1983). However, the composition of organic matter is much more strongly affected by local factors, such as rates of primary and secondary productivity, which are ultimately linked with ocean redox state and chemical composition (e.g., Bekker et al. 2008), than is carbonate

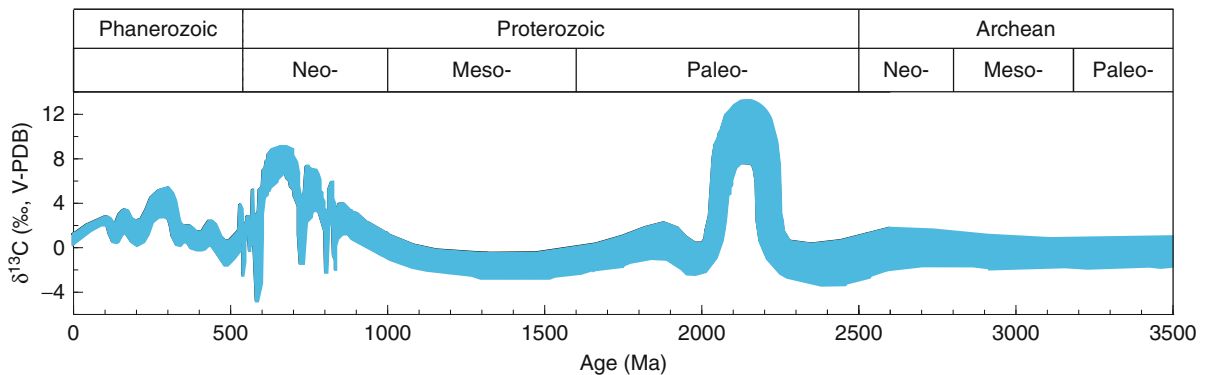
carbon. Therefore, carbon isotope studies of carbonates and organic matter from open-marine settings hold the potential (when used with caution) to constrain past organic and carbonate burial fluxes, even if samples are billions of years old.

Use of these methodologies has yielded a surprising result: the $\delta^{13}\text{C}$ values of marine carbonates have remained relatively constant throughout Earth's history (Fig. 2). Almost all marine carbonates, dating back to 3.5 billion years ago, have a $\delta^{13}\text{C}$ value of $\sim 0\%$ (Schidlowski et al. 1975). This indicates that even in the Earth's early history there was significant and continuous burial of isotopically light carbon, suggesting autotrophic primary production. Further, it implies that despite dramatic changes to the biosphere, such as the evolution of land plants and calcareous phytoplankton, the relative burial of organic versus carbonate carbon has remained essentially constant. This relative stasis is a testament to the importance of stabilizing feedbacks at work in Earth's **biogeochemical cycles**. Short-lived (<5 million years) isotope excursions are relatively common in the Phanerozoic (the eon encompassing the last 542 million years of Earth's history). The magnitude of these excursions is typically less than 5‰ and, in most cases, they can be linked to temporary increased or decreased organic carbon burial. For instance, transient shifts to anoxic deep-sea conditions in the Cretaceous Period resulted in burial of organic-rich black shales and, consequently, positive carbonate carbon isotope excursions (e.g., Sageman et al. 2006). Additionally, there are two major periods in Earth's history with long-lived carbon isotope excursions. Foremost, the mid-Paleoproterozoic (~ 2.3 to 2.1 billion years ago) record is notable for an abundance of carbonates with markedly positive carbon isotope values, in some

cases reaching even above 10‰ (Karhu and Holland 1996; Bekker et al. 2003, 2008). In the Neoproterozoic Era (~ 800 –650 million years ago) markedly positive and negative carbonate carbon isotope excursions are also common (Kaufman and Knoll 1995; see Fig. 2). These isotope signatures are traditionally interpreted to mark periods of enhanced or decreased organic carbon burial. It has also been recently suggested that Neoproterozoic carbonate carbon isotope variations may reflect the dynamics of a large dissolved organic carbon reservoir (Rothman et al. 2003).

Beyond tracking global processes, carbon isotopes provide a means to trace local carbon fixation pathways and carbon transformations on a small scale. In contrast to the global carbon cycle, in isolated systems the isotopic fractionations associated with abiogenic processes can be very important. For instance, the small kinetic isotope fractionation caused by carbon dioxide degassing during evaporation can generate ^{13}C -enriched dissolved inorganic carbon (DIC) pool (e.g., Stiller et al. 1985; see for contrary view Lazar and Erez 1990), since evaporation in a closed system allows for expression of Rayleigh distillation effects. Similarly, although the fractionation associated with carbonate mineral precipitation is very small, in settings with efficient distillation mechanisms this process can form isotopically distinct carbon pools. There are also ancient diagenetic carbonates that record the isotopic composition of porewater rather than the $\delta^{13}\text{C}$ value of DIC of water column. Porewater isotopic composition can be strongly influenced by organic matter remineralization and thermal decarboxylation.

Methane cycling can also produce markedly negative and positive carbon isotope values. Methane on Earth is almost



Carbon Isotopes as a Geochemical Tracer. Figure 2 Generalized record of the $\delta^{13}\text{C}$ values of marine carbonates through time (Modified from Karhu 1999)



entirely directly or indirectly biologically-produced (Fiebig et al. 2009); foremost during organic matter fermentation by methanogens, which can generate methane with $\delta^{13}\text{C}$ values $< -80\text{‰}$. Although the presence of isotopically light methane is commonly assumed to provide a signature of microbial processes, abiogenic **▶ serpentization** can also produce methane with highly negative $\delta^{13}\text{C}$ values (Foustoukos and Seyfried 2004). Experimentally-controlled serpentization reactions can produce methane with $\delta^{13}\text{C}$ values $< -50\text{‰}$ (e.g., Horita and Berndt 1999). The presence of $\delta^{13}\text{C}_{\text{org}}$ values as low as -60‰ in ca. 2.7 billion-year-old sediments on several continents has been suggested to indicate aerobic methane oxidation (Hayes 1994; Eigenbrode and Freeman 2006) and may therefore date the rise of aerobic ecosystems. However, methane oxidation can also be linked with ferric oxide, nitrate, or sulfate reduction (Orphan et al. 2001; Raghoebarsing et al. 2006; Beal et al. 2009) and these oxidants can be formed in an anoxic ocean–atmosphere system. High temperature and pressure metal-catalyzed reactions (e.g., Fischer–Tropsch reactions) can also create a wide range of isotopically depleted simple organic molecules other than methane (e.g., Foustoukos and Seyfried 2004; Fiebig et al. 2009) and are a potential source of abiogenic light organic carbon in the geologic record. Consequently, carbon isotopes are a powerful geochemical tracer, but there is often more than one explanation for the $\delta^{13}\text{C}$ values. Therefore, whether the end goal is to trace the global carbon cycle, constrain carbon pathways in an isolated system, or to find evidence of biological activity, a strong geological context is an essential prerequisite to using carbon isotopes to derive a unique explanation.

Future Directions

Carbon isotopes have greatly improved our understanding of the carbon cycle on Earth. Carbon isotopes will undoubtedly play a significant role in unravelling aspects of the carbon cycle on other planets. With recent advances in in-flight technology (e.g., mobile TDLAS systems) the idea of carbon isotope studies on other planets is no longer a distant prospect in astrobiological studies.

See also

- ▶ Biogeochemical Cycles
- ▶ Biomarkers, Isotopic
- ▶ Carbon Cycle (Biological)
- ▶ Carbon Isotopes as a Geochemical Tracer
- ▶ Mantle Volatiles
- ▶ Serpentinization

References and Further Reading

- Beal EJ, House CH, Orphan VJ (2009) Manganese- and iron-dependent marine methane oxidation. *Science* 325:184–187
- Bekker A, Karhu JA, Eriksson KA, Kaufman AJ (2003) Chemostratigraphy of Paleoproterozoic carbonate successions of the Wyoming Craton: tectonic forcing of biogeochemical change? *Precambrian Res* 120:279–325
- Bekker A, Holmden C, Beukes NJ, Kenig F, Eglinton B, Patterson WP (2008) Fractionation between inorganic and organic carbon during the Lomagundi (2.22–2.1 Ga) carbon isotope excursion. *Earth Planet Sci Lett* 271:278–291
- Bjerrum CJ, Canfield DE (2004) New insights into the burial history of organic carbon on the early Earth. *Geochem Geophys Geosys* doi:10.1029/2004GC000713
- Broecker WS (1970) A boundary condition on the evolution of atmospheric oxygen. *J Geophys Res* 75:3553–3557
- de Laeter JR, Böhlke JK, De Bièvre P, Hidaka H, Peiser HS, Rosman KJR, Taylor PDP (2003) Atomic weights of the elements. *Pure Appl Chem* 75:683–800
- Deines P, Harris JW, Robinson DN, Gurney JJ, Shee SR (1991) $\delta^{13}\text{C}$ and $\delta^{18}\text{O}$ variations in diamond and graphite eclogites from Orapa, Botswana, and the nitrogen content of their diamonds. *Geochim Cosmochim Acta* 55:515–524
- Eigenbrode JL, Freeman KH (2006) Late Archean rise of aerobic microbial ecosystems. *Proc Natl Acad Sci* 103:15759–15764
- Fiebig J, Woodland AB, D'Alessandro W, Puttmann W (2009) Excess methane in continental hydrothermal emissions is abiogenic. *Geology* 37:495–498
- Fischer WW, Schroeder S, Lacassie JP, Beukes NJ, Goldberg T, Strauss H, Horstmann UE, Schrag DP, Knoll AH (2009) Isotopic constraints on the late archean carbon cycle from the Transvaal Supergroup along the western margin of the Kaapvaal Craton, South Africa. *Precambrian Res* 169:15–27
- Foustoukos DI, Seyfried WE Jr (2004) Hydrocarbons in hydrothermal vent fluids: the role of chromium-bearing catalysts. *Science* 304:1002–1005
- Hayes JM (1994) Global methanotrophy at the Archean – Proterozoic transition. In: Bengtson S (ed) *Early life on earth* (Nobel symposium 84). Columbia University Press, New York, pp 220–236
- Hayes JM (2001) Fractionation of the isotopes of carbon and hydrogen in biosynthetic processes. *Rev Mineral Geochem* 43:225–278
- Hayes JM, Waldbauer JR (2006) The carbon cycle and associated redox processes through time. *Philos Trans R Soc* 361:931–950
- Hayes JM, Kaplan IR, Wedeking KW (1983) Precambrian organic geochemistry: preservation of the record. In: Schopf JW (ed) *Earth's earliest biosphere: its origin and evolution*. Princeton University Press, Princeton, NJ, pp 93–134
- Holland HD (1978) *The chemistry of the atmosphere and oceans*. Wiley, New York, p 351
- Horita J, Berndt M (1999) Abiogenic methane formation and isotopic fractionation under hydrothermal conditions. *Science* 285:1055–1057
- Hotinski RM, Kump LR, Arthur MA (2004) The effectiveness of the Paleoproterozoic biological pump: A $\delta^{13}\text{C}$ gradient from platform carbonates of the Pethei Group (Great Slave Lake Supergroup, NWT). *Geol Soc Am Bull* 116:539–554
- Karhu J (1999) Carbon isotopes. In: Marshall CP, Fairbridge RW (eds) *Encyclopedia of geochemistry*. Kluwer Academic Publishers, Dordrecht, pp 67–73
- Karhu JA, Holland HD (1996) Carbon isotopes and the rise of atmospheric oxygen. *Geology* 24:867–870

- Kaufman AJ, Knoll AH (1995) Neoproterozoic variations in the carbon isotopic composition of seawater: stratigraphic and biogeochemical implications. *Precambrian Res* 73:27–49
- Kump LR, Arthur MA (1999) Interpreting carbon-isotope excursions: carbonates and organic matter. *Chem Geol* 161:181–198
- Lazar B, Erez J (1990) Extreme ^{13}C depletions in seawater-derived brines and their implications for the past geochemical carbon cycle. *Geology* 18:1191–1194
- MacKenzie FT, Lerman A (2006) Carbon in the geobiosphere: Earth's outer shell, *Topics in Geobiology-25*. Springer-Verlag, New York, p 402
- Orphan VJ, House CH, Hinrichs K-U, McKeegan KD, DeLong EF (2001) Methane-consuming archaea revealed by directly coupled isotopic and phylogenetic analysis. *Science* 293:484–487
- Raghoebarsing AA, Pol A, van de Pas-Schoonen KT, Smolders AJ, Ettwig KE, Rijpstra WI, Schouten S, Damsté JS, Op den Camp HJ, Jetten MS, Strous M (2006) A microbial consortium couples anaerobic methane oxidation to denitrification. *Nature* 440:878–879
- Rothman DH, Hayes JM, Summons RE (2003) Dynamics of the neoproterozoic carbon cycle. *Proc Natl Acad Sci* 100:8124–8129
- Sageman BB, Meyers SR, Arthur MA (2006) Orbital time scale and new C-isotope record for Cenomanian-Turonian boundary stratotype. *Geology* 34:125–128
- Schidlowski M (1988) A 3800-million-year isotopic record of life from carbon in sedimentary rocks. *Nature* 333:313–318
- Schidlowski M (2001) Carbon isotopes as biogeochemical recorders of life over 3.8 Ga of Earth history: evolution of a concept. *Precambrian Res* 106:117–134
- Schidlowski M, Eichmann R, Junge CE (1975) Precambrian sedimentary carbonates: carbon and oxygen isotope geochemistry and implications for the terrestrial oxygen budget. *Precambrian Res* 2:1–69
- Scott EM (2003) The fourth international radiocarbon intercomparison (FIRI). *Radiocarbon* 45:135–285
- Stiller M, Rounick JS, Shasha S (1985) Extreme carbon-isotope enrichments in evaporating brines. *Nature* 316:434–435

Carbon Monosulfide

Synonyms

CS

Definition

The diatomic molecule carbon monosulfide, CS, is widespread in interstellar ► [molecular clouds](#), in our ► [Milky Way](#), and in external galaxies. Its emission at millimeter wavelengths is frequently used to estimate the density in these regions, since these pure rotational transitions require densities greater than about 10^5 molecules per cubic centimeter to be excited by collisions. Various isotopic variants have been observed astronomically, including those with ^{13}C , ^{34}S , and ^{33}S , as well as the most abundant $^{12}\text{C}^{32}\text{S}$. CS is also observed in cometary comae.

History

Interstellar CS was first detected by radio astronomers in 1971.

See also

- [Comet](#)
- [Milky Way](#)
- [Molecular Cloud](#)
- [Sulfur](#)

References and Further Reading

- Penzias AA, Solomon PM, Wilson RW, Jefferts KB (1971) Interstellar Carbon Monosulfide. *Astrophys J* 168:L53–L58

Carbon Monoxide

THOMAS MCCOLLOM

Laboratory for Atmospheric and Space Physics, University of Colorado, Boulder, CO, USA

Definition

Carbon monoxide is a diatomic compound with the chemical composition CO. At terrestrial atmospheric pressure, the melting point of pure carbon monoxide is -205°C and the boiling point is -191.5°C .

Overview

Carbon monoxide is not known to occur as a pure substance in natural environments, but instead occurs primarily as a minor component in gas and ice mixtures. Carbon monoxide has been observed in interstellar space, and spectroscopic observations indicate it composes several percent of the icy component of ► [comets](#) (which is predominantly water ice). These observations indicate carbon monoxide was a significant reservoir of carbon during formation of the solar system. In planetary bodies, carbon monoxide primarily occurs as a trace component in atmospheres (~ 0.1 parts per million on the present Earth) and in volcanic gases.

Transformations between carbon monoxide and ► [carbon dioxide](#) (CO_2) proceed fairly readily through photochemical reactions in planetary atmospheres and through mechanisms such as the so-called water-gas shift reaction in geologic environments ($\text{CO} + \text{H}_2\text{O} \leftrightarrow \text{CO}_2 + \text{H}_2$). The latter is an oxidation-reduction reaction, and at the prevailing oxidation state of the Earth's interior, carbon dioxide is strongly favored by chemical thermodynamics relative to carbon monoxide. Consequently,

CO₂:CO ratios in volcanic gases on Earth are typically in range of 10³ to 10⁵. Carbon monoxide may also be generated from dehydration of ► [formic acid](#), and vice versa (HCOOH ↔ CO + H₂O).

Carbon monoxide readily forms complexes with transition metals, such as iron carbonyl [Fe(CO)₅] (carbonyl is the name given to the CO radical). Formation of carbonyls from carbon monoxide can also occur on the surface of transition metal-bearing minerals and alloys. Carbonyls are highly reactive, and carbonyls derived from carbon monoxide have been hypothesized to be a key reactant for the in situ formation of prebiotic organic compounds in several scenarios for the ► [origin of life](#) (e.g., Huber and Wächtershäuser 1997). One such reaction that is frequently invoked for the formation of organic matter in the early solar system is Fischer–Tropsch synthesis, a surface-catalyzed process for conversion of gaseous mixtures of CO and H₂ to hydrocarbons and other functionalized organic compounds such as fatty acids. Potential environments for the surface-catalyzed conversion of carbon monoxide to prebiotic organic compounds by the Fischer–Tropsch synthesis or other processes include dust grains in the early solar system, volcanic fumaroles, and hydrothermal systems.

See also

- [Carbon Dioxide](#)
- [Comet](#)
- [Fischer-Tropsch-Type Reaction](#)
- [Formic Acid](#)
- [Origin of Life](#)
- [Prebiotic Chemistry](#)

References and Further Reading

Huber C, Wächtershäuser G (1997) Activated acetic acid by carbon fixation on (Fe, Ni)S under primordial conditions. *Science* 276:245–247

Carbon Nitride

- [Cyanogen](#)

Carbon Source

Definition

Carbon source refers to any carbon containing molecule (carbohydrate, amino acid, fatty acid, CO₂) used by an

organism for the synthesis of its organic molecules. Carbon is a basic element for sustaining life as we know it and the main element in all classes of macromolecules. All cells require carbon as a major nutrient. On a dry weight basis, a typical cell is 50% carbon. Depending on their carbon source, organisms are either heterotrophs, requiring one or more organic compounds as their carbon source, or autotrophs, where CO₂ is the carbon source.

See also

- [Biosynthesis](#)
- [Carbon Cycle \(Biological\)](#)
- [Carbon Dioxide](#)
- [Chemotroph](#)
- [Macronutrient](#)
- [Metabolism \(Biological\)](#)
- [Phototroph](#)

Carbonaceous Chondrite

Synonyms

[Carbonaceous meteorite](#); CC

Definition

Carbonaceous chondrites constitute a subcategory of ► [chondrites](#) – which in turn are stony ► [meteorites](#). carbonaceous chondrites are the most primitive meteorites yet found and are mostly regarded as remnants of the first solid bodies to accrete in the ► [solar nebula](#). The main components of carbonaceous chondrites are ► [chondrules](#) and ► [CAIs](#) (Ca–Al-rich inclusions), which are embedded in a matrix of micrometer-sized dust particles. Since carbonaceous chondrites contain the highest concentration of volatile elements of the chondrites, they are concluded to have formed at the lowest temperatures. Their chemical composition is very similar to that of the Sun (albeit depleted in ► [hydrogen](#) and helium), and thus they can be considered (apart from ► [comets](#)) to be the most primitive ► [Solar System](#) materials.

See also

- [CAI](#)
- [Chondrite](#)
- [Chondrule](#)
- [Comet](#)
- [Hydrogen](#)
- [Meteorites](#)
- [Solar Nebula](#)
- [Solar System Formation \(Chronology\)](#)



Carbonaceous Chondrites (Organic Chemistry of)

CONEL MICHAEL O'DONEL ALEXANDER

Department of Terrestrial Magnetism, Carnegie Institution of Washington, NW Washington, DC, USA

Keywords

► [Amino acids](#), ► [asteroids](#), carbonaceous, chondrites, comets, ► [enantiomeric excess](#), ► [interplanetary dust particles](#), interstellar medium, isotope anomalies, meteorites, molecular cloud, nucleic acids, organic matter, ► [protoplanetary disk](#)

Definition

Carbonaceous chondrites are a class of primitive ► [meteorite](#) that formed in the ► [asteroid](#) belt and have remained relatively unmodified since their formation in the early Solar System. Some carbonaceous chondrites contain diverse suites of soluble and insoluble organic matter, including nucleic acids and amino acids with L enantiomeric excesses. This organic matter may have genetic links to organic matter in comets, and has a complex heritage, probably including synthesis in the interstellar medium, in the solar protoplanetary disk, and in the parent asteroids of the meteorites.

Overview

Most, if not all, chondrites probably accreted some organic matter when they formed, but generally thermal processes in their parent asteroids have destroyed or heavily modified it. The carbonaceous chondrites are a diverse class of meteorite comprised of eight recognized groups and a number of ungrouped meteorites. In three of these groups (CI, CM, and CR) the organic matter has been reasonably well preserved, although it has been modified to varying degrees by aqueous alteration (akin to low temperature ► [serpentinization](#)) and/or shock heating.

The organic matter in the CI-CM-CR chondrites is broadly divided into solvent soluble and insoluble fractions. The insoluble fraction (>70% of the total organic carbon) is a structurally complex, macromolecular material composed of small aromatic moieties that are cross-linked by short, highly branched aliphatic chains. It has a bulk elemental composition of $\sim\text{C}_{100}\text{H}_{75}\text{N}_3\text{O}_{15}$, which is similar to the average of comet Halley CHON particles, and is dispersed in chondrite matrices as particles that are typically <1 μm across. In bulk, the insoluble

material is significantly enriched in ^2H and ^{15}N . Even more extreme isotopic enrichments can be found in localized (usually $\leq 2\text{--}3\ \mu\text{m}$ across) “hotspots,” some of which are associated with so-called ► [globules](#) – spherical to irregular organic particles that are often hollow. Similar globules, isotopic “hotspots” and/or bulk isotopic enrichments are found in the organic matter of chondritic interplanetary dust particles and comet 81P/Wild two samples, suggesting that there is a common origin between both types of particles.

The solvent-extractable organic material is a complex suite of compounds that include: amino acids, N-heterocycles, hydroxy acids, carboxylic acids, sulphonic and phosphonic acids, polyols, amines, amides, alcohols, aldehydes, ketones, and aliphatic and ► [aromatic hydrocarbons](#). Concentrations range from hundreds of parts-per-million to a few parts-per-billion. Many of these compounds show almost complete structural diversity for a given carbon number, and also have large enrichments in ^2H and, if they contain N, in ^{15}N . Some CI-CM-CR chondrites contain α -dialkyl amino acids that do not readily racemize and that are not common terrestrial contaminants, but exhibit up to $\sim 20\%$ L-enantiomeric excesses. These L-enantiomeric excesses, which appear to be products of hydrothermal alteration, are consistent with the theory that the exogenous delivery of amino acids to the early Earth led to the left handedness of amino acids in living systems.

The origins of the soluble and insoluble fractions have yet to be definitively established. The ^2H and ^{15}N isotopic enrichments point to synthesis in very cold environments, either in the early Solar System or in the protosolar molecular cloud. However, it is less clear whether it was the existing organic material or its precursors that formed there.

See also

- [Aliphatic Hydrocarbon](#)
- [Amino Acid](#)
- [Aromatic Hydrocarbon](#)
- [Asteroid](#)
- [Carbonaceous Chondrite](#)
- [Comet \(Nucleus\)](#)
- [Enantiomeric Excess](#)
- [Globule \(Nanoglobule\)](#)
- [Interplanetary Dust Particles](#)
- [Interstellar Dust](#)
- [Interstellar Medium](#)
- [Meteorites](#)
- [Meteorite \(Murchison\)](#)
- [Protoplanetary Disk](#)



- ▶ [Racemization](#)
- ▶ [Serpentinization](#)

References and Further Reading

- Alexander CMO'D, Fogel M, Yabuta H, Cody GD (2007) The origin and evolution of chondrites recorded in the elemental and isotopic compositions of their macromolecular organic matter. *Geochim Cosmochim Acta* 71:4380–4403
- Busemann H, Young AF, Alexander CMO'D, Hoppe P, Mukhopadhyay S, Nittler LR (2006) Interstellar chemistry recorded in organic matter from primitive meteorites. *Science* 314:727–730
- Gilmour I (2003) Structural and isotopic analysis of organic matter in carbonaceous chondrites. In: Davis AM (ed) *Meteorites, comets and planets*. Elsevier-Pergamon, Oxford, pp 269–290
- Glavin DP, Dworkin JP (2009) Enrichment of the amino acid L-isovaline by aqueous alteration on CI and CM parent bodies. *Proc Natl Acad Sci* 106:5487–5492
- Gourier D, Robert F, Delpoux O, Binet L, Vezin H, Moissette A, Derenne S (2008) Extreme deuterium enrichment of organic radicals in the Orgueil meteorite: revisiting the interstellar interpretation? *Geochim Cosmochim Acta* 72:1914–1923
- Martins Z, Sephton M (2009) Extraterrestrial amino acids. In: Hughes AB (ed) *Origins and synthesis of amino acids*. Wiley-VCH, Weinheim, pp 3–42
- Martins Z, Botta O, Fogel ML, Sephton MA, Glavin DP, Watson JS, Dworkin JP, Schwartz AW, Ehrenfreund P (2008) Extraterrestrial nucleobases in the Murchison meteorite. *Earth Planet Sci Lett* 270:130–136
- Nakamura-Messenger K, Messenger S, Keller LP, Clemett SJ, Zolensky ME (2006) Organic globules in the Tagish Lake meteorite: remnants of the protosolar disk. *Science* 314:1439–1442
- Pizzarello S, Cooper GW, Flynn GJ (2006) The nature and distribution of the organic material in carbonaceous chondrites and interplanetary dust particles. In: Lauretta DS, McSween HY Jr (eds) *Meteorites and the early solar system II*. University of Arizona Press, Tucson, pp 625–651
- Pizzarello S, Huang Y, Alexandre MR (2008) Molecular asymmetry in extraterrestrial chemistry: insights from a pristine meteorite. *Proc Natl Acad Sci* 105:3700–3704

Carbonaceous Meteorite

- ▶ [Carbonaceous Chondrite](#)
- ▶ [Meteorite \(Murchison\)](#)
- ▶ [Meteorites](#)

Carbonate

Synonyms

Calcareous sediment; Limestone

Definition

Carbonate refers either to a mineral or to a rock. Examples of carbonate minerals are calcite (CaCO_3) and dolomite ($\text{MgCa}(\text{CO}_3)_2$), which are common constituents of limestones and other calcareous sediments; siderite (FeCO_3), which also occurs in [▶ sedimentary rocks](#); magnesite (MgCO_3), an alteration product of ultramafic rock; and malachite $\text{Cu}_2(\text{CO}_3)(\text{OH})_2$, smithsonite (ZnCO_3), and cerusite (PbCO_3), which result from superficial alteration of metallic ore deposits. The term is also applied to sediments or sedimentary rocks such as limestones or dolostones that are composed predominantly of carbonate minerals. Most Phanerozoic carbonates are composed mainly of the shells, tests, and spicules from marine organisms cemented by secondary carbonates; other rarer carbonates precipitate directly from sea- or lake water. Carbonate sediments are rare in Archean sequences. Carbonate minerals detected by Martian rovers may provide evidence of the presence of water of the surface early in the history of [▶ Mars](#).

See also

- ▶ [Mars](#)
- ▶ [Sedimentary Rock](#)

Carbonate (Extraterrestrial)

Definition

The term carbonate can either refer to carbonate [▶ minerals](#), which are dominated by the carbonate ion CO_3^{2-} , or to carbonate rocks, which are mainly composed of carbonate minerals. The crystal system of carbonate minerals can be monoclinic (e.g., azurite), orthorhombic (e.g., aragonite), or trigonal (e.g., calcite, dolomite, magnesite). So far, extraterrestrial carbonates were only found on [▶ Mars](#), that is, magnesium carbonates in the Nili Fossae region. Whereas the bulk of terrestrial [▶ carbonates](#) are biogenic in origin, carbonate minerals on Mars are expected to be an alteration product of [▶ water](#) and basaltic [▶ rocks](#) in an atmosphere containing CO_2 .

See also

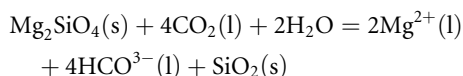
- ▶ [Mars](#)
- ▶ [Mineral](#)
- ▶ [Phyllosilicates \(Extraterrestrial\)](#)
- ▶ [Sulfates \(Extraterrestrial\)](#)



Carbonation

Definition

A *carbonation* reaction describes the breakdown of silicates by dissolved carbon dioxide. The reaction of olivine carbonation reads:



Carbonation enhances the drawdown of volcanic CO_2 by ► [weathering](#); it limits the P_{CO_2} and therefore the greenhouse effect. In addition, the alkalinity liberated in the reaction (HCO_3^{3-}) keeps the pH of the ocean high enough for the carbonate ion to be abundant and enhances the precipitation of calcium carbonates.

See also

► [Weathering](#)

Carbonization

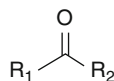
► [Pyrolysis](#)

Carbonyl

Definition

In organic chemistry, a carbonyl is a functional group consisting of a carbon atom doubly bonded to an oxygen atom (Fig. 1). Some examples of carbonyl-group-containing compounds include carboxylic acids and their derivatives (e.g., amides, esters and anhydrides), aldehydes, and ketones. The term carbonyl can also refer to carbon monoxide as a ligand in an organometallic complex (e.g., iron pentacarbonyl, $\text{Fe}(\text{CO})_5$).

Since oxygen is more electronegative than carbon, the oxygen atom in a carbonyl group pulls electron density toward itself and away from carbon making the bond polar. The carbonyl carbon thus tends to be electrophilic,



Carbonyl. Figure 1 General structure of carbonyl compounds

and more reactive with nucleophiles. The electronegative oxygen can react with an electrophile.

Protons bonded to carbon atoms alpha to a carbonyl group are considerably more acidic (by ~ 3 $\text{p}K_a$ units) than typical aliphatic C–H bonded protons. This is because a carbonyl group is in tautomeric resonance with an enol configuration. Deprotonation of this enol produces an enolate anion, which is nucleophilic and can alkylate electrophiles such as other carbonyls.

See also

► [Aldehyde](#)

Carbonyldiamide

► [Urea](#)

Carboxylic Acid

Definition

In chemistry, carboxylic acids are generally weak organic acids that contain a carboxyl functional group. The general formula of a carboxylic acid is R-COOH. Carboxylic acids are proton donors. Some common examples are ► [formic acid](#) H-COOH, and ► [acetic acid](#) CH_3COOH . There are many carboxylic acids of biological importance, for example, fatty acid esters are important components of many cell membranes, proteins are polymers of amino acids, and many compounds in intermediary metabolism are carboxylic acids. Common prebiotic syntheses of carboxylic acids proceed via the hydrolysis of precursor nitriles.

Because they are both hydrogen-bond acceptors and hydrogen-bond donors, they are able to participate in hydrogen bonding. Carboxylic acids tend to have higher boiling points than water partly because of their tendency to form hydrogen-bonded dimers. Carboxylic acids are polar: short-chain aliphatic carboxylic acids (for example, those containing 1–5 carbon atoms) are soluble in water, whereas higher carboxylic acids are less soluble due to the increasingly hydrophobic nature of their aliphatic components.

Carboxylic acids form various derivatives in combination with other functional group-containing compounds,

for example, esters in combination with alcohols, amides in combination with amines, and anhydrides in combination with another carboxylic acid.

See also

- ▶ [Acetic Acid](#)
- ▶ [Aliphatic Carboxylic Acids](#)
- ▶ [Amide](#)
- ▶ [Ester](#)
- ▶ [Formic Acid](#)
- ▶ [Nitrile](#)

Carboxylic Acids, Geological Record of

JENNIFER EIGENBRODE

NASA Goddard Space Flight Center, Greenbelt, MD, USA

Synonyms

[Fatty acids](#)

Keywords

Carbonyl, Fatty acids, Hydroxyl, Organic acid, Carboxyl, Lipids

Definition

▶ [Carboxylic acids](#) are a class of organic compounds that contain one or more carboxyl groups per molecule. Each carboxyl group, which is a combination of ▶ [carbonyl](#) and hydroxyl groups, has the formula $-C(=O)OH$ (or $-COOH$). Carboxylic acids are polar and proton donors. Carboxylic acids are widespread in nature, often combined with other functional groups, and ubiquitous in biology, recent sediments, and carbonaceous meteorites. As they degrade during diagenesis and thermal maturation in the rock record, they generally transform into esters, carboxylates (i.e., hydroxyl group replaced with salts or anions), and, eventually, alkanes.

Overview

Carboxyl groups are polar. The carbonyl group is a hydrogen-bond acceptor and the hydroxyl group is a hydrogen-bond donor. Consequently, carboxylic acids participate in hydrogen bonding, particularly with each other and with minerals such as phyllosilicates, oxyhydroxides, and other oxides. In addition, the “self-association” of carboxylic acids that results from hydrogen

bonding generates stabilized dimeric pairs in nonpolar media. The dimers have decreased volatility. The bonds must be broken chemically or thermally for the carboxyl group to be reactive to other geochemicals. The stabilization of dimers and the nonreactive nature of the alkyl side chain (or other carbon skeleton) contribute to the refractory nature of carboxylic acids during diagenesis compared to more polar organic molecules.

Carboxylic acids having more than five carbons in an alkyl chain are not soluble in water unless at high temperatures and exhibit both hydrophilic (carboxyl) and hydrophobic (alkyl) regions in the same molecule. The amphiphilic nature of these molecules leads to the formation of non-biological monolayers on the water and mineral surfaces or micelles, sphere-shaped clusters, in solution. Biology takes advantage of the amphiphilic nature of carboxylic acids to form fatty-acid lipid bilayers of cellular ▶ [membranes](#). Formation of non-biological monolayers was likely critical for the formation of the earliest cellular life.

Carboxylic acids are weak acids that only partially dissociate into H^+ cations and $RCOO^-$ anions in pH neutral aqueous solution. In the presence of a base, carboxylic acids become carboxylates. These moieties are important in geological and biogeochemical processes because they can be siderophores, chelating with metals, such as ferric iron.

The carbon atom of a carboxyl group is in a relatively high ▶ [oxidation](#) state and can be partially reduced by sulfur or other organic molecules during diagenesis under reducing conditions. ▶ [Oxidation](#) of the carboxyl carbon commonly occurs in oxidizing environments to form carbon dioxide (decarboxylation reaction). Depending on the geochemical or biological reaction, the alkyl side-chain may end up reduced to an alkane or oxidized, often with the addition of an anion or salt. In both cases, decarboxylation results in the loss of a carbon from the carbon skeleton and the product can then be preserved in the rock record.

See also

- ▶ [Acid Hydrolysis](#)
- ▶ [Carbonaceous Chondrites \(Organic Chemistry of\)](#)
- ▶ [Carbonyl](#)
- ▶ [Carboxylic Acid](#)
- ▶ [Cell Wall](#)
- ▶ [Complex Organic Molecules](#)
- ▶ [Fatty Acids, Geological Record of](#)
- ▶ [Kerogen](#)
- ▶ [Membrane](#)
- ▶ [Oxidation](#)

References and Further Reading

- Eigenbrode JL (2007) Fossil lipids for life-detection: a case study from the early earth record. *Space Sci Rev* 135:161–185
- Kraemer SM, Butler A, Borer P, Cervini-Silva J (2005) Siderophores and the dissolution of iron bearing minerals in marine systems. *Rev Mineralogy Geochem* 59:53–76
- Kraemer SM, Crowley D, Kretzschmar R (2006) Siderophores in plant iron acquisition: geochemical aspects. *Adv Agron* 91:1–46
- Sephton MA (2005) Organic matter in carbonaceous meteorites: past, present and future research. *Philos Trans R Soc A* 363:2729–2742
- Wade LG (2009) *Organic chemistry*, 7th edn. Prentice-Hall, New Jersey, pp 1320

Carboxysomes

Definition

Carboxysomes are bacterial organelles that contain enzymes involved in carbon dioxide fixation. These structures are found in cyanobacteria and many chemoautotrophic bacteria.

See also

- ▶ [Autotroph](#)
- ▶ [Autotrophy](#)
- ▶ [Chemoautotroph](#)
- ▶ [Cyanobacteria](#)
- ▶ [Genome](#)

Cassini

Definition

Giovanni Domenico Cassini (or Jean-Dominique Cassini) (1625–1712), was born in Perinaldo, near Naples, and was Professor at Bologna. In 1669, he became a member of the French Académie des Sciences, and in 1671, he became the first Director of the Observatoire de Paris, from which the Paris Meridian was defined. Its first scientific aims were metrology, celestial mechanics, and positional astrometry. Cassini made important discoveries regarding solar-system objects: determination of Mars' rotation, Jupiter's rotation, Jupiter's satellites' revolutions, identification of several of Saturn's satellites (Iapetus, Rhea, Thetys, and Dione), as well as the Cassini Division within Saturn's rings. Cassini also recorded observations of the zodiacal light. The Cassini space mission, launched in 1987 and presently exploring the ▶ [Saturn](#) system, was named after him.

See also

- ▶ [Planetary Rings](#)
- ▶ [Saturn](#)

Cassini Division

Definition

The Cassini Division is a gap between the A and B rings of ▶ [Saturn](#). It was first identified by Giovanni Domenico Cassini in 1675 and can be observed with a small telescope. It extends between 117,500 and 122,000 km from the center of Saturn. Observations by the Cassini orbiter have shown that the Cassini division is not devoid of matter, as previously thought, but it consists in a region where the density of particles is lower. The existence of the Cassini division is probably due to a gravitational interaction with ▶ [Mimas](#), as the Cassini division is in resonance with the orbit of this satellite. There are other divisions in Saturn's rings (Encke division, Keeler division).

See also

- ▶ [Mimas](#)
- ▶ [Planetary Rings](#)
- ▶ [Saturn](#)

Cassini Mission

- ▶ [Cassini–Huygens Space Mission](#)

Cassini Spacecraft

- ▶ [Cassini–Huygens Space Mission](#)

Cassini State

Definition

When an orbiting body is affected by tides, its spin axis, spin rate, and orbital plane can reach an equilibrium state in which obliquities (tilts) are nonzero. Cassini states are observed in the Earth–Moon system, Triton–Neptune, and possibly Europa–Jupiter. In these cases, the satellite's obliquity is locked at a small nonzero value, but in general, with large inclinations, the obliquity could be large.

See also

- ▶ [Tides \(Planetary\)](#)

Cassini Titan's Probe

► [Huygens \(Probe\)](#)

Cassini–Huygens Space Mission

ATHENA COUSTENIS

Laboratoire d'Etudes Spatiales et d'Instrumentation en Astrophysique (LESIA) (Bât. 18), Observatoire de Paris-Meudon, Meudon Cedex, France

Synonyms

[Cassini mission](#); [Cassini spacecraft](#)

Keywords

Cassini–Huygens, Cassini orbiter, Enceladus, Huygens probe, kronian satellites, rings, Saturn, Titan

Definition

Cassini–Huygens is a large, ► [NASA](#)–► [ESA](#)–► [ASI](#) mission, composed of the ► [Saturn](#) orbiter (► [Cassini](#)) and the ► [Titan](#) lander (► [Huygens](#)). Cassini–Huygens reached Saturn in 2004 after a 7-year trip, and has since then been investigating the Saturnian environment, carrying out the first detailed survey of the ► [planet](#), its rings, and the 62 currently known ► [satellites](#), with a focus on ► [Titan](#). The Cassini instruments have returned a great amount of data that have revolutionized our view of the Saturnian system. The orbiter will remain operational at least until 2017.

History

An ambitious and international mission to explore the Saturn system was initially proposed to the National Aeronautics and Space Administration (NASA) and the European Space Agency (ESA) in 1982 by a team of European and US scientists. After extensive discussions between ESA and NASA, the initial concepts eventually evolved by 1989 into Cassini–Huygens, a mission composed of an American orbiter and a European descent probe. This made it the first truly international planetary mission, in addition to its other breakthroughs. The Italian Space Agency (ASI) is responsible for the spacecraft's radio antenna and portions of three scientific instruments. Cassini–Huygens arrived in the saturnian system in July 2004. The Huygens probe executed its mission in January 2005. After two extensions, the Cassini orbiter continues its exploration of the saturnian system until 2017.

Overview

Trajectory and Operations

The Cassini–Huygens mission is a fruitful collaboration between ESA, NASA, and ASI which has been investigating the saturnian system since 2004, bringing spectacular new insights on the primary planet, its rings, and its natural satellites, of which Titan, the largest moon, is a special target. The mission has thus been instrumental in enhancing our understanding of the environment around Saturn.

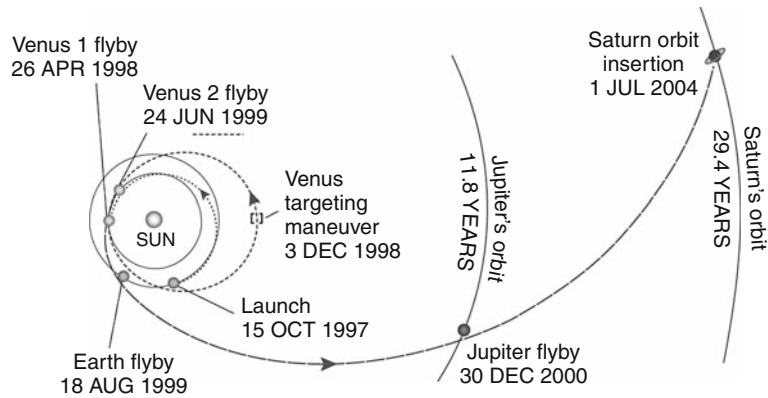
The Cassini–Huygens spacecraft consists of two main elements: the NASA Cassini orbiter, named after the Italian-French astronomer Giovanni Domenico Cassini, who gave his name to the ► [Cassini Division](#) in the rings and discovered several of Saturn's major satellites, and the ESA-provided Huygens probe, named after the Dutch astronomer, mathematician, and physicist Christiaan Huygens, who discovered Titan in 1625. The Cassini–Huygens mission was launched on October 15, 1997, on a Titan IV-Centaur rocket from Cape Canaveral and performed flybys of ► [Venus](#), ► [Earth](#), and ► [Jupiter](#) before entering into orbit around Saturn on July 1, 2004 ([Fig. 1](#)).

One particular target of Cassini–Huygens was Titan, also visited in situ by the ► [Huygens probe](#): on December 25, 2004, the Huygens probe separated from the orbiter and reached Titan on January 14, 2005, where it made an atmospheric descent to the moon's surface and relayed scientific information (Lebreton et al. 2008). Mission control activities for Cassini are conducted from the Space Flight Operations Facility at the Jet Propulsion Laboratory (► [JPL](#)), where the project is headquartered.

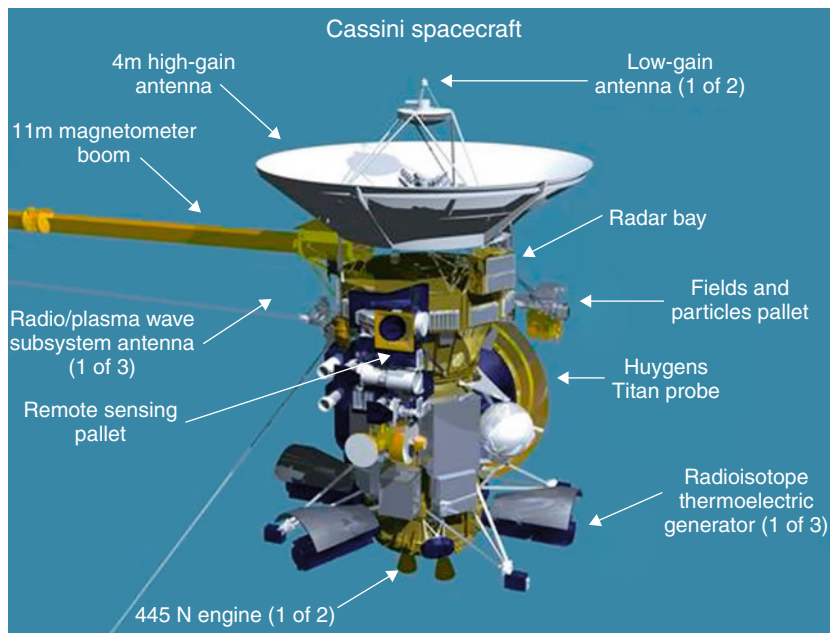
The Spacecraft and Its Payload

The spacecraft, including the orbiter and the probe, is the largest and most complex interplanetary spacecraft built to date. The orbiter has a mass of 2,150 kg (plus fuel), and the probe has a mass of 350 kg. The Cassini spacecraft is more than 6.8 m high and more than 4 m wide ([Fig. 2](#)). The complexity of the spacecraft is warranted by the ambitious program of scientific observations the spacecraft is performing. Due to its weight and complexity, the spacecraft wasn't injected into a direct trajectory to Saturn but made use of gravity-assisted maneuvers at Venus, Earth, and Jupiter. These maneuvers increased the duration of the voyage, which lasted about 7 years, but allowed to test the instruments during the different flybys and to improve their calibration.

The main body of the orbiter is nearly cylindrical and consists of a lower equipment platform, a propulsion module and an upper equipment platform, topped by a 4-m



Cassini–Huygens Space Mission. Figure 1 The trajectory of the Cassini–Huygens mission from launch to Saturn orbit insertion



Cassini–Huygens Space Mission. Figure 2 Diagram of the Cassini spacecraft carrying the Huygens probe

diameter high-gain antenna. Attached about halfway up the trunk is a remote sensing pallet, which carries cameras and other remote sensing instruments, and a fields and particles pallet, which carries instruments that study magnetic fields and charged particles. In order to point the instruments in the correct observing direction, the entire spacecraft must be turned, although three of the instruments possess their own single-axis articulation capability.

Cassini's orbiter instrumentation (Fig. 2) consists of a synthetic-aperture RADAR mapper, a charge-coupled device ► [imaging](#) system, a visible/infrared mapping

spectrometer, a composite infrared spectrometer, a cosmic dust analyzer, a radio and plasma wave experiment, a plasma spectrometer, an ultraviolet imaging spectrograph, a magnetospheric imaging instrument, a magnetometer, and an ion/neutral mass spectrometer. Telemetry from the communications antenna and other special transmitters are also used to make observations of the atmospheres of Titan and Saturn and to measure the gravity fields of the planet and its satellites. On its orbit around Saturn, Cassini finds itself between 8.2 and 10.2 astronomical units (AU) from the Earth. Because of this, it takes

between 68 and 84 min for radio signals to travel from Earth to the spacecraft, and vice versa.

More details and updates on the Cassini–Huygens mission can be found at: <http://saturn.jpl.nasa.gov/>; <http://www.esa.int/SPECIALS/Cassini-Huygens/index.html>; http://www.nasa.gov/mission_pages/cassini/main/index.html

Major Discoveries

The Cassini–Huygens mission has brought a host of new and exciting discoveries in the Saturnian system (Coustenis and Taylor 2008; Lorenz and Mitton 2008; Brown et al. 2009; Dougherty et al. 2009). They concern the distribution and composition of the rings, the nature of the satellites and their interactions with the rings, the planet’s atmospheric envelope and its ► [magnetosphere](#).

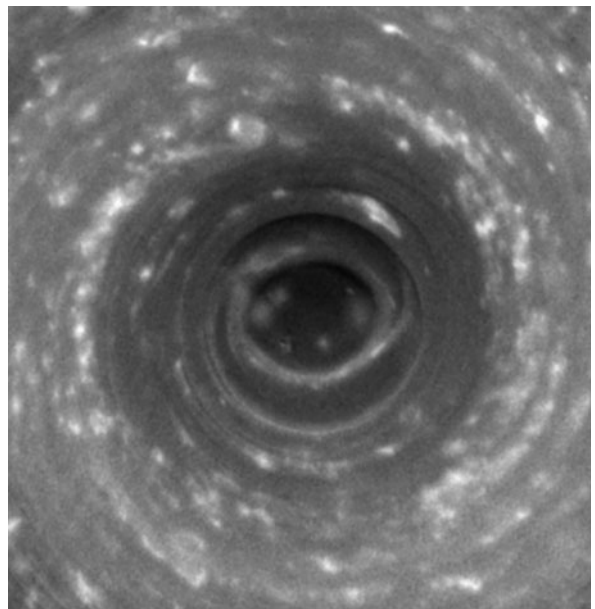
In the first few days of 2001 the Cassini spacecraft hurtled past Jupiter, temporarily joining the ► [Galileo mission](#) in orbit around the gas giant. This brief conjunction of the two probes, complemented by simultaneous observations from the Earth-orbiting ► [Hubble Space Telescope](#) and Chandra X-ray Observatory, provided an unprecedented opportunity for the intimate study of the Solar System’s largest planet. The results from this encounter greatly contributed to our enhanced understanding of Jupiter’s radio emission and aurorae and their interaction with the ► [solar wind](#). Jupiter’s magnetosphere and radiation belts and the interactions between the magnetosphere and ► [Io](#), ► [Ganymede](#) and ► [Europa](#) were explored (Fig. 3).

Given the long duration of the mission, the complexity of the payload onboard the Cassini Orbiter and the amount of data gathered on the primary planet, the satellites, and rings, it would be impossible to describe all the new discoveries made (the reader can find detailed reviews in Dougherty et al. 2009; Brown et al. 2009). We will therefore cite here only a few of the breakthroughs showing how Cassini’s data have opened up a whole new chapter in Solar System exploration and in particular have contributed to our understanding of the astrobiological aspects of many of the Saturnian bodies (Lunine and Raulin 2010).

In studying the primary planet, Cassini found lightning on Saturn whose power is said to be approximately 1,000 times that of lightning on Earth (Dougherty et al. 2009). In addition, in October 2006, the probe detected an 8,000 km diameter hurricane with an eyewall at Saturn’s South Pole (Fig. 4). Scientists believe that the storm is the strongest of its kind ever seen. This observation is particularly notable because eyewall clouds had not previously been seen on any planet other than Earth.

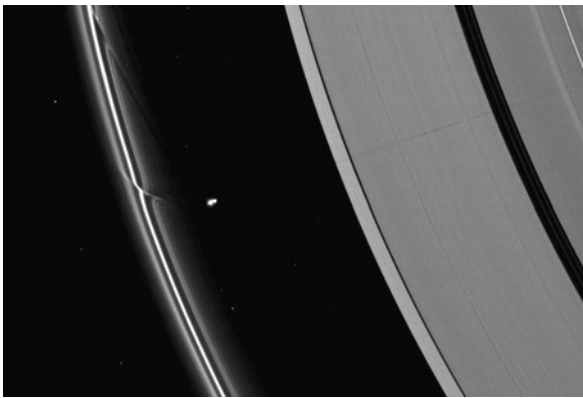


Cassini–Huygens Space Mission. Figure 3 A view of Jupiter’s satellite Io as it passes in front of the cloudtops of the planet as seen by the Cassini spacecraft on Jan. 1, 2001, 2 days after Cassini’s closest approach to Jupiter



Cassini–Huygens Space Mission. Figure 4 This Cassini image shows a large hurricane-like storm at Saturn’s south pole. The dark eye of the “hurricane” spans about 8,000 km and it is surrounded by rings of clouds that tower about 30–75 km above it. Contrary to the Earth, Saturn’s storm is fixed in place – above the South Pole – and is not powered by an ocean, since Saturn is a gaseous planet

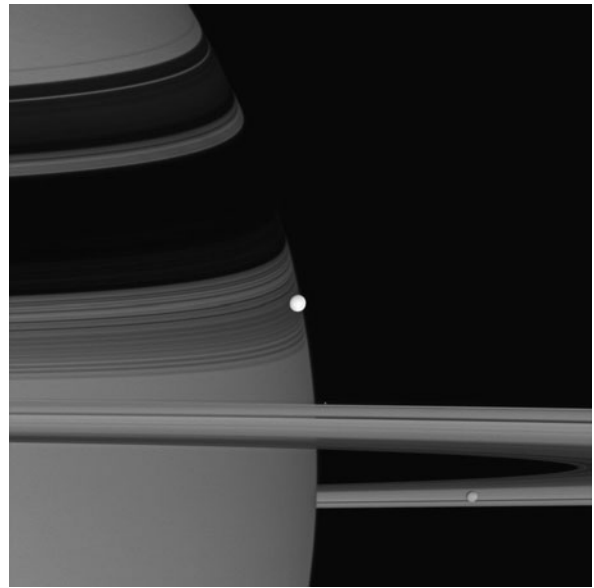
Saturn is probably best known for its system of ► **planetary rings**, which makes it the most visually remarkable object in the solar system. They extend from 6,630 to 120,700 km above Saturn’s equator, average approximately 20 m in thickness, and are composed of 93 percent ► **water ice** with a smattering of ► **tholin** impurities, and 7% ► **amorphous carbon**. The particles that make up the rings greatly vary in size. On September 20, 2006, a Cassini photograph revealed a previously undiscovered planetary ring, outside the brighter main rings of Saturn and inside the G and E rings. Apparently, the source of this ring is the result of the crashing of a meteoroid off two of the moons of Saturn (Dougherty et al. 2009). Indeed, the interactions and material exchange between the rings and the satellites are a significant breakthrough in our understanding of the saturnian system provided by the Cassini spacecraft (Fig. 5). Thus, on 6 October 2009, another discovery was announced of a tenuous outer disk of material in the plane of ► **Phoebe’s** orbit. The ring is from 128 to 207 times the radius of Saturn, and is thought to originate from micrometeoroid impacts on the satellite Phoebe, which orbits at an average distance of 215 Saturn radii. The ring material should thus share Phoebe’s retrograde orbital motion, and after migrating inward would



Cassini–Huygens Space Mission. Figure 5 Cassini captures the effects of the small moon Prometheus on two of Saturn’s rings in this image taken on July 30, 2009, at a distance of approximately 1.8 million kilometers from Saturn. A long, thin shadow cast by the moon stretches across the A ring on the right. The gravity of the small moon Prometheus periodically creates streamer-channels in the F ring, as can be seen on the left of the image. Prometheus is overexposed in this image. Bright specks in the image are background stars. This view looks toward the northern, dark side of the rings from about 28° above the ringplane

encounter ► **Iapetus’** leading face, which could help explain the dramatic two-faced nature of this satellite. While the infalling material cannot be directly responsible for the observed pattern of light and dark regions on Iapetus, it is believed to have initiated a runaway thermal self-segregation process in which ice sublimates from warmer regions and condenses onto cooler regions. This leaves contrasting areas of dark ice-depleted residue and bright ice deposits.

From 2004 to November 2, 2009, the probe has discovered and confirmed eight new satellites, bringing the number up to 62. In the satellite system the Cassini orbiter has produced a large range of new results, demonstrating that these small bodies are far from being icy, dead worlds, but rather active bodies with resurfacing and cryovolcanic features. The moons of Saturn are a diverse collection (Fig. 6). Cassini has explored their icy landscapes in



Cassini–Huygens Space Mission. Figure 6 On June 28, 2007, the Cassini cameras captured this trio of icy moons against Saturn’s atmosphere and rings (Dougherty et al. 2009). Enceladus is located on the planet’s shadow-draped limb at the center; Pandora is a bright speck hovering near the rings; and Mimas is seen at lower right. The view was obtained at a distance of approximately 291,000 km from Enceladus, looking toward the sunlit side of the rings from about a degree below the ringplane. Scale in the image ranges from 17 km per pixel on Enceladus to 32 km per pixel on Saturn in the background

unprecedented detail, solving long-standing mysteries and sharing many new surprises: ▶ **Iapetus** has an enormous ridge along its equator, in addition to its two sides of remarkably different brightness. ▶ **Rhea** may have its own faint rings. And sponge-looking Hyperion is so porous that impacts tend to just punch into the surface, and its gravity is so low that what material does get ejected tends to leave the moon altogether.

In addition to the surface investigations, Cassini also discovered the presence of organics (hydrocarbons mainly) on several of Saturn's satellites seen through their signatures in several of the instruments' data, not only on Titan and ▶ **Enceladus**, but also on Iapetus and Phoebe and ▶ **Dione**, with Cassini VIMS showing that the dark material in the Saturn system could be organics (Dougherty et al. 2009).

A big surprise came from February 2010 observations of ▶ **Mimas** showing large temperature differences across the surface with no surface brightness features to explain it. The differences are believed to be due to Mimas' thermal inertia being considerably higher in the colder regions than the hotter. In such a case, heat could soak into the Mimas interior more easily, rather than raise the temperature of the surface. This supposes that the thermal conductivity of the satellite has to be at least ten times greater in the cold regions with respect to the warmer regions, while there are no apparent differences in the visible-wavelength observations. The fact that the giant crater, Herschel, is within this cold region may be just a coincidence.

More surprises came from the combined investigations of the orbiter and of the Huygens probe in the case of Titan (Coustenis and Taylor 2008; Lorenz and Mitton 2008), but also from very close Cassini flybys of Enceladus (Brown et al. 2009). In some ways, the moons Titan and Enceladus have turned out to be the stars of the ▶ **Cassini mission**, making the saturnian system's exploration very relevant to the search for ▶ **life** in the Solar System. Titan, with its thick atmosphere, clouds, dunes, and rivers and lakes of liquid ▶ **methane**-ethane on its surface (Stofan et al. 2007; Brown et al. 2008), is a rich laboratory for chemistry and processes that may resemble early Earth in a deep freeze, but with a different solvent (Coustenis and Taylor 2008). And with its towering south polar plume of icy particles, Enceladus has geological activity, simple organic compounds, and possibly liquid water beneath its frozen surface, making it incredibly important to the study of potentially habitable environments for life. Both of these moons are tempting targets for future exploration. Hereafter, we detail the Cassini–Huygens major results on these two bodies with high relevance to Astrobiology, the ▶ **origin of life**, and habitability.

Titan

The Cassini orbiter and the Huygens descent probe were designed to be part of a common strategy to uncover the mysteries shrouding the enigmatic satellite of Saturn, ▶ **Titan**. Titan is an organic paradise that is certain to tell us much about the chemical evolution that may lead to life. Water ice and ▶ **carbon dioxide** ice have been reported to exist currently on the surface. Transient episodes of melting of the water ice by either geologic activity or impacts would expose organics to aqueous alteration, as well as contact with carbon dioxide, leading potentially to reaction pathways that mimic those that occurred on the prebiotic Earth. No other place in the solar system has this type of ongoing chemistry. The Cassini–Huygens era of investigation has furthered our understanding of Titan as the largest ▶ **abiotic** organic factory in the Solar System.

Some essential breakthroughs related to Astrobiology within the realm of Saturn are summarized hereafter.

Titan's Atmosphere

Measurements throughout the Titan atmosphere, both remotely and in situ, have indicated the presence of numerous hydrocarbon and ▶ **nitrile** gases, as well as a complex layering of organic ▶ **aerosols** that persists all the way down to the surface of the moon. Thus, the organic chemistry detected in the higher atmosphere by the Ion and Neutral Mass Spectrometer (INMS) provided feedback and useful information for all studies and models of the satellite's chemical composition, complemented by measurements in the ▶ **stratosphere** made by the Composite Infrared Spectrometer (CIRS, Coustenis et al. 2010) and by the chemistry inferences from the Gas Chromatograph-Mass Spectrometer (GC-MS, Niemann et al. 2005), as well as density and temperature data retrieved by the Huygens Atmospheric Structure Instrument (HASI, Fulchignoni et al. 2005) during the descent to the surface near Titan's equator. The highly complex organic species in the ionosphere found by INMS are the precursors of the hydrocarbons and nitriles found in the stratosphere (Waite et al. 2007), which form aggregates and eventually condense out on the surface (Niemann et al. 2005). Some of these chemical components are molecules of prebiotic interest (like hydrogen cyanide, HCN, Raulin et al. 2008). Thus, it appears that Titan is a chemical factory in which the formation of complex positive and negative ions is initiated in the high thermosphere as a consequence of magnetospheric–ionospheric–atmospheric interactions involving solar ▶ **EUV**, ▶ **UV** radiation, and energetic ions and electrons.

With the current picture of Titan's organic chemistry, the chemical evolution of the main atmospheric

constituents – ► **dinitrogen** (N_2) and methane – thus produces complex refractory organics through ► **photolysis** and ► **photochemistry**. The products accumulate on the surface, together with condensed volatile organic compounds such as ► **HCN** and benzene. The abundance of methane and its organic products in the atmosphere, seas, and dunes exceeds by more than an order of magnitude the carbon inventory in the Earth’s ocean, biosphere, and fossil fuel reservoirs. Indeed, the measured value of the irreversible conversion of the methane in the atmosphere into higher-order organic/nitrile compounds that eventually end up deposited on the surface of Titan is near that of our terrestrial reference, indicating that methane is re-supplied and converted at a rate that prevents the buildup of the heavier ► **isotopologue** over time as is the case of ► **nitrogen**.

The Cassini cameras and spectrometers, as well as the Huygens instruments, showed the presence of clouds and storms in Titan’s atmosphere and described the distribution of the aerosols (haze) throughout the atmosphere (Fig. 7).

Cassini–Huygens has also provided important information on the origin and evolution of Titan’s atmosphere by measuring the ► **noble gas** concentrations (like argon for the first time) and their isotopic ► **abundances**, as well as the nitrogen and carbon stable isotopic ratios. These measurements also provide important clues about the overall role of escape, chemical conversion, outgassing, and recycling in the evolution of Titan’s atmosphere.

Titan’s Surface

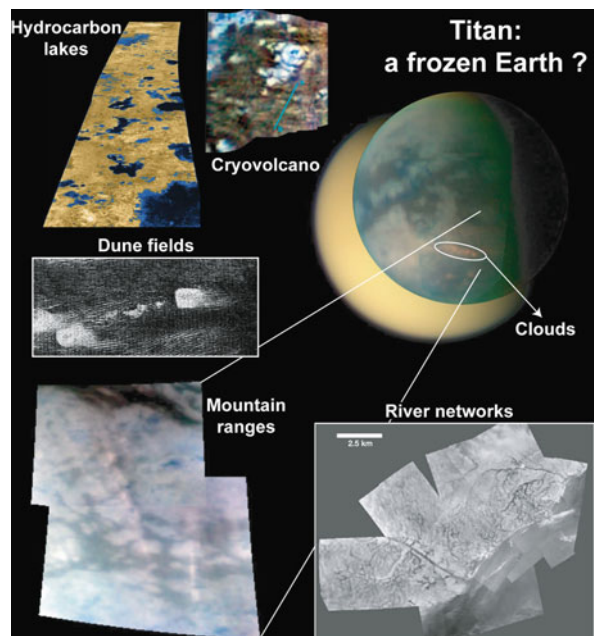
Only with Cassini–Huygens did it become possible to acquire a clear picture of Titan’s complex and exciting



Cassini–Huygens Space Mission. Figure 7 Artwork showing the Cassini orbiter observing the Huygens probe landing site with VIMS and UVIS in 2008

terrain. One of the most efficient applications of the synergy between the orbiter and the probe is the mapping of Titan’s surface. While the Cassini orbiter provided detailed views of Titan’s surface with its camera, mapping spectrometer, and radar, the Huygens probe, descending through the atmosphere on January 14, 2005, returned extraordinarily detailed images with resolutions ranging from 10 m at 10 km down to centimeters at the surface (Fig. 8). The Huygens Atmospheric Structure Instrument (HASI) gave the conditions of pressure and temperature on Titan’s surface to be 1.5 bar and 93.7 K.

Similarly to the atmosphere, for the surface discoveries the context is provided by the Cassini radar (RADAR), Visual and Infrared Mapping Spectrometer (VIMS) and Imaging Science Subsystem (ISS) data (Porco et al. 2005), while the ground truth was obtained by several of the Huygens instruments at the probe’s ► **landing site**, like the images and spectra of Descent Imager/Spectral Radiometer (DISR, Tomasko et al. 2005) or the composition measurements of the ► **GC-MS** (Niemann et al. 2005). Radar observations suggest that the ultimate fate of this aerosol precipitation is the generation of expansive



Cassini–Huygens Space Mission. Figure 8 Some of the major discoveries that the Cassini–Huygens mission made on Titan: transient atmospheric phenomena (clouds) and several geomorphological features (dunes, cryovolcanoes, channels, mountains and lakes) are shown in this composite. Credit: G. Tobie

organic-laden dunes (Lorenz et al. 2006; Radebaugh et al. 2008) that were observed around Titan’s equator for the first time by Cassini (Fig. 8). These dunes are remarkable in being exactly the same size and shape as linear (longitudinal) dunes on Earth such as those found in the Namibian and Saharan deserts. This type of dune forms in a fluctuating wind regime, which on Titan may be provided by the tides in the atmosphere due to Saturn’s gravitation acting over Titan’s eccentric orbit.

Radar-bright channels (probably cobbled streambeds like that at the Huygens landing site) have been observed at low and mid-latitudes, while channels incised to depths of several hundred meters are seen elsewhere, and at high latitudes radar-dark, meandering channels are seen that suggest a lower-energy environment where deposition of fine-grained sediment occurs (Soderblom et al. 2007a; Lorenz et al. 2008a). Fluvial modification of the surface was very evident at the Huygens landing site (Tomasko et al. 2005). Radar and near-infrared imagery has revealed channels on much larger scales than those seen by Huygens (Soderblom et al. 2007b; Lorenz et al. 2008a).

Furthermore, in July 2006, Cassini found the first proof of hydrocarbon lakes near Titan’s north pole (Stofan et al. 2007), which was confirmed in January 2007 (Mitri et al. 2007; Hayes et al. 2008). In March 2007, additional images near Titan’s north pole discovered hydrocarbon “seas.” These very dark features at the high northern latitudes of Titan were finally shown to be liquid-filled (most probably with ethane rich mixtures, Brown et al. 2008; Raulin 2008) basins – “lakes.” The features range in size from less than 10 km² to at least 100,000 km². They are confined to the region poleward of 55°N. To date some 655 such features have been identified and mapped (Fig. 8). Other small lakes exist more to the South, like the Ontario Lacus.

Thus, the diversity of the terrains on Titan depicted by the Cassini–Huygens instruments includes a host of geologic features (Fig. 8):

- Erosional features such as channels and dendritic networks, possible lakes and seas, fluvial erosional deltas and other erosional and depositional constructs such as dunes (Radebaugh et al. 2008), possible glacial-flow constructs, etc
- Impacts: the very low ► crater frequency is indicative of active geological surface processes
- Volcano-tectonic features: domes, possible cryovolcanic flows, and bright spots (Sotin et al. 2005, Nelson et al. 2007) as well as mountain chains (Radebaugh et al. 2007), many of these features may be active regions on Titan’s surface

The features Cassini–Huygens discovered on Titan’s surface were more complex than any expected, with landforms that seem to resemble the landscapes on Earth, including hills, dunes, a deflated lakebed, but all composed of completely different constituents, many of which could be ices and organic material. The ambient conditions and direct measurement of methane evaporating from under the landed probe imply that the working erosive agent is liquid methane, not liquid water.

The surface of Titan, as revealed by the Cassini orbiter and the Huygens probe, offers us an opportunity to stretch our current models in an effort to explain the presence of dunes, rivers, lakes, ► cryovolcanoes, and mountains in a world where the rocks are composed of water ice rather than silicates and the liquid is methane or ethane rather than liquid water.

Titan’s tectonism involves a number of very-large-scale linear features seen optically, notably the dark dune-filled basins. Some linear mountain ranges have been detected, several forming a chevron pattern near the equator, with a large bright terrain (Xanadu) extending over 3,400 km in diameter. RADAR/SAR (Synthetic-aperture radar (SAR)) imagery shows Xanadu to be extremely rugged.

As said before, the N₂–CH₄ byproducts in Titan’s atmosphere eventually end up as sediments on the surface, where they accumulate presently at a rate of roughly 0.5 km in 4.5 Gyr. Since no large source was detected by Cassini to re-supply methane, cryovolcanic outgassing has been hypothesized, yet over what timescales and through which internal processes is unknown. Cassini–Huygens also found that the balance of geologic processes – impacts, tectonics, fluvial, aeolian – is somewhat similar to the Earth’s, more so than for Venus or Mars. Titan may well be the best analogue to an active terrestrial planet in the sense of our home planet, albeit with different working materials (Coustenis and Taylor 2008).

In addition, the detection of Argon 40, and observations of what appear to be flows from cryovolcanoes, suggests that the interior of Titan is geologically active; theoretical calculations suggest a heat flow at present of about 8% that of the Earth, sufficient to mobilize water as liquid in the interior as the working fluid for ► cryovolcanism. Cryovolcanism is a process of particular interest at Titan because of the known astrobiological potential of liquid water erupting onto photochemically produced organic molecules. Several likely cryovolcanic structures have been identified in Cassini near-infrared and radar images (Fig. 8). Although definitive evidence for active volcanism has not yet been produced, there are apparent surface changes in Cassini data that require explanation.

Titan’s overall density (1.88 g/cm^3) requires it to have roughly equal proportions of rock and ice. After its accretion, Titan was probably warm enough to allow differentiation into a rocky core with a water/ice envelope, but whether an iron or iron–sulfur core formed during the subsequent evolution remains uncertain. Thermal evolution models suggest that Titan may have an icy crust between 50 and 150 km thick, lying atop a liquid-water ocean a couple of hundred kilometers deep, with some amount (a few to 30%, most likely $\sim 10\%$) of ammonia dissolved in it, acting as an anti-freeze. Beneath lies a layer of high-pressure ice. Cassini’s measurement of a small but significant non-synchronous contribution to Titan’s rotation is most straightforwardly interpreted as a result of decoupling of the crust from the deeper interior by a liquid layer (Lorenz et al. 2008b). Could such a water-liquid environment be a host to life?

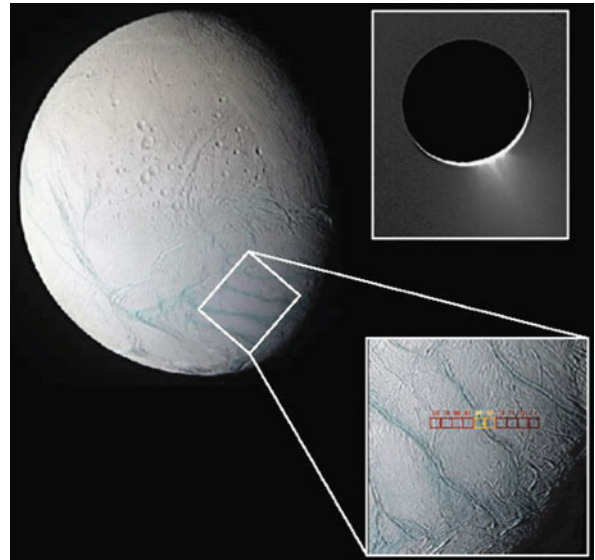
With impact craters, dark plains with some brighter flows, mysterious linear black features possibly related to winds, sand dunes, snow dunes and a host of possible agents: solids, liquids, ices, precipitation, evaporation, flow, winds, volcanism, etc. to be included, Titan has proven to be a much more complex world than originally thought and much more difficult to interpret. Future long-term exploration would bring new insights.

Enceladus

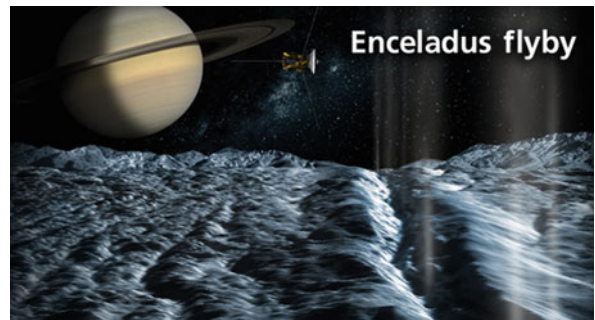
When Cassini had its first encounter with [▶ Enceladus](#) on Feb. 17, 2005, the magnetometer instrument saw a bending of Saturn’s magnetic field, with the plasma being slowed and deflected as it passed Enceladus. Data collected during the March 9, 2005 flyby provided further evidence of the existence of an atmosphere around the southern pole of Enceladus. The cosmic dust analyzer recorded thousands of hits from tiny particles of dust or ice, possibly coming from a cloud around the moon or from the adjacent E ring. The Cassini spacecraft provided definitive proof that Enceladus is currently geologically active when multiple Cassini instruments detected plumes of gas and ice particles emanating from a series of warm fractures centered on the south pole, dubbed the “tiger stripes” (Fig. 9).

On March 10, 2006, Cassini images strongly suggested the presence of liquid-water reservoirs that erupt in geysers on Saturn’s moon Enceladus. Images had also shown particles of water in its liquid state emitted by icy jets and towering plumes. Several flybys of Enceladus followed bringing more data and revealing an extremely intriguing world (Fig. 10).

In March 2008, Cassini swept by Enceladus’ South pole at an altitude of 52 km and plunged into a south polar plume, scooping up particles and gases to sample



Cassini–Huygens Space Mission. Figure 9 Cassini’s major breakthroughs in our understanding of the Enceladus environment are connected to the southern polar region, where the magnetometer and the cameras detected plumes of gas and ice particles emanating from a series of warm fractures, dubbed the “tiger stripes”



Cassini–Huygens Space Mission. Figure 10 One of the Cassini flybys of Enceladus when the spacecraft flew at quite low altitudes into the satellite’s plumes

their composition. The gases that were tasted by Cassini’s INMS bore a strong resemblance to the gases that issue from comets. All of the “fields and particles” Cassini instruments (the ones that measure the abundance, compositions, and motions of plasma, ions, atoms, molecules, particles, and magnetic fields in situ, wherever Cassini travels) have been sampling the plumes.



Enceladus is thus the second cryovolcanically active icy satellite that has been identified (Triton is the only other known active icy satellite, but the process driving its cryovolcanism may not be linked to an internal heat source) and can be used to study active processes that are thought to have once played an important role in shaping the surfaces of other icy satellites. These processes include tidal heating, cryovolcanism, and ice tectonism, which all can be studied as they currently happen on Enceladus. Moreover, the plume source region on Enceladus samples a warm, chemically rich, environment that may facilitate complex organic chemistry and biological processes. CIRS on Cassini has demonstrated that the Enceladus south pole was the warmest portion of this moon, shockingly much warmer than the equator.

Enceladus is arguably a place in the solar system where exploration is most likely to find a demonstrably habitable environment, and several researches point to the possibility that Enceladus' plumes, tectonic processes, and possible liquid-water ocean may create a complete and sustainable geochemical cycle that may allow it to support life. While other moons in the solar system have liquid-water oceans covered by kilometers of icy crust, in the case of Enceladus, the pockets of liquid water may be no more than tens of meters below the surface. Cassini has thus discovered a new potential ► [habitat](#) in our Solar System, well outside the traditional ► [habitable zone](#).

Future Directions

The primary mission for *Cassini* ended on July 30, 2008. However, given the excellent condition of the orbiter, the mission was extended to 2010. On February 3, 2010, NASA announced another extension for Cassini, this one for 6-1/2 years until 2017. The extension enables another 155 revolutions around the planet, 54 flybys of Titan, and 11 flybys of Enceladus.

However, even after these extensions, several questions and scientific themes remain that cannot be addressed by Cassini in its current configuration or with its present instrumentation. The two major themes in Titan exploration – the methane cycle as an analogue to the terrestrial hydrological cycle (Atreya et al. 2006) and the chemical transformations of ► [complex organic molecules](#) in the atmosphere and the surface – render Titan a very high priority if we are to understand how volatile-rich worlds evolve and how organic chemistry and planetary evolution interact on large spatial and temporal scales. Both are of keen interest to planetology and astrobiology.

To answer the several remaining vital questions that Cassini has raised for Titan and for Enceladus, a new mission (the Titan Saturn System Mission, TSSM) was proposed and studied in 2008 by both ESA and NASA. This new mission would bring the required long-term exploring capabilities combining an orbiter and two in situ elements (a montgolfière balloon and a lander) with state-of-the-art technology and instruments (see www.lesia.cosmicvision/tssm/tssm-public). Other, simpler but also exciting, mission concepts are also being studied for a return to the Saturnian system within the next two or three decades.

See also

- [Abiotic](#)
- [Abundances of Elements](#)
- [Aerosols](#)
- [ASI](#)
- [Atmosphere, Structure](#)
- [Cassini](#)
- [Cassini Division](#)
- [Clouds](#)
- [Complex Organic Molecules](#)
- [Cryovolcanism](#)
- [Dinitrogen](#)
- [Enceladus](#)
- [ESA](#)
- [Galileo](#)
- [Gas Chromatography](#)
- [Giant Planets](#)
- [GC/MS](#)
- [Habitable Zone](#)
- [Habitat](#)
- [Hubble Space Telescope](#)
- [Huygens](#)
- [Huygens \(Probe\)](#)
- [Hydrogen Cyanide](#)
- [Iapetus](#)
- [Imaging](#)
- [Infrared Spectroscopy](#)
- [Isotopic Ratio](#)
- [JPL](#)
- [Landing Site](#)
- [Life](#)
- [Magnetosphere](#)
- [Mass Spectrometry](#)
- [Methane](#)
- [Mimas](#)
- [Molecular Abundances](#)
- [NASA](#)
- [Nitrile](#)

- ▶ Nitrogen
- ▶ Noble Gases
- ▶ Organic Material Inventory
- ▶ Organic Molecule
- ▶ Origin of Life
- ▶ Photochemistry (Atmospheric)
- ▶ Photolysis
- ▶ Planetary Rings
- ▶ Prebiotic Chemistry
- ▶ Refractory Molecules
- ▶ Rhea
- ▶ Satellite or Moon
- ▶ Saturn
- ▶ Spectroscopy
- ▶ Stratosphere
- ▶ Terrestrial Analog
- ▶ Tholins
- ▶ Titan
- ▶ Visible
- ▶ Volatile
- ▶ Water

References and Further Reading

- Atreya SK, Adams EY, Niemann HB, Demick-Montelara JE, Owen TC, Fulchignoni M, Ferri F, Wilson EH (2006) Titan's methane cycle. *Planet Space Sci* 54:1177–1187
- Brown RH, Soderblom LA, Soderblom JM, Clark RN, Jaumann R, Barnes JW, Sotin C, Buratti B, Baines KH, Nicholson PD (2008) The identification of liquid ethane in Titan's Ontario Lacus. *Nature* 454:607–610
- Brown RH, Lebreton J-P, Waite H (eds) (2009) *Titan from Cassini-Huygens*. Springer, New York, p 535. ISBN 10:1402092148
- Coustenis A, Taylor F (2008) *Titan: Exploring an earth-like world*. World Scientific Publishing, Singapore
- Coustenis A et al (2010) Titan trace gaseous composition from CIRS at the end of the Cassini-Huygens prime mission. *Icarus* 207:461–476
- Dougherty M, Esposito L, Krimigis T (eds) (2009) *Saturn from Cassini-Huygens*. Springer, New York, p 805. ISBN 10: 1402092164
- Fulchignoni M et al (2005) In situ measurements of the physical characteristics of Titan's environment. *Nature* 438(7069):785–791
- Hayes A, Aharonson O, Callahan P, Elachi C, Gim Y, Kirk R, Lewis K, Lopes R, Lorenz R, Lunine J, Mitchell K, Mitri G, Stofan E, Wall S (2008) Hydrocarbon lakes on Titan: distribution and interaction with a porous regolith. *Geophys Res Lett* 35:L09204
- Lebreton J-P, Coustenis A, Lunine J, Raulin F, Owen T, Strobel D (2008) Results from the Huygens probe on Titan. *Astron Astrophys Rev* 17:149–179
- Lorenz RD, Mitton J (2008) *Titan unveiled*. Cambridge University Press, Cambridge
- Lorenz RD et al (2006) The sand seas of Titan: Cassini RADAR observations of longitudinal dunes. *Science* 312:724–727
- Lorenz RD et al (2008a) Fluvial channels on Titan: initial Cassini RADAR observations. *Planet Space Sci* 56:1132–1144
- Lorenz RD et al (2008b) Titan's rotation reveals an internal ocean and changing zonal winds. *Science* 319:1649–1651
- Lunine J, Raulin F (2010) Titan and the Cassini-Huygens mission. In: Gargaud M, Lopez-Garcia P, Martin H (eds) *Origin and evolution of life: an astrobiology perspective*, Chap 29. Cambridge University Press, (in press)
- Mitri G, Showman AP, Lunine JI, Lorenz RD (2007) Hydrocarbon lakes on Titan. *Icarus* 186:385–394
- Nelson RM, Brown RH, Radebaugh J, Lorenz RD, Kirk RL, Lunine JI, Stofan ER, Lopes RMC, Wall SD, The Cassini Radar Team (2007) Mountains on Titan observed by Cassini radar. *Icarus* 192:77–91
- Niemann H et al (2005) The abundances of constituents of Titan's atmosphere from the GCMS instrument on the Huygens probe. *Nature* 438:779–784
- Porco C et al (2005) Imaging of Titan from the Cassini spacecraft. *Nature* 434:159–168
- Radebaugh J, Lorenz RD, Kirk RL, Lunine JI, Stofan ER, Lopes RMC, Wall SD, The Cassini Radar Team (2007) Mountains on Titan observed by Cassini Radar. *Icarus* 192(1):77–91
- Radebaugh J, Lorenz RD, Lunine JI, Wall SD, Boubin G, Reffet E, Kirk RL, Lopes RM, Stofan ER et al (2008) Dunes on Titan observed by Cassini radar. *Icarus* 194:690–703
- Raulin F (2008) Planetary science: organic lakes on Titan. *Nature* 454:587–589
- Raulin F, Gazeau M-C, Lebreton JP (2008) Latest news from Titan. *Planet Space Sci* 56(5):571–572
- Soderblom LA, Tomasko MG, Archinal BA, Becker TL et al (2007a) Topography and geomorphology of the Huygens landing site on Titan. *Planet Space Sci* 55:2015–2024
- Soderblom LA, Kirk RL, Lunine JI et al (2007b) Correlations between Cassini VIMS spectra and RADAR SAR images: implications for Titan's surface composition and the character of the Huygens probe landing site. *Planet Space Sci* 55:2025–2036
- Sotin C et al (2005) Release of volatiles from a possible cryovolcano from near-infrared imaging of Titan. *Nature* 435:786–789
- Stofan ER, Elachi C, Lunine JI et al (2007) The lakes of Titan. *Nature* 445:61–64
- Tomasko MG et al (2005) Results from the descent imager/spectral radiometer (DISR) instrument on the Huygens probe of Titan. *Nature* 438:765–778
- Waite H et al (2007) The process of tholin formation in Titan's upper atmosphere. *Science* 316:870–875

C-Asteroid

Definition

▶ **Asteroid** taxonomic systems are based on spectral features observed in reflected sunlight, with letters of the alphabet used to denote different taxonomic types. A C-type asteroid is one with a relatively flat and featureless reflection spectrum in visible light, similar to that of ▶ **carbonaceous chondrite** ▶ **meteorites** and with a low ▶ **albedo** (typically 0.03–0.1), characteristics indicative of a carbonaceous (carbon-rich) mineralogy. C-type asteroids are common in the outer ▶ **main belt** but are also present in the near-Earth asteroid population. Many C-type asteroids have weak absorption features in the

near-infrared region of the spectrum, apparently due to the presence of water-bearing ► [minerals](#).

See also

- [Albedo](#)
- [Asteroid](#)
- [Asteroid Belt, Main](#)
- [Carbonaceous Chondrite](#)
- [Meteorites](#)
- [Mineral](#)
- [Near-Earth Objects](#)

Catabolism

Definition

Catabolism is the subset of metabolic networks by which organic compounds are degraded to simpler organic or inorganic compounds. Catabolism includes oxidation reactions – coupled to the reduction of coenzymes such as NAD^+ or FAD – and sometimes substrate-level phosphorylation steps leading to ATP synthesis.

See also

- [Anabolism](#)
- [Metabolism \(Biological\)](#)

Cataclysmic Pole Shift Hypothesis

- [True Polar Wander, Theory of](#)

Catalyse

- [Catalyst](#)

Catalyst

HENDERSON JAMES (JIM) CLEAVES II
Geophysical Laboratory, Carnegie Institution of
Washington, Washington, DC, USA

Synonyms

Catalyse

Definition

In chemistry, catalysts are compounds that change the rate of a reaction but are not consumed in the reaction, as a reagent would be. Catalysts may speed up or slow down reaction rates and may participate in reactions multiple times. In a general sense, anything that increases the rate of a process is a “catalyst,” a term that is derived from the Greek *καταλύειν*, meaning to dissolve or loosen. Catalysts may be metals, mineral surfaces, ► [enzymes](#), ► [ribozymes](#), or small organic molecules, among other possibilities.

Overview

Catalysts operate by changing the rate-limiting free energy change to the transition state relative to that of the corresponding uncatalyzed reaction, resulting in a larger or smaller reaction rate at a given temperature. The physical mechanism of catalysis can be complex. Catalysts may affect the reaction environment, or bind to the reagents to polarize bonds forming intermediates that do not occur in the cognate uncatalyzed reactions. Catalysts have no effect on the chemical equilibrium of a reaction because the rates of both the forward and reverse reactions are affected.

In catalyzed reactions, as in uncatalyzed reactions, the overall reaction rate depends on the frequency of collision of the reactants in the rate-limiting step. The catalyst usually acts in this limiting step, and rate changes are proportional to the amount of catalyst present. As catalysts are not consumed in a reaction, only small amounts may be needed to increase the rate of the reaction significantly. In reality, however, catalysts are sometimes inhibited, deactivated, or destroyed via secondary processes. Substances that reduce the activity of catalysts are called inhibitors if the reduction is reversible, and poisons if the reduction is irreversible.

Catalysts can be heterogeneous or homogeneous, depending on whether they exist in the same phase as the substrate. Heterogeneous catalysts act in a different phase than the reactants, for example, solids that act on liquid or gaseous substrates. Homogeneous catalysts function in the same phase as the reactants, for example, cytosolic enzymes are examples of homogeneous catalysts.

See also

- [Clay](#)
- [Enzyme](#)
- [Protein](#)
- [Ribozyme](#)



Catena, Catenae

Synonyms

Crater chain

Definition

A catena is a linear, slightly curved, or sinuous chain of circular to elliptical depressions. The depressions can be surrounded by raised rims and are contiguous or separate. A crater chain may originate from volcanic or impact processes. Depressions in volcanic catenae are generally rimless. Raised rims and a more-or-less uniform size distribution of the depressions are characteristic of impact ► [Crater chains](#). Impact catenae are created (a) either by fragments of a projectile that disintegrated prior to impact, or (b) by material ejected when a crater is formed, forming chains of secondary craters.

See also

- [Crater, Impact](#)
- [Fumarole](#)
- [Olympus Mons](#)
- [Patera, Paterae](#)

Cavitation Zone

- [Spallation Zone](#)

Cavus, Cavi

Definition

It is a hollow, irregular steep-sided depression usually in arrays or clusters (definition by the International Astronomical Union; <http://planetarynames.wr.usgs.gov/jsp/append5.jsp>). It is used as a descriptor term for naming surface features on ► [Mars](#).

See also

- [Mars](#)

CC

- [Carbonaceous Chondrite](#)

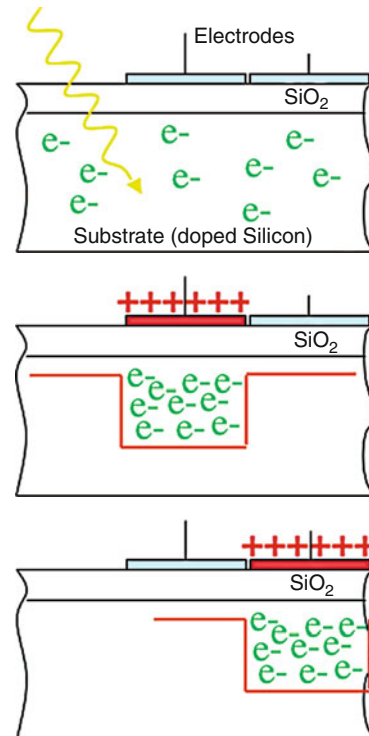
CCD

Synonyms

Charge coupled device

Definition

CCD is the abbreviation for Charge Coupled Device. A CCD is a photo-electronic imaging device commonly used for astronomical observations in the visible domain. A CCD is a solid-state Silicon-based detector where each of the numerous pixels (up to 10 million) stores in a potential well the electrons produced by photons (one to one). At the end of the exposure, charges are transferred from one pixel to the next, up to the output amplifier, by manipulation of voltages applied to surface electrodes see ([Fig. 1](#)). Back-illuminated (or thinned) CCDs feature



CCD. **Figure 1** The principle of charge transfer from one pixel to the next one in a CCD. *Top:* photons penetrate the substrate and create electrons; *Middle:* the electrons are attracted and stored below an electrode polarized with a positive voltage and isolated from the substrate thanks to a thin layer of silicon oxide; *Bottom:* a voltage is applied to the next electrode and reset on the first one so that electrons travel one step. The procedure is repeated until all pixels are read at the end of the chain

an excellent quantum efficiency for wavelengths up to $\lambda = 1 \mu\text{m}$. Because of their better efficiency and the convenience of obtaining directly a digital image at the output, CCDs definitely replaced the photographic plates in the 1980s, especially when it has been possible to tile side by side several CCDs (up to several tens) and produce cameras with a wide sensitive surface.

See also

► [Imaging](#)

CD

► [Circular Dichroism](#)

Celestial Equator

Definition

The celestial equator is the projection of the Earth's equator on the sky, represented as a great circle on the imaginary celestial sphere. As a result of the Earth's axial tilt, the celestial equator is inclined by $\sim 23.5^\circ$ with respect to the ecliptic plane. The celestial equator is the origin of declination, one of the two coordinates used to locate an object in the sky.

See also

► [Coordinate, Systems](#)
 ► [Declination](#)
 ► [Ecliptic](#)

Cell

ANGELES AGUILERA

Laboratorio de Extremófilos, Centro de Astrobiología (INTA-CSIC), Torrejón de Ardoz, Madrid, Spain

Keywords

Cell structure, endosymbiotic theory, microscopy, organelles

Definition

The cell is the smallest unit of living matter capable of performing all the activities necessary for life (Alberts et al.

1994). In fact is the smallest structure with a complete metabolism because it has all the physical and chemical components needed for its own maintenance and growth. All living organisms are made of cells. The simplest forms of life are individual cells that propagate by division, while more complex organisms are multicellular, that is, their bodies are cooperatives of many kinds of specialized cells that could not survive for long time by themselves.

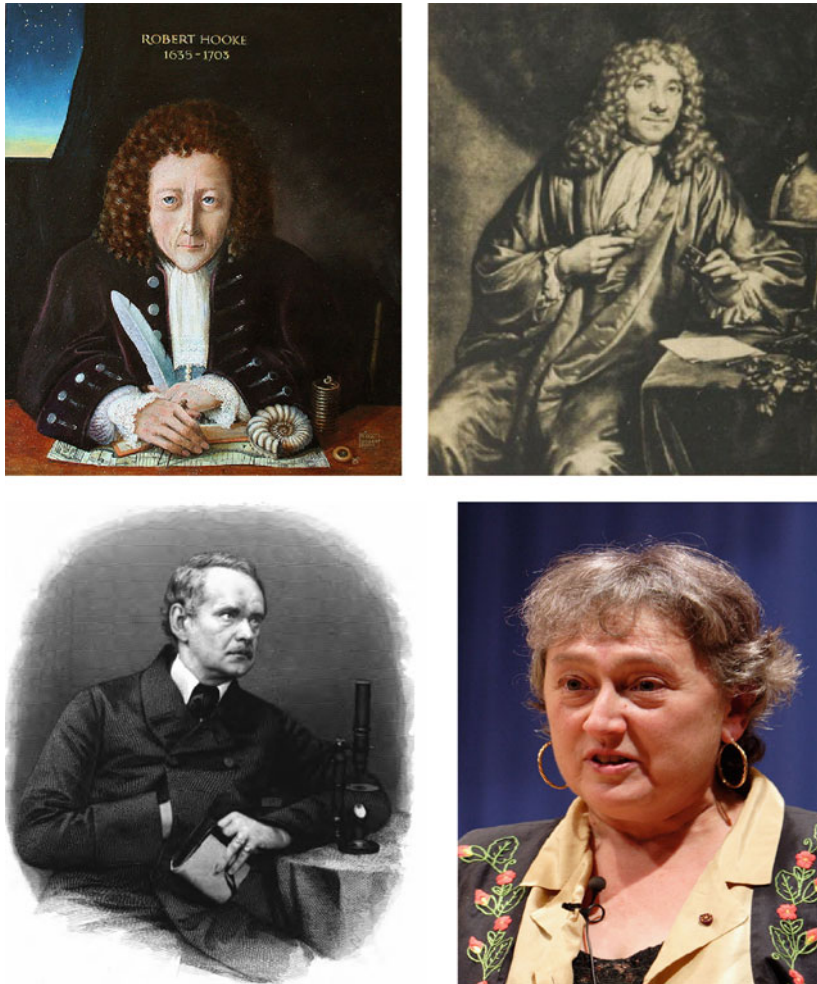
History

The first person to use the word cell was Robert Hook (1665) who described what he called the *cella* in a piece of cork ([Fig. 1](#)). He used this term because the cork appeared to be composed of thousands of small chambers that resembled the individual sleeping rooms in monasteries. However, Antonie Philips van Leeuwenhoek (1632–1723) using his handcrafted microscopes was the first to observe and describe single-celled microbial organisms, which he originally referred to as *animalcules*. After Van Leeuwenhoek, in 1838 a botanist, Matthias Jakob Schleiden, and a zoologist, Theodor Schwann, formally proposed “The Cell Theory” stating that: (1) all organisms are composed of one or more cells, (2) all cells come from preexisting cells, (3) vital functions of an organism occur within cells, and (4) all cells contain the hereditary information necessary for regulating cell functions and for transmitting information to the next generation of cells. Their theory, which nowadays seems so obvious, was a milestone in the development of modern biology. The cell theory was extended in 1855 by Rudolf Virchow, who stated that new cells come into existence only by the division of previously existing cells. Cells cannot arise by spontaneous generation from nonliving matter (Campbell and Reece 2002).

Overview

At first sight, cells exhibit a staggering diversity. Some lead a solitary existence, others live in communities; some have defined geometric shapes, others have flexible boundaries; some swim, some are sedentary. However, all cells have several basic features in common: they are bounded by a ► [plasma membrane](#) that physically separates them from the outside environment. Within the membrane is a semifluid substance, cytosol, composed mostly of water (70–90%). In the cytosol is where a variety of specialized structures named ► [organelles](#) are located. All cells contain also chromosomes, carrying genes for synthesizing all the proteins needed for cell growth, repair, and reproduction.

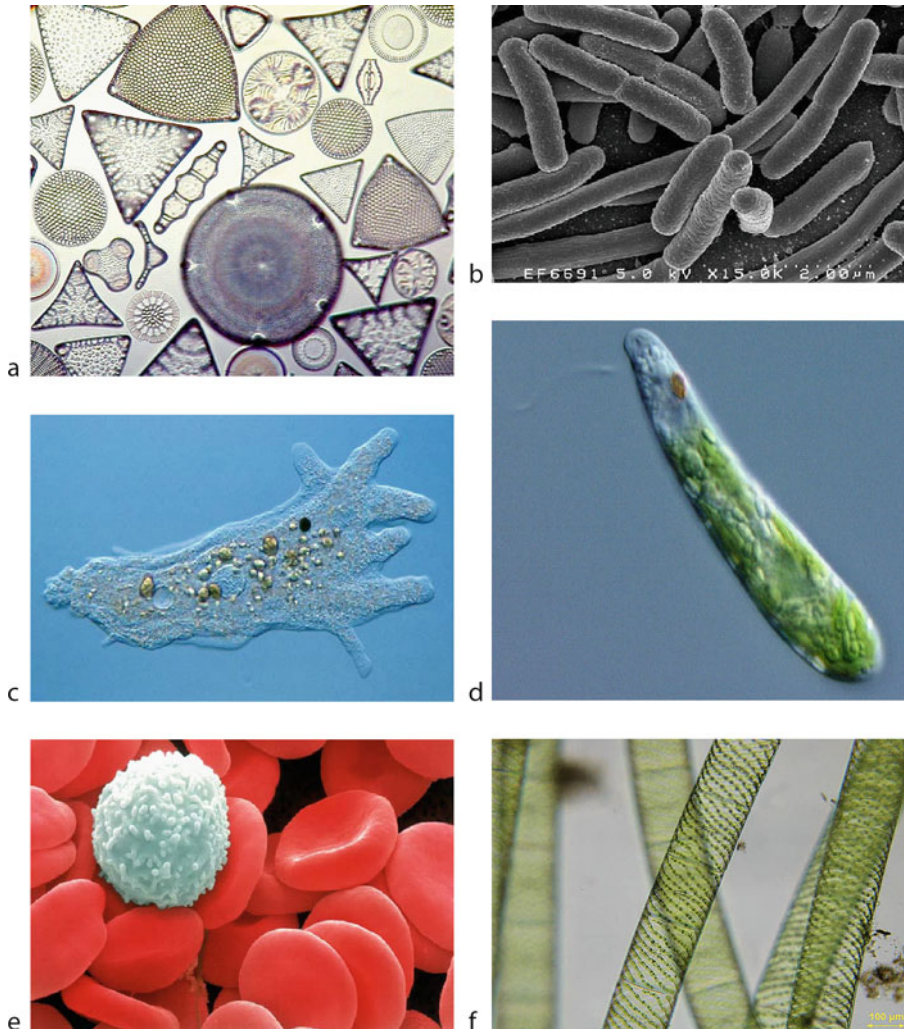
Despite all the different cell morphologies, it is surprising that there are only two types of cells.



Cell. Figure 1 Portraits of Robert Hook, Antonie Philips van Leeuwenhoek, two of the founders of cell biology and microbiology. Below them, the portraits of Matthias Jakob Schleiden and Lynn Margulis, known for their cell theory and endosymbiotic theory respectively

Based on differences in compartmentalization, cells can be divided into ► **prokaryotic** cell, the simplest, and the more complex ► **eukaryotic** cell (Fig. 2). By definition, prokaryotes are those organisms whose cells are not subdivided by membranes into a separate nucleus and cytoplasm. All prokaryote cell components are located together in the same compartment; the genetic material (DNA) is concentrated in a region called the nucleoid, but no membrane separates this region from the rest of the cell. On the contrary, eukaryotic cells contain a membrane-bound organelle named nucleus where the genetic material is contained. Only bacteria and archaea are prokaryotic cells. Protists, plants, fungi, and animals are eukaryotic cells (Bolsover et al. 1997).

Prokaryotic cells are simpler and generally smaller than eukaryotic cells and are thought to have evolved first (Fig. 3). Fossils show that prokaryotic organisms antedate by at least 2 billion years the first eukaryotes, which appeared some 1.5 billion years ago. It is likely that eukaryotes evolved from prokaryotes. The most plausible explanation of this process is known as the endosymbiotic theory, first articulated by the Russian botanist Konstantin Mereschkowsky in 1905. The endosymbiotic theory was advanced and substantiated with microbiological evidence by Lynn Margulis in a 1967 paper, *The Origin of Mitosing Eukaryotic Cells*. The basis of this theory concerns the origins of mitochondria and plastids (e.g., chloroplasts), which are organelles of eukaryotic

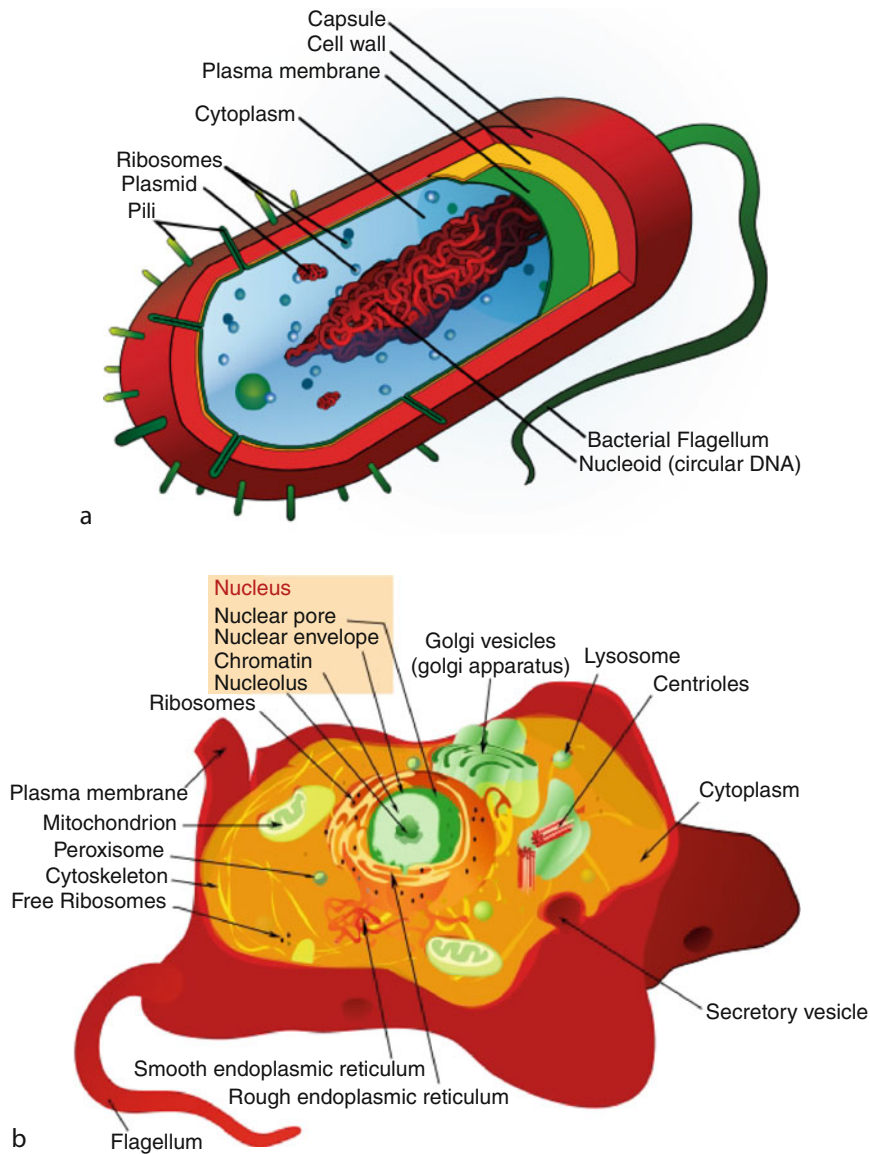


Cell. Figure 2 Although all the cells have several basic features in common, there is a great variety of specific cellular body plans. Some cells are organisms in their own right, and some make up the bodies of multicellular organisms. **(a)** Mixed diatoms, these algae are single-cell or colonial and are surrounded by a rigid siliceous envelope named theca. **(b)** Bacterial cells belonging to the species *Escherichia coli* a rod-shaped bacterium that is commonly found in the lower intestine of warm-blooded organisms. **(c)** Amoeba cell, this small protozoan uses tentacular protuberances called pseudopodia to move and phagocytose smaller unicellular organisms, which are enveloped inside the cell's cytoplasm in a food vacuole, where they are slowly broken down by enzymes. **(d)** *Euglena* cell, a photosynthetic protist with at least 150 described species. The cells are cylindrical with a rounded anterior and tapered posterior. The chloroplasts are well-developed and can glide and swim using their flagella. **(e)** White and red blood cells also referred to them as leucocytes and erythrocytes principal cells of the immune system involved in defending the body against both infectious disease and foreign materials and cells involved in delivering oxygen to the body tissues via the blood flow through the circulatory system. **(f)** *Spirogyra* cells, a filamentous green algae named for the helical or spiral arrangement of the chloroplasts. It is commonly found in freshwater areas, and there are more than 400 species of *Spirogyra* in the world. *Spirogyra* measures approximately 10 to 100 μm in width and may stretch centimeters long

cells. According to this theory, these organelles originated as separate prokaryotic organisms that were taken inside the cell as endosymbionts. Mitochondria developed from proteobacteria (in particular, Rickettsiales or

close relatives) and chloroplasts from cyanobacteria (Margulis 1967).

In addition, prokaryotic cells also lack most other membrane-bound organelles typical of eukaryotic cells.



Cell. Figure 3 Schematic representation of the cell composition. (a) prokaryotic cells, (b) eukaryotic animal cells. Despite their apparent differences, both cell types have a lot in common. They perform most of the same kinds of functions, and in the same ways. All are enclosed by plasma membranes, filled with cytoplasm, and loaded with small structures called ribosomes. They have DNA which carries the archived instructions for operating the cell. Physiologically they are very similar in many ways. For example, the DNA in the two cell types is precisely the same kind of DNA, and the genetic code for a prokaryotic cell is exactly the same genetic code used in eukaryotic cells

In some prokaryotic cells the plasma membrane is folded inward to form a complex of internal membranes (the mesosome) along which the reactions of cellular respiration are thought to take place. Photosynthetic prokaryotes contain chlorophyll associated with flat membranes called lamellae. On the contrary, eukaryotic cells have many

types of membrane-bound organelles that partition the cytoplasm into compartments.

Typically, each prokaryotic cell has a single chromosome carrying a full set of genes providing it with the genetic information necessary to operate as a living organism. Each chromosome has 3,000–4,000 genes although

some has as few as 500. A typical prokaryotic cell is rod shaped and about 2–3 μm long and 1 μm wide (1 μm = 0.001 mm). However, bacteria are not limited to a rod shape; spherical, filamentous, or spirally twisted bacteria are also found. Eukaryotic cells are generally much bigger than prokaryotes. Size is a general aspect of cell structure that relates to function. At the lower limit, the smallest cells known are bacteria called Mycoplasmas, which have diameters between 0.1 and 1.0 μm . Eukaryotic cells are typically ten times bigger than bacteria.

There are two distinct types (Domains) of prokaryotes, the ► **Bacteria** and ► **Archaea**, which are no more genetically related to each other than either group is to the eukaryotes. Both show the typical prokaryotic structure where the nucleus and other internal membranes are lacking. Despite this visual similarity to bacteria, archaea possess genes and several metabolic pathways that are more closely related to those of eukaryotes: notably the proteins involved in transcription and translation. Other aspects of archaean biochemistry are unique, such as their reliance on ether lipids in their cell membranes and cell wall. The cell wall of bacteria is always made of peptidoglycan, a molecule unique to this group or organisms. Archaea often have cell walls, but peptidoglycan is never present. Thus, the only well defined cellular structures presented by prokaryotes, the cell membrane and cell wall, are chemically quite different in these two groups or organisms. Initially, archaea were seen as extremophiles that lived in harsh environments, such as hot springs and salt lakes, but they have since been found in a broad range of habitats, such as soils, oceans, and marshlands. Archaea are particularly numerous in the oceans, and the archaea in plankton may be one of the most abundant groups of organisms on the planet (Clark 2005).

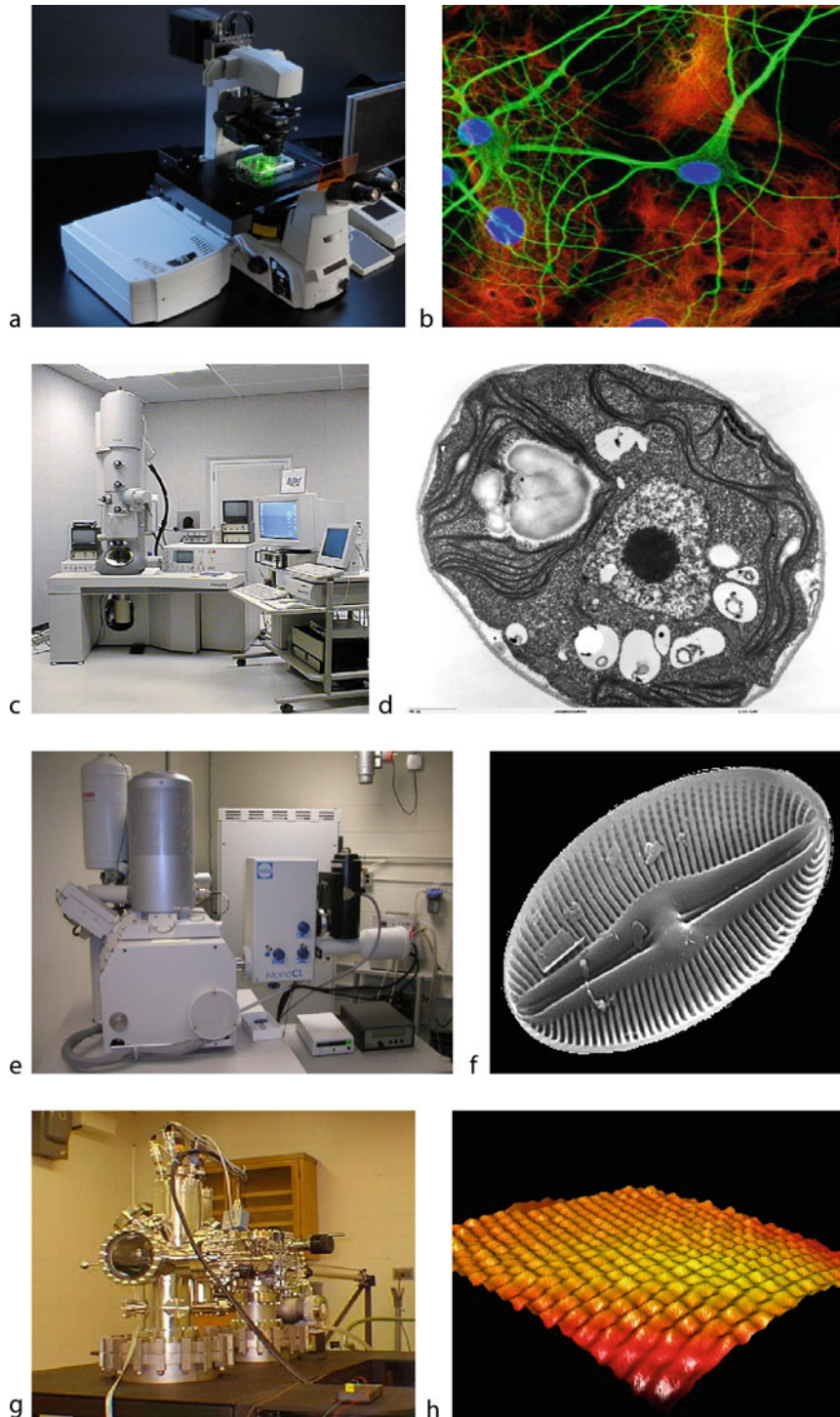
In addition to the plasma membrane, a eukaryotic cell has extensive and elaborately arranged internal membranes, which partition the cells into compartments. The nucleus is surrounded by a double membrane, the nuclear membrane, which separates the nucleus from the cytoplasm, but allows some communication with the cytoplasm via nuclear pores. The nucleus contains most of the genes in the eukaryotic cell (although some genes are located in the mitochondria and chloroplasts). The genome of eukaryotes usually consists of 10,000–50,000 genes carried on several ► **chromosomes**. In a cell that is not dividing, DNA is organized along with proteins forming an irregular network of strands termed chromatin. When the cells began the process of nuclear division (mitosis), the chromatin coils and condenses into discrete chromosomes containing several thousand genes arranged in a specific linear order. Most eukaryotes are diploid, with

two copies of each chromosome. Consequently, they possess at least two copies of each gene.

Besides nucleus, eukaryotic cells contain a variety of ► **organelles**, which are subcellular structures that carry out specific tasks. Some of them are separated from the rest of the cytoplasm by membranes but others are not. Many of the different membranes of the eukaryotic cell are forming an extensive complex of branching tubules, named endoplasmic reticulum (ER) that is continuous with the nuclear envelope and permeates the cytoplasm. The ER manufactures membranes and performs many other biosynthetic functions such as synthesis of lipids, metabolism of carbohydrates, and detoxifications of drugs and toxins. The ER also functions as a system for transporting materials from one part of the cell to another and perhaps to the outside environment as well. The Golgi apparatus is a stack of flattened membrane sacs and associated vesicles that is involved in the secretion of the proteins manufactured along the ER. The proteins are released from the ER in sealed-off little vesicles that fuses with the membranes of the Golgi complex. Within the Golgi complex the proteins are modified in various ways (i.e., adding carbohydrates forming glycoproteins). The Golgi apparatus in plant cells produces polysaccharides used to construct the cell wall.

Other organelles related to cell metabolism are the lysosomes, membrane-bound structures specialized for digestion that contain hydrolytic enzymes that cells use to digest macromolecules. About 40 different enzymes have been identified in lysosomes. In addition, ► **mitochondria** and ► **chloroplasts** are the main energy transducers of cells. Mitochondria are generally rod-shaped organelles bounded by a double membrane. They resemble bacteria in their size and shape; it is thought that mitochondria are indeed evolved from bacteria that took up residence in the primeval ancestor of eukaryotic cells. Like bacteria, mitochondria contain a circular molecule of DNA similar to a bacterial chromosome, although much smaller. Mitochondria are the site of most of the chemical reactions that convert the chemical energy present in inorganic compounds to another form of energy, ATP, that cells can use for work. These organelles are the sites for cellular respiration, the catabolic process that generates ATP by extracting energy from sugars, fats, and other compounds with the help of oxygen. This contrasts with bacteria, where the respiration chain is located in the cytoplasmic membrane, as no mitochondria are present (Davis et al. 1990).

► **Chloroplasts** are also membrane-bound organelles that produce and store food materials in algae and plant cells. Chloroplasts contain the light-absorbing pigment



Cell. Figure 4 Microscopes and their images. **(a)** A confocal microscope creates sharp images of a specimen that would otherwise appear blurred when viewed with a conventional optical microscope. This is achieved by excluding most of the light from the specimen that is not from the microscope's focal plane. **(b)** A glia neuron cell viewed using confocal microscopy. **(c)** Transmission electron microscope (TEM) uses a high energy electron beam transmitted through a very thin sample to image

chlorophyll, along with enzymes and other molecules that function in the photosynthetic production of reduced carbon molecules by trapping light energy. Like mitochondria, chloroplasts contain a circular DNA molecule and are thought to have evolved from a photosynthetic bacteria. Chloroplasts also contain a variety of yellow and orange pigments known as carotenoids. Although a unicellular alga may have only a single large chloroplast, cells of complex plants may possess 20–100 of these organelles.

Besides for the presence of chloroplasts, plant cells differ from animal cells in several other ways. Although all cells are limited by plasma membranes, plant cells are also surrounded by ► **cell walls** of cellulose, which limits any change of position and shape. In addition, most plants have one large or several small compartments called vacuoles, used for storing nutrients and waste products, and certain organelles such as centrioles and lysosomes are absent.

There are still other structures that support the cells, connect them with other cells, and help them move. Cytoskeletal elements, such as microtubules or microfilaments, give cells their shape and allow the movement. Centrioles are tiny organelles that function in nuclear division, usually located within a dense area of cytoplasm, the centrosome. Cells are able to swim or move by using their cilia and flagella, which are specialized arrangements of microtubules (Maton et al. 1997).

Cell Origin and Evolution

Synthesis and accumulation of biologically relevant molecules in the early Earth would have been the first step in the path to the primitive cells. It is generally assumed that RNA was the first information storage molecule and that DNA came later. The primitive cell vaguely resembled a bacterium (Bada and Lazcano 2010).

Life began remarkably early in Earth's history, and those first organisms were ancestral to the great diversity of life we observe today. The Earth was formed about 4.5 billion years ago. However, the oldest fossils of

organisms known are 3.5 billion years old. These microfossils resemble certain bacteria that still exist today. For bacteria so complex to have evolved by 3.5 billion years ago, it is a reasonable hypothesis that life originated much earlier, when Earth began to cool to a temperature at which liquid water could exist. The fossil record supports the presumption that prokaryotes were the earliest organisms. Photosynthesis probably evolved very early also in prokaryotic history. The photosynthetic bacteria that generate and release oxygen to the atmosphere, named cyanobacteria, probably evolved over 2.7 billion years ago. The accumulation of atmospheric oxygen was gradual and had an enormous impact on life since oxygen attacks chemical bonds and was toxic for many of the existing prokaryotic groups. Although some prokaryotic species survived in habitats that remained anaerobic, a variety of different adaptations to the oxidizing atmosphere evolved, including cellular respiration, using oxygen to obtain energy from organic and inorganic molecules.

The oldest fossils of eukaryotes are 2.1–2.7 billion years old, and look like simple single-celled algae. This range of time places the earliest eukaryotes during a time when the oxygen evolution was changing Earth's environments dramatically. Development of chloroplasts may be part of the explanation for this temporal correlation.

It seems reasonable to suggest that eukaryotes evolved from a single prokaryotic ancestor that gradually accumulated greater structural complexity. But evidences show that the eukaryotic cell originated from a symbiotic coalition of multiple prokaryotic ancestors not just one. The theory of ► **serial endosymbiosis** proposes that mitochondria and chloroplasts were formerly small prokaryotes living within larger cells (Margulis 1967; Davis et al. 1990). The proposed ancestors of mitochondria were aerobic heterotrophic prokaryotes, related to alpha-proteobacteria, that became endosymbionts. The proposed ancestors of chloroplasts were photosynthetic prokaryotes related to cyanobacteria. These ancestors probably gained entry to the host cell as undigested prey or parasites. Evidences supporting this idea are the structural similarity

and analyze the microstructure of materials with atomic scale resolution. The electrons are focused with electromagnetic lenses and the image is observed on a fluorescent screen, or recorded on film or digital camera. **(d)** A TEM image of the green alga *Chlamydomonas* we can observe the ultrastructure of the nuclei, chloroplasts and pyrenoid. **(e)** Scanning electron microscope (SEM), while TEM allows us to study the inner structure of objects (tissues, cells, viruses) and SEM is used to visualize the surface of tissues, macromolecular aggregates and materials. **(f)** A SEM image of a diatom, brown algae. We can see the silica theca that surround the cells with their characteristic patterns specific for each species. **(g)** The scanning tunneling microscope (STM) provides a picture of the atomic arrangement of a surface by sensing corrugations in the electron density of the surface that arise from the positions of surface atoms. **(h)** A STM image of palladium crystals

between bacteria, mitochondria and chloroplasts, both organelles are able to replicate by a splitting process reminiscent of binary fission in bacteria, and each organelle contains a genome consisting of a single circular DNA molecule not associated with histones or other proteins, as in most prokaryotes. Furthermore, the organelles contain all the enzymatic equipment necessary to transcribe and translate their DNA into proteins. During the evolution from endosymbiont to organelle, the vast majority of the original bacterial genes has been lost or transferred to the host nucleus; so the organellar genomes are very reduced in comparison to their closest free-living counterparts.

Basic Methodology

Living cells are composed of many progressively smaller components. Most levels of biological organization are imperceptible to the human senses, so that to study them we must make use of a variety of instruments and indirect techniques. Microscopy is the most useful technique to study cell structure and related issues. The light microscope, gradually improved since Hooke's time, uses visible light as the source of illumination. During the last decades, the development of the electron microscope has enabled researchers to study the fine detail, called ultrastructure of cells. Nowadays, the scanning tunneling electron microscope allows us to study the relationship between molecules.

Magnification is the ratio of the size of the image to the size of the specimens. Whereas the ordinary light microscope can magnify a structure about 1,000 times, the electron microscope can magnify up to 250,000 times or even more. Besides, the electron microscope has far superior resolving power, which is the ability to reveal fine detail, and is expressed as the minimum distance between two points that can be distinguished as separate and distinct points.

Optical and electron microscopy involve the diffraction, reflection, or refraction of electromagnetic radiation/electron beams interacting with the subject of study, and the subsequent collection of this scattered radiation in order to build up an image. This process may be carried out by wide-field irradiation of the sample (e.g., standard light microscopy and transmission electron microscopy) or by scanning of a fine beam over the sample (e.g., confocal laser scanning microscopy and scanning electron microscopy) (Fig. 4).

Optical or light microscopy involves passing visible light transmitted through or reflected from the sample through a single or multiple lenses to allow a magnified view of the sample. The resulting image can be detected

directly by the eye. To be viewed with the light microscope, specimens must be very thin. Single cell organisms can be observed *in vivo*. There are important limitations to the standard optical microscopy: the technique can only image dark or strongly refracting objects efficiently, diffraction limits resolution to approximately 0.2 μm , and out of focus light from points outside the focal plane reduces image clarity. Live cells generally lack sufficient contrast to be studied successfully. Internal structures of the cell are colorless and transparent.

The electron microscope uses a beam of electrons as a source of illumination instead of light. The microscope has a greater resolving power than a light-powered optical microscope, because it uses electrons that have wavelengths about 100,000 times shorter than visible light (photons), and can achieve magnifications of up to 1,000,000 times. The electron microscope uses electrostatic and electromagnetic "lenses" to control the electron beam and focus it to form an image. Two types of electron microscopes in common use are the transmission electron microscope and the scanning electron microscope (Murphy 2002).

See also

- ▶ [Archea](#)
- ▶ [Bacteria](#)
- ▶ [Cell Membrane](#)
- ▶ [Cellular Theory, History of](#)
- ▶ [Cytoplasm](#)
- ▶ [Eukary](#)
- ▶ [Evolution \(Biological\)](#)
- ▶ [Prokaryote](#)

References and Further Reading

- Alberts B, Bray D, Lewis J, Raff M, Roberts K, Watson JD (1994) *Molecular biology of the cell*, 3rd edn. Garland Publ, New York, p 1294
- Bada JL, Lazcano A (2010) The origin of life. In: Ruse M, Travis J (eds) *The Harvard companion of evolution*. Harvard University Press, Cambridge, Belknap
- Bolsover SR, Hyams JS, Jones S, Shephard EA, White HA (1997) *From genes to cells*. Wiley, New York, p 424
- Campbell NA, Reece JB (2002) *Biology*, 6th edn. Benjamin Cummings Publ, San Francisco, p 1247
- Clark DP (2005) *Molecular biology – understanding the genetic revolution*. Elsevier Academic Press, Burlington, p 783
- Davis PW, Solomon EP, Berg LR (1990) Cell structure and function. In: *The World of Biology*. Saunders College Publ, Fort Worth, pp 79–107
- Margulis L (1967) On the origin of mitosing cells. *J Theor Biol* 14(3):255–274
- Maton A, Hopkins JJ, LaHart S, Warner SQ, Wright M, Jill D (1997) *Cells building blocks of life*. Prentice Hall, New Jersey, p 267
- Murphy DB (2002) *Fundamentals of light microscopy and electronic imaging*. Springer, Heidelberg, p 262

Cell Communication

- ▶ [Quorum Sensing](#)

Cell Membrane

Synonyms

[Cytoplasmic membrane](#); [Plasma membrane](#)

Definition

The ▶ [cell](#) membrane is the boundary that envelops all cells and provides a semi-permeable barrier for their separation from the extracellular environment. It is constituted by a 5–8 nm thick lipid bilayer – mainly composed by amphiphilic phospholipids – in which membrane proteins are interspersed. The cell membrane is involved in different cellular processes including active and passive traffic of substances, signal transduction, and cell adhesion and fusion. In addition to the cell membrane, inside the eukaryotic cytoplasm there are membrane-enclosed ▶ [organelles](#). These specialized compartments include the nucleus, mitochondria, plastids, Golgi apparatus, vacuoles, vesicles, lysosomes, peroxisomes, and endoplasmic reticulum. Mitochondria – present in almost all eukaryotes – and plastids – in photosynthetic eukaryotes – are double-membrane organelles, a feature indicative of their endosymbiotic origin. ▶ [Bacteria](#) and archaea lack membrane-enclosed compartments, with certain exceptions such as the magnetosomes present within the nucleocytoplasm of magnetotactic bacteria and the cell compartments observed in bacteria from the phylum *Planctomycetes*. Some ▶ [virus](#) families – the so-called lipid coated viruses – are also surrounded by a membrane during their extracellular phase, derived from the host cell previously infected.

See also

- ▶ [Amphiphile](#)
- ▶ [Archea](#)
- ▶ [Bacteria](#)
- ▶ [Cell](#)
- ▶ [Cell Wall](#)
- ▶ [Eukarya](#)
- ▶ [Lipid Bilayer](#)
- ▶ [Membrane](#)
- ▶ [Membrane Potential](#)
- ▶ [Organelle](#)
- ▶ [Virus](#)

Cell Models

DAVID DEAMER

Department of Biomolecular Engineering, University of California, Santa Cruz, CA, USA

Synonyms

[Artificial cells](#); [Protocell](#); [Synthetic cells](#)

Keywords

Compartments, encapsulation, lipid vesicles, permeability, replication, translation

Definition

Cell models are laboratory versions of simple cellular structures that exhibit some of the properties of the living state. They consist of a compartment, usually microscopic lipid vesicles, with encapsulated functional polymers such as enzymes and nucleic acids.

History

The idea that it might be possible to assemble model ▶ [cells](#) can be traced back to 1965, when Alec Bangham discovered that phospholipids spontaneously ▶ [self-assemble](#) into closed compartments (now called liposomes) when dispersed in aqueous phases (see review by Bangham 1993). The boundary of such compartments is a ▶ [lipid bilayer](#) that is relatively permeable to water and small molecules like water but much less permeable to ionic solutes such sodium and potassium ions. Efraim Racker took the next step toward cell models when he and his co-workers showed that it was possible to use detergents such as deoxycholic acid to disperse membranous components of cells (see Racker 1970). When the detergent was removed, small vesicles formed that contained the original lipids and functional proteins. Using this method, Racker and his colleagues were able to reconstitute electron transport reactions of mitochondrial and chloroplast membranes.

Similar techniques were soon applied to other biological structures and functions. For instance, Oesterhelt and Stoeckenius (1971) reconstituted the proton pump of purple membranes isolated from a halophilic bacterial species that uses the energy of a proton gradient to synthesize ATP. Racker and Stoeckenius then collaborated to produce a system of reconstituted membrane vesicles containing both the proton pump of halobacteria and the ATP synthase of mitochondria (Racker and Stockenius 1974). The hybrid structures could synthesize ATP using

light as an energy source, which strongly confirmed Peter Mitchell's chemiosmotic hypothesis that proton gradients could drive ATP synthesis (Mitchell 1976).

When it was realized that lipid vesicles could incorporate enzymatic functions, the next step toward model cells became feasible, in which a polymerase encapsulated in liposomes would be able to synthesize a ► **nucleic acid**. This was first attempted by Chakrabarti et al. (1994) and Walde et al. (1994) both reporting that encapsulated polynucleotide phosphorylase could synthesize an RNA homopolymer from its substrate, in this case ADP.

Overview

The point of this brief history is that relatively complex biological functions can be reconstituted by ► **self-assembly** of their dispersed components, so it is reasonable to consider the possibility that similar techniques might allow artificial cells to be fabricated under laboratory conditions. If this turns out to be possible, perhaps it will help define "life" and even elucidate the major steps that led to the origin of cellular life nearly four billion years ago.

Basic Methodology

What would such a system do? This question can be answered by listing the properties and functions of model cells that could conceivably be assembled in the laboratory. For the purposes of this list, it is assumed that all the nutrients and energy needed for growth and replication will be provided so that a complex metabolism will not be required:

1. Self-assembly of lipid molecules generates cellular compartments defined by boundary membranes.
2. Macromolecules are encapsulated in the compartments, yet smaller substrate molecules can cross the membrane barrier.
3. The macromolecules have the potential to grow by polymerizing the substrate molecules.
4. The membrane itself can grow by addition of lipid molecules.
5. Some of the encapsulated polymers are catalysts that can speed the growth process, and the catalysts are reproduced during growth by polymerization.
6. Genetic information is contained in the sequence of monomers in a second set of polymers, and is used to direct the growth of catalytic polymers.
7. The catalytic polymers catalyze the polymerization of the genetic molecules.
8. Following a certain amount of growth, the membrane-bounded system of macromolecules divides

into smaller structures, each containing the catalysts and copies of genetic information.

9. Genetic information is passed between generations by duplicating the gene sequences and sharing them between daughter cells.
10. Occasional mistakes (mutations) occur during replication or transmission of genetic information so that the system can evolve through selection.

Key Research Findings

Several research groups are beginning to study systems of genetic and catalytic molecules that are steps toward fulfilling this list of properties. For instance, Mansy et al. (2008) demonstrated that it was possible to encapsulate a short DNA template in fatty acid vesicles, then add activated nucleotides outside. The nucleotides were sufficiently permeable to enter the vesicle interior and support the sequence-dependent elongation of the DNA. In a related advance, Lincoln and Joyce (2009) developed a pair of ribozymes, each of which could catalyze the synthesis of the other by a ligation reaction that joined two smaller non-catalytic oligonucleotides. This system is not encapsulated and does not replicate a complete base sequence, but illustrates in principle how an evolving system of paired ribozymes could function. The Rasmussen group in Denmark have stepped away from biologically inspired molecular systems and are attempting to assemble a very different version of model cells (DeClue et al. 2009). In their system, the reactions occur on the surface of vesicles, rather than the interior, thereby bypassing the requirement for membrane transport of the nutrients. Furthermore, they are attempting to drive the polymerization reaction by an input of light energy, rather than supplying activated monomers.

Another approach to model cells is to encapsulate ribosomes and translation systems in lipid vesicles. Luigi Luisi and his co-workers at the Eigennössische Technische Hochschule in Zurich, Switzerland made the first attempt to assemble a translation system in lipid vesicles by encapsulating ribosomes and an RNA homopolymer that codes for phenylalanine (Oberholzer et al. 1995). The phenylalanine was attached to transfer RNA so that it was ready to be used by ribosomes for peptide synthesis. However, the lipid bilayer was impermeable to the transfer RNA, so peptide bond formation was limited to the small number of tRNA–amino acid complexes that were encapsulated within the vesicles. This limitation makes the point that model cells need to have some way to transport nutrients inward across their boundary membrane.

Noireaux and Libchaber (2004) reported an elegant solution to the permeability problem. They disrupted

E. coli cells and captured samples of the bacterial cytoplasm in lipid vesicles. The samples included ribosomes, transfer RNAs, and the hundred or so other components required for protein synthesis. The researchers then chose two genes to translate, one for green fluorescent protein (GFP), a marker for protein synthesis, and a second gene for a pore-forming protein called alpha hemolysin. If the system had worked as planned, the GFP would have accumulated in the vesicles as a visual marker for protein synthesis and the hemolysin would have allowed externally added “nutrients” in the form of amino acids and ATP to cross the membrane barrier and supply the translation process with energy and monomers. The system was functional, and the newly synthesized hemolysin allowed synthesis of GFP to continue for as long as four days. The GFP in the vesicles was monitored by its green fluorescence. A more recent example of a model cell system is the encapsulated “genetic cascade” fabricated by Ichihashi et al. (2010), in which a gene on a plasmid was transcribed by RNA polymerase to mRNA, which in turn directed the synthesis of green fluorescent protein.

The model cells containing ribosomes clearly demonstrate one fundamental property of life: they can use genetic information to synthesize a protein. Although they can grow by synthesizing one or more specific proteins, no other cellular components are produced. To approach the definition of a living system, the vesicles would need to incorporate genetic information required for a hundred or more different proteins and RNA species, over half of which are the components of the ribosomes themselves. They would need genes for polymerase enzymes so that the DNA could be replicated as part of the growth process, and a way for lipid to be synthesized, because the membranous boundary must grow to accommodate the internal growth. Transport proteins must be synthesized and incorporated into the lipid bilayer, otherwise the vesicles have no access to external sources of nutrients and energy. A whole set of regulatory processes must be in place so that all of these functions are coordinated. Finally, when the vesicles grow to approximately twice their original size, there must be a way for them to divide into daughter cells that share the original genetic information.

It seems impossible that the first forms of life sprang into existence with such a complex system of interacting molecules. There must have been something simpler, a kind of scaffold life that was left behind in the evolutionary process leading to today’s life. Can we reproduce that scaffold? This is the challenge for research on model cells and the origin of life.

Applications

A functioning system of artificial cells will represent a major breakthrough in biotechnology. At present, the pharmaceutical industry must use recombinant DNA techniques and bacterial cultures to synthesize protein products. Model cells are simplified versions of bacterial cells, and if they can be designed to produce a desired protein in large quantities, the result would be a much more efficient, flexible, and inexpensive system for producing important therapeutic agents. See review by Pohorille and Deamer 2002.

Future Directions

One promising approach to model cells is suggested by the results reported by Lincoln and Joyce (2009). It is possible that a pair of ribozymes will be found that can catalyze their own complete synthesis using genetic information encoded in their base sequences. If the ribozymes could then function in a membrane-bounded compartment using nucleotides present in the external medium, the system could rightly be claimed to have the essential properties that are lacking so far in artificial cell models: reproduction of the catalysts and genetic information in a cellular compartment.

See also

- ▶ Cell
- ▶ Lipid Bilayer
- ▶ Nucleic Acids
- ▶ Protocell
- ▶ Self Assembly

References and Further Reading

- Bangham AD (1993) Liposomes: the Babraham connection. *Chem Phys Lipids* 64:275–285
- Chakrabarti A, Breaker RR, Joyce GF, Deamer DW (1994) Production of RNA by a polymerase protein encapsulated within phospholipid vesicles. *J Mol Evol* 39:555–559
- Deamer D, Szostak J (eds) (2010) *Origins of life*. Cold Spring Harbor Press, Woodbury
- Deamer DW, Dworkin JP, Sandford SA, Bernstein MP, Allamandola LJ (2002) The first cell membranes. *Astrobiology* 2:371–382
- DeClue MS, Monnard PA, Bailey JA, Maurer SE, Collis GE, Ziock HJ, Rasmussen S, Boncella JM (2009) Nucleobase mediated, photocatalytic vesicle formation from an ester precursor. *J Am Chem Soc* 131:931–933
- Hanczyc MM, Szostak JW (2004) Replicating vesicles as models of primitive cell growth and division. *Curr Opin Chem Biol* 8:660–664
- Ichihashi N, Matsuura T, Kita H, Sunami T, Suzuki H, Yomo T (2010) Constructing partial models of cells. In: Deamer D, Szostak J (eds) *Origins of Life*, Cold Spring Harb Perspect Biol. 2010
- Lincoln TA, Joyce GF (2009) Self-sustained replication of an RNA enzyme. *Science* 323:1229–1232

- Luisi PL (2006) *The emergence of life: from chemical origins to synthetic biology*. Cambridge University Press, Cambridge
- Mansy SS, Schrum JP, Krishnamurthy M, Tobé S, Treco DA, Szostak JW (2008) Template-directed synthesis of a genetic polymer in a model protocell. *Nature* 454:122–125
- Mitchell P (1976) Possible molecular mechanisms of the protonmotive function of cytochrome systems. *J Theor Biol* 62:327–367
- Monnard PA, Luptak A, Deamer DW (2007) Models of primitive cellular life: polymerases and templates in liposomes. *Philos Trans R Soc Lond B Biol Sci* 362:1741–1750
- Morowitz HJ (2009) *Beginnings of cellular life*. Yale University Press, New Haven
- Noireaux V, Libchaber A (2004) A vesicle bioreactor as a step toward an artificial cell assembly. *Proc Natl Acad Sci USA* 101:17669–17674
- Oberholzer TR, Wick R, Luisi PL, Biebricker CK (1995) Protein expression in liposomes. *Biochem Biophys Res Commun* 207:250
- Oesterhelt D, Stoekenius W (1971) Rhodopsin-like protein from the purple membrane of *Halobacterium halobium*. *Nat New Biol* 233:149–152
- Pohorille A, Deamer DW (2002) Artificial cells: prospects for biotechnology. *Trends Biotech* 20:123
- Racker E (1970) *Membranes of mitochondria and chloroplasts*. Van Nostrand Reinhold, New York
- Racker E, Stockenius W (1974) Reconstitution of purple membrane vesicles catalyzing light-driven proton uptake and adenosine triphosphate formation. *J Biol Chem* 249:662–663
- Schrum JP, Ricardo A, Krishnamurthy M, Blain JC, Szostak JW (2009) Efficient and rapid template-directed nucleic acid copying using 2'-amino-2',3'-dideoxyribonucleoside-5'-phosphorimidazole monomers. *J Am Chem Soc* 131:14560–14570
- Sunami T, Kita H, Hosoda K, Matsuura T, Suzuki H, Yomo T (2009) Detection and analysis of protein synthesis and RNA replication in giant liposomes. *Methods Enzymol* 464:19–30
- Szostak JW, Bartel DP, Luisi PL (2001) Synthesizing life. *Nature* 409:387–390
- Walde P, Goto A, Monnard P-A, Wessicken M, Luisi PL (1994) Oparin's reactions revisited: enzymatic synthesis of poly(adenylic acid) in micelles and self-reproducing vesicles. *J Am Chem Soc* 116:7541–7547
- Zhu TF, Szostak JW (2009) Coupled growth and division of model protocell membranes. *J Am Chem Soc* 131:5705–5713

Cell Motility

- [Motility](#)

Cell Wall

Definition

The cell wall is an external layer that surrounds some types of ► [cells](#). It has structural, protective, and functional roles

(filtering capacities for the selective uptake of substances for cell metabolism). It is located outside the cell membrane. The cell wall is found in plants, bacteria, fungi, algae, and some Archaea. The main functions of cell walls are (1) to provide tensile strength and limited plasticity to the cell, (2) to provide mechanical support, (3) cutinized, it is used to prevent water loss, (4) to provide mechanical protection, and (5) to contribute to cell–cell communication. The structure of the cell wall differentiates Gram positive from ► [Gram negative bacteria](#), a property of important phylogenetic value.

See also

- [Cell](#)
- [Cell Membrane](#)
- [Gram Negative Bacteria](#)
- [Gram-Positive Bacteria](#)
- [Peptidoglycan](#)
- [Protoplast](#)

Cellular Automata

MARCO TOMASSINI

Information Systems Department, University of Lausanne, Lausanne, Switzerland

Synonyms

[Tessellation automata](#)

Keywords

Automata, complex systems, discrete dynamics, simulation

Definition

Cellular automata (CA) are dynamical systems in which space and time are discrete. A cellular automaton consists of an array of cells, each of which can be in one of a finite number of possible states, updated synchronously in discrete time steps, according to a local, identical interaction rule. The state of a ► [cell](#) at the next time step is determined by its own current state and the current states of a surrounding neighborhood of cells (Wolfram 1994).

Overview

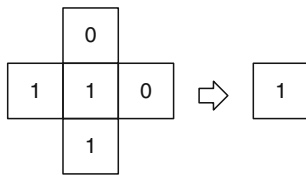
Cellular automata were originally conceived by Ulam and von Neumann in the 1940s to provide a formal framework

for investigating the behavior of complex, extended systems (von Neumann 1966). In particular, von Neumann asked whether we could use purely mathematical–logical considerations to discover the specific features of automata that make them formally analogous with self-constructing and ► **self-replicating** biological systems.

Thanks to their simplicity and appeal, over the years, CA have been applied to the study of general phenomenological aspects of the world, including communication, computation, construction, growth, reproduction, competition, and evolution. CA have also been used successfully as an easy way to program models for studying phenomena of interest in several scientific fields, including physics, biology, and computer science.

Basic Methodology

As an example, let us consider the *parity rule* for a 2-state, 5-neighbor, two-dimensional CA. Each cell is assigned a state of 1 at the next time step if the combined parity of its current state and the states of its four neighbors in the *N*, *E*, *S*, and *W* directions is odd, and is assigned a state of 0 if the parity is even. There are 32 different combinations for the states of the neighbors, including the central cell itself. The rule table consists of entries of the form:



This means that if the current state of the cell is 1 and the states of the north, east, south, and west cells are 0, 0, 1, 1, respectively, then the state of the central cell at the next time step will be 1 (because three bits in the neighborhood

are in state 1). The rule is completely specified by the rule table given in Table 1. Figure 1 demonstrates patterns that are produced by the parity CA.

The simplest CA are one dimensional with only two possible states per cell and a neighborhood constituted of the cell itself and its immediate right and left neighboring cells. Figure 2 shows an example of the time evolution of an elementary CA.

More formally, a cellular automaton A is a quadruplet

$$A = (S, G, d, f)$$

where S is a finite set of states, G is the cellular neighborhood, $d \in \mathbb{Z}^+$ is the dimension of A , and f is the local cellular interaction rule, also referred to as the transition function.

Given the position of a cell \mathbf{i} , $\mathbf{i} \in \mathbb{Z}^d$, in a regular d -dimensional uniform lattice, or *grid* (i.e., \mathbf{i} is an integer vector in a d -dimensional space), its *neighborhood* G is defined by

$$G_{\mathbf{i}} = \{\mathbf{i}, \mathbf{i} + \mathbf{r}_1, \mathbf{i} + \mathbf{r}_2, \dots, \mathbf{i} + \mathbf{r}_n\},$$

where n is a fixed parameter that determines the neighborhood size, and \mathbf{r}_j is a fixed vector in the d -dimensional space.

The *local transition rule* f

$$f : S^n \rightarrow S$$

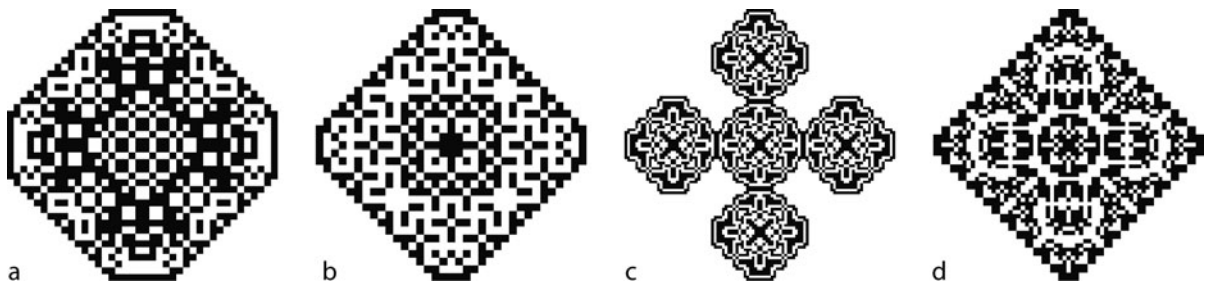
maps the state $s_{\mathbf{i}} \in S$ of a given cell \mathbf{i} into another state from the set S , as a function of the states of the cells in the neighborhood $G_{\mathbf{i}}$.

Consider a one-dimensional CA with only two states $S = \{0, 1\}$. In this case, f is a function $f: \{0, 1\}^n \rightarrow \{0, 1\}$ and the neighborhood size n is usually taken to be $n = 2r + 1$ such that

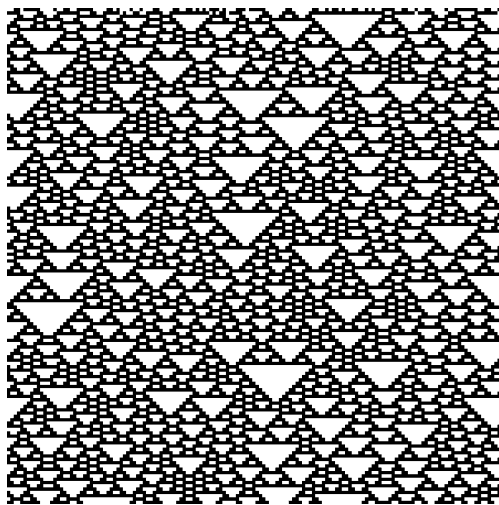
$$s_i(t + 1) = f(s_{i-r}(t), \dots, s_i(t), \dots, s_{i+r}(t)),$$

Cellular Automata. Table 1 Parity rule table. CNESW denotes the current states of the center, north, east, south, and west cells, respectively. S_{next} is the state of the central cell state at the next time step

CNESW	S_{next}	CNESW	S_{next}	CNESW	S_{next}	CNESW	S_{next}
00000	0	01000	1	10000	1	11000	0
00001	1	01001	0	10001	0	11001	1
00010	1	01010	0	10010	0	11010	1
00011	0	01011	1	10011	1	11011	0
00100	1	01100	0	10100	0	11100	1
00101	0	01101	1	10101	1	11101	0
00110	0	01110	1	10110	1	11110	0
00111	1	01111	0	10111	0	11111	1



Cellular Automata. Figure 1 Patterns produced by the parity rule, starting from a 20×20 rectangular pattern. White squares represent cells in state 0, black squares represent cells in state 1. (a) after 30 time steps ($t = 30$), (b) $t = 60$, (c) $t = 90$, (d) $t = 120$



Cellular Automata. Figure 2 A one-dimensional elementary CA is shown, where the horizontal axis depicts the configuration at a certain time t and the vertical axis depicts successive time steps (increasing down the page). The system starts in a randomly generated configuration of zeroes and ones

where $r \in \mathbb{Z}^+$ is a parameter, known as the *radius*, representing the standard one-dimensional cellular neighborhood. Considering the $r = 1$ case, one obtains so-called *elementary* CAs, for which the neighborhood size is $n = 3$:

$$f : \{0, 1\}^3 \rightarrow \{0, 1\}, \quad s_i(t+1) = f(s_{i-1}(t), s_i(t), s_{i+1}(t)).$$

In this case, the domain of f is the set of all 2^3 triplets, which gives rise to $2^8 = 256$ distinct elementary rules (Wolfram 1994). For finite-size grids, spatially periodic boundary conditions are frequently assumed, resulting in a circular grid. An example of an elementary rule has been shown in Fig. 2.

For a CA of size N , a *configuration* of the grid at time t is defined as

$$C(t) = (s_0(t), s_1(t), \dots, s_{N-1}(t)),$$

where $s_i(t) \in S$ is the state of cell i at time t . The progression of the CA in time is then given by the iteration of the *global mapping* F :

$$F : C(t) \rightarrow C(t+1), \quad t = 0, 1, \dots$$

through the simultaneous application in each cell of the local transition rule f . The global dynamics of the CA can be described as a directed graph, referred to as the CA's *phase space* (Wolfram 1994).

Key Research Findings

Cellular automata have been proved to be universal computing devices and, as such, they can compute any computable function (Wolfram 1994). The question of whether cellular automata can model not only general phenomenological aspects of our world, but also directly model the laws of physics themselves was raised by (Fredkin and Toffoli 1982). A primary theme of this research is the formulation of computational models of physics that are *information-preserving*, and thus retain one of the most fundamental features of microscopic physics, namely, reversibility (Fredkin and Toffoli 1982; Margolus 1984; Toffoli 1980). This approach has been used to provide extremely simple models of common differential equations of physics, such as the heat and wave equations (Toffoli 1984) and the Navier–Stokes equation (Frisch et al. 1986). CA also provide a useful model for a branch of dynamical systems theory which studies the emergence of well-characterized collective phenomena, such as order, turbulence, chaos, symmetry breaking, and fractality, in discrete systems (Chopard and Droz 1998; Vichniac 1984).

Applications

For engineers and scientists, cellular automata are a particularly useful modeling device when the phenomenon to be studied does not lend itself to a clear mathematical model such as those represented by differential equations. In this case, simple local rules that are motivated by the phenomenon at hand may give rise to a global behavior that approaches that of the original system. Examples of this range from ► [chemotaxis](#), to snow transport by the wind, and to car traffic, just to name a few (Chopard and Droz 1998). Of course, how to choose the local cellular automata rules in order to produce the desired global behavior is a hard problem. It can be approached by trial and error or by heuristics such as evolutionary algorithms (Sipper 1997; Crutchfield et al. 2003) in which good rules evolve out of a population of possible candidate rules by the ► [Darwinian](#) principles of variation and selection. CA have thus been used as a simple and easy to implement model for studying phenomena of interest in several scientific fields, including physics, biology, engineering, and computer science.

Future Directions

In summary, CA suggest a new approach in which complex behavior arises in a bottom-up manner from nonlinear, spatially extended, local interactions and provide a simple and useful model for many complex systems arising in the sciences and in engineering.

CA exhibit massive parallelism, locality of cellular interactions, and simplicity of basic hardware components. As a consequence, in recent years, there has been a growing interest in the utilization of CA as actual embedded computing devices, e.g., in low-level vision, pseudorandom number generation, and cryptography (Chaudhuri et al. 1997). A trend that could become important in the future is the search for practical quantum computing CA devices, a concept that is potentially capable of revolutionizing computation and its applications; quantum cellular automata belong to this class (Pérez-Delgado and Cheung 2007).

See also

- [Autopoiesis](#)
- [Biological Networks](#)
- [Chaotic Region \(Chaos\)](#)
- [Self Replication](#)

References and Further Reading

- Chaudhuri PP, Chowdhury DR, Nandi S, Chattopadhyay S (1997) Additive cellular automata: theory and applications. IEEE Computer Society, Los Alamitos, CA
- Chopard B, Droz M (1998) Cellular automata modeling of physical systems. Cambridge University Press, Cambridge

- Crutchfield JP, Mitchell M, Das R (2003) Evolutionary design of collective computation in cellular automata. In: Crutchfield JP, Schuster P (eds) Evolutionary dynamics: exploring the interplay of selection, Accident, neutrality, and function. Oxford University Press, Oxford, pp 361–411
- Fredkin E, Toffoli T (1982) Conservative logic. *Int J Theor Phys* 21:219–253
- Frisch U, Hasslacher B, Pomeau Y (1986) Lattice-gas automata for the Navier-Stokes equation. *Phys Rev Lett* 56:1505–1508
- Margolus N (1984) Physics-like models of computation. *Phys D* 10:81–95
- Pérez-Delgado C, Cheung D (2007) Local unitary quantum cellular automata. *Phys Rev A* 76:032320
- Sipper M (1997) Evolution of parallel cellular machines: the cellular programming approach. Springer-Verlag, Heidelberg
- Toffoli T (1980) Reversible computing. In: De Bakker JW, Van Leeuwen J (eds) Automata, languages and programming. Springer-Verlag, Berlin, pp 632–644
- Toffoli T (1984) Cellular automata as an alternative to (rather than an approximation of) differential equations in modeling physics. *Phys D* 10:117–127
- Vichniac G (1984) Simulating physics with cellular automata. *Phys D* 10:96–115
- Von Neumann J (1966) Theory of self-reproducing automata. University of Illinois Press, Illinois. Edited and completed by Burks AW
- Wolfram S (1994) Cellular automata and complexity. Addison-Wesley, Reading

Cellular Theory, History of

STÉPHANE TIRARD

Faculté des Sciences et des Techniques de Nantes, Centre François Viète d'Histoire des Sciences et des Techniques EA 1161, Nantes, France

Keywords

Chromosomes, globules

Abstract

The cellular theory was produced in two steps by Schleiden and Schwann (1838–1839) and then by Remak (1855) and Virchow (1855–1858). This theory claimed that cells were universal and microscopic entities, constituting living beings and that a cell was always produced by the division of another cell. Since that period up to now, the cell has become a central concept in biology.

History

The cellular theory was formulated after more than one and a half century of microscopic observations. Indeed,

the invention of microscope during the seventeenth century offered new investigations to naturalists. Robert Hooke (1635–1703) in his *Micrographia* (1665), Antoni van Leeuwenhoek (1632–1723), Jan Swammerdam (1737–1780). . . observed microscopical objects: individual entities, often named animalcules, and parts of organisms. However, they did not have concepts to consider all these new observations. For example, it is important to notice that when Hooke used the word cell to name some little spaces that he had observed in vegetable organism he did not expect to conceptualize anything, his intention was only descriptive.

During all the eighteenth century, microscopic observations were more and more accurate. They showed a broad diversity of animalcules and microscopic structures in living beings. At the beginning of the nineteenth century, some theories claimed that there could be a unity in the microscopic structure. The French botanist Charles-François Brisseau de Mirbel (1776–1854) suggested that plants were constituted by a set of membranes with a lot of pores. A few years later, René Joachim Henri Dutrochet (1776–1847), who had discovered the osmotic phenomenon, claimed that cells constituted plants. However, in the wall of these cells there could be some little globules that could be the fundamental entities. Then, François-Vincent Raspail (1794–1878) (the inventor of the microscopic colorations) considered that living beings were made of globules that were to be formed in the wall of other globules which would fit into each other.

In the period? Lorenz Okenfuss (Oken) (1779–1851) claimed that living beings were a synthesis of infusorians. All these proposals have in common the fact that they are conceptions about the possibility of a microscopic and universal structure.

In 1838, the German botanist Matthias Schleiden (1804–1881) claimed that vegetable organisms were composed of cells in which there was a systematic structure, the cytoblast (that will be later named nucleus). Besides, Schleiden suggested that cells were the result of the accumulation of a liquid, the cytoblastem, between the cytoblast and the membrane. His colleague, Theodor Schwann (1810–1882), a specialist of animal physiology, generalized this theory to animals and indicated that the cytoblastem came from the interstitial fluid.

During the 1850s, Robert Remak (1815–1865) and Rudolph Virchow (1821–1902) independently (Remak in 1855 and Virchow in 1855–1858) asserted that every cell was the result of the division of a previous cell. From this time forth, the concept of cell has become central in biology.

During the end of the nineteenth century, the progress of microscopy led to observations of chromosomes and to the description of mitosis (Fleming 1882) and meiosis (Boveri, Hertwig 1887–1892).

See also

- ▶ [Cell](#)
- ▶ [Protoplasmic Theory of Life](#)
- ▶ [Spontaneous Generation \(History of\)](#)

References and Further Reading

Duchesneau F (1987) *Genèse de la théorie cellulaire*. Bellarmin-Vrin, Paris

Cenancestor

Synonyms

[Last universal common ancestor](#)

Definition

The cenancestor is the most recent ancestor from which all currently living species have evolved. The idea that all present day life could be related by common ancestry was already suggested by Charles Darwin in *The Origin of the Species* (1859). Nowadays, this hypothesis is strongly supported by the similarities at the biochemical and genetic level of all organisms belonging to the three domains. However, the nature of this ancestral entity continues to be a matter of debate. Its level of complexity (in number of genes in its genome), the chemical nature of its genome (whether DNA or RNA), or its prokaryotic-like nature have been discussed along with other aspects of its biology.

See also

- ▶ [Common Ancestor](#)
- ▶ [Darwin's Conception of Origins of Life](#)
- ▶ [Domain \(Taxonomy\)](#)
- ▶ [Homology](#)
- ▶ [Last Universal Common Ancestor](#)
- ▶ [Phylogeny](#)

Centaur (Asteroids)

Definition

The Centaur are outer ▶ [asteroids](#) whose orbits are mostly confined between those of Jupiter and Neptune.

Due to giant planets' perturbations, these objects have transient orbits with typical lifetimes of a few million years. There are a few tens of Centaurs presently known, among them (2060) Chiron (also named 95P/Chiron), (5145) Pholus, and (10199) Chariklo, the biggest Centaur found to date with a diameter of 260 km. Saturn's satellite Phoebe is believed to be a captured Centaur. This population appears to be intermediate between asteroids and ► [comets](#), as any Centaur coming close enough to the Sun is expected to show cometary activity.

See also

- [Asteroid](#)
- [Comet](#)
- [Kuiper Belt](#)
- [Trans-Neptunian Object](#)

Center of Mass

- [Barycenter](#)

Center of Mass Velocity

Synonyms

[Barycenter velocity](#)

Definition

The center of mass velocity of a system of masses is the velocity of the point where the resultant force of gravitational attraction acts. The system's whole mass can be considered to be concentrated at this point, for the purpose of calculations. The motion of the center of mass of an object in free fall is the same as the motion of a point object located there.

Centre National d'études Spatiales

- [CNES](#)

Ceres

RALF JAUMANN

German Aerospace Center (DLR), Institute of Planetary Research, Berlin, Germany

Department of Earth Sciences, Institute of Geosciences, Remote Sensing of the Earth and Planets, Freie Universität Berlin, Germany

Keywords

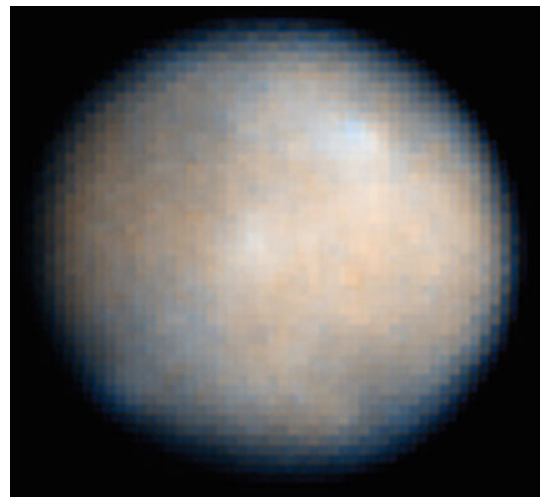
Asteroid, dwarf planet, Dawn mission

Definition

Discovered in 1801 by Guiseppe Piazzi, 1Ceres is the largest and one of the oldest and most intact objects in the ► [asteroid belt](#), cataloged by the IAU as a ► [dwarf planet](#) in 2006. Ceres orbits the ► [Sun](#) at a distance of 2.77 AU and differs from any other ► [asteroid](#) visited so far. Its surface seems to be covered with ice and ► [clay](#), a hydrated ► [rock](#) alteration product, and might have regions covered with frost. This is consistent with thermal models making Ceres an icy object that has been subject to ► [differentiation](#) and hydrothermal activity, and that might host a liquid subsurface layer even today.

Overview

1Ceres ([Fig. 1](#)) is an oblate spheroid with an equatorial radius of 487 ± 2 km and a polar radius of 455 ± 2 km, a mass of $(9.43 \pm 0.05) \cdot 10^{20}$ kg, a density of $2,077 \text{ kg/m}^3$,



Ceres. **Figure 1** Hubble Space Telescope image of Ceres, January 24, 2004 (NASA; HST ACS/HRC)

a rotation period of ~ 9 h, and an orbital period of 4.6 years (Thomas et al. 2005; McCord and Sotin 2005). The physical properties of Ceres are consistent with a rocky ► **core** and a thick outer ► **mantle** of ► **water ice** and possibly even a global ocean of water beneath that ice (McCord and Sotin 2005). Its surface temperatures vary with latitude from 130 K at the poles to 180 K at the equator, reaching a maximum of 235 K (cf. Castillo-Rogez and McCord 2009; Li et al. 2006). This is greater than any creep temperature for known icy compositions, implying Ceres' icy shell to be in ► **hydrostatic equilibrium**. Surface ► **albedo** varies from ~ 0.04 to ~ 0.09 (Li et al. 2006), which is suggestive of surface processes such as tectonics and impact cratering, although no specific geological feature has been identified at the surface of Ceres so far (besides some bright and dark spots that move with Ceres' rotation) (Thomas et al. 2005; Li et al. 2006).

Ceres is classified as a C- or G-type asteroid, sharing similarities with ► **carbonaceous chondrites**. Microwave dielectric measurements suggest that Ceres is covered with dry clay-like material at least 3 cm thick (Webster et al. 1988). Thermal emission spectroscopy also indicates the presence of iron-poor olivine, implying the presence of dry silicate, possibly on top of ► **phyllosilicates** (Witteborn et al. 2000). Spectral signatures of ► **carbonates** and iron-rich phyllosilicates have also been identified on the surface of Ceres and are distributed globally in constant amount throughout the surface (Rivkin et al. 2006). A 3–4 μm feature is attributed to ► **ammonia** bearing clay, either ammoniated saponite or montmorillonite (King et al. 1992; Rivkin et al. 2006) implying temperatures since formation of less than 400 K.

Models constrained by the thermal and compositional conditions demonstrate that Ceres almost certainly differentiated, involving processes such as the formation of a silicate core, a liquid water mantle, and a solid ice crust and crustal evolution by tectonics and probable ► **cryovolcanism** (Castillo-Rogez and McCord 2009). Ceres' relatively thin ► **hydrosphere** might imply a connection between endogenic activity and features on the surface, indicating some remarkably recent processes and some astrobiological potential.

Ceres will be explored in detail by the Dawn mission (launched 2007) (Russell et al. 2007) that will orbit Ceres for 9 months in 2015.

See also

- **Albedo**
- **Albedo Feature**
- **Ammonia**

- **Asteroid**
- **Asteroid Belt, Main**
- **Carbonaceous Chondrite**
- **Carbonate (Extraterrestrial)**
- **C-Asteroid**
- **Clay**
- **Core, Planetary**
- **Crater, Impact**
- **Crust**
- **Cryovolcanism**
- **Differentiation (Planetary)**
- **Dwarf Planet**
- **Heat Flow (Planetary)**
- **Heat Transfer (Planetary)**
- **Hydrosphere**
- **Hydrostatic Equilibrium**
- **Hydrothermal Environments**
- **Interior Structure (Planetary)**
- **Mantle**
- **Minor Planet**
- **Phyllosilicates (Extraterrestrial)**
- **Primordial Heat**
- **Regolith (Planetary)**
- **Rock**
- **Rotation Planet**
- **Silicate Minerals**
- **Space Weathering**
- **Sun (and Young Sun)**
- **Water**
- **Water Activity**

References and Further Reading

- Castillo-Rogez JC, McCord TB (2009) Ceres' evolution and present state constrained by shape data. *Icarus* 203:443–459. doi:10.1016/j.icarus.2009.04.008
- King TVV, Clark RN, Calvin WM, Sherman DM, Brown RH (1992) Evidence for ammonium-bearing minerals on Ceres. *Science* 255:1551–1553
- Li J-Y, McFadden LA, JWm P, Young EF, Stern SA, Thomas PC, Russell CT, Sykes MV (2006) Photometric analysis of 1 Ceres and surface mapping from HST observations. *Icarus* 182:143–160
- McCord TB, Sotin C (2005) Ceres: evolution and current state. *J Geophys Res* 110:E05009
- Rivkin AS, Volquardsen EL, Clark BE (2006) The surface composition of Ceres: discovery of carbonates and iron-rich clays. *Icarus* 185:563–567
- Russell CT, Capaccioni F, Coradini A, de Sanctis MC, Feldman WC, Jaumann R, Keller HU, McCord TB, McFadden LA, Mottola S, Pieters CM, Prettyman TH, Raymond CA, Sykes MV, Smith DE, Zuber MT (2007) Dawn mission to Vesta and Ceres. *Earth Moon Planets* 101:65–91
- Thomas PC, JWm P, McFadden LA, Russell CT, Stern SA, Sykes MV, Young EF (2005) Differentiation of the asteroid Ceres as revealed by its shape. *Nature* 437:224–226



Webster WJ, Johnston KJ, Hobbs RW, Lamphear ES, Wade CM, Lowman PD, Kaplan GH, Seidelmann PK (1988) The microwave spectrum of asteroid ceres. *Astron J* 95:1263–1268. doi:10.1086/114722

Witteborn FC, Roush TL, Cohen M (2000) Thermal emission spectroscopy of 1 Ceres: evidence for olivine, thermal emission spectroscopy and analysis of dust, disks, and regoliths. In: Sitko ML, Sprague AL, Lynch DK (eds) *Proceedings of a meeting held at LPI April 1999*: Astronomical Society of the Pacific Conference Series, vol 196, pp 197–203

Cerium (Anomalies of)

Definition

Cerium (Ce) is the second rare-earth element (REE), most of which are trivalent at the conditions prevalent in the mantle, the crust, and planetary surfaces. In the modern ocean, the redox boundary between trivalent and tetravalent Ce is close enough to the O_2-H_2O equilibrium that a substantial fraction of this element is oxidized and rapidly scavenged by Fe and Mn oxides. Excess Ce with respect to adjacent REE La and Pr is common in Mn nodules and encrustations, which leaves seawater, phosphates, and carbonates with a deficit. Cerium anomalies in sediments and sedimentary rocks are useful proxies for the state of oxidation in the ocean and the atmosphere in the past.

See also

- ▶ Chert
- ▶ Great Oxygenation Event
- ▶ Ocean, Chemical Evolution of
- ▶ Oxygenation of the Earth's Atmosphere

CH

- ▶ Methylidyne

CH⁺

- ▶ Methylidyne Cation

CH₂

- ▶ Methylene

CH₃

- ▶ Methyl Radical

CH₂CHCN

- ▶ Vinyl Cyanide

CH₃CCH

- ▶ Propyne

CH₃CH₂CHO

- ▶ Propionaldehyde

CH₃CH₂CN

- ▶ Ethyl Cyanide

CH₃CHCH₂

- ▶ Propylene

CH₃CN

- ▶ Acetonitrile

CH₃OCH₃

- ▶ Dimethyl Ether

CH₃SH

- ▶ [Methanethiol](#)

CH₄

- ▶ [Methane](#)

Chalcedony

- ▶ [Chert](#)

Chalcophile Elements

Definition

In the Berzelius–Goldschmidt classification, *chalcophile elements* are elements with a low affinity for oxygen and which preferentially bond with sulfur to form sulfides. Their name derives not from sulfur, but from copper, which also forms sulfides. This group comprises transition elements (Cu, Zn, Cd, Ag, Hg), heavy metals (Ga, In, Sn, Pb, Po, Bi, Tl), and metalloids (Ge, S, Sb, Se, Te, As). As a consequence of their relatively low condensation temperatures (500–1100 K), most of these elements are depleted in terrestrial planets with respect to chondrites.

See also

- ▶ [Lithophile Elements](#)
- ▶ [Siderophile Elements](#)

Chance and Randomness

FRANCESCA MERLIN

University of Paris-Sorbonne, Paris, France

Synonyms

[Haphazardness](#); [Indeterminacy](#); [Stochasticity](#); [Uncertainty](#)

Keywords

Chance, determinism, indeterminism, probability, randomness, unpredictability

Definition

Chance and randomness are usually considered as synonymous; however, they can have different meanings, in several scientific fields as in everyday contexts. In particular, chance has a broader scope than randomness, the latter being often interpreted according to more specific mathematical connotations. Broadly speaking, both are used to qualify events that are unpredictable in the sense that they have no particular aim or direction (unbiased events), and that they occur in an irregular and disordered (haphazard) way which makes it difficult to make money betting.

Overview

Chance is a double-faced notion including subjective chance, which concerns our knowledge of real events, and objective chance, which refers to an inherent property of the structure of the world, independently of our knowledge. Chance and randomness are often used as counterparts to determinism: a random process is said to be non-deterministic in the sense that, from a set of starting conditions, it can produce different outcomes according to some law of probability. However, neither notion is necessarily incompatible with the assumption of determinism. Subjective chance, when defined as ignorance of the real underlying causes, implies that there is no chance in the real world, but for human knowledge: for instance, we might assign a 50% chance to both possible outcomes of the flip of a fair coin (“heads” and “tails”) because we ignore the underlying causes (e.g., the way the coin is flipped). This recalls the Laplacian notion of chance, which is a deterministic notion; nevertheless, subjective chance is also compatible with indeterminism in so far as the underlying causes that we do not know about might still be the result of an indeterministic process. Objective chance can refer to an event that is not planned (or by design), as in Aristotle’s accidental meeting with the person who owed him money. This notion implies the confluence of two or more independent causal chains: in this sense, Cournot claimed that the fact that two brothers serving in different armies died the same day is a matter of chance. Chaotic processes provide an example of chance as sensitivity to initial conditions in the sense that small differences in initial conditions may yield radically different outcomes. Whereas all notions of chance mentioned above are noncommittal to determinism nor indeterminism, this is not the case for chance according to the Copenhagen interpretation of quantum mechanics,

according to which indeterminism is considered a true description of the microlevel world. Randomness mostly has a mathematical connotation, like in algorithmic information theory where a binary sequence is said to be Kolmogorov-random if and only if it is incompressible, i.e., it is shorter than any computer program that can produce it. Other formal definitions of a random sequence (e.g., Martin-Löf's) have been recently formulated, each of which tries to capture our intuitive notion of randomness.

See also

- ▶ [Materialism](#)
- ▶ [Physicalism](#)
- ▶ [Reductionism](#)
- ▶ [Vitalism](#)

References and Further Reading

- Aristotle (1984) *Physics*. In: Barnes J (ed) *The complete works of Aristotle*, vol I and II. Princeton University Press, Princeton
- Calude CS (ed) (2007) *Randomness and complexity from Leibniz to Chaitin*. World Scientific, Singapore
- Cournot AA (1843) *Exposition de la Théorie des Chances et des Probabilités*. Hachette, Paris
- Earman J (1986) *A primer on determinism*. D. Reidel Publishing, Dordrecht
- Hacking I (1995) *The taming of chance*. Cambridge University Press, Cambridge, 1990
- Heisenberg W (1958) *Physics and philosophy*. Harper, New York
- Laplace P-S (1814) *A philosophical essay on probabilities* (English edition: Laplace P-S 1951). Dover, New York
- Martin-Löf P (1966) The definition of random sequences. *Inf Control* 9:602–619
- Poincaré H (1921) *The foundations of science: science and hypothesis, the value of science, science and method* (trans: Halsted GB). The Science Press, New York

Chandrasekhar's Limit

Definition

Chandrasekhar's limit, named after the Indian astrophysicist Subrahmanyan Chandrasekhar, is a critical mass of about 1.4 solar masses that the core of a star can attain, before collapsing to become a neutron star or a black hole. This core is built from the heavy elements that the star synthesizes during its lifetime through nuclear fusion. Beyond this critical mass, the relativistic electron degeneracy pressure is unable to counteract the gravitational forces. Stars with mass higher than 8 solar mass develop

a degenerate core, whose mass will grow until it exceeds this limit, leading to a ▶ [supernova](#) explosion.

See also

- ▶ [Supernova](#)
- ▶ [White Dwarf](#)

Channels

- ▶ [Valley Networks](#)

Chaotic Region (Chaos)

Synonyms

[Chaotic terrains](#)

Definition

A chaotic region is a distinctive area of broken terrain. They are characterized by a textured matrix featuring mesas and knobs. Chaoses can be primarily found on ▶ [Mars](#) in a region called “Chaotic Terrains.” The latter is located east of ▶ [Valles Marineris](#) and represents parts of the huge ▶ [outflow channel](#) floors. The Martian chaoses are thought to have formed from disruption and collapse of an icy ▶ [Permafrost](#) layer initiated by pressurized groundwater. However, the formation of these regions is still debated. Chaos regions can also be found on ▶ [Jupiter's moon](#) ▶ [Europa](#), which are suggested to be sites of melt-through from the subsurface.

See also

- ▶ [Europa](#)
- ▶ [Jupiter](#)
- ▶ [Mars](#)
- ▶ [Outflow Channels](#)
- ▶ [Permafrost](#)
- ▶ [Valles Marineris](#)

Chaotic Terrains

- ▶ [Chaotic Region \(Chaos\)](#)



Characterization of Microfossils

- ▶ [Microfossils, Analytical Techniques](#)

Charge Coupled Device

- ▶ [CCD](#)

Charge Exchange

- ▶ [Charge Transfer](#)

Charge Transfer

STEVEN B. CHARNLEY

NASA Goddard Space Flight Center, Solar System Exploration Division, Code 691, Astrochemistry Laboratory, Greenbelt, MD, USA

Synonyms

[Charge exchange](#)

Keywords

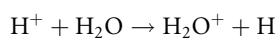
Chemical reactions

Definition

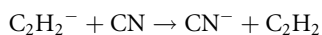
Charge transfer is a chemical process whereby charge is transferred from a positive or negative ion (cation or ▶ [anion](#)) to a neutral atom or molecule.

Overview

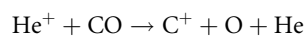
Simple charge transfer reactions between atomic ions and neutral atoms and molecules are important in many astronomical environments, ranging from ▶ [planetary nebulae](#) to ▶ [comets](#), to dark ▶ [molecular clouds](#). Reactions of the type



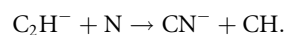
and



are ▶ [exothermic](#), rapid, and proceed with no molecular rearrangement. On the other hand, dissociative charge transfer reactions involve the breaking of chemical bonds, examples of which are:



and



See also

- ▶ [Anions](#)
- ▶ [Comet](#)
- ▶ [Exothermic](#)
- ▶ [Molecular Cloud](#)
- ▶ [Planetary Nebula](#)

References and Further Reading

Millar TJ, Williams DA (eds) (1988) *Rate coefficients in astrochemistry*. Kluwer, Dordrecht

Charon

Definition

Charon, discovered in 1978 by James Walter Christy, is orbiting around ▶ [Pluto](#) at a distance of 19,640 km or 17 Pluto radii. The orbital period of the Pluto-Charon system is 6.4 days. Its diameter is 1,206 km and its density is 1.8 g/cm³. With a mass ratio of about 9, both Pluto and Charon can be considered as parts of a Pluto-Charon system. Charon's properties have been studied through photometry during mutual eclipses and transits and stellar occultations. Unlike Pluto's, the surface of Charon is mostly made of water ice with no evidence of atmosphere. Numerical simulations indicate that Charon was formed after a giant impact that took place some 4.5 Gy ago, in a scenario comparable to the Earth-Moon formation.

See also

- ▶ [Kuiper Belt](#)
- ▶ [Pluto](#)
- ▶ [Trans-Neptunian Object](#)

Chasma, Chasmata

Synonyms

[Canyon](#)



Definition

A chasma (plural: chasmata) is a broad, deep, elongate trough or depression. Chasmata are bounded by steep scarps that can form a series of terraces. A chasma is preferentially created by extensional tectonic forces. On the ► [terrestrial planets](#), ► [Venus](#) and ► [Mars](#) have a large number of chasmata. In the outer ► [Solar System](#), chasmata are major surface features on the icy ► [satellites](#) of ► [Saturn](#) and ► [Uranus](#).

See also

- [Fossa, Fossae](#)
- [Mars](#)
- [Rima, Rimae](#)
- [Rupes, Rupēs](#)
- [Satellite or Moon](#)
- [Saturn](#)
- [Solar System Formation \(Chronology\)](#)
- [Sulcus, Sulci](#)
- [Terrestrial Planet](#)
- [Uranus](#)
- [Venus](#)

Chemical Adsorption

- [Chemisorption](#)

Chemical Bistability

Definition

Chemical Bistability in astrochemistry refers to the existence of multiple steady states known to occur in chemical models of dense interstellar clouds. For certain combinations of model (control) parameters (cosmic ray ionization rate, elemental depletions, etc.), three steady states can appear, comprising two stable states connected by an unstable one; i.e., the solutions exhibit hysteresis.

History

Chemical bistability in astrochemical models was first positively identified by Le Bourlot et al. (1993).

See also

- [Molecular Cloud](#)

References and Further Reading

Le Bourlot J, Pineau des Forets G, Roueff E, Schilke P (1993) Bistability in dark cloud chemistry. *Astrophys J* 416:L87–L91

Chemical Evolution

ANDRÉ BRACK

Centre de Biophysique Moléculaire CNRS, Orléans
cedex 2, France

Synonyms

[Prebiotic chemistry](#)

Keywords

Autotrophic life, cellular world, primitive life, primordial soup, RNA world

Definition

Chemical evolution refers to the suite of natural reactions that led to the first living systems from abiotically synthesized molecules on the primitive Earth. Since this was a historical process, and we have no relics of the compounds formed in this process, chemists can only model chemical evolution by running experiments, chemical reconstructions also known as prebiotic chemistry.

Overview

Although primitive life is generally believed to have been organic, that is, based on ► [carbon](#) chemistry, the precise sequence of steps that allowed for the formation of living systems from abiotic chemistry remains poorly constrained and somewhat speculative. Chemical evolution is the study of the processes that led from simple molecules to biochemistry.

There are presently numerous scenarios for this process which scientists consider plausible. Among them is the idea that a genetic mineral material presenting suitable properties such as the ability to store and replicate information has been proposed (Cairns-Smith 1982). Another hypothesis favors a heterotrophic origin of life in a “► [primordial soup](#),” involving self-assembling, preformed carbon-based molecules. An autotrophic origin of life via direct reduction of carbon oxides in a “metabolism first” scenario has also been proposed (Wächtershäuser 2007).

While it is clear that all contemporary life shares a common heritage, it is possible that there were earlier, more primitive states that life evolved through which might have borne little resemblance to modern

biochemistry. Some believe that primitive life emerged as a cell-like system requiring at least pre-RNA molecules capable of storing and transferring the information needed for reproduction, pre-enzymes providing the basic chemical work, and pre-membranes able to isolate the system from the aqueous environment. Since RNA has been shown to be able to act as an information molecule and also as a catalytic molecule, RNA has been considered as a candidate for the first living system that preceded the cellular world. The spontaneous organization of amphiphilic molecules to form vesicles has also been postulated as the first step toward the origin of life (Harold Morowitz 1992). Chemists are also tempted to consider that primitive self-replicating systems depended on simple autocatalytic molecules adsorbed on solid surfaces, which could solve some of the problems of the likely high dilution of organics in the primitive oceans.

See also

- ▶ [Abiotic](#)
- ▶ [Carbon](#)
- ▶ [Chronological History of Life on Earth](#)
- ▶ [Origin of Life](#)
- ▶ [Prebiotic Chemistry](#)
- ▶ [Primordial Soup](#)
- ▶ [RNA World](#)

References and Further Reading

- Cairns-Smith AG (1982) Genetic takeover. Cambridge University Press, Cambridge
- Morowitz H (1992) Beginnings of cellular life. Yale University Press, New Haven/London
- Wächtershäuser G (2007) On the chemistry and evolution of the pioneer organism. *Chem Biodiv* 4:584–602

Chemical Fossil

- ▶ [Biomarkers](#)

Chemical Reaction Network

RAPHAËL PLASSON
Nordita, Stockholm, Sweden

Synonyms

[Automaton](#), [Chemical](#); [Chemical system](#); [Reaction network](#)

Keywords

Metabolism, stoichiometric matrix

Definition

A chemical reaction network consists of a set of chemical reactions and a set of chemical compounds. Each chemical compound is a node of the network. Each chemical reaction is a directed vertex of the network, connecting the chemical compounds involved in the reaction, from the reactants towards the products.

Overview

A complex chemical system can contain a large number of chemical compounds, involved in a large number of chemical reactions. This system forms a chemical reaction network that can be studied as a whole, rather than being simply considered as the sum of its different elements.

A reaction network is typically described by its stoichiometric matrix v . The $v_{i,j}$ element is the stoichiometric coefficient of the compound i in the reaction j , i.e., the number of molecule of i that is involved in the reaction j . This number is by convention negative for the reactants (that are disappearing) and positive for the products (that are formed). The mathematical analysis of this matrix gives information about the structure of the reaction network (Schilling et al. 2000). The identification of matter fluxes and of patterns of mass conservation leads to the description of the reaction network in terms of transformation pathways (Papin et al. 2004) and of conserved moieties (Schuster and Hilgetag 1995). This mathematical analysis only gives static information about the reaction network. Adding the kinetic data relative to each chemical reaction allows establishment of the set of ordinary differential equations (ODE) describing the reaction network. Its numerical integration gives the dynamical behavior of the system (Alves et al. 2006).

The description of chemical reaction networks is used in very different fields. This is typically the case of biosystems, especially for the description of ▶ [metabolism](#) (Schuster and Hilgetag 1995; Schilling et al. 2000; Papin et al. 2004; [Metabolism databases](#)), but also in abiotic systems as in astrochemistry (Woodall et al. 2007), combustion modeling (Manion et al. 2008), etc. The precise description of these complex chemical systems generally relies on the existence of extensive databases, summing up thermodynamic and kinetic data.

In the field of astrobiology, ▶ [prebiotic chemistry](#) can be seen as a bridge between ▶ [abiotic](#) and biotic chemical reaction networks. The purpose is to understand how a reaction network consisting of very simple compounds can spontaneously evolve into a more complex and

structured network, and how complex behaviors can be generated by the association of several simple reactions (e.g., network ► [autocatalysis](#), energy coupling, ► [self-replication](#), etc.) (Wagner and Ashkenasy 2009).

See also

- [Automaton, Chemical](#)
- [Chemical Evolution](#)
- [Cosmochemistry](#)
- [Interstellar Chemical Processes](#)
- [Metabolism \(Biological\)](#)
- [Prebiotic Chemistry](#)

References and Further Reading

- Alves R, Antunes F, Salvador A (2006) Tools for kinetic modeling of biochemical networks. *Nat Biotechnol* 24:667–672
- Manion JA, Huie RE, Levin RD, Burgess DR Jr, Orkin VL, Tsang W, McGivern WS, Hudgens JW, Knyazev VD, Atkinson DB, Chai E, Tereza AM, Lin CY, Allison TC, Mallard WG, Westley F, Herron JT, Hampson RF, Frizzell DH (2008) NIST chemical kinetics database. National Institute of Standards and Technology, Gaithersburg, <http://kinetics.nist.gov/>
- Metabolism databases: KEGG, <http://www.genome.ad.jp/kegg/reaction/>; Biocyc, <http://biocyc.org/>; UniPathway, <http://www.grenoble.prabi.fr/obiwarehouse/unipathway>
- Papin JA, Stelling J, Price ND, Klamt S, Schuster S, Palsson BO (2004) Comparison of network-based pathway analysis methods. *Trends Biotechnol* 22:400–405
- Schilling C, Letscher D, Palsson BO (2000) Theory for the systemic denition of metabolic pathways and their use in interpreting metabolic function from a pathway-oriented perspective. *J Theor Biol* 203:229–248
- Schuster S, Hilgetag C (1995) What information about the conserved-moiety structure of chemical reaction systems can be derived from their stoichiometry? *J Phys Chem* 99:8017–8023
- Wagner N, Ashkenasy G (2009) Symmetry and order in systems chemistry. *J Chem Phys* 130:164907
- Woodall J, Agúndez M, Markwick-Kemper AJ, Millar TJ (2007) The UMIST database for astrochemistry 2006. *Astron Astrophys* 466:1197–1204

Chemical System

- [Chemical Reaction Network](#)

Chemical Zones

- [Redox Zonation](#)

Chemiosmotic Potential

- [Proton Motive Force](#)

Chemisorption

Synonyms

[Chemical adsorption](#)

Definition

Chemisorption involves the formation of covalent chemical bonds between an adsorbed atom or molecule (or its dissociation products) and the molecules present in a solid surface, such as that of an interstellar grain. This strong bonding contrasts with the weaker bonding during ► [physisorption](#).

See also

- [Adsorption](#)
- [Interstellar Dust](#)
- [Physisorption](#)

Chemoautotroph

Definition

Chemoautotrophs are organisms that obtain their energy from a chemical reaction (chemotrophs) but their source of carbon is the most oxidized form of carbon, carbon dioxide (CO₂). The best known chemoautotrophs are the chemolithoautotrophs that use inorganic ► [energy sources](#), such as ferrous iron, hydrogen, hydrogen sulfide, elemental sulfur or ammonia, and CO₂ as their ► [carbon source](#). All known chemoautotrophs are prokaryotes, belonging to the ► [Archaea](#) or ► [Bacteria](#) domains. They have been isolated in different extreme habitats, associated to deep-sea vents, the deep biosphere or acidic environments. This form of ► [energy conservation](#) is considered one of the oldest on Earth. These microorganisms are of astrobiological interest because they could develop in the extreme conditions existing in different extraterrestrial planetary bodies, like Mars or Europa.

See also

- [Acidophile](#)
- [Archea](#)
- [Autotroph](#)



- ▶ Autotrophy
- ▶ Bacteria
- ▶ Bioenergetics
- ▶ Carbon Source
- ▶ Chemolithoautotroph
- ▶ Chemotroph
- ▶ Deep-Sea Microbiology
- ▶ Deep-Subsurface Microbiology
- ▶ Energy Conservation
- ▶ Energy Sources
- ▶ Extreme Environment
- ▶ Extremophiles
- ▶ Hot Vent Microbiology
- ▶ Iron Cycle
- ▶ Lithotroph
- ▶ Prokaryote
- ▶ Respiration

Chemolithoautotroph

Synonyms

Hydrogen-oxidizers; Iron-oxidizers; Nitrifying bacteria; Sulfur-oxidizers

Definition

A chemolithoautotroph is an autotrophic microorganism that obtains energy by oxidizing inorganic compounds. Most ▶ [chemolithotrophs](#) are autotrophs. Examples of relevant inorganic electron donors include hydrogen, hydrogen sulfide, ferrous iron, and ammonia. Winogradsky described the concept of chemolithoautotrophy for the first time while studying the ammonia-oxidizing bacteria. Chemolithoautotrophic organisms have ▶ [electron transport](#) complexes, similar to those of chemoorganotrophs, which are used to generate a ▶ [protein motive force](#). The proton motive force drives the synthesis of ATP. In this case, the reduction of CO₂ requires the use of ATP and reducing power, which is, most often, obtained through the use of the electron transport chain in reverse mode, consuming energy. Sulfur, iron, and ammonia oxidizers are fundamental elements in the biogeochemical cycles of these elements. Chemolithoautotrophic organisms are of special interest to astrobiology due to their minimal requirements for development and their ability to readily adapt to extreme conditions.

See also

- ▶ ATP Synthase
- ▶ Bioenergetics

- ▶ Carbon Dioxide
- ▶ Chemotroph
- ▶ Electron Transport
- ▶ Nitrification
- ▶ Proton Motive Force

Chemolithotroph

RICARDO AMILS

Departamento de Planetología y Habitabilidad
Centro de Astrobiología (CSIC-INTA), Universidad
Autónoma de Madrid Campus Cantoblanco, Torrejón de
Ardoz, Madrid, Spain

Synonyms

Chemolithotrophy

Definition

A chemolithotroph is an organism that is able to use inorganic reduced compounds as a source of energy. This mode of metabolism is known as chemolithotrophy.

History

▶ [Chemolithotrophy](#) was discovered by Winogradsky while studying the microorganisms involved in the oxidation of sulfur compounds.

Overview

Chemolithotrophy is found only in prokaryotes and is widely distributed among Bacteria and Archaea. The spectrum of inorganic compounds that can be used as ▶ [electron donors](#) by chemolithotrophs is rather broad (H₂S, S⁰, S₂O₃²⁻, H₂, Fe²⁺, NO₂⁻ or NH₃). Some microorganisms are rather specific regarding the inorganic substrates they can use to generate energy, while others are able to use different compounds (versatile). The best characterized chemolithotrophs are aerobic respirers, which use oxygen as the ▶ [electron acceptor](#), although the list of chemolithotrophs capable of employing ▶ [anaerobic respiration](#) is increasing rapidly. Chemolithotrophs have ▶ [electron transport](#) systems similar to those of ▶ [chemoorganotrophs](#), which are used for the generation of a ▶ [proton motive force](#). The only difference is that chemolithotrophs donate electrons directly to the electron transport chain, while chemoorganotrophs must generate cellular reducing power (▶ [NADH](#)) from the ▶ [oxidation](#) of reduced organic compounds, which are

then used to donate electrons to the electron transport system. This proton motive force is used to generate ATP or any cellular functions that might require this type of energy (active transport, movement, etc). An important distinction between chemolithotrophs and chemoorganotrophs is their source of carbon. Chemoorganotrophs use organic compounds as both energy and carbon sources, while chemolithotrophs are generally autotrophs (with few exceptions, known as mixotrophs, that use reduced organic compounds as a source of carbon). Chemolithotrophs can obtain the reducing power needed to assimilate CO₂ directly from the inorganic substrate (only H₂ oxidizers) or by the reverse electron transport reaction (the rest of chemolithotrophs), in this case using proton motive force as a source of energy.

Hydrogen is a common product of geochemical reactions and microbial metabolism, and a number of chemolithotrophs are able to use it as an electron donor in energy metabolism. A wide variety of anaerobic H₂-oxidizing Bacteria and Archaea are known, differing in the electron acceptor they use (nitrate, sulfate, ferric iron, etc).

The most common sulfur compounds used as electron donors are hydrogen sulfide (H₂S), elemental sulfur (S⁰), and thiosulfate (S₂O₃²⁻). The final product of sulfur oxidation is sulfate (SO₄²⁻), although an intermediate step is the formation of elemental sulfur, which in some cases is stored as an alternative source of energy. One of the products of sulfur oxidation reaction is the generation of protons (H⁺), consequently one result of the oxidation of reduced sulfur compounds is the acidification of the environment by the production of sulfuric acid.

The aerobic oxidation of ferrous iron (Fe²⁺) to ferric iron (Fe³⁺) is an energy-yielding reaction, used by some prokaryotes to conserve energy. Only a small amount of energy is generated by this reaction, thus iron-oxidizing microorganisms must oxidize large amounts of reduced iron to grow. Ferrous iron is oxidized very rapidly in the presence of oxygen, while it is very stable at acidic conditions. This is probably the reason why many iron-oxidizing microorganisms are acidophilic. Despite the instability of ferrous iron at neutral pH, there are a number of iron-oxidizing bacteria that can thrive at circumneutral pH. Some anoxygenic phototrophic bacteria can use ferrous iron as a source of environmental reducing power. Recently it has been shown that some denitrifying bacteria can anaerobically respire (oxidize) reduced iron. The use of ferrous iron to obtain energy is widely distributed in nature, a property that was ignored until recently, due to thermodynamic considerations.

The most common nitrogen compounds used as electron donors for energy conservation are ammonia (NH₃)

and nitrite (NO²⁻). Both compounds can be oxidized aerobically by chemolithotrophic nitrifying bacteria. Some nitrifying microorganisms oxidize ammonia to nitrite, while another group oxidizes nitrite to nitrate. The complete oxidation of ammonia requires the concerted activity of these two types of microorganisms. A special case of nitrogen-oxidizing microorganisms corresponds to those capable of carrying out the anoxic oxidation of ammonia, a process known as anamox. In this case the electron acceptor is nitrite, and the product of the metabolic reaction in addition to proton motive force is the generation of N₂. This metabolic reaction is carried out by a special type of microorganisms belonging to the Planctomycetes phylum of Bacteria.

Due to their metabolic properties, chemolithotrophs are of astrobiological interest and also critical elements of the ► [biogeochemical cycles](#).

See also

- [Acidophile](#)
- [Aerobic Respiration](#)
- [Anaerobic Respiration](#)
- [ATP Synthase](#)
- [Autotrophy](#)
- [Bioenergetics](#)
- [Biogeochemical Cycles](#)
- [Chemoautotroph](#)
- [Chemolithoautotroph](#)
- [Chemoorganotroph](#)
- [Electrochemical Potential](#)
- [Electron Acceptor](#)
- [Electron Carrier](#)
- [Electron Donor](#)
- [Electron Transport](#)
- [Energy Conservation](#)
- [Energy Sources](#)
- [Iron](#)
- [Iron Cycle](#)
- [NADH, NADPH](#)
- [Nitrogen Cycle \(Biological\)](#)
- [Oxidation](#)
- [Proton Motive Force](#)
- [Sulfur Cycle](#)

References and Further Reading

- Ehrlich HL, Newman DK (2009) *Geomicrobiology*, 5th edn. CRC Press, New York
- Fernandez-Remolar DC, Morris RV, Gruener JE, Amils R, Knoll AH (2005) The Rio Tinto basin, Spain: mineralogy, sedimentary geobiology, and implications for interpretation of outcrop rocks at Meridiani Planum, Mars. *Earth Planet Sci Lett* 240(1):149–167. doi:10.1016/j.epsl.2005.09.043

- González-Toril E, Gómez F, Malki M, Amils R (2006) Isolation and study of acidophilic microorganisms. In: Rainey F, Oren A (eds) *Methods in microbiology*, vol 35. Elsevier, Oxford, pp 463–502
- Leininger S, Urich T, Schloter M, Schwark L, Qi J, Nicol GW, Prosser JL, Schuster SC, Schleper C (2006) Archaea predominate among ammonia-oxidizing prokaryotes in soils. *Nature* 442:806–809
- Madigan MT, Martinko JM, Dunlap PV, Clark DP (2009) *Brock biology of microorganisms*, 12th edn. Benjamin Cummings
- Strous M, Fuerst JA, Kramer EH et al (1999) Missing lithotroph identified as new planctomycete. *Nature* 400(6743):446–449. doi:10.1038/22749
- Winogradsky S (1949) *Microbiologie du Sol*. Masson, Paris
- Yamanaka T (2008) Chemolithoautotrophic bacteria, *Biochemistry and Environmental Biology*, XIV. Springer, Japan

Chemolithotrophy

- ▶ [Chemolithotroph](#)
- ▶ [Lithotrophy](#)

Chemoorganotroph

Synonyms

[Fermentation](#); [Heterotrophs](#); [Respiration](#)

Definition

A chemoorganotroph is an organism that obtains energy from the oxidation of reduced organic compounds. The list of compounds from which chemoorganotrophic organisms can generate energy and their sources of carbon are very long, making these microorganisms extremely versatile. Two mechanisms for energy conservation are known for chemoorganotrophs: ▶ [fermentation](#) and ▶ [respiration](#). In the case of fermentation, cellular energy in the form of ATP is obtained by cytoplasmic soluble catalytic reactions involved in substrate-level phosphorylation. In the case of respiration, ATP is produced at the expense of the ▶ [proton motive](#) force resulting from coupling the substrate oxidation reactions via the generation of reducing power to the electron transport chain. Due to their type of metabolism, chemoorganotrophs are fundamental elements of the carbon cycle.

See also

- ▶ [Aerobic Respiration](#)
- ▶ [ATP Synthase](#)
- ▶ [Catabolism](#)
- ▶ [Chemotroph](#)
- ▶ [Energy Sources](#)
- ▶ [Proton Motive Force](#)

Chemotaxis

IRMA MARÍN

Departamento de Biología Molecular, Universidad Autónoma de Madrid, Madrid, Spain

Keywords

Motility, two components system

Definition

Chemotaxis is the process by which motile bacteria sense changes in their chemical environment and move to more favorable conditions.

Overview

Bacteria, Archaea, and some eukaryotes use two-component signaling pathways to detect environmental conditions and bring about appropriate changes in cellular behavior. This process has been studied in *Escherichia coli* over the past 40 years.

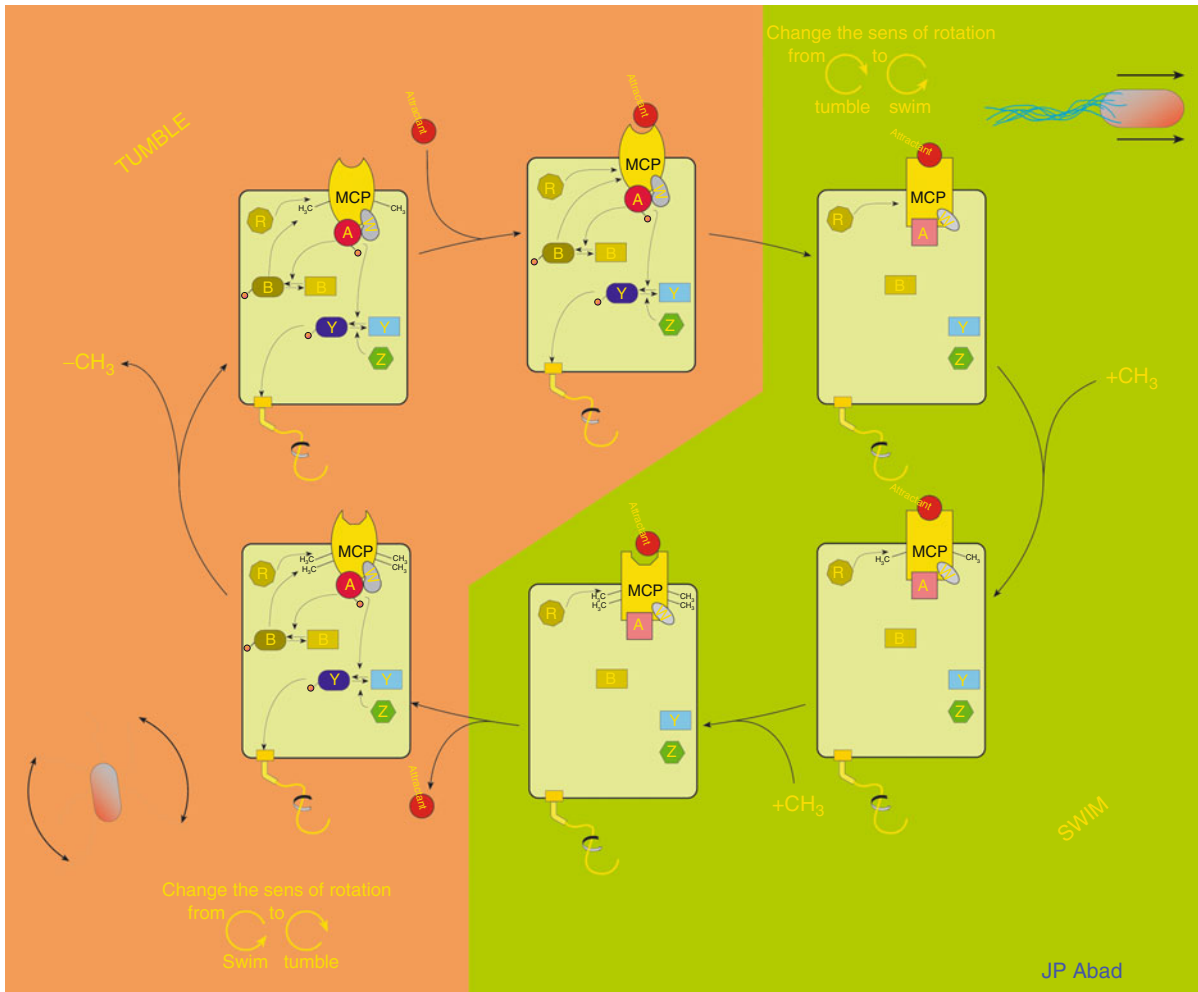
E. coli has several flagella per cell (4–19) that can rotate in two ways: counterclockwise (CCW) that aligns the flagella causing the bacterium to swim in a straight line, and clockwise (CW) that causes the bacterium to tumble since each flagellum rotates independently.

Bacteria monitor chemical concentrations using multiple transmembrane receptors, named methyl-accepting chemotaxis proteins (MCPs). Five MCP-mediating responses to specific attractant and repellent stimuli have been reported in *E. coli*: Tar, Tsr, Trg, Aer, and Tap. The signals from these receptors are transmitted across the cell membrane into the cytoplasm, where Che proteins (CheA, CheB, CheW, CheY, CheR, and CheZ) are activated.

Signals from the receptors are received by the CheA histidine kinase. CheA is coupled to transmembrane receptors (MCP) by the adaptor protein CheW. The activation of the receptor causes autophosphorylation of CheA that also phosphorylates CheB and CheY. CheY~P binds then to the flagellar motor protein FliM, inducing a change from CCW to CW rotation of flagella, thus increasing the frequency of tumbles of the bacterium (Fig. 1).

A feedback mechanism that modulates the methylation level of the MCP receptors controls adaptation. Two enzymes, CheB and CheR, are involved in this mechanism by interacting with the receptor and chemically modifying them.

CheB, activated by CheA, acts as a methylesterase that removes methyls from the cytoplasmic part of the



Chemotaxis. Figure 1 Model of chemotaxis mechanism as described in the text. A, B, R, W, Y, Z are CheA, CheB, CheR, CheW, CheY and CheZ proteins, respectively

receptor. It works antagonistically with CheR, which is a methyltransferase. The higher the amount of methylated residues of the receptor, the lower the sensitivity to stimuli. The result is an enhancement of CheA autophosphorylation and, thereby, transmission of a CW signal. When an attractant generates a signal, demethylation of the receptor is induced, closing the feedback loop.

The system is continuously adjusted to environmental chemical levels, remaining sensitive to small changes even under extreme chemical concentrations, since the system compares concentrations along the movement path. When necessary this is switched to go closer to, or further away from a higher concentration of attractant or a repellent, respectively. Other mechanisms are involved in increasing the absolute value of the sensitivity on

a given background. *E. coli*, but not *B. subtilis*; possesses the protein CheZ that enhances the rate of CheY dephosphorylation.

See also

► [Motility](#)

References and Further Reading

- Bren, Eisenbac M (2000) How signals are heard during bacterial chemotaxis: protein-protein interactions in sensory signal propagation. *J Bacteriol* 182:6865–6873
- Madigan, MT, Martinko JM, Dunlap PV, Brock DP (2008) *Biology of microorganisms*, 12 edn. Clark Benjamin Cumming, San Francisco
- Prescott, Harley, Klein (2007) *In Microbiology*, 7th edn. Willey, McGraw-Hill Science, New York

Chemoton

- ▶ [Automaton, Chemical](#)

Chemotroph

Definition

Chemotrophs are organisms that obtain energy by the oxidation of reduced compounds. The substrates used by chemotrophs can be organic (organotrophs) or inorganic compounds (lithotrophs). According to the carbon source, chemotrophs can be either chemoautotrophs or chemoheterotrophs. Because chemoheterotrophs use reduced organic compounds as a source of energy and a source of carbon, they are usually called heterotrophs, although the term is misleading because, strictly, it only refers to the carbon source. Chemoautotrophs use inorganic energy sources and are known as chemolithoautotrophs or lithoautotrophs. Chemolithoheterotrophs are a special kind of chemotroph that use inorganic compounds as an energy source and reduced organic compounds as a carbon source. They are known as mixotrophs. Chemotrophs use ▶ [fermentation](#) and ▶ [respiration](#) to obtain energy. Fermentation is restricted to organotrophs.

See also

- ▶ [Aerobic Respiration](#)
- ▶ [Anaerobic Respiration](#)
- ▶ [Autotrophy](#)
- ▶ [Bioenergetics](#)
- ▶ [Carbon Dioxide](#)
- ▶ [Chemoautotroph](#)
- ▶ [Chemolithoautotroph](#)
- ▶ [Chemolithotroph](#)
- ▶ [Chemolithotrophy](#)
- ▶ [Chemoorganotroph](#)
- ▶ [Energy Conservation](#)
- ▶ [Fermentation](#)
- ▶ [Respiration](#)

Chengjiang Biota, China

Definition

The Chengjiang biota is an assemblage of fossils first discovered in 1984 at Maotianshan, near Chengjiang, Yunnan Province, China, and dated to ca. 520 Ma, within

the Cambrian Period of geologic time. Exceptional preservation of soft-bodied marine organisms provides a rare, detailed view of Cambrian life, yielding insights into early animal evolution and the Cambrian explosion. The Chengjiang biota provides an early Cambrian counterpart to the exceptionally preserved biota of the middle Cambrian Burgess Shale, Canada.

See also

- ▶ [Burgess Shale Biota](#)
- ▶ [Cambrian Explosion](#)

Chert

TANJA ELSA ZEGERS

Faculty of Geosciences, Paleomagnetic Laboratory “Fort Hoofdijk”, Utrecht, CD, The Netherlands

Synonyms

[Chalcedony](#); [Flint](#); [Jasper](#)

Keywords

Archean, (micro)fossils, hydrothermal alteration, sediments

Definition

Chert is a microcrystalline rock consisting almost exclusively of silica. Chert may occur as stratiform units, with often-spectacular laminar alteration of colors (red, white, black, green), in dykes crosscutting the stratigraphy, or, in modern limestones, as nodules. Stratiform cherts in Archean greenstone belts represent the earliest sedimentary rocks, some of which preserve the oldest evidence for life (▶ [Apex Chert](#), ▶ [Pilbara Craton](#), Western Australia).

History

The oldest preserved chert units occur in the highly metamorphic and deformed 3.6–3.7 Ga supracrustal units of the ▶ [Isua Supracrustal Belt](#) in West Greenland (Nutman et al. 1984). The Isua cherts may have a sedimentary origin or may represent volcanic rocks that were hydrothermally altered and layered as a consequence of intense plastic deformation (Nutman and Friend 2009; Polat and Frei 2005). Trace elements indicate that the chert/▶ [banded iron formations](#) units have seawater-like signatures suggesting at least a component of sedimentary origin (marine chemical precipitate).

In both the ► **Pilbara** (Australia) and the ► **Barberton** (South Africa) greenstone belts, the oldest well-preserved volcanic sequences contain stratiform chert units (Byerly et al. 1996; Van Kranendonk et al. 2002) formed between 3.5 and 3.3 Ga. Despite the good preservation of the greenstone sequence, the origin of the stratiform chert units is still controversial. Van den Boorn et al. (2007) distinguished three different end-members of silica derivation on the basis of Si isotopic signatures: direct precipitation of silica from seawater on the seafloor; alteration of a precursor rock (usually volcanic, but also dolomite) by addition of silica from seawater, and silica alteration and precipitation from hydrothermal vents. Only in the first case, does the chemical and isotopic composition of chert reflect the chemistry and temperature of the Archean seawater.

Once chert is formed, it remains very resistant to surface weathering and associated chemical alteration. Therefore, chert is often considered to be the ideal agent for the preservation of very ancient biosignatures, and potentially of extraterrestrial biosignatures (Westall 2008).

Overview

Cherts, both sedimentary (authigenic) and as a secondary alteration product, form by precipitation from water. The solubility of silica (Dove and Rimstidt 1994; Fleming and Crerar 1982) in water is largely independent of pH for pH lower than 9, but increases exponentially for pH >9. Solubility of silica increases with increasing temperature and with increasing quantity of dissolved salt. During the Archean, precipitation of silica is most likely abiogenic and derived originally from ocean floor hydrothermal vents. In more recent times, from around 1.8 Ga (Maliva et al. 2005) the silica cycle in the oceans was, and still is, governed by silica-secreting organisms (radiolarians), using mostly silica derived from continental weathering and delivered by rivers to the oceans (Laruelle et al. 2009).

For our understanding of the evolution and conditions of early life, the chert units found in Early Archean stratigraphic sequences such as those outcropping in the Pilbara craton (Australia) and Barberton Greenstone Belt (South Africa) are most important. Both sequences, the Warrawoona Group in the Pilbara craton and the Onverwacht Group in the Barberton Greenstone Belt, consist predominantly of mafic to ultramafic volcanic units, with minor felsic volcanic and associated volcanoclastic units (3.47–3.3 Ga). Both sequences are so similar that they may have been part of a single terrain at the time of deposition (Zegers et al. 1998). Chert units (typically less than 20 m thick) cap volcanic sequences,

and can frequently be traced over large (>50 km) distances (Kato and Nakamura 2003). A few thicker chert units occur in both the Pilbara Craton and Barberton Greenstone Belt: the Strelley Pool Chert and the Buck Reef Chert (350 m, Hofmann and Harris 2008), respectively. The detailed study of the Strelley Pool Chert (~3.43Ga) by Allwood et al. (2006) showed that the chert consists of at least four members with different characteristics and compositions, some of which show excellently preserved ► **stromatolites**. The unit was most likely deposited as a dolomite/carbonate reef on a shallow platform consisting of felsic volcanoclastic sediments. Tice and Lowe (2004) studied in detail the Buck Reef Chert, and sedimentary structures were interpreted to represent deposition in a shallow to deep marine environment, with organic matter resulting from photosynthetic microbial mats.

Other chert units in the earliest greenstone sequences show no strong evidence for carbonaceous and clastic sedimentary deposition, but are more likely to represent deposition of silica directly from seawater, typically as a result of oversaturation of the water with silica by the release from ocean floor hydrothermal vents. They show no stromatolitic textures, but they have been studied for microtextures that might be indicative of fossilized microorganisms and microbial mats (Schopf et al. 2002; Westall et al. 2006; Westall 2008). Some of the most famous putative microtextures were found in the ► **Apex Chert** (Schopf et al. 2002). The claim that those wormlike textures represent evidence for life at 3.45 Ga was countered by studies showing that very similar textures can be generated in hydrothermal systems by Fischer–Tropsch-type abiotic processes (Brasier et al. 2002).

Because chert is so resistant to erosion, it provides a good record for any study of early ► **Earth conditions**. Samples from the Marble Bar Chert (Pilbara) have been used for paleomagnetic studies (Suganuma et al. 2006). Oxygen and Si isotopic compositions in chert have been used to infer the temperature of the Archean ocean (Knauth and Lowe 2003; Robert and Chaussidon 2006) up to 70°C. However, van den Boorn et al. (2010) showed that the samples used in those studies were most likely deposited from hot hydrothermal water, rather than from ambient seawater. They suggest a maximum temperature of ambient seawater of 55°C.

Because of its formation by precipitation from water, and the potential to preserve textural and geochemical proxies for fossil life, chert is one of the targets for life detection on Mars (Westall 2008). The ► **Mars Exploration Rover Spirit** found recently amorphous silica (i.e., chert) in the Gusev Crater (Rice et al. 2010).

Key Research Findings

Chert units in Archean greenstone belts represent the oldest sedimentary units in otherwise entirely volcanic sequences. Stratiform chert units may be the result of direct precipitation from oversaturated seawater, or may represent hydrothermal deposits. In some cases, units that originally contain largely carbonate (dolomite, siderite) have been silicified to chert. Some of those units contain stromatolites and other micromorphological indications of biological activity.

Applications

Chert is very resistant to weathering and chemical alteration under surface conditions. This makes chert units, if they can be shown to have formed in the Archean, ideal recorders of Archean conditions, to be probed by a variety of techniques.

Future Directions

Chert units will continue to be studied as some of the best recorders of the conditions of early life. To correctly interpret micromorphological and geochemical signatures it remains of extreme importance to study the context of chert units and their surroundings. A unit recognized as chert today may either have been deposited originally as chert, or may be the result of later silicification. Silicification may have occurred soon after deposition (Hofmann and Harris 2008), but in the extreme case may be the result of relatively recent meteoric processes. To obtain a continuous stratigraphic sequence, unaltered by surface conditions, and unaffected by lightning strikes (for paleomagnetic studies), it will be important to drill cores through chert units. Such core samples should be studied collaboratively using different techniques and methods to obtain a more accurate insight into the conditions of life in the Archean. Amorphous silica deposits on Mars deserve full attention in preparation for future missions such as ExoMars and Mars Sample Return.

See also

- ▶ Alteration
- ▶ Apex Basalt, Australia
- ▶ Apex Chert
- ▶ Apex Chert, Microfossils
- ▶ Archean Drilling Projects
- ▶ Archean Environmental Conditions
- ▶ Banded Iron Formation
- ▶ Barberton Greenstone Belt
- ▶ Barberton Greenstone Belt, Sedimentology
- ▶ Barberton Greenstone Belt, Traces of Early Life
- ▶ Biomarkers

- ▶ Biomarkers, Morphological
- ▶ Carbonate
- ▶ Hydrothermal Environments
- ▶ Microfossils
- ▶ Pilbara Craton
- ▶ Precambrian Oceans, Temperature of

References and Further Reading

- Allwood AC, Walter MR, Kamber BS, Marshall CP, Burch IW (2006) Stromatolite reef from the Early Archaean era of Australia. *Nature* 441(7094):714–718
- Brasier MD, Green OR, Jephcoat AP, Klepepe AK, Van Kranendonk MJ, Lindsay JE, Steele A, Grassineau NV (2002) Questioning the evidence for Earth's oldest fossils. *Nature* 416(6876):76
- Byerly G, Kroner A, Lowe D, Todt W, Walsh M (1996) Prolonged magmatism and time constraints for sediment deposition in the early Archean barberton greenstone belt: evidence from the upper onverwacht and fig tree groups. *Precambrian Res* 78(1–3):125–138
- Dove P, Rimstidt J (1994) silica-water interactions: silica: physical behavior. *Geochem Materials Appl* 29:259
- Fleming B, Crerar D (1982) silicic-acid ionization and calculation of silica solubility at elevated-temperature and pH - application to geothermal fluid processing and reinjection. *Geothermics* 11(1):15–29
- Hofmann A, Harris C (2008) Silica alteration zones in the Barberton greenstone belt: A window into seafloor processes 3.5–3.3 Ga ago. *Chem Geol* 257(3–4):224–242
- Kato Y, Nakamura K (2003) Origin and global tectonic significance of Early Archean cherts from the Marble Bar greenstone belt, Pilbara Craton Western Australia. *Precambrian Res* 125(3–4):191–243
- Knauth L, Lowe D (2003) High Archean climatic temperature inferred from oxygen isotope geochemistry of cherts in the 3.5 Ga Swaziland Supergroup, South Africa. *Geol Soc Am Bull* 115(5):566–580
- Laruelle G, Roubeix V, Sferratore A, Brodherr B, Ciuffa D, Conley D, Durr H, Garnier J, Lancelot C, Phuong Q, Meunier J, Meybeck M, Michalopoulos P, Moriceau B, Longphuit S (et al) (2009) Anthropogenic perturbations of the silicon cycle at the global scale: Key role of the land-ocean transition: *Global Biogeochemical Cycles*, v. 23
- Maliva R, Knoll A, Simonson B (2005) Secular change in the Precambrian silica cycle: Insights from chert petrology. *Geol Soc Am Bull* 117(7–8):835–845
- Nutman A, Friend C (2009) New 1:20,000 scale geological maps, synthesis and history of investigation of the Isua supracrustal belt and adjacent orthogneisses, southern West Greenland A glimpse of Eoarchaean crust formation and orogeny. *Precambrian Res* 172(3–4):189–211
- Nutman A, Allaart J, Bridgewater D, Dimroth E, Rosing M (1984) Stratigraphic and geochemical evidence for the depositional environment of the early Archean Isua supracrustal belt Southern West Greenland. *Precambrian Res* 25(4):365–396
- Polat A, Frei R (2005) The origin of early Archean banded iron formations and of continental crust, Isua, southern West Greenland. *Precambrian Res* 138(1–2):151–175
- Rice M, Bell J, Cloutis E, Wang A, Ruff S, Craig M, Bailey D, Johnson J, de Souza P, Farrand W (2010) Silica-rich deposits and hydrated minerals at Gusev Crater Mars: Vis-NIR spectral characterization and regional mapping. *Icarus* 205(2):375–395
- Robert F, Chaussidon M (2006) A palaeotemperature curve for the Precambrian oceans based on silicon isotopes in cherts. *Nature* 443(7114):969–972

- Schopf J, Kudryavtsev A, Agresti D, Wdowiak T, Czaja A (2002) Laser-Raman imagery of Earth's earliest fossils. *Nature* 416(6876):73–76
- Suganuma Y, Hamano Y, Niitsuma S, Hoashi M, Hisamitsu T, Niitsuma N, Kodama K, Nedachi M (2006) Paleomagnetism of the Marble Bar Chert Member, Western Australia: Implications for apparent polar wander path for Pilbara craton during Archean time. *Earth Planet Sci Lett* 252(3–4):360–371
- Tice M, Lowe D (2004) Photosynthetic microbial mats in the 3, 416-Myr-old ocean. *Nature* 431(7008):549–552
- van den Boorn S, van Bergen M, Nijman W, Vroon P (2007) Dual role of seawater and hydrothermal fluids in Early Archean chert formation: evidence from silicon isotopes. *Geology* 35(10):939–942
- van den Boorn S, van Bergen M, Vroon P, de Vries S, Nijman W (2010) Silicon isotope and trace element constraints on the origin of similar to 3.5 Ga cherts: Implications for Early Archaean marine environments. *Geochim Cosmochim Acta* 74(3):1077–1103
- Van Kranendonk M, Hickman A, Smithies R, Nelson D, Pike G (2002) Geology and tectonic evolution of the archeon North Pilbara terrain, Pilbara Craton Western Australia. *Econ Geol Bull Soc* 97(4):695–732
- Westall F (2008) Morphological biosignatures in early terrestrial and extraterrestrial materials. *Space Sci Rev* 135(1–4):95–114
- Westall F, de Vries S, Nijman W, Rouchon V, Orberger B, Pearson V, Watson J, Verchovsky A, Wright I, Rouzaud J, Marchesini D, Severine A (2006) The 3.466 Ga “Kitty’s Gap Chert,” an early Archean microbial ecosystem: Processes on the Early Earth, no. 405, pp 105–131
- Zegers T, de Wit M, Dann J, White S (1998) Vaalbara, Earth's oldest assembled continent? A combined structural, geochronological, and palaeomagnetic test. *Terra Nova* 10(5):250–259

Chicken or Egg Problem

Definition

Chicken or egg problems are apparent causality problems; for example, which came first, the chicken or the egg? This is paradoxical because chickens are required to lay eggs, and yet chickens hatch from eggs. An apparent paradox in modern biochemistry is the fact that nucleic acids (both DNA and RNA) are required to make coded proteins, and at the same time, coded proteins are required to make nucleic acids. In the origin and early evolution of life then, it is not apparent which of these two must have come first. One possible solution to this problem is offered by the discovery of ribozymes, RNA molecules which could potentially code for their own replication and serve as catalysts for their replication as well.

See also

- ▶ [Genetic Code](#)
- ▶ [Nucleic Acids](#)
- ▶ [Origin of Life](#)
- ▶ [Protein](#)
- ▶ [RNA World](#)

Chicxulub Crater

PHILIPPE CLAEYS

Earth System Science, Vrije Universiteit Brussel, Brussels, Belgium

Keywords

Carbonaceous chondrites, dinosaurs, impact craters, mass extinctions, meteorites

Definition

The Chicxulub structure is an impact crater formed 65 Ma ago and located at the tip of the Yucatan Peninsula (Mexico). With a diameter between 180 and 220 km, the Chicxulub structure is the third largest impact crater known on Earth. The Chicxulub impact is considered by many authors as a cause of the important biological crisis at the KT boundary that led to mass extinction of 50–60% of the fauna and flora on the continent and in the oceans, including organisms such as ammonites and in particular the non-avian dinosaurs.

Overview

The Chicxulub structure formed 65 million years ago by the collision of a projectile, most likely a 10–12 km in size carbonaceous chondrite meteorite, with the Earth crust. The impact took place on a shallow-water carbonate platform; the underlying target rocks were composed of ~2–3 km of sediments (carbonates and evaporites) overlying a 600 Ma old gneiss-granitic basement. Geophysical methods give a good image of the crater that lies buried under ~1 km of Cenozoic sediments. Seismic data show the concave morphology of the structure. Measurements of the gravity field clearly outline a central-peak ring surrounded by a region of lower density forming the trough zone. A magnetic anomaly, caused by the presence of iron-rich rocks corresponds to the uplifted central peak area. The crater was drilled first for oil exploration purposes. In 2002, the International Continental Scientific Drilling Program drilled the crater for scientific research. The cores yielded ▶ [suevite](#) (a breccia of melt and solid fragments floating in a fine pulverized clastic matrix) and impact melt-rock containing evidence of high-pressure metamorphism, such as ▶ [shocked quartz](#) and diaplectic glass (i.e., formed by impact shockwaves). The identified melt phases have a ^{40}Ar – ^{39}Ar age of 65.46 ± 0.50 Ma, corresponding to the age of the KT boundary. The ▶ [impactites](#) are linked geochemically to the ▶ [ejecta](#) material spread all over the Gulf of Mexico. The energy

liberated by the impact amounted to $\sim 1,024$ J. The crater excavation injected into the upper atmosphere vast quantities of water vapor (200 Gt), CO_2 (350–3,500 Gt), SO_x (40–560 Gt) produced by the vaporization of the target material, along with a huge volume of fine dust. The dust and sulfur aerosols led to a yearlong darkness and brutal cooling all over the Earth, strongly reducing photosynthesis. Climate models suggested that a CO_2 -induced greenhouse warming followed. These events likely caused or contribute to the important biological crisis precisely at the ► [KT boundary](#) that led to the mass extinction of more than 60% of the fauna and in particular of the non-avian dinosaurs.

See also

- [Crater, Impact](#)
- [Deccan Trapps](#)
- [Ejecta](#)
- [Impactite](#)
- [KT Boundary](#)
- [Mass Extinctions](#)
- [Shocked Quartz](#)
- [Suevite](#)

References and Further Reading

- Morgan J, Warner M (1999) Chicxulub: the third dimension of a multi-ring impact basin. *Geology* 27:407–410
- Pierazzo E et al (2003) Chicxulub and climate: radiative perturbations of impact-produced S-bearing gases. *Astrobiology* 3:99–118
- Schulte P et al (2010) The Chicxulub asteroid impact and mass extinction at the cretaceous-paleogene boundary. *Science* 327:1214–1218
- Swisher CC et al (1992) Coeval $^{40}\text{Ar}/^{39}\text{Ar}$ ages of 65.0 million years ago from Chicxulub crater melt rock and Cretaceous-Tertiary boundary tektites. *Science* 257:954–958
- Urrutia-Fucugauchi J et al (2004) The Chicxulub scientific drilling project (CSDP). *Meteorit Planet Sci* 39:787–790

China National Space Administration

- [CNSA](#)

Chiral Excess

- [Enantiomeric Excess](#)

Chiral Pairs of Molecules

- [Stereoisomers](#)

Chirality

STANLEY I. GOLDBERG

Department of Chemistry, University of New Orleans,
New Orleans, LA, USA

Synonyms

[Handedness](#)

Keywords

Biochirality problem, chiral influence, conglomerate crystals, diastereomeric effect, diastereomers, enantiomers, homochirality, meteorites, racemic, racemic compounds

Definition

When a molecule is chiral, its three-dimensional structure lacks all elements of reflection symmetry. As a consequence, chiral molecules and their nonsuperimposable mirror images (called ► [enantiomers](#)) are distinct compounds. The nonsuperimposable, object–mirror image relationship of our right and left hands is a readily observable example of the enantiomeric condition of chiral objects.

In contemporary biochemistry, however, one enantiomeric form of each chiral biomolecule is nearly always absent, and the remaining enantiomer is usually of a preferred handedness or configuration (arrangement in space) as the other members of its compound class, for example amino acids. Thus, almost all chiral amino acids and chiral carbohydrates are not only present in essentially 100% enantiomeric purity but exist in states of configurational one-sidedness as well. The *L*-amino acids and the *D*-carbohydrates and their biopolymers in the contemporary biosphere are thus configurationally homogeneous, that is, homochiral.

Overview

The abiotic synthesis of chiral compounds generally results in the formation of equal quantities of enantiomers, known as ► [racemic](#) mixtures. Simply put, the central problem concerning the origin of biochirality asks the question: how did initially formed racemic mixtures

come to preferentially lose one enantiomer to become the enantiopure, configurationally homogeneous materials of the contemporary biosphere?

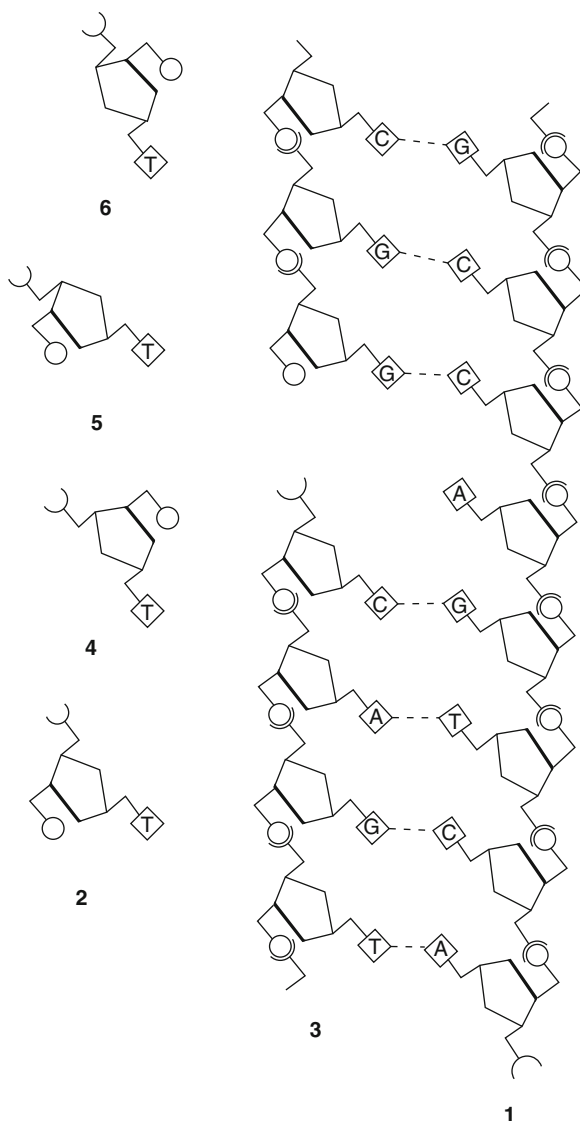
This problem has resisted solution for many years because enantiomers possess identical physical and chemical properties (Eliel and Wilen 1994). Therefore, differences upon which to base a possible separation scheme are not easily evoked, unless the scheme is carried out in the presence of an interaction with some other nonracemic chiral influence. This point will be developed below.

► **Homochirality** is believed to be an indispensable property of contemporary biochemistry. It provides a basis for the unique spatial interactions needed for the stunning specificities of the myriad essential interactions of living systems. Very high degrees of prebiotic configurational homogeneity (homochirality) may have been needed for the emergence of life. Here are two reasons why:

First, if biopolymers such as polypeptides were initially necessary, a homochiral prebiotic world would have neatly avoided the problem of having an impossibly large number of configurational isomers generated from the random assembly of enantiomeric monomers (the so-called *D*- and *L*-isomers in biochemistry). Even the formation of a polypeptide of modest size, say one consisting of only 25 amino acid residues would have meant the stereorandom synthesis of 225 or 33,554,432 configurationally isomeric polypeptides, only one of which would have been the all *L*-polypeptide found in contemporary life. With only *L*-amino acids available, *L*-polypeptides would have been the only ones possible.

The second reason rests on the reasonable requirement that any definition of life must include a replicating system, that is, to be alive is to be able to reproduce. That system may have been based on RNA, the so-called RNA World model. RNA must be homochiral to be able to carry out the essential tasks of replication and translation. Homochirality or a level of enantio-enrichment very close to homochirality may then have been required for life to emerge via this model. With even a small number of deviations from homochirality, the two helical strands of ribonucleic acids may not have been able to replicate. As William Bonner in a 1998 review of the chirality problem succinctly put it, "No homochirality, no life." This concept is illustrated by the simplified representations shown in Fig. 1.

During replication the double helical strands of DNA begin to unwind. Hydrogen bonds between complementary bases – A with T and C with G – are formed along each template strand, one segment of which is represented by 1, with each of its building blocks derived from



Chirality. Figure 1 Only when all components are configurationally homogeneous (homochiral) will replication of the daughter strand 3 take place. This means that not units 4, 5, or 6, but only unit 2, which possesses the same chirality present in the homochiral, template strand 1, will fit and allow replication by completing 3

β -D-deoxyribofuranosyl units, represented by 2. Strand 1 is therefore homochiral. The replicating daughter strand segment 3 is shown with two already-formed homochiral regions, needing only one more building block to connect them. Even though each of the four possible isomeric building blocks, 2, 4, 5, and 6 possess the correct base T needed to qualify as the bridging building block, only the unit 2, which maintains homochirality, will fit so that

the ball and socket representing its linking parts will allow completion of the segment of the daughter strand **3**. The presence of the others, competing for occupancy of the vacant site, will inhibit or halt the replication process. Note that isomer **4** is the nonsuperimposable mirror image (enantiomer) of **2**, belonging to the *L* stereochemical family of carbohydrates. The other inhibiting isomers, **4** and **5**, represent nonribosylated compounds.

This idea puts a critical constraint on proposed solutions to the chirality problem. It excludes those starting with racemic modifications or even slightly resolved racemic mixtures and proceeding on to living systems where they could achieve the homochiral state found in biochemistry.

Because enantiomers possess identical physical and chemical properties, the only way they can be detected or separated is through interaction with a nonracemic chiral influence to convert the enantiomeric condition into a pair of diastereomerically related results, which differ in physical and chemical properties. Some application of this principle must operate in every case where enantiomers are discriminated on a molecular level (Eliel and Wilen 1994). This fundamental principle, called the diastereomeric effect, is represented symbolically in Eq. 1, where the two-dimensionally chiral letters **L** and its mirror image **J** stand for the enantiomeric condition, while **G** denotes some interacting nonracemic chiral influence. The interaction of **G** with each enantiomer produces **L • G** and **J • G**, diastereomers, which (unlike enantiomers), possess different chemical and physical properties. Every manifestation of an enantiomeric condition must be the end product of an interaction leading to a diastereomeric result. In a classical chemical resolution, **G** is the resolving agent, in a biochemical process **G** is the enzyme, in enantioselective photolysis **G** may be circularly polarized ultraviolet radiation, and so on.



The numerous detections of nonracemic compounds, including amino and hydroxyl acids in carbonaceous meteorites (Pizzarello 2006) is evidence for the earlier action of an extraterrestrial chiral influence, possibly some source of chiral radiation, such as circularly polarized light, with appropriate energy, which caused selective enantiomeric depletions in racemic material on interstellar dust particles before that material was incorporated into meteors (and comets) and delivered to Earth's surface. Thus, a possible solution to the symmetry-breaking portion of the biochirality problem may be provided by these observations.

Plausible solutions to the other part of the problem – the problem of increasing the enantiomeric purity of meteoritic materials to levels which may have allowed the emergence of life – have also been experimentally developed. These depend on differences between enantiomers and their racemic modifications.

While it is true that in the absence of a nonracemic chiral influence enantiomers are identical, this is not necessarily the case when an enantiomer on the molecular level is compared to an associated state of enantiomers within the same system. In such circumstances, when an enantiomer is present in even slight excess, it may be discriminated from those in an associated state, which is usually the crystalline state. Most enantiomers have solubilities different from those of their crystalline racemic mixtures.

In the case of chiral compounds that form racemic conglomerate crystals, which are equimolecular mixtures of enantiopure crystals, the pure enantiomeric components are always less soluble than their conglomerates, and recrystallization under equilibrium conditions always results in an increase in enantiomeric purity of the more abundant enantiomers. Furthermore, as several experimental studies have shown, when such systems are not at equilibrium, recrystallization not only amplifies the enantiomeric purity of the more abundant enantiomer, but causes a significant increase in its quantity as well (Jacques et al. 1981a). These facts, combined with the discoveries of nonracemic compounds in meteorites have been cited as a possible solution to the biochirality problem (Goldberg 2000).

In mixtures with low levels of enantiomeric purity of substances that crystallize as racemic compounds, forms in which the stoichiometric ratio of enantiomers is equal to one, treatment with a small amount of solvent concentrates almost the entire ► **enantiomeric excess** in the solution phase, from which almost enantiopure material may be obtained (Jacques et al. 1981b). Recent experimental work has extended the applicability of this equilibrium saturation process to amino acids (Klussmann et al. 2006) and ribonucleosides (Breslow et al. 2010).

An entirely new enantiomeric enrichment phenomenon was discovered recently (Goldberg 2007) when an aqueous solution of a chiral, nonracemic compound was allowed to evaporate onto a clay or silica surface. The crystals formed were enriched in the more abundant enantiomer. The process was shown to work for several amino and hydroxy acids, giving up to a six-fold enrichment over the initial enantiomeric excess in one case. It was also projected as the main component of a spontaneous and continuous amplification system

operating on the prebiotic Earth leading to high levels of configurational homogeneity, which may have been required for the emergence of life. The process was built into a laboratory model which had a “beach” gently sloping up from a “sea” containing a dilute solution of a chiral compound with an initially low enantiomeric excess. Heat supplied by an infrared lamp (“the sun”) to a section of the “beach” provided enantiomerically enriched crystals, which were washed back into the “sea” by rain or tidal action. In this way, the enantiomeric purity of the test compound in the “sea” was continually raised up to a factor of 3.6 over the 3 months period before the model was shut down.

If the idea suggested by the presence of nonracemic, biosignificant compounds in the carbonaceous meteorites, that the prebiotic Earth was sufficiently supplied with nonracemic and accessible extraterrestrial material is even partially true, then this, taken together with the enantiomeric enrichment processes mentioned here may be elements of a solution to the biological homochirality problem.

See also

- ▶ [Enantiomeric Excess](#)
- ▶ [Enantiomers](#)
- ▶ [Homochirality](#)
- ▶ [Origin of Life](#)
- ▶ [Racemic \(Mixture\)](#)

References and Further Reading

- Bonner W (1998) Homochirality and life. In: Jolles P (ed) *D-amino acids in sequences of secreted peptides of multicellular organisms*. Birkhauser Verlag, Basel, pp 159–188
- Breslow R, Levine M, Cheng Z (2010) Imitating prebiotic homochirality on earth. *Orig Life Evol Biosph* 40:11–26
- Eliel E, Wilen S (1994) *Stereochemistry of organic compounds*. John Wiley and Sons, New York, Chap 6
- Goldberg S (2000) A solution to the origin of biochirality based on observational and experimental evidence. In: Celniker L, Van J (eds) *Frontiers of life*. Gioi, Vietnam, pp 51–2
- Goldberg S (2007) Enantiomeric enrichment on the prebiotic earth. *Orig Life Evol Biosph* 37:55–60
- Jacques J, Collet A, Wilen S (1981a) Enantiomers, racemates, and resolutions. John Wiley and Sons, New York, pp 181–182
- Jacques J, Collet A, Wilen S (1981b) Enantiomers, racemates, and resolutions. John Wiley and Sons, New York, pp 195–196
- Klussmann M, Iwamura H, Mathew S, Wells D, Pandya U, Armstrong A, Blackmond D (2006) Thermodynamic control of asymmetric amplification in amino acid catalysis. *Nature* 441:621–623
- Miller S, Orgel L (1974) *The origin of life on earth*. Prentice-Hall/Engelwood Cliffs, New Jersey, pp 166–174
- Pizzarello S (2006) The chemistry of life’s origin: a carbonaceous meteorite perspective. *Acc Chem Res* 39:231–237

Chiron

Definition

Chiron, discovered in 1977, was first identified as the asteroid 2060 Chiron. In 1989, as the object was moving toward perihelion, a coma was discovered and it was also designed as the comet 95 P/Chiron. Chiron is the first identified object among the class of the ▶ [Centaurs](#) which orbit between Jupiter and Neptune. Its period is 50 years and its perihelion distance is 8.4 AU. Its diameter is about 180 km and its albedo is about 0.05. Chiron belongs to the C-type class of asteroids. Like other Centaurs, Chiron is assumed to be originally a ▶ [trans-Neptunian object](#) which escaped from the ▶ [Kuiper Belt](#).

See also

- ▶ [Centaurs \(Asteroids\)](#)
- ▶ [Kuiper Belt](#)
- ▶ [Trans-Neptunian Object](#)

Chlorophylls

Definition

Chlorophylls are a class of pigments derivative of protoporphyrin complexed with magnesium. Chlorophylls function in photosynthetic organisms both as light receptors and special photochemical devices in photosynthetic reaction centers.

See also

- ▶ [Bacteriochlorophyll](#)
- ▶ [Photosynthesis](#)

Chloroplast

Definition

Chloroplast is a ▶ [chlorophyll](#)-containing organelle of phototrophic eukaryotes responsible for the generation of energy from radiation. A major feature of eukaryotic cells, absent from prokaryotic cells, is the presence of membrane-enclosed structures called ▶ [organelles](#). These include mitochondria and chloroplasts, the latter only in photosynthetic cells. Like mitochondria, chloroplasts have a permeable outermost membrane, a much less permeable inner membrane, and an intermembrane space. The inner

membrane surrounds the lumen of the chloroplast, called stroma. Chlorophyll and all other components needed for ► [photosynthesis](#) are located in a series of flattened membrane discs called thylakoids. The thylakoid membrane is highly impermeable to ions and other metabolites because its function is to establish the ► [proton motive force](#) necessary for ATP synthesis. In green ► [algae](#) and plants, thylakoids are typically stacked into discrete structural units called grana. The chloroplast stroma contains large amounts of the enzyme ribulose biphosphate carboxylase (RubisCO). RubisCO is a key catalyst of the ► [Calvin cycle](#), the series of biosynthetic reactions by which most photosynthetic organisms convert CO₂ to organic compounds. RubisCO makes up over 50% of the total chloroplast protein and catalyzes the formation of phosphoglyceric acid, a key compound in the biosynthesis of glucose. The permeability of the outermost chloroplast membrane allows glucose and ATP produced during photosynthesis to diffuse into the cytoplasm where they can be used to build new cell material. On the basis of their relative autonomy, size, and morphological resemblance to prokaryotes, it was suggested that chloroplasts were descendants of bacteria by ► [endosymbiosis](#). There are different structural, functional, and molecular evidences that support the endosymbiotic origin of chloroplasts: existence of a small genome, presence of ribosomes, anti-biotic specificity, and molecular phylogeny.

See also

- [Algae](#)
- [ATP Synthase](#)
- [Autotrophy](#)
- [Calvin–Benson Cycle](#)
- [Carbon Dioxide](#)
- [Chlorophylls](#)
- [Endosymbiosis](#)
- [Organelle](#)
- [Oxygenic Photosynthesis](#)
- [Photoautotroph](#)
- [Photosynthesis](#)
- [Photosynthetic Pigments](#)
- [Proton Motive Force](#)

Chondrite

Definition

Chondrites are undifferentiated stony ► [meteorites](#) and represent the majority among stony meteorites.

The term literally means “with ► [chondrules](#)” and therefore underlines the main difference to ► [achondrites](#). Chondrites consist of a fine-grained matrix of micrometer-sized dust particles, surrounding roughly millimeter-sized, rounded inclusions (► [chondrule](#)), refractory ► [CAIs](#) ► ([Ca–Al-rich inclusion](#))), particles enriched in metallic Fe–Ni and sulfides, and other individual mineral grains. The matrix also contains presolar grains that formed elsewhere in the Galaxy before the Solar System came into being. The presence of ► [chondrules](#) may suggest that chondrites formed by accretion of thermally processed dust particles, whereas their primitive parent bodies never experienced partial melting and recrystallization. The class of chondrites has been divided into enstatite (EH and EL types), Rumuruti (R type), ordinary (H, L, and LL types), and carbonaceous (C types), the latter subject to aqueous alteration and thought to be the most primitive meteorites. H, L, and LL indicate high iron, low iron, and low iron/metal contents, respectively.

See also

- [Achondrites](#)
- [CAIs](#)
- [Chondrule](#)
- [Meteorites](#)

Chondrule

Definition

Chondrule comes from the Greek word “chondros” for grain or seed. They are the major component of ► [chondrites](#) and can make up to 80% of the volume of a given ► [meteorite](#). In general, chondrules are rounded inclusions, roughly millimeter-sized ► [silicates](#). Their formation is not fully understood, but they did go through a transient heating process which was followed by a cooling period, so that molten or partly molten droplets came together before these pieces accreted to their parent body. Chondrules together with the ► [CAIs](#) ([Ca–Al-rich inclusion](#)) constitute the oldest material of our ► [Solar System](#).

See also

- [CAIs](#)
- [Chondrite](#)
- [Meteorites](#)
- [Silicate](#)
- [Solar System Formation \(Chronology\)](#)

Chromatographic Co-elution

Synonyms

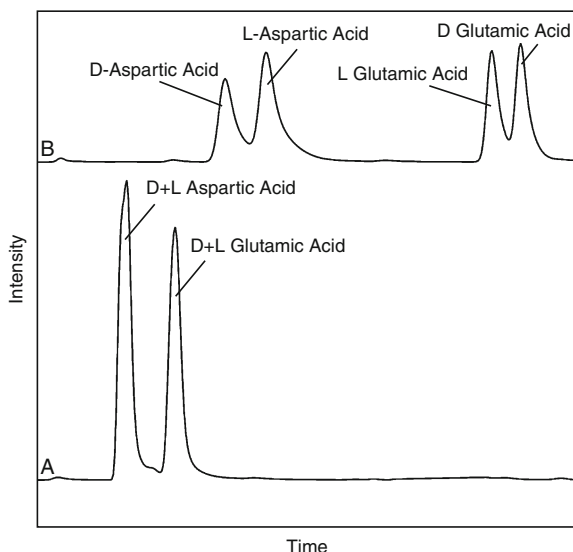
Co-elution

Definition

Chromatographic co-elution occurs when two (or more) compounds do not chromatographically separate due to the fact that both species have retention times that differ by less than the resolution of the method. This can be solved by increasing the selectivity and/or efficiency of the ► [chromatography](#) or by employing different detection techniques that can differentiate the co-eluting compounds. Changing the chemistry of the mobile phase, stationary phase, temperature, and column or plate length are good methods to increase the separation. Techniques such as mass spectrometry and optical spectroscopy are common ways to distinguish between co-eluting compounds that cannot be resolved.

See also

- [Chromatography](#)
- [Gas Chromatography](#)
- [GC/MS](#)



Chromatographic Co-elution. Figure 1 Chromatographic co-elution can be resolved by adjusting the chromatographic conditions. In these reverse phase HPLC traces, fluorescently labeled amino acids are resolved by decreasing the methanol concentration in the mobile phase. (See Glavin et al. 2006 for methods)

- [Ion-exchange Chromatography](#)
- [Liquid Chromatography-Mass Spectrometry](#)
- [Pyrolysis GC/MS](#)

References and Further Reading

Glavin DP, Dworkin JP, Aubrey A, Botta O, Doty III JH, Martins Z, Bada JL (2006) Amino acid analyses of Antarctic CM2 meteorites using liquid chromatography-time of flight-mass spectrometry. *Met Planet Sci* 41:889–902

Chromatography

JASON P. DWORKIN

NASA Goddard Space Flight Center, Astrochemistry Laboratory, Code 691, Greenbelt, MD, USA

Keywords

Column chromatography, GC, hyphenated techniques, LC, planar chromatography, separation science, solid phase extraction

Definition

Chromatography (either preparative or analytical) is a qualitative or quantitative experimental method based on the properties of all molecules to partition more or less selectively from one phase into another and therefore to migrate at different rates when they are carried across a solid or liquid stationary phase by a mobile phase, which can be a gas, liquid, or supercritical fluid.

Overview

Chromatography is a broad laboratory method for physically separating compounds from a mixture based on the preferential partitioning of different molecules across two different phases. The analyte is carried in the mobile phase (gas, liquid, or supercritical fluid), then passes through a stationary phase (liquid or solid), and some analytes are retained more efficiently than others. Different types of chromatography are based on the geometry (through a stationary phase-filled tube or “column” or over plate or “plane” with stationary phase), the type of mobile/stationary phase interaction (gas/liquid, gas/solid, liquid/liquid, liquid/solid, supercritical fluid/solid), and the nature of the analyte/stationary phase interaction (e.g., host/guest chemistry, hydrophobic interactions, ion exchange, hydrodynamic volume, volatility, etc.). ► [Electrophoresis](#), while not strictly chromatography, is closely related.

While planar chromatography (e.g., paper and thin layer (TLC)) is typically qualitative, column chromatography is well suited for real-time interrogation of the eluting compounds with detectors. Common types of gas-liquid chromatography (GC) detection techniques are flame ionization detection, thermal conductivity, and any number of mass spectrometric techniques (GC-MS). Common detectors in liquid-solid chromatography (LC or ► **HPLC**) are ultraviolet absorbance, fluorescence, refractive index, and various mass spectrometric methods (LC-MS). The addition of more elaborate detectors with a chromatographic or capillary electrophoretic “front end” (or “inlet”) is collectively referred to as hyphenated or hybrid techniques. Combinations of chromatography with ► **mass spectrometry**, nuclear magnetic resonance, and optical spectroscopy increase the ability of an analytical chemist to study small quantities of complex mixtures.

Conversely, preparative chromatography (either column or planar) is used to purify large quantities of a compound of interest. While GC or supercritical fluid chromatography is sometimes used, the most popular method is LC (or electrophoresis). One popular method is solid-phase extraction (SPE).

While the majority of chromatography is conducted in laboratories or industry, the process can be found elsewhere. Naturally occurring chromatography is typically fractional distillation or geochromatography, where, for example, compounds dissolved in water are roughly separated as they pass through rocks or sediment columns. Chromatography (GC-MS) has also been used in robotic planetary science missions to study Mars; Saturn’s moon, Titan; and comets.

See also

- **Affinity Chromatography**
- **ExoMars**
- **Electrophoresis**
- **Gas Chromatography**
- **GC/MS**
- **Ion-Exchange Chromatography**
- **Liquid Chromatography-Mass Spectrometry**
- **Mars Science Laboratory**
- **Mass Spectrometry**
- **Pyrolysis GC/MS**
- **Viking**

References and Further Reading

- Ettre LS (1993) Nomenclature for Chromatography. *Pure Appl Chem*, 65, 819–872. <http://chromatographyonline.com/>
- Miller JM (2004) *Chromatography: concepts and contrasts*. Wiley-Interscience, Hoboken, p 490

Chromophore

Definition

Chromophores are chemical groups that absorb ► **electromagnetic radiation**, for example, in the visible, near-infrared, or ultraviolet ranges, though the original derivation of the word comes from the Greek for color, implying absorption of visible radiation. They may contain systems of conjugated multiple bonds, transition element ions, or both. In biological systems, light absorption by chromophores forms the basis of vision, ► **photosynthesis**, and in the case of ► **ultraviolet light**, ► **mutation** and vitamin D synthesis. Chromophores are responsible for the colors of dyes, pigments, minerals, and many organisms, though some colors, particularly blues and iridescent effects, are produced by diffraction.

See also

- **Bacteriochlorophyll**
- **Chlorophylls**
- **Circular Dichroism**
- **Electromagnetic Radiation**
- **Extreme Ultraviolet Light**
- **Fluorophore**
- **Mutation**
- **Photosynthesis**
- **Photosynthetic Pigments**

Chromosome

Definition

Chromosome is a structure consisting of or containing ► **DNA** with essential genetic information for the cell. In most prokaryotes, it is a circular, double-stranded DNA, normally attached to the cell membrane, with a folded structure (also known as nucleoid) with some attached proteins. In eukaryotic cells, usually the number of chromosomes is characteristic of the species – polyploid plants are a remarkable exception. Somatic cells possess two sets of homologous chromosomes (diploid number or $2n$), one originating from the male progenitor, the other from the female. In contrast, germ-line cells are haploid (n). Eukaryotic chromosomes are located inside the ► **nucleus** and consist of a double-stranded DNA molecule highly folded and complexed with proteins (histones) also known as chromatin. The term chromosome also applies

to the DNA molecules located in mitochondria and plasmids and also applies to the genome of DNA viruses.

See also

- ▶ [DNA](#)
- ▶ [Genome](#)
- ▶ [Nucleus](#)
- ▶ [Replication \(Genetics\)](#)
- ▶ [Transcription](#)

Chronology of the Solar System Formation

- ▶ [Solar System Formation \(Chronology\)](#)

Chronology, Cratering and Stratigraphy

STEPHAN VAN GASSELT, GERHARD NEUKUM

Planetary Sciences and Remote Sensing, Institute of Geological Sciences, Free University of Berlin, Berlin, Germany

Synonyms

[Cratering chronology](#); [Planetary chronostratigraphy](#); [Planetary surface ages](#)

Keywords

Chronostratigraphy, cratering chronologies, impact crater, production function, radiometric ages, stratigraphy

Definition

The term chronology with respect to planetary surfaces generally refers to the timing of events when rock surface units were formed or modified and describes the position of a geological unit within its stratigraphic context. The term chronology furthermore encompasses the method of deriving ages of planetary surface units by means of radiometric age determinations as well as by analyses of impact-crater size-frequency distributions based on knowledge or assumptions of the flux and size-distribution of planet-impacting bodies in the history of the solar system.

Overview

The chronology of planetary surfaces refers to the sequence of geological events that have led to deposition

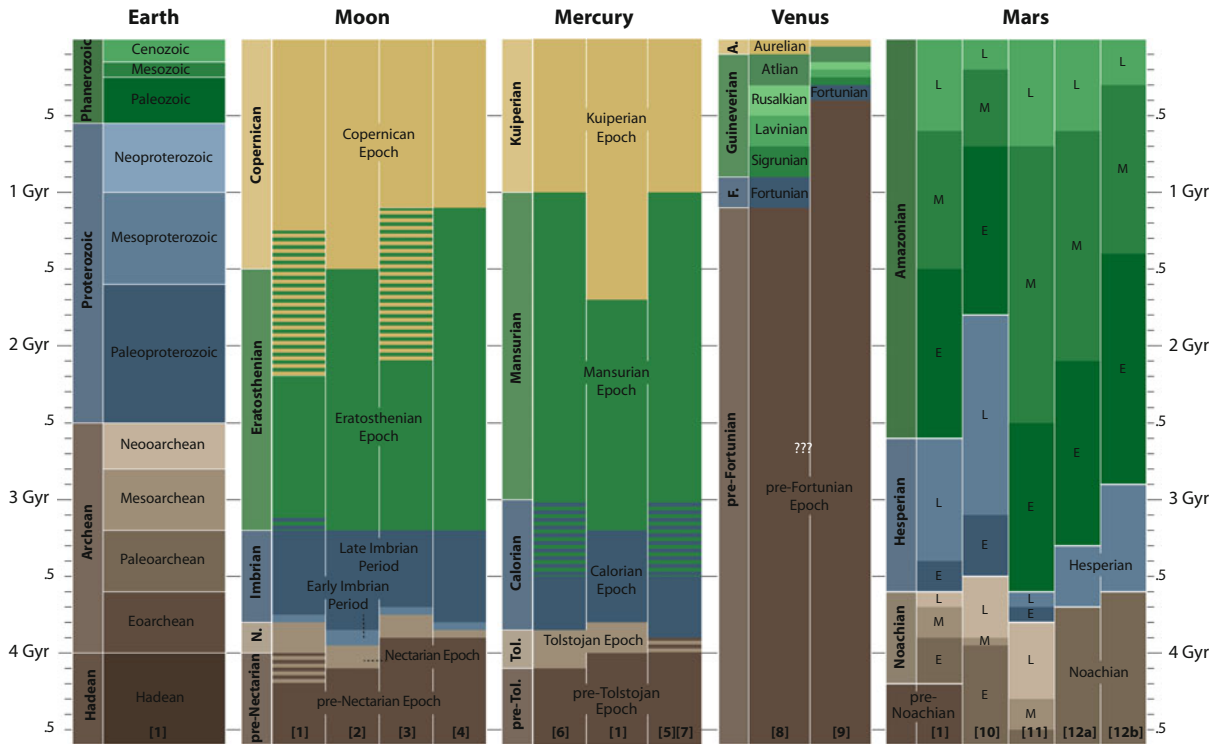
and emplacement of rock-forming units on a planetary surface. The sequence of events and the geologic materials, i.e., the rock-forming units (Wilhelms et al. 1987; Greeley and Batson 1990), are the planet's chronostratigraphic record and have to be seen in a specific planetary context as each planetary body evolves in a different way.

While the chronology in general refers to the timing and sequence of such events, the stratigraphic record of a planet is defined by divisions of geologic time and boundaries of geologic units on a global scale. Divisions of time are characterized by primary or secondary markers considered to be characteristic of that surface. While the geologic time unit (chronologic unit, see Fig. 1) refers to an age derived by various methods as discussed below, a chronostratigraphic unit consists of rocks formed on a global scale during a specific geologic time (Ogg et al. 2008).

The knowledge we have today about the chronostratigraphy and chronology of terrestrial planetary surfaces other than the Earth is based upon the knowledge we have gained during planetary exploration of the ▶ [Moon](#) (Wilhelms et al. 1971) and was later expanded to other terrestrial surfaces, in particular ▶ [Mercury](#) and ▶ [Mars](#) for which formal stratigraphic systems have been developed (Tanaka and Hartmann 2008).

The establishment of time scales for planetary surfaces is based upon geological mapping of planetary surfaces as defined by surface properties, e.g., morphologies, textures, spectral compositions, and, as delineated by geologic contacts, the superposition of individual units following basic stratigraphic principles. Relative ages can be derived by measuring the size-frequency distribution of ▶ [impact craters](#) that have accumulated in a planet's history through time, which means that densely cratered surfaces are older than less-densely cratered surface units. Thus, a geologic unit records the age as expressed by the number of impact craters formed during meteoritic bombardment and the time a unit was exposed to the projectile impact flux (Öpik 1960; Baldwin 1964; Hartmann 1966; Neukum et al. 1975).

Absolute ages for surface units are constrained by samples returned from the Moon in the course of the lunar Apollo and Luna mission programs. Derived radiometric ages of surface samples have established a calibration for the size-frequency distribution of the Moon's surface as observed by remote-sensing imaging. This process allows us to measure model ages for other planetary surfaces either (a) by estimating the relative cratering rates in comparison with the Moon or (b) by directly assessing cratering rates under consideration of impact probabilities and impactor sizes and sources



Chronology, Cratering and Stratigraphy. Figure 1 Chronology units in terms of epochs and periods for the terrestrial planets as compiled from different sources, see main text for description; the two columns for Venus' chronology depict the upper and lower estimates for $T = 800$ Myr and $T = 288$ Myr, respectively. (1, Ogg et al. (2008); 2, Neukum and Ivanov (1994); 3, Stöer and Ryder (2001); 4, Wilhelms (1987); 5, Neukum et al. (2001); 6, Strom and Neukum (1988); 7, Spudis and Guest (1988); 8, Basilevsky and Head (1998); 9, Basilevsky and Head (2002); 10, Tanaka (1986); 11, Neukum and Wise (1976); 12a, Hartmann and Neukum (2001) Neukum model; 12b, Hartmann and Neukum (2001) Hartmann model)

(Neukum and Ivanov 1994; Tanaka and Hartmann 2008) as well as crater scaling laws that describe the relationship between projectile size and impact condition parameters, e.g., velocity, angle, density, and surface parameters, such as surface gravity, density, compositions, and strength of surface materials (Croft 1985; Holsapple 1987; Schmidt and Housen 1987).

For planetary surface chronologies the number of stratigraphic systems for planetary objects has advanced with new data that have become available in the context of planetary exploration mission. Stratigraphic systems cover the terrestrial (inner) planets as well as the Moon and also the major icy satellites of the jovian and saturnian planetary systems.

Basic Methodology

There are different methods of assessing the stratigraphy of planetary surfaces with respect to the relative or absolute age of individual geologic units and their relation to

neighboring units. Ages of rocky planetary surface material are determined by means of the decay of radioactive isotopes and decay products if decay rates are known and if samples of surface material are available. In cases where planetary surfaces are observed by remote-sensing methods, ages of surface forming units can only be determined by analyses of impact-crater size-frequency measurements, i.e., by comparing the size-frequency distribution of impact craters with the modeled size-distribution and impact flux of meteorites on a given planetary surface.

While *relative* age determinations of units allow to assess and estimate the relative sequence of unit-forming events within an area of interest and in comparison with an established global distribution of impact-crater size-frequency observations, age determinations of geologic units based on remotely sensed data with the help of either appropriate scaling laws or modeling of impactor flux allow us to derive *absolute* ages. Except for the Earth, only the Moon has been directly sampled thus far and

therefore forms the only natural calibration target for establishing planetary chronostratigraphies and surface chronologies.

Radiogenic Isotope Measurements

Radioactive (or radiometric) dating, i.e., determination of radiogenic isotope ages of rock samples in the context of chronology, makes use of the constancy of rates of radioactive decay by which a radioactive nuclide is transformed to its daughter product. Radiogenic isotope ages for lunar material have been derived using decay measurements of Rb-Sr, Sm-Nd, and Ar⁴⁰-Ar³⁹. Such methods are described in detail by, e.g., Dalrymple and Ryder 1991; Albarède 2009.

For the Moon, over 380 kg of rock material in over 2000 samples were returned to Earth during the six manned Apollo missions. During the Soviet robotic Luna missions, several hundred grams were collected during three Luna missions and analyzed after return to Earth. Samples are mainly from basaltic rock and impact glass from the lunar ► **mare** areas (Apollo 11, 12, 15, 17, Luna 16, 24) as well as from highland terrain (Apollo 14–17, Luna 20). In addition, a number of meteorites found on Earth have a lunar origin (or martian) and could be radiometrically dated in laboratory measurements; their exact location of origin is, however, unknown.

Lunar rocks on the surface are exposed to cosmic weathering processes and recurrent meteoritic bombardment and therefore are altered. This leads to reprocessing of rocky material and to formation of second or third-generation rocks (Stöffler et al. 2006). By making use of radio-isotope measurements, different ages are usually derived, i.e., (a) crystallization ages, (b) ages of formation of impact breccia, and (c) exposure ages. The crystallization age gives the age of events that led to formation of rock minerals by magmatic or in situ melting processes. Ages for formation of impact breccia give insight into the age rock material and minerals were transformed to breccias, while the exposure age of rock material gives the age since the rock was exposed to cosmic weathering by cosmic rays (Stöffler et al. 2006). It has, however, been shown that direct radiometric age determinations are only possible for lunar mare basalts, as highland material collected at the lunar surface cannot be related directly to its source area. None of the collected samples were derived from bedrock material due to a several meters thick surface coverage of lunar regolith (e.g., Heiken et al. 1991 and references therein).

Radiogenic isotope measurements for deriving absolute ages of localized samples help to establish boundary age values, but without a careful interpretation of the

photogeological settings and the geological context such measurements cannot contribute to establishing a planet-wide chronology and chronostratigraphic system.

Relative Age Determinations

The easiest accessible approach to assess the time-sequence of rock-forming events on a planetary surface is to measure the size-frequency distribution of impact diameters within a geologic unit and to compare this to other geologic units of the same planetary body: the higher the number of impact craters that have accumulated over time per area, the older the surface, which means that a crater frequency measured on a specific geologic unit is representative of the relative age or crater retention age of that unit (Arvidson et al. 1979). A geologic unit or rock-stratigraphic unit is a morphologically distinct entity formed at a specific time by a distinct geologic process (Stöffler et al. 2006). The derived relative surface age does not necessarily reflect the true relative age when a geologic unit was formed, as subsequent processes, generally termed resurfacing, might have led to eliminating impact craters in a given diameter-size range. The main problems arise from accurately identifying and delineating a geologic unit at a given scale, as this significantly depends on the appearance of a particular unit and its relation to surrounding units in the image data used for photogeologic interpretations (Shoemaker and Hackman 1962; Wilhelms 1987).

By employing cumulative crater size-frequency diagrams, the measured impact-crater diameters of all impact craters within a given geologic unit are usually plotted against their cumulative frequency in a log-log diagram. The impact-crater size-frequency distribution derived in such a way provides a measure for the surface age with older units, i.e., units with increasing crater retention ages, shifted upwards on the frequency axis (apparent shift towards larger impact-crater diameters) while distributions of younger units are shifted downwards on the frequency axis leading to an apparent shift toward smaller impact-crater diameter sizes (Hartmann et al. 1981; Wilhelms 1987).

While relative surface age determinations are based upon the interpretation of remotely sensed data by means of determining the superposition of individual rock surface units and by determining impact crater size frequencies, age determinations leading to absolute age values need additional pieces of information.

Absolute Age Determinations

There are two methods of obtaining absolute ages of rock surface units of planetary bodies. One method links

radiogenic isotope ages obtained for the Moon with crater retention ages, i.e., relative ages, obtained through photo-geological mapping (Hartmann et al. 1981; Neukum 1983; Neukum and Ivanov 1994). In the other approach, models for rates for formation of impact craters are employed and are transferred to other planetary objects considering their specific environment, e.g., position and size, atmosphere, target properties (Neukum and Wise 1976; Neukum and Hiller 1981; Hartmann et al. 1981; Croft 1985; Holsapple 1987; Schmidt and Housen 1987).

For the ► **terrestrial planets** in the Inner Solar System, surface ages can only be obtained by models of the crater forming rates on each one of these bodies. Shapes of crater size-frequency distributions (SFDs) measured on the terrestrial planets, including the Moon, were shown to be more or less similar which indicates (a) the same family of bodies, preferentially asteroids (Main Belt, Near Earth asteroids, etc.), impacting these planets, and (b) that time dependences of impact and cratering rates are similar to that for the Moon (Neukum and Hiller 1981; Neukum and Wise 1976; Neukum and Ivanov 1994; Neukum et al. 2001; Strom et al. 2005).

Lunar-like cratering chronology models were derived for Mercury (Strom and Neukum 1988; Neukum et al. 2001b), ► **Venus** (McKinnon et al. 1997), and Mars (Neukum and Wise 1976; Neukum and Hiller 1981; Hartmann and Neukum 2001). Crater-size frequency measurements were conducted also for a number of asteroids, e.g., 951 Gaspra (Neukum and Ivanov 1994; Chapman et al. 1996), 243 Ida (Neukum and Ivanov 1994), and 253 Mathilde (Chapman et al. 1998).

The impact-cratering chronology model for the Moon is characterized by an exponentially declining impact and crater formation rate in the first 1 Gyr following planetary formation 4.55 Gyr ago (e.g., Neukum 1977; Neukum and Ivanov 1994).

Since about 3.8 Gyr ago, impact and cratering rates have dropped considerably and reached a more or less constant level at 3–3.3 Gyr ago (Wetherill 1975; Neukum 1983; Neukum and Ivanov 1994, Neukum et al. 2001a). Some authors interpreted a peak in radiometric ages of lunar rocks at about 3.9 Gyr as indication for a strong peak in impact and cratering rate (e.g., Tera et al. 1974). They concluded that this so-called Late Heavy Bombardment (LHB) was characterized by a terminal lunar cataclysm rather than by a smooth, exponential decay in impact rate with time. The lunar cataclysm theory has been challenged by dynamic, geologic and stratigraphic arguments (Wetherill 1975; Neukum and Ivanov 1994; Baldwin 2006).

Absolute ages obtained with an impact chronology model are generally termed cratering model ages, and

their units are given in Giga-years (Ga = Gyr = 1 billion years) or Mega-years (Ma = Myr = 1 million years).

Crater-size frequency distributions obtained from crater size-frequency measurements are represented using several techniques, of which three are commonly adopted. In principle, crater-size diameters are grouped into pseudo-logarithmic or logarithmic bins and plotted on the abscissa (Arvidson et al. 1979; Neukum et al. 2001; Michael and Neukum 2009). The ordinate gives the crater size-frequency values as a function of log diameters. This frequency can either be based upon the cumulative crater-diameter sizes (cumulative plots) in which the number of craters with diameters equal or greater than D : $N = N(\geq D)$ are presented, or in differential form where the derivative dN/dD of the cumulative size-frequency distribution gives the number of craters in equal diameter bins. The incremental form provides the frequency as a function of the geometric average of fixed-diameter increments (usually $\sqrt{2}$). The relative distribution (R-plot) is the deviation of the size-frequency distribution from a power law: $R = D^3 (dN/dD)$. The choice depends on the details that need to be depicted and highlighted and the analyses that are carried out subsequently.

The size-frequency distribution of an impact crater population can be approximated using either three step-wise power-law segments (Hartmann et al. 2000) obtaining coefficients for the approximation that are characteristic for each SFD. In contrast to the approach by Hartmann, Neukum proposed an analytical polynomial fit (Neukum 1983; Neukum and Ivanov 1994; Ivanov et al. 2001; Neukum et al. 2001). These functions are termed production functions and are characteristic of each planetary body and derived from numerous observations and measurements of impact craters. Once the production function is fitted, the frequency of impact craters larger than a given diameter (usually N for $D \geq 1$ or N for $D \geq 10$ km) is obtained. This frequency value is subsequently used to derive a surface age from the chronology function obtained earlier which represents the impact-cratering record in the planet's history.

Stratigraphic schemes have been established in principle for all terrestrial bodies. These schemes are based upon stratigraphic marker horizons that are defined by geologic criteria which are different for each object, and they take into account the superimposed crater-size frequencies considered to be characteristic of a particular unit (Wilhelms 1987). The geologic history of each planet is subdivided into so-called time-stratigraphic systems. Such chronostratigraphic divisions are termed systems and are further divided into several (e.g., lower, middle, or upper) series. Time-stratigraphic systems and series correspond

to periods and epochs as chronologic or chronometric divisions (Wilhelms 1987). The beginning of each period or epoch is defined by the cratering model age derived from the SFD measurement on the unit which defines the base of each system.

Key Research Findings

Stratigraphic sequences have been established in principle for all terrestrial bodies in the solar system, in particular for the inner solar system planets and the Moon. The main stratigraphic sequences and unit-forming events are summarized below and ages are provided whenever possible. However, age uncertainties are excluded for all model ages and the reader is referred to references listed in each section. While for several bodies, such as the Moon and Mars, chronostratigraphic systems are well established and applicable, other objects are partly still unknown when it comes to high resolution data needed for cratering analysis and statistics. Consequently, differences in absolute age dating for each planet between various groups of investigators are due to differences in assumptions of the impact and cratering rates, and many preliminary results are expected to be improved in the course of ongoing planetary missions.

The Moon

The Earth and its moon are the only bodies in the solar system for which radiometric ages of rock surface units and soil samples have been obtained. Robotic as well as manned missions to the Moon have provided the most extensive data set concerning stratigraphy and surface ages available (Wilhelms 1987).

The lunar geologic history is subdivided into periods defined by impact events and impact crater occurrences ranging from the pre-Nectarian (oldest period), Nectarian, Imbrian, Eratosthenian to the Copernican period (youngest). The Imbrian period is subdivided by the Orientale impact into a late (upper) and early (lower) Imbrian epoch (Wilhelms 1987).

- The pre-Nectarian covers that section of geologic history which predates the Nectarian period, i.e., older than 3.92 (Wilhelms 1987; Stöffler and Ryder 2001) to 4.1 Gyr ago (Neukum and Ivanov 1994). The chronostratigraphic system comprises a number of 30 impact basins among which is the South Pole Aitken basin. No traces for volcanic or tectonic processes during the pre-Nectarian period have been found thus far. Traces of pre-Nectarian surface units are mainly found on the lunar farside and samples returned during the Apollo and Luna missions are later-generation material reworked as breccias in the

course of subsequent impact processes (Wilhelms 1987; Stöffler et al. 2006).

- The Nectarian period is defined as the time period between formation of the Nectaris basin (Janssen Formation) and the Imbrium impact event and comprises at least 11 other large impact-basin forming events. Although some Nectarian-aged volcanic material has been observed (Wilhelms 1987), much of this unit is covered by later impact events that masked Nectarian units. According to recent studies, mare volcanism started already during the Nectarian period with ages of 3.92 Gyr ago and continuing up to 1.2 Gyr ago (Hiesinger et al. 2003). The chronostratigraphic basis, i.e., the lowermost unit, for the Nectarian system is set between 3.92 (Wilhelms 1987; Stöffler and Ryder 2001) to 4.1 Gyr ago (Neukum and Ivanov 1994).
- The Imbrian period is defined by the impact-basin event forming the Imbrium impact crater on the lunar near side with the Fra Mauro Formation at its base. The Late Imbrian epoch starts with the Orientale basin formation (Hewelius Formation); its upper limit is defined through impact crater sizes only. Two thirds of the lunar mare volcanic deposits are of Late Imbrian age. Apart from extensive mare-type volcanism, dark mantling deposits are thought to be of Late Imbrian age (Stöffler et al. 2006). Formation of the Orientale basin is suggested to be 3.72 Gyr (Stöffler and Ryder 2001) to 3.8 Gyr (Wilhelms 1987) or 3.84 Gyr (Neukum and Ivanov 1994; Neukum et al. 2001) ago depending on the chronology model.

The Early Imbrian epoch covers the time range between Imbrium (Fra Mauro Formation) and Orientale basin formation (Hewelius Formation) corresponding to 3.77 Gyr (Stöffler and Ryder 2001) to 3.84 Gyr (Wilhelms 1987) or even 3.92 Gyr (Neukum and Ivanov 1994; Neukum et al. 2001) ago depending on the chronology model. The epoch is characterized by extensive volcanism and impact cratering but without formation of larger impact basins, except for the Schrödinger basin. Many of the light plains have a Lower Imbrian age (Stöffler et al. 2006).

- The Eratosthenian period is defined through the appearance of younger impact craters covering most of other lunar units but showing no signs of rayed ejecta; a criterion that has led to discussions regarding boundary ambiguities (Stöffler et al. 2006; Stöffler and Ryder 2001). Some of the mare basalts were emplaced during the Eratosthenian, but these units are much less extensive than those in the Imbrian period. The basis of the Eratosthenian is generally set to 3.2 Gyr ago

(Wilhelms 1987; Stöffler and Ryder 2001; Neukum and Ivanov 1994; Neukum et al. 2001).

- The Copernican period is defined through the occurrence of rayed craters on the Moon with Copernicus being the most prominent rayed impact crater. These impact craters are superimposed on all other units and show traces of ejecta material all over the Moon despite their relatively small size. Due to its definition, the basis for the Copernican period is not well constrained with ages ranging from 1.1 Gyr (Wilhelms 1987) to 1.5 Gyr (Neukum and Ivanov 1994; Neukum et al. 2001) up to 1.1–2.1 Gyr (Stöffler and Ryder 2001). The Copernican period continues up to the present time.

Mercury

Mercury's surface is visually comparable to the lunar one as expressed by numerous impact craters and large impact basins, as well as a rich variety of tectonic features probably caused by rapid cooling and tidal despinning (Spudis and Guest 1988; Neukum et al. 2001). Mercury's surface shows a global dichotomy in terms of major geologic units: the densely cratered terrain (highlands) with interspersed smoother areas (inter-crater plains) and the less-densely cratered lowland plains (smooth plains) (Trask and Guest 1975; Spudis and Guest 1988). In contrast to the lunar surface, the smooth plains and highland terrain are comparable in relative albedo. Notwithstanding the surficial resemblance of Mercury and the Moon, crater-size frequencies of the heavily cratered highland terrain of Mercury are less than that of the Moon (Spudis and Guest 1988) with a general paucity of impact craters in the 30 km diameter range (Neukum et al. 2001b). The stratigraphic system of Mercury was established by geologic mapping at scales of 1:5,000,000 in the late 1970s and early 1980s on image data of Mariner 10 flybys.

Mercury's surface resemblance to the Moon led to establishing a stratigraphic system comparable to that of the lunar one with impact events characterizing bases of stratigraphic periods. Mercury's geologic history is therefore subdivided into five periods starting with the Pre-Tolstojan as the oldest unit to the Kuiperian as the youngest period (Spudis and Guest 1988).

- The Pre-Tolstojan period closely compares to the lunar Pre-Nectarian and encompasses geologic units older than 3.97 Gyr (Neukum et al. 2001) to 4.1 Gyr (Strom and Neukum 1988) ago and is related to crater materials and multiring basins as well as inter-crater plains (Neukum et al. 2001; Tanaka and Hartmann 2008; Spudis and Guest 1988).

- During the Tolstojan period which is equivalent to the lunar Nectarian period the dominant geologic units are the Goya formation that marks the basis of the Tolstoj system and which hosts deposits of the Tolstoj basin as well as materials of small impact basins and craters. Its base is estimated to be approximately 3.9–4.0 Gyr (Spudis and Guest 1988) up to 4.06 Gyr (Strom and Neukum 1988) old. Recent age estimates based on new chronology models put the Tolstojan basis at 3.97 Gyr ago (Neukum et al. 2001b).
- The Calorian period compares to the lunar Imbrian period and is mainly characterized by Caloris-group units, i.e., mountain material, intermontane plains, hummocky plain, the Calorian plains, as well as impact crater materials and materials of small impact basins. Its time-stratigraphic base is estimated to be in the range of 3.77 Gyr (Neukum et al. 2001), 3.85 Gyr (Strom and Neukum 1988) to 3.9 Gyr (Spudis and Guest 1988) and is defined by the Caloris impact event that is considered to be the youngest impact basin on Mercury (McCauley et al. 1981).
- The Mansurian period is equivalent to the lunar Eratosthenian period and its chronostratigraphic base is defined by the impact event of Mansur. With some uncertainties, its crater model age is estimated at 3–3.5 Gyr (Spudis and Guest 1988; Strom and Neukum 1988, Neukum et al. 2001). As for the Kuiperian system, major units are of impact-crater origin mainly.
- The Kuiperian period represents the youngest period in Mercury's history and its base is defined by the age of impact crater Kuiper which occurred ~ 1 Gyr ago, equivalent to the lunar Copernican system (Wilhelms 1987; Spudis and Guest 1988; Strom and Neukum 1988; Neukum et al. 2001). As for the Moon, the period is predominantly characterized by young impact crater materials.

Venus

Radar mapping investigations of Venus's surface in the context of the 1990s Magellan mission have shown that the impact crater frequency on Venus is extremely low. This indicates that the surface as it is observed today has an age of few 100 Myr only (Basilevsky and Head 1998). Widespread volcanism and intensive tectonic disruptions have shaped the surface and deleted most of the older geologic units and the planet's impact crater record. Consequently, the stratigraphic system is not constrained throughout all of Venus's history and could not be established until the late 1990s, on the basis of photogeologic interpretation of a few selected

regions that proved to be statistically significant for establishing a global stratigraphic system (Basilevsky and Head 1998).

The current stratigraphic record represents only 10–20% of Venus's history and covers only 30% of Venus's surface as mapped at scales of 1:3 M–1:10 M (Basilevsky and Head 1998). Specific geologic time units (periods) are defined mainly on the basis of large impact events and volcanic plains formation events, and which helped to establish four major periods: the pre-Fortunian (oldest), Fortunian, Guineverian, and Aurelian (youngest unit). Due to the paucity of impact craters and statistically relevant average estimates of surface ages, absolute ages are usually provided as ratios with respect to the global impact crater frequency ($T = 1.98 \times 10^{-6}$ craters/km²) corresponding to an average surface age of 288 Myr (+311/–98 Myr) according to Strom et al. 1994, 400–800 Myr according to Phillips et al. 1992, or as high as 800 Myr (+800/–400) according to Zahnle and McKinnon (1996) as discussed in Basilevsky and Head 1998 in detail.

- The Pre-Fortunian period is not constrained in terms of geologic surface units and spans the time before 1.47 T.
- The Fortunian period is characterized by intensive tectonic deformation with formation of the ancient ► *tessera* terrain that covers about 8% of Venus's surface. Tesserae formation occurred at 1.47 T (1.93–1.01 T in previous estimates) which is considered to form the time basis of the Fortunian period (Basilevsky and Head 1998).
- During the Guineverian period extensive volcanic plains were formed with a peak at 1.1 T (Tanaka et al. 1997). The period has been proposed to be a super-group consisting of four plains-forming sub units by Basilevsky and Head 1998. These groups (youngest to oldest unit) follow the proposal by Basilevsky and Head 1998 and the Atla Group, consisting of relatively undisturbed mafic lava, Rusalka Group lava materials covering up to 75% of Venus's surface, the Lavinia Group characterized by ridged and fractured plains, and the Sigrun Group consisting of densely fractured plains material emplaced as mafic lavas. The Guineverian period covers most of Venus's known geologic record and terminates at around 0.1–0.2 T according to most recent estimates (Basilevsky and Head 1998). A period of younger volcanic activity peaking at 0.4–0.5 T ago with formation of Venus's coronae and rifts as well as formation of large volcanoes at 0.3 T were proposed as a fourth major unit in Tanaka et al. 1997.

- The Aurelian period is characterized by materials associated with the youngest impact craters; its basis is set to 0.1 T containing approximately 10% of Venus's visible cratering record (Tanaka et al. 1997 and references therein) and translating to an age of ~50 Myr using a conservative estimate of the mean surface age.

Mars

On Mars, impact cratering and plains volcanism played a dominant role in shaping the planet's surface throughout history. Additionally, a rich variety of processes related to fluvial, glacial, and eolian resurfacing have significantly contributed to the morphologies that are observed nowadays. Mars' global topography is divided into the densely cratered and old highland terrain in the south and the smooth, less-densely cratered younger northern plains. The subdivision of the stratigraphic system of Mars is based on marker horizons that are formed by plains-forming volcanism (Scott and Carr 1978; Tanaka 1986; Tanaka et al. 1992). Martian geologic time periods are from oldest to youngest: the Noachian (with late, middle, and early epochs), the Hesperian (with a late and early epoch), and the Amazonian (with a late, middle, and early epoch) (Scott and Carr 1978; Tanaka 1986; Tanaka et al. 1992). For Mars, several chronology models were proposed and modified in the course of the availability of new higher resolution data. Some of these efforts have been combined lately to form the recent chronology model by Hartmann and Neukum (2001). Stratigraphic boundaries (boundaries of time periods) are slightly different, which has led to a Hartmann model (HM) and a Neukum model (NM).

- A Pre-Noachian period is informally established although the Noachian basis is not exposed; however, radiometrically derived ages for the Martian meteorite ALH84001 with a crystallization age of 4.5 Gyr fits into this period (Mittlefehldt 1994).
- The Noachian system is characterized by the oldest, densely cratered units in the highlands covering a time range of older than 3.97 Gyr ago to 3.74 Gyr ago for the Noachian system (Tanaka et al. 1992; Hartmann and Neukum 2001). Its basis is defined by highland material of the Noachis Terra located between the Argyre and Hellas Planitiae impact basins (Tanaka et al. 1992). The system is generally characterized by Heavy Bombardment impacts, large-scale volcanism peaking in the Tharsis region and the highland volcanic provinces, global tectonism and extensive valley network formation indicating fluvial processes, and a much denser atmosphere and warmer climate.

The Late Noachian period spans 3.86–3.74 Gyr ago (Hartmann and Neukum 2001), and is characterized by cratered plateau material mainly. During that period, the crustal dichotomy has been morphologically shaped. The Middle Noachian epoch which covers the time span between 3.97 and 3.86 Gyr ago (Hartmann and Neukum 2001) is characterized by cratered highland terrain shaped by impact cratering and the Argyre Planitia impact-basin event. During the late Early Noachian (>3.97 Gyr), the Hellas and Isidis impact basins formed, and global volcanism shaped the Tharsis region with the formation of Paterae and Tholi, and the circum-Hellas Planitia Highland volcanoes (Tanaka et al. 1992). Recently, the Noachian period was characterized in terms of geochemical alteration by Bibring et al. 2006, suggesting that formation of clay minerals, i.e., phyllosilicates, peaked during the Early and Middle Noachian epochs.

- The Hesperian period is subdivided into the Early and Late Hesperian epochs spanning 3.74 Gyr to 2.9 Gyr ago and is characterized by the Hesperia Planum ridged plains material northeast of the Hellas Planitia impact basin. Impact-cratering rates were significantly lower when compared to the Noachian period, marking the end of the Heavy Bombardment period. Vanishing fluvial activity was replaced by large-scale volcanism in the lowland units (Tanaka et al. 1992 and ref's therein). The disappearance of surface water has led to the assumption that most of the water is stored as permafrost under the surface. Catastrophic release of water led to formation of outflow channels on Mars in the circum-Chryse and eastern Hellas Planitia regions along with formation of the Martian chaotic terrain and the Valles Marineris system (Tanaka et al. 1992). The Hesperian is also characterized by extensive sulfate deposits (Bibring et al. 2006) primarily in the Valles Marineris region. The Early Hesperian period covers the age range of 3.74 to 3.65 Gyr ago (Hartmann and Neukum 2001) and is defined through the Hesperia Planum ridged plains units. Geologic materials of the Late Hesperian, covering the period between 3.65 Gyr and 2.9 Gyr ago (Hartmann and Neukum 2001), are defined through the plains material of the northern plains Vastitas Borealis unit.
- The Amazonian period spans much of Martian history and starts 2.9 Gyr ago according to the Hartmann model (HM), and up to 3.31 Gyr ago according to the Neukum chronology model (NM). The period is generally defined through processes related to the northern lowland units and plains materials and is

characterized by extensive resurfacing processes. Late-stage volcanism and eolian resurfacing shaped large areas of Mars and obliterated older units (Tanaka et al. 1992). The Amazonian also shows late-stage outflow activity in the circum-Chryse Planitia area and an abundance of ice-related surface processes predominantly near the global dichotomy escarpment and circum-Tharsis volcanoes as well as the circum-Hellas/Argyre Planitiae regions. Surface alteration by formation of anhydrous ferric oxides led to the planet's characteristic red surface color (Bibring et al. 2006).

The basis of the Upper Amazonian series (Late Amazonian epoch) is defined by flood plains material of the southern Elysium Planitia area and starts 0.3 Gyr (HM) to 0.6 Gyr (NM) ago (Tanaka 1986; Hartmann and Neukum 2001). Characteristic materials of the Upper Amazonian are predominantly found near the seasonally changing polar caps of Mars and in the young deposits and flow fields delineating the northern hemispheric volcanoes. The Middle Amazonian is defined by the age of Amazonis Planitia lava flow materials (Tanaka 1986; Hartmann and Neukum 2001) and covers the time range between 2.1 Gyr and 0.6 Gyr ago (NM) or 1.4 Gyr to 0.3 Gyr ago (HM). The basis for the Early Amazonian epoch is set to 3.3 Gyr (NM) to 2.9 Gyr (HM) ago and is defined by the smooth plains materials of Acidalia Planitia (Tanaka 1986; Hartmann and Neukum 2001).

Outer Solar System Objects

In contrast to the currently accepted chronology models proposed for the inner planets which are based upon the lunar chronology model with impactors from the asteroid belt, planetary objects in the outer solar system are treated in a different way. While one group favors the lunar-like distribution and chronology model for all objects in the solar system, i.e., lunar-like time dependence of the cratering rate, the second group favors nearly-constant cratering rates by cometary impactors. A number of researchers developed lunar-like chronology models for the Jovian and Saturnian system (Shoemaker and Wolfe 1982; Boyce and Plescia 1985; Neukum 1985; Neukum 1997). Based on present-day estimates of sizes and dynamics, a constant cratering rate chronology for the icy satellites was put forward with impactors originating in the Kuiper Belt (Zahnle et al. 1998).

The two competing cratering chronology models agree well for old, densely cratered surfaces on the icy satellites but they are different by more than an order of magnitude for younger, resurfaced units. These issues are discussed in

detail in, e.g., Neukum et al. 1997; Neukum et al. 1998; Zahnle et al. 1998.

Imaging data of the Voyager and Galileo missions to the outer solar system provided the basis for impact-crater size-frequency statistics and estimates of surface ages of the Galilean satellites. The surface of Europa is considered to be relatively young under assumption of primarily cometary impacts with average ages in the range of 30–70 Myr, as suggested by the less-densely cratered surface of Europa when compared to Callisto or Ganymede (Lucchitta and Soderblom 1982; Zahnle 2003). Employing a lunar-like chronology model with the asteroid belt as main impactor source, surface ages of Europa are in the range of 0.5–1.5 Gyr. However, individual units can be as young as approximately 200 Myr or less (Neukum et al. 1998).

The heavily cratered dark plains on Callisto and Ganymede are on the order of 4 Gyr and older in both asteroidal and cometary-source chronology models (Neukum et al. 1998; Zahnle et al. 1998; Zahnle et al. 2003). For the younger resurfaced, tectonically disrupted terrain on Ganymede, the lunar-like chronology model gives ages in the range of 3.6–3.9 Gyr ago (Neukum et al. 1997, 1998) while the cometary chronology model gives an age of about 2 Gyr (Zahnle et al. 2003) up to few hundred million years (Zahnle et al. 1998).

The densely cratered surfaces of Saturn's icy satellites are estimated to be in the range 3.8–4 Gyr old by applying the lunar-like impact chronology model. However, resurfaced units, in particular on Enceladus and Dione, show lower ages at approximately 1.5 Gyr ago (Boyce and Plescia 1985; Neukum 1985).

Current efforts focus on updating existing chronology models with the help of new spacecraft data (e.g., Zahnle et al. 2003) and imply ages far below 1 Gyr for the resurfaced terrain on Enceladus and ages as old as 4 Gyr for the older terrain, using a constant-rate chronology model with mainly cometary contribution of impactors. Mimas' surface crater-impact density is close to saturation, suggestive of an old age, but it lacks larger impact craters beyond 30 km implying a much younger surface age. For Saturn's moon Titan, the small number of observed impact craters suggests very young surface ages. A closer look at the data and impact conditions, however, shows that much of Titan's surface is probably as old as 2 Gyr (Jaumann and Neukum 2009).

See also

- ▶ Crater, Impact
- ▶ Mare, Maria
- ▶ Mars

- ▶ Mercury
- ▶ Moon, The
- ▶ Terrestrial Planet
- ▶ Tessera, Tesseræ
- ▶ Venus

References and Further Reading

- Albarède F (2009) *Geochemistry: an introduction*. Cambridge University Press, Cambridge
- Arvidson RE, Boyce J, Chapman C, Cintala M, Fulchignoni M, Moore H, Neukum G, Schultz P, Soderblom L, Strom R, Woronow A, Young R (1979) Standard techniques for presentation and analysis of crater size-frequency data. *Icarus* 37:467–474
- Baldwin RB (1964) Lunar crater counts. *Astron J* 69:377
- Baldwin RB (2006) Was there ever a terminal lunar cataclysm? With lunar viscosity arguments. *Icarus* 184(2):308–318
- Basilevsky AT, Head JW (1998) The geologic history of Venus: a stratigraphic view. *J Geophys Res* 103:8531–8544
- Basilevsky AT, Head JW (2002) Venus: timing and rates of geologic activity. *Geology* 30:1015
- Bibring J-P, Langevin Y, Mustard JF, Poulet F, Arvidson R, Gendrin A, Gondet B, Mangold N, Pinet P, Forget F (2006) Global mineralogical and aqueous Mars history derived from OMEGA/Mars express data. *Science* 312:400–404
- Boyce JM, Plescia JB (1985) Chronology of surface units on the icy satellites of Saturn. In: Klinger J, Benest D, Dollfus A, Smoluchowski R (eds) *Ices in the solar system*. D. Reidel, Dordrecht
- Chapman C, Veverka J, Belton MJS, Neukum G, Morrison D (1996) Cratering on Gaspra. *Icarus* 120(1):231–245
- Chapman CR, Merline W, Thomas P, Near MSI-Nis Team (1998) Cratering of the C-Type Asteroid Mathilde. *Meteorit Planet Sci* 33:A30
- Croft SK (1985) Ganymede and Callisto: beauty is only skin deep. *J Geophys Res Suppl* 90:12–14
- Dalrymple GB, Ryder G (1991) Ar-40/Ar-39 ages of six Apollo 15 impact melt rocks by laser step heating. *Geophys Res Lett* 18:1163–1166
- Greeley R, Batson RM (1990) *Planetary Mapping*. In: Greeley R, Batson RM (eds) *Planetary mapping*. Cambridge University Press, Cambridge
- Hartmann WK (1966) Early lunar cratering. *Icarus* 5:406–418
- Hartmann WK, Strom RG, Grieve RAF, Weidenschilling SJ, Diaz J, Blasius KR, Chapman C, Woronow A, Shoemaker EM, Dence MR, Jones KL (1981) Chronology of planetary volcanism by comparative studies of planetary cratering. In: Project, B. V. S (ed) *Basaltic volcanism on the terrestrial planets*. Pergamon Press, New York, pp 1049–1128
- Hartmann WK, Ryder G, Dones L, Grinspoon D (2000) Time-dependent intense bombardment of the primordial earth/moon system. In: Canup RM, Righter K (eds) *Origin of the earth and moon*. University of Arizona Press, Tucson, p 493
- Hartmann WK, Neukum G (2001) Cratering chronology and the evolution of Mars. *Space Sci Rev* 96:165–194
- Heiken G, Vaniman D, French BM (eds) (1991) *Lunar sourcebook: a user's guide to the Moon*. Cambridge University Press, New York, p 756
- Hiesinger H, Head JW, Wolf U, Jaumann R, Neukum G (2003) Ages and stratigraphy of mare basalts in Oceanus Procellarum, Mare Nubium, Mare Cognitum, and Mare Insularum. *J Geophys Res* 108:E75065
- Holsapple KA (1987) Impact crater scaling laws. *Intl J Impact Eng* 5:343

- Jaumann R, Neukum G (2009) The surface age of Titan, 40th Lun Planet Sci Conf 1641, The Woodlands, TX
- Lucchitta BK, Soderblom LA (1982) The geology of Europa. In: Morrison D (ed) *Satellites of Jupiter*. University of Arizona Press, Tucson, p 521
- McCauley JE, Guest JE, Schaber GG, Trask NJ, Greeley R (1981) Stratigraphy of the Caloris basin, Mercury. *Icarus* 47:184–202
- McKinnon WB, Zahnle KJ, Ivanov BA, Melosh HJ (1997) Cratering on Venus: models and observations. In: Bougher SW, Hunten DM, Phillips RJ (eds) *Venus II*. University of Arizona Press, Tucson, pp 969–1014
- Michael G, Neukum G (2009) Planetary surface dating from crater size – frequency distribution measurements: partial resurfacing events and statistical age uncertainty. *Earth Planet Sci Lett* (in press)
- Mittlefehldt DW (1994) ALH84001, a cumulate orthopyroxenite member of the Martian meteorite clan. *Meteoritics* 29:214–221
- Neukum G, Koenig B, Arkani-Hamed J (1975) A study of lunar impact crater size-distributions. *Moon* 12:201–229
- Neukum G, Wise DU (1976) Mars – A standard crater curve and possible new time scale. *Science* 194:1381–1387
- Neukum G (1977) Lunar Cratering, paper presented at discussion on the Moon – A new appraisal from space missions and laboratory analyses. Royal Society Philosophical Transactions, London
- Neukum G, Hiller K (1981) Martian ages. *J Geophys Res* 86:3097–3121
- Neukum G (1983) *Meteoritenbombardement und Datierung planetarer Oberflächen*. Dissertation for Faculty Membership, University of Munich, Munich
- Neukum G (1985) Cratering records of the satellites of Jupiter and Saturn. *Adv Space Res* 5(8):107–116
- Neukum G, Ivanov BA (1994) Crater size distributions and impact probabilities on Earth from Lunar, terrestrial-planet, and asteroid cratering data. In: Gehrels T, Matthews MS, Schumann A (eds) *Hazards due to comets and asteroids*. University of Arizona Press, Tucson, p 359
- Neukum G (1997) Bombardment history of the jovian system. In: *The three Galileos: the man, the spacecraft, the telescope*. Kluwer, Padova
- Neukum G, Wagner R, Wolf U, Ivanov BA, Head JW III, Pappalardo RT, Klemaszewski JE, Greeley R, Belton MJS, Galileo SSI Team (1998) *Cratering Chronology in the Jovian System and Derivation of Absolute Ages*. Lun Planet Sci Conf, 1742, Houston, TX
- Neukum G, Ivanov BA, Hartmann WK (2001a) Cratering records in the inner solar system in relation to the lunar reference system. *Space Sci Rev* 96:55–86
- Neukum G, Oberst J, Hoffmann H, Wagner R, Ivanov BA (2001b) Geologic evolution and cratering history of Mercury. *Planet Space Sci* 49:1507–1521
- Ogg JG, Ogg G, Gradstein FM (eds) (2008) *The concise geologic time scale*. Cambridge University Press, New York, p 77
- Öpik EJ (1960) The lunar surface as an impact counter. *Mon Not R Astron Soc* 120:404
- Phillips RJ, Raubertas RF, Arvidson RE, Sarkar IC, Herrick RR, Izenberg N, Grimm RE (1992) Impact craters and Venus resurfacing history. *J Geophys Res* 97:15923
- Schmidt RM, Housen KR (1987) Some recent advances in the scaling of impact and explosion cratering. *Int J Impact Eng* 5:543–560
- Scott DH, Carr MH (1978) *Geologic map of Mars, I-1083*. U. S. Geological Survey, Reston
- Shoemaker EM, Hackman RJ (1962) Stratigraphic basis for a lunar time scale. Paper presented at *The Moon*, n/a 1, 1962
- Shoemaker EM, Wolfe RF (1982) Cratering time scales for the Galilean satellites. In: Morrison D (ed) *Satellites of Jupiter*. University of Arizona Press, Tucson, p 277
- Spudis PD, Guest JE (1988) Stratigraphy and geologic history of Mercury. In: Vilas F, Chapman CR, Matthews MS (eds) *Mercury*. University of Arizona Press, Tucson, pp 118–164
- Stöffler D, Ryder G (2001) Stratigraphy and isotope ages of lunar geologic units: chronological standard for the inner solar system. *Space Sci Rev* 96(1/4):9–54
- Stöffler D, Ryder G, Ivanov BA, Artemieva NA, Cintala MJ, Greve RA (2006) Cratering history and lunar chronology. In: Jolliff BL, Wieczorek MA, Shearer CK, Neal CR (eds) *New views of the Moon*. Mineralogical Society of America, Geochemical Society, Chantilly, pp 519–588
- Strom RG, Neukum G (1988) The cratering record on Mercury and the origin of impacting objects. In: Vilas F, Chapman CR, Matthews MS (eds) *Mercury*. University of Arizona Press, Tucson
- Strom RG, Schaber GG, Dawson DD (1994) The global resurfacing of Venus. *J Geophys Res* 99:10899
- Strom RG, Malhotra R, Ito T, Yoshida F, Kring DA (2005) The origin of planetary impactors in the inner solar system. *Science* 309(5742):1847–1850
- Tanaka KL (1986) The stratigraphy of Mars. *J Geophys Res* 91:139
- Tanaka KL, Scott DH, Greeley R (1992) *Global stratigraphy*. In: Kieffer HH (ed) *Mars*. University of Arizona Press, Tucson, pp 345–382
- Tanaka KL, Senske DA, Price M, Kirk RL (1997) Physiography, geomorphic/geologic mapping, and stratigraphy of Venus. In: Bougher SW, Hunten DM, Phillips RJ (eds) *Venus II*. University of Arizona Press, Tucson, pp 667–694
- Tanaka KL, Hartmann WK (2008) Planetary time scale. In: Ogg JG, Ogg G, Gradstein FM (eds) *The concise geologic time scale*. Cambridge University Press, New York, pp 13–22
- Tera F, Papanastassiou DA, Wasserburg GJ (1974) Isotopic evidence for a terminal lunar cataclysm. *Earth Planet Sci Lett* 22:1
- Trask NJ, Guest JE (1975) Preliminary geologic terrain map of Mercury. *J Geophys Res* 80:2461–2477
- Wetherill GW (1975) Late heavy bombardment of the moon and terrestrial planets, paper presented at Lunar Science Conference March 17–21, Pergamon Press, Houston
- Wilhelms DE, McCauley JE, Chao ECT (1971) Summary of lunar stratigraphy and structure: a perspective for lunar sample analysis. *Meteoritics* 6:324–326
- Wilhelms DE, Squyres SW (1984) The martian hemispheric dichotomy may be due to a giant impact. *Nature* 309:138–140
- Wilhelms DE (1987) *The geologic history of the moon*. U.S. Geological Survey, Washington, DC, pp 1348
- Zahnle K, McKinnon WB (1996) Age of the surface of Venus, paper presented at *Bulletin of the American Astronomical Society*, September 1, 1996
- Zahnle K, Dones L, Levison HF (1998) Cratering rates on the Galilean satellites. *Icarus* 136:202
- Zahnle K (2003) Cratering rates in the outer solar system. *Icarus* 163(2):263–289

Chury

- ▶ [Comet, Churyumov-Gerasimenko](#)
- ▶ [Comet](#)

CIP Rules

- ▶ [Cahn Ingold Prelog Rules](#)

Circular Dichroism

Synonyms

[CD](#)

Definition

In chemistry, circular dichroism (CD) refers to the differential absorption of left and right-handed circularly polarized light by optically active ▶ [chiral](#) molecules. Electromagnetic radiation consists of electric and magnetic fields that oscillate perpendicular to one another and to the direction of propagation. Linearly polarized light occurs when the electric field vector oscillates only in one plane and changes in magnitude, while circularly polarized light occurs when the electric field vector rotates about its propagation direction and retains constant magnitude. It thus forms a helix propagating in space.

When circularly polarized light passes through an optically active light-absorbing medium, the velocities and wavelengths of its right and left polarizations differ as does the extent to which they are absorbed. CD is the difference in the amount of absorption between the two. Since circularly polarized light is “chiral,” it interacts differently with different chiral molecules. At the quantum mechanical level, the information provided by circular dichroism and optical rotation measurements are identical. Depending on the wavelength employed, CD can be used to investigate the structures of proteins, nucleic acids, small organic molecules, and charge-transfer transitions.

See also

- ▶ [Chirality](#)
- ▶ [Polarized Light and Homochirality](#)

Circumplanetary Disk

- ▶ [Planetary Rings](#)

Circumstellar Disk

- ▶ [Protoplanetary Disk](#)

Circumstellar Dust Disks

- ▶ [Debris Disk](#)

Cirrus Cloud

Definition

In astronomy, cirrus clouds are sources of infrared (IR) emission detected by the ▶ [InfraRed Astronomy Satellite \(IRAS\)](#), a joint project of the US, the UK, and the Netherlands which surveyed the sky at wavelengths of 12, 25, 60, and 100 μm . The spatial distribution of this IR emission is similar in appearance to terrestrial cirrus clouds, although the latter have nothing to do with the interstellar clouds. The astronomical emission arises from interstellar dust in our galaxy, particularly that associated with the diffuse portions of interstellar clouds.

See also

- ▶ [Infrared Astronomical Satellite](#)
- ▶ [Interstellar Dust](#)

Cistron

- ▶ [Gene](#)

Citric Acid Cycle

JULI PERETÓ

Cavanilles Institute for Biodiversity and Evolutionary Biology and Department of Biochemistry and Molecular Biology, University of València, València, Spain

Synonyms

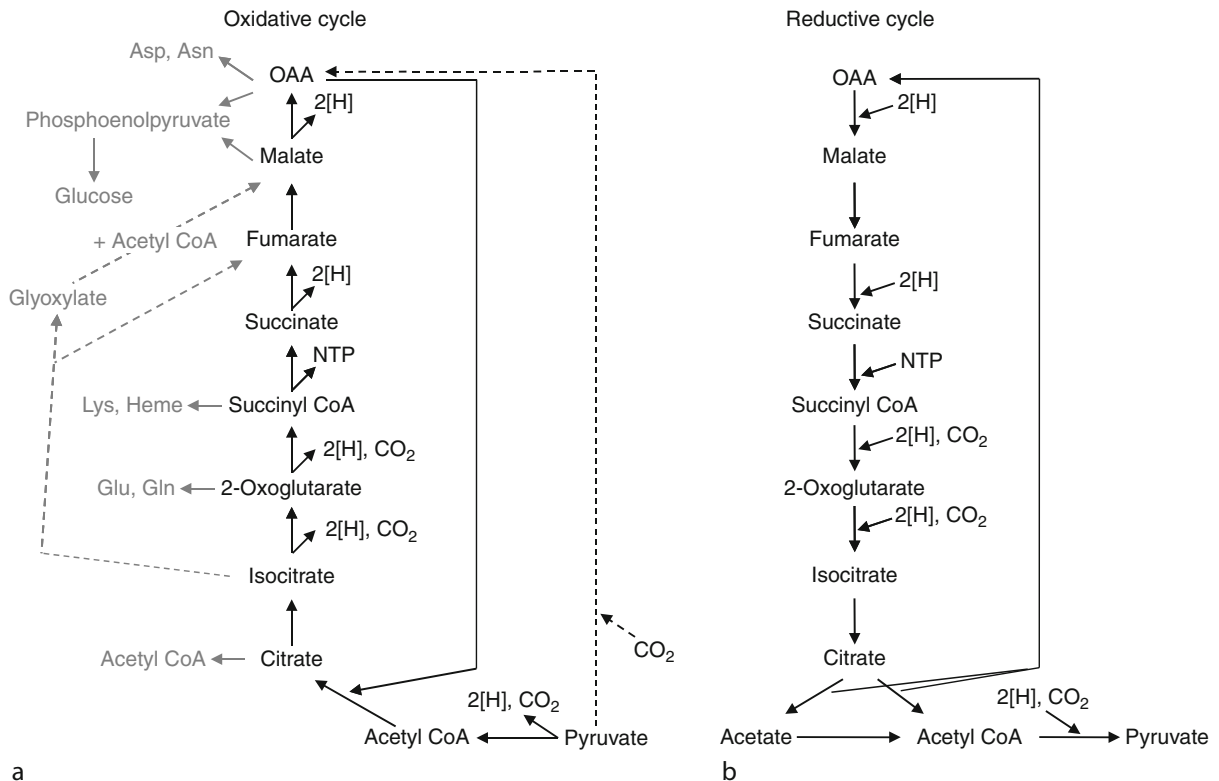
[Krebs cycle](#); [Tricarboxylic acid \(TCA\) cycle](#)

Keywords

Anaplerosis, cataplerosis, catalytic cycle, oxidative metabolism

Definition

Citric acid cycle is a metabolic pathway often regarded as the final step for the complete oxidation of fuel molecules.



Citric Acid Cycle. Figure 1 The citric acid cycle. **(a)** Oxidative cycle. An anaplerotic reaction is shown (broken black line), as well as some biosynthetic branches starting from cycle intermediates (in gray). The glyoxylate shunt is also shown (broken gray line). **(b)** Reductive cycle

Stoichiometrically, a 2-C molecule (acetyl CoA) condenses with a 4-C molecule (oxaloacetate) to yield citrate (Fig. 1a). Two consecutive oxidative decarboxylations transform the initial 2-C unit into two CO_2 molecules. The regeneration of oxaloacetate closes the cycle through an oxidative process. In addition to the electrons taken up by redox coenzymes ($NAD(P)^+$ and FAD), a part of the energy is conserved in a substrate-level phosphorylation step yielding GTP. The citric acid cycle can also be regarded as a source of biosynthetic precursors. In some organisms, the cycle operates in reverse, reductively, thus functioning as an autotrophic pathway (Fig. 1b).

History

In an elegant series of experiments on substrate oxidation in respiratory animal tissues, performed among others by Albert Szent-Györgyi (1893–1986), Carl Martius (1906–1993), and Franz Knoop (1875–1946), fragments of a sequence of the metabolic transformations were established. Those observations were completed by Hans A. Krebs (1900–1981) who proposed, in a paper

co-authored by William A. Johnson, the cyclic nature of the pathway in 1937 (Krebs and Johnson 1937).

Overview

The citric acid cycle occupies a central position in the metabolic network both as a **catabolic**, oxidative process and as a supplier of biosynthetic precursors. The cycle is more a roundabout (or traffic circle) than a carousel: There is a permanent flux of metabolites in and out the cycle. Some metabolites are used for biosynthetic purposes (e.g., 2-oxoglutarate as glutamate precursor or succinyl CoA for the biosynthesis of heme group or lysine, see Fig. 1a). The catalytic nature of the citric acid cycle, as well as the consumption of intermediates as biosynthetic precursors, imposes the necessity of the net synthesis and replacement of those intermediates. This process is termed anaplerosis. Anaplerotic reactions include the synthesis of oxaloacetate by pyruvate carboxylation, and the synthesis of oxaloacetate or 2-oxoglutarate from aspartate or glutamate, respectively, by transamination. On the other hand, the 4-C and 5-C skeletons derived from amino acid

catabolism must leave the cycle to be fully oxidized (this process has been called cataplerosis (Owen et al. 2002).

In some autotrophic microorganisms, the citric acid cycle operates in a reverse, reductive way (Fig. 1b). This pathway (also known as the Arnon-Buchanan cycle) allows the net synthesis of Acetyl CoA from CO₂. Firstly described by Daniel I. Arnon and Robert B. Buchanan in 1966 as the autotrophic carbon fixation pathway in the green sulfur bacterium *Chlorobium limicola* (Evans et al. 1966), it is also present in some proteobacteria and some members of the domain Archaea (Berg et al. 2010).

See also

- ▶ Anabolism
- ▶ Carbon Dioxide
- ▶ Catabolism
- ▶ Glycolysis
- ▶ Metabolism (Biological)

References and Further Reading

- Berg IA, Kockelkorn D, Ramos-Vera WH, Say RF, Zarzycki J, Hügler M, Alber BE, Fuchs G (2010) Autotrophic carbon fixation in archaea. *Nat Rev Microbiol* 8:447–460
- Evans MCW, Buchanan BB, Arnon DI (1966) A new ferredoxin-dependent carbon reduction cycle in a photosynthetic bacterium. *Proc Natl Acad Sci USA* 55:928–934
- Krebs HA, Johnson WA (1937) The role of citric acid in intermediate metabolism in animal tissues. *Enzymologia* 4:148–156
- Owen OE, Kalhan SC, Hanson RW (2002) The key role of anaplerosis and cataplerosis for citric acid cycle function. *J Biol Chem* 277:30409–30412

Classification

- ▶ Taxonomy

Clastation

- ▶ Weathering

Clathrate

Definition

In chemistry, a clathrate is an inclusion complex, also known as a clathrate compound, cage or a host–guest

complex, in which a molecule, aggregate of molecules or crystal lattice of molecules (the “host”) noncovalently traps or encloses another, usually small, gas molecule (the “guest”), rendering it incapable of escaping by diffusion. The word is derived from the Latin word *clatratus*, meaning “with bars” or “a lattice.”

Especially important naturally occurring types of clathrates are ▶ **clathrate hydrates**, formed from water ices and various gases such as methane, ammonia or CO₂, and zeolite minerals.

See also

- ▶ Clathrate Hydrate

Clathrate Hydrate

Definition

Clathrate hydrates are ice-like solids in which a “host” hydrogen-bonded H₂O lattice entraps a nonpolar “guest” gas molecule such as CH₄ or CO₂. It has been speculated that clathrate hydrates are important components of many outer solar system bodies including comets, the outer planets, and their icy moons. Methane clathrate hydrates are also widely distributed in terrestrial seafloor sediments where the ambient temperature and pressure allows their existence. It is thought that their breakdown during periods of increasing temperature releases methane, a strong greenhouse gas, which may contribute significantly to global warming.

See also

- ▶ Clathrate

Clay

ALICIA NEGRÓN-MENDOZA

Instituto de Ciencias Nucleares, Universidad Nacional Autónoma de México, Coyoacán, DF, Mexico

Synonyms

Argillaceous earth; Clay minerals

Keywords

Chemical evolution, clay, clay minerals, montmorillonite, phyllosilicates

Definition

Clay is a generic term for a ► **mineral** group of complex hydrated aluminophyllosilicates that mainly form from feldspar ► **weathering** and as low-temperature hydrothermal alteration products of many rocks.

Clays are natural, soft, fine-grained materials less than 2 μm in size; they are plastic when mixed with an appropriate amount of ► **water** but hard when fired. Clays are composed of a silicon tetrahedral layer and an aluminum octahedral layer with water trapped between silicate sheets (Guggenheim and Martin 1995).

History

Clays and clay minerals have been mined since the Stone Age, once prehistoric man discovered clay's useful properties. Clay tablets were used as the first writing medium, while clays sintered in fire were used to make the first ceramic objects. Many ancient religions and philosophies have posed that mankind was originally created from clay; for example, in the Bible, the first man, Adam, whose name means "of the ► **earth**," was made from clay.

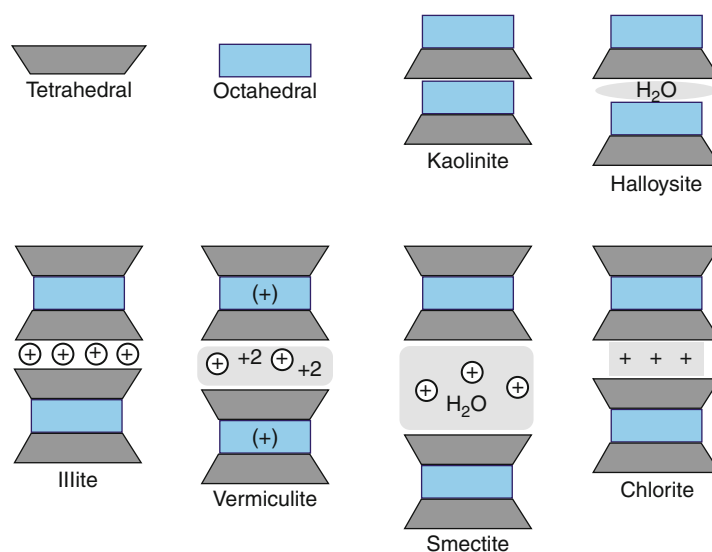
Overview

Structure

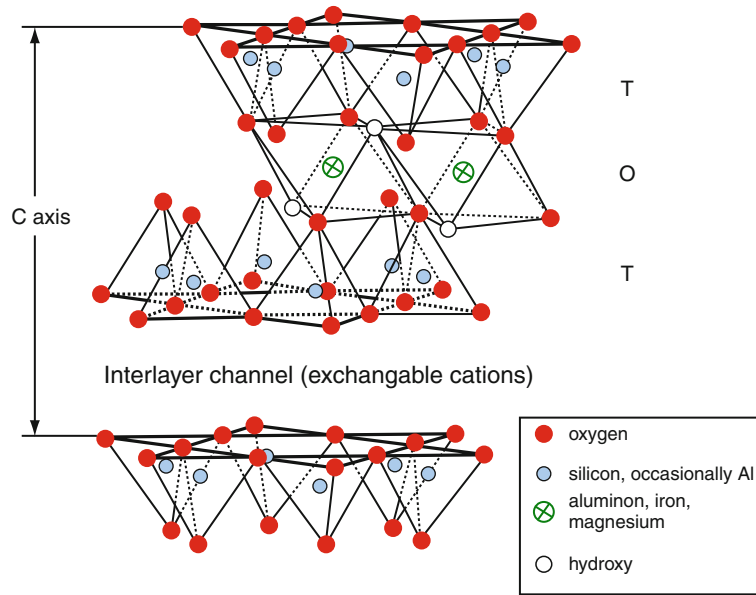
Clays' simple crystal structure consists of two basic components: a silicon tetrahedron-oxygen layer (the tetrahedral silicon can, in part, be replaced by Al^{3+} or Fe^{3+}), and an octahedron layer, in which an atom of aluminum, magnesium, and/or iron is surrounded by six anions

(oxygen atoms or hydroxyl groups). The individual units are stacked in parallel plates, one above the other, and depending upon the arrangement, different types of clays are produced. They are classified first according to the number of tetrahedral and octahedral sheets that have combined into "layer types" and then into "groups," which are differentiated by the kinds of isomorphic cation substitutions that have taken place. The layer types are illustrated in Fig. 1. The 1:1 (tetrahedral-octahedral or TO) layer type consists of one tetrahedral sheet fused to an octahedral sheet and is represented by the ► **kaolinite** group. Type 2:1 clay (or TOT) is made up of an octahedral sheet sandwiched between two tetrahedral sheets; examples include kaolinite, illite, and smectites, such as ► **montmorillonite**. This composite unit is continuous in two directions of a plane in the c-direction see (Fig. 2) and forms packets of 2–15 elementary units (Meunier 2010). Figure 2 depicts a TOT layer type crystal structure.

At all ► **pH** values above 2, clay particles carry a net negative charge in the space between the silica layers, referred to as the interlayer or interlamellar channel. The distance between these layers varies, depending upon the layers of water or intercalated organics (Swartzen-Allen and Matijevic 1974). The negative charge can originate from several different factors, including lattice imperfections, isomorphic substitution, broken bonds, and exposed structural hydroxyl groups. The presence of a positive counterion, such as Na^+ , K^+ , or Ca^{2+} , compensates for the negative charge. The edges of the crystal are positively charged in the neutral and acid pH ranges



Clay. Figure 1 Types of clays (see text)



Clay. Figure 2 TOT layer type crystal structure

(Swartzen-Allen and Matijevic 1974). These structural characteristics give rise to the special properties of clays. For example, *montmorillonite* can take up organic molecules of various kinds. The molecule may be adsorbed on the clay lattice by cation interchange, ion-dipole forces, ► [van der Waals forces](#), or hydrogen bonds.

Importance

Clays are important minerals in nature as well as in human activities. They are an integral part of terrestrial ► [biogeochemical cycles](#). These cycles influence microbial ► [life](#) and the cycling of elements on planetary surfaces. They also play a role in the buffering capacity of the oceans; it has also been proposed that they played a central role in ► [chemical evolution](#) and the ► [origin of life](#) (Negrón-Mendoza et al. 2010). The investigation of the role of clays in prebiotic organic synthesis ranges from their potential use as catalytic substrates to the controversial claim that it was initially clays that were the functional templates (Cairns-Smith and Hartman 1988). These uses are due to their capacity to adsorb organic molecules and catalyze reactions in various different ways (Theng 1974; Laszlo 1987; Yariv and Cross 2002). Clays are among the most important minerals used by the manufacturing and environmental industries, such as in the field of construction ceramics, like tiles and bricks, and in pottery.

Alongside sand and silt, clay is one of the three principal types of sediment and primarily forms from the weathering of rocks and soil at the surface of the Earth.

Clays are ubiquitous minerals on Earth; it also seems likely that their presence can be traced to the early stages of the planet's formation. While various clays probably formed on the continents of the Earth in the Archaean, the largest area of clay production would have been the sea floor. The genesis of continental smectites can be traced back to 3 or 4 billion years ago (Odin 1988).

The presence of clays in extraterrestrial environments, such as in ► [meteorites](#), on ► [Mars](#), and in the ► [comet Tempel 1](#) (Lisse et al. 2006), is important to understanding the conditions of aqueous alteration that prevailed in the early stage of the history of the solar system, as the primary requirement for the formation of clay minerals is the presence of liquid water.

See also

- [Biogeochemical Cycles](#)
- [Buffer](#)
- [Chemical Evolution](#)
- [Comet Tempel 1](#)
- [Earth](#)
- [Earth, Formation and Early Evolution](#)
- [Environment](#)
- [Hydrogen Bond](#)
- [Hydrothermal Reaction](#)
- [Kaolinite](#)
- [Life](#)
- [Mars](#)
- [Meteorites](#)

- ▶ [Mineral](#)
- ▶ [Montmorillonite](#)
- ▶ [Organic Molecule](#)
- ▶ [Origin of Life](#)
- ▶ [pH](#)
- ▶ [Silicate Minerals](#)
- ▶ [Van der Waals Forces](#)
- ▶ [Water](#)
- ▶ [Weathering](#)

References and Further Reading

- Cairns-Smith AG, Hartman H (1988) *Clay minerals and the origin of life*. Cambridge University Press, Cambridge
- Guggenheim S, Martin RT (1995) Definition of clay and clay minerals: join report of the AIPEA nomenclature and CMS nomenclature committees. *Clay Clay Min* 43:255–256
- Laszlo P (1987) Chemical reactions on clays. *Science* 235:1473–1477
- Lisse CM, Van Cleve J, Adams AC, Ahearn ME, Fernández YR, Farnham TL, Armus CML, Grillmair CJ, Ingalls J, Belton MJS, Groussin O, McFadden LA, Meech KJ, Schultz PH, Clark BC, Feaga LM, Sunshine JM (2006) Spitzer spectral observations of the deep impact ejecta. *Science* 313:635–640
- Meunier A (2010) *Clays*. Springer, Berlin
- Negrón-Mendoza A, Ramos-Bernal S, Mosqueira FG (2010) The role of clay interactions in chemical evolution. In: Basiuk V (ed) *Astrobiology: emergence, search and detection of life*. American Scientific Publishers, Los Angeles, pp 214–233
- Odin GS (1988) The origin of clays on Earth. In: Cairns-Smith AG, Hartman H (eds) *Clay minerals and the origin of life*. Cambridge University Press, Cambridge, pp 81–89
- Swartzen-Allen SL, Matijevic E (1974) Surface and colloid chemistry of clays. *Chem Rev* 74:385–399
- Theng BKG (1974) *The chemistry of clay-organic reactions*. Adam Hilger/Wiley, London/New York
- Yariv S, Cross H (2002) *Organo-clay complexes and interactions*. Marcel Dekker, New York

Clay Minerals

- ▶ [Clay](#)
- ▶ [Phyllosilicates \(Extraterrestrial\)](#)

Clean Room

Definition

A clean room is a work place, generally a room, where the air is permanently filtered to remove the particles. In some cases, the temperature and atmospheric humidity are also

controlled while the number of particles is monitored. The access is strictly limited to trained personnel entering through a double door after they dress with protective garment to avoid the spreading of skin particles and hair. In such clean rooms, the laboratory hardware, the lab wear of the personnel, the number of people working simultaneously is also specified to limit the spreading of dust and particles. Clean rooms are used in industry to perform the tasks requiring the maximum cleanliness such as the production of microprocessors, hard disk drives, and precision optical elements.

Minimizing the number of particles minimizes also the number of airborne ▶ [microorganisms](#) and subsequently the contamination of the surfaces.

Clean rooms are required for the assembly of the satellites and of the interplanetary probes following planetary protection policy. In practice, the clean rooms are often known by the number of particles with size under 0.5 μm by cubic feet (class 10,000, class 1,000, Class 100, . . .). A strict definition is proposed by the international standard organization (▶ [ISO](#)) in the standard *ISO 14644-1*. This definition applies also to small working area limited to a tent or to working cabinets.

See also

- ▶ [ISO](#)
- ▶ [Microorganism](#)
- ▶ [Planetary Protection](#)

Cleanliness

Definition

For ▶ [planetary protection](#), the cleanliness of an environment or spacecraft hardware is the level of contamination by something which is not wanted for the achievement of a goal. The maximum amount of the unwanted item is generally specified. For instance the biological cleanliness can be measured by the number of remaining microorganisms after the cleaning process. Depending on the final goal the living microorganisms, the dead microorganisms, or both could be considered. The chemical cleanliness refers to maximal specified amounts of each chemical per unit of surface or volume.

See also

- ▶ [Bioburden](#)
- ▶ [Planetary Protection](#)
- ▶ [Sterilization](#)

Cloning

Definition

Cloning is the process of obtaining replicative molecules, cells, or organisms that are genetically identical to a common ancestor. DNA recombinant techniques – or ► [genetic engineering](#) – allow the synthesis, replication, and expression of DNA fragments of any size – up to complete synthetic molecules the size of a small bacterial genome – in appropriate receptor cells. The cloning of cells and organisms – e.g., plants and animals – using the methods of tissue culture and in vitro cell differentiation is also possible.

See also

► [Amplification \(Genetics\)](#)

Clouds

MARK S. MARLEY¹, LISA KALTENEGGER^{2,3}

¹NASA Ames Research Center, Moffett Field, CA, USA

²Harvard University, Cambridge, MA, USA

³MPIA, Heidelberg, Germany

Synonyms

[Condensate layer](#)

Keywords

Albedo, atmosphere, clouds, extrasolar planets, spectra, spectroscopy

Definition

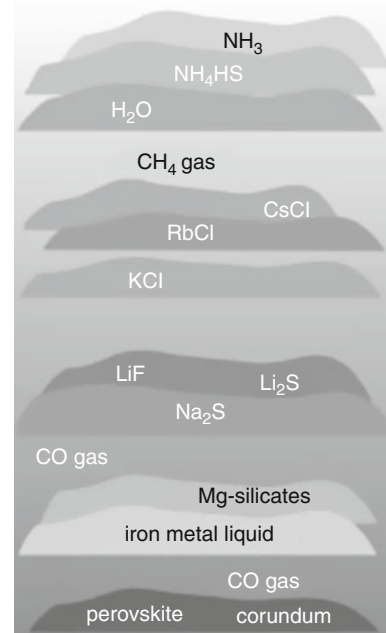
Clouds play an important role in planetary atmospheres. Since clouds scatter and absorb incident stellar radiation as well as emergent thermal radiation, they control both the appearance and thermal structure of a planet. Furthermore, a cloud deck can both limit the depth an external observer can “see” into an atmosphere and thus hide molecular species, and it can alter a planet’s ► [albedo](#). For such reasons, a basic understanding of the role clouds play is required to interpret exoplanet spectra.

Overview

To understand cloud structure, we imagine an air parcel moving upward from the deep atmosphere. We start at a set temperature and slowly raise the gas parcel up; as the

gas rises, it cools adiabatically (without exchanging heat with the remainder of the atmosphere) while the partial pressure of the condensable species remains constant. As the temperature falls, however, the saturation vapor pressure, which measures how much of the condensable species the gas parcel can hold, decreases very rapidly. When the condensable species’ partial pressure equals the saturation vapor pressure the parcel is said to be saturated and under equilibrium conditions a solid or liquid condensate forms. This is where we expect to find a cloud base. In reality, condensation often occurs later, somewhat higher in an atmosphere, when the parcel is slightly supersaturated.

► [Jupiter’s](#) atmosphere provides a point of departure for understanding the diversity of giant planet atmospheres that we expect to encounter outside of the solar system. Assuming we start at a temperature of about 2,000 K ([Fig. 1](#)), the first constituents to condense in a rising gas parcel are refractory oxides such as perovskite and corundum, followed by various magnesium silicates including enstatite and forsterite. As we move upward in the atmosphere, the temperature continues to fall and eventually water clouds form, removing H₂O from the gas phase. Above the water clouds, the atmosphere continues to cool until ammonia clouds form. It is the



Clouds. **Figure 1** Cloud structure expected on a Jupiter-like planet depending on its temperature (hot: *bottom*, cool: *top*). Figure modified from Lodders (2004)

ammonia clouds of Jupiter, dusted by various photochemical pollutants, that we see reflecting sunlight back from the planet. In a warmer Jupiter, the atmosphere would never become saturated in water and ammonia vapor, and these species would stay in the gas phase, thus removing the bright clouds and substantially altering the appearance and color of the planet.

Likewise, for terrestrial planets, clouds play a crucial role. Typically, the reflectivity of water clouds in the visible and near-infrared wavelength range is high in comparison to surface features. Thus, a cloudy planet is brighter and has a higher albedo than either a rocky, airless world or a planet with a deep, clear atmosphere. Thick clouds can limit the height from which thermal flux is emitted in an atmosphere and thus hide underlying regions which might otherwise produce significant spectral features. Clouds must be considered in any calculation of the location of the ► [Habitable Zone](#), as they can both raise the Bond albedo, thus lowering the surface temperature, and limit thermal emission, which has the opposite effect.

Clouds can also hide the presence of absorbers which lie beneath. For Venus, the sulfuric acid (H₂SO₄) cloud deck obscures any information from below the cloud deck and thus prevents sampling the whole atmosphere or the surface.

Future Directions

Clouds are intrinsically difficult to model from a priori physical considerations (see, e.g., Yau and Rogers 1989; Yung and DeMore 1999; Ackerman and Marley 2001; Marley et al. 2007; Helling et al. 2008; Kasting 1991; Forget and Pierrehumbert 1997). The detailed behavior of the terrestrial cloud cover as a function of atmospheric temperature is the leading source of uncertainty in global climate models. Although the chemistry is thought to be well understood, predicting cloud behavior for extrasolar planets, including such issues as particle sizes, vertical distribution, and any horizontal patchiness is difficult. Accounting for the effects of these clouds has proven challenging, and such issues must be carefully considered when spatially resolved exoplanet spectra eventually become available.

See also

- [Adiabatic Processes](#)
- [Albedo](#)
- [Atmosphere, Structure](#)
- [Exoplanets, Modeling Giant Planets](#)
- [Greenhouse Effect](#)
- [Habitable Planet \(Characterization\)](#)
- [Habitable Zone](#)
- [Jupiter](#)

References and Further Reading

- Ackerman A, Marley M (2001) Precipitating condensation clouds in substellar atmospheres. *J Astrophys* 556:872–884
- Forget F, Pierrehumbert RT (1997) Warming early Mars with carbon dioxide clouds that scatter infrared radiation. *Science* 278 (5341):1273
- Helling C et al (2008) Comparative study of dust cloud modelling for substellar atmospheres. *Mon Not R Astron Soc* 391(4):1854–1873
- Kaltenegger L, Jucks K, Traub W (2007) Spectral evolution of an Earth-like planet. *Astrophys J* 658:598
- Kasting J (1991) *Icarus* (ISSN 0019-1035), vol 94, p 1–13
- Kitzmann D et al (2010) Clouds in the atmospheres of extrasolar planets. I. Climatic effects of multi-layered clouds for Earth-like planets and implications for habitable zones. *Astron Astrophys* 511:A66
- Lodders K (2004) *Science* 303:323
- Marley MS, Fortney J, Seager S, Barman T (2007) Atmospheres of extrasolar giant planets. *Protostars Planets V* 733
- Niemann HB et al (1998) The composition of the Jovian atmosphere as determined by the Galileo probe mass spectrometer. *J Geophys Res* 103:22831
- Yau MK, Rogers RR (1989) Short course in cloud physics. International Series in Natural Philosophy, 3rd edn. Butterworth-Heinemann, Woburn
- Yung YL, Demore WB (1999) Jovian Planets. In: Yung YL, DeMore WB (eds) Photochemistry of planetary atmospheres. Oxford University Press, New York

CMB

- [Cosmic Background Radiation](#)

CN

- [Cyanogen Radical](#)

CNES

Synonyms

[Centre National d'études Spatiales](#); [French Space Agency](#)

Definition

The French Space Agency was established in 1961 and was tasked to implement and coordinate space policy as decided by government, through its own teams and with national and international partners in science and industry. France is a founding member of the European Space Agency (► [ESA](#)) and Centre National d'Études Spatiales

(CNES) represents the country in its council and boards. The 2,500 employees working in 2010 at CNES are spread among the 4 main centers. The headquarters are located downtown Paris, while the directorate for launchers is located in Evry (south of Paris). The large Technical Center is located in Toulouse in the south of France. Finally, CNES is also in charge of the launch base of Kourou located in French Guyana. This base is the European Spaceport from which the European launchers are operated since 1973. Besides ArianeV, Soyouz and Vega rockets are to be launched also from this base. The CNES is supporting through grants and industrial contracts most of the French activities related to space prototyping either commercial or institutional applications, supporting science in space or activities related to defence and security.

CNES was involved in manned space flight through cooperation with the Soviet Union leading to the flight of Jean-Lou Chretien in 1981 and with the United States leading to the flight of Patrick Baudry in 1985. Since then, several flights and experiments related to exobiology flew onboard the MIR space Station (► [COMET](#), ► [Exobio](#)) as well as the US Space Shuttle. Since the International Space station era, CNES is supporting manned space flight activities mainly under the auspices of ESA.

CNES is also playing a major role in the exploration of the solar system through numerous contributions to missions sponsored by United States, Soviet Union then Russia, India, Japan, and China. France is through CNES mixing the mandatory and the optional programs, the first contributor to ESA.

See also

- [Comet](#)
- [ESA](#)
- [Exobiologie Experiment](#)
- [Expose](#)

CNO Cycle

Definition

The CNO cycle is a series of nuclear reactions converting H to He and using C, N, and O isotopes as catalysts; thus, the total amount of these latter species is not affected by the operation. There are three such cycles, each converting 4 protons to one ${}^4\text{He}$ nucleus and releasing about 6.6 MeV/nucleon or $5 \cdot 10^{18}$ erg/g. At temperatures higher than $17 \cdot 10^6$ K, encountered in stars more massive than $1.3 M_{\odot}$, depending on metallicity, rotation, etc., the CNO

cycle is the dominant source of energy production, while in lower mass stars, the proton-proton ► [\(p-p\) chains](#) dominate. Although the sum of C + N + O abundances is conserved, ${}^{12}\text{C}$ and ${}^{16}\text{O}$ are converted to ${}^{14}\text{N}$.

History

The CNO cycle is also called the Bethe-Weizsäcker cycle. Hans Bethe won the 1967 Nobel Prize in physics for his 1938 discovery of energy production in stars.

See also

- [P-P Chains](#)

CNSA

Synonyms

[China National Space Administration](#)

Definition

The China National Space Administration (CNSA) was established in 1993, as a governmental institution to develop and fulfill China's due international obligations, with the approval by the Eighth National People's Congress of China (NPC). Then CNSA was assigned as an internal structure of the Commission of Science, Technology and Industry for National Defense (COSTIND).

China National Space Administration assumes the main responsibilities for signing governmental agreements in the space area on behalf of organizations; intergovernmental scientific and technical exchanges; and also being in charge of the enforcement of national space policies and managing the national space science, technology, and industry.

CNSA is backed by numerous independent organizations, ruling the industry for launchers and satellites, manned space flights, etc. The China Aerospace Corporation, the three launch bases, the China Astronaut Research, and Training Center, the Beijing Aerospace Control Center are some of these entities.

China while developing the manned space flights is developing science exploration of the ► [Moon](#) (Chang'e 1 and 2) and ► [Mars](#) (► [Yinghuo-1](#)).

Up to now, China has signed governmental space cooperation agreements with Brazil, Chile, France, Germany, India, Italy, Pakistan, Russia, Ukraine, the United Kingdom, the United States, and some other countries.

See also

- [Yinghuo-1](#)

CO₂ Ice Cap (Mars)

Definition

Mantles of CO₂ ice deposited above 50° latitude in both hemispheres of ► [Mars](#) during fall and winter. They form by condensation of CO₂ gas, the main constituent of the atmosphere, and can reach thicknesses of 50 cm to 1m. Their surface temperature is controlled by solid–gas equilibrium with the atmosphere and ranges between 142 and 150 K. In the northern hemisphere, the CO₂ ice cap completely disappears during spring. In the southern hemisphere, the CO₂ ice does not completely sublime, leaving a perennial ► [polar caps \(Mars\)](#) 300 km across and several meters thick near the south pole.

See also

- [Carbon Dioxide](#)
- [Mars](#)
- [Polar Caps \(Mars\)](#)

CO₂ Ice Clouds (Mars)

Definition

Clouds composed of CO₂ ice form when CO₂ gas (the main constituent of the ► [Mars](#) atmosphere) condenses out in the atmosphere. CO₂ ice clouds have been observed in the lower Martian atmosphere in the winter polar night of both hemispheres (Pettengill and Ford 2000), and in Mars' mesosphere (around 80–100 km altitude) near the equator (Montmessin et al. 2007). Thick CO₂ ice clouds may have been present in the ► [planet's](#) denser early atmosphere, more than 3.5 billion years ago. They could have contributed to warming the surface through the process of the scattering ► [greenhouse effect](#) (Forget and Pierrehumbert 1997).

See also

- [Carbon Dioxide](#)
- [Greenhouse Effect](#)
- [Mars](#)
- [Planet](#)

References and Further Reading

Forget F, Pierrehumbert RT (1997) Warming early Mars with carbon dioxide clouds that scatter infrared radiation. *Science* 278:1273–1276

Montmessin F, Gondet B, Bibring JP, Langevin Y, Drossart P, Forget F, Fouchet T (2007) Hyper-spectral imaging of equatorial CO₂ ice clouds on Mars by OMEGA on Mars Express. *J Geophys Res* 112: E11, CiteID E11S90

Pettengill GH, Ford PG (2000) Winter clouds over the north Martian polar cap. *Geophys Res Lett* 27:609–613

Co-elution

- [Chromatographic Co-elution](#)

Coagulation in Planetary Disks

Definition

Coagulation in the context of ► [planet formation](#) refers to a statistical model for particle growth in the ► [protoplanetary disk](#) in ► [planet formation](#). This model (usually) assumes that particle sizes and velocities are well-modeled by an analytic function, and that no outliers exist (e.g., a particle orders of magnitude larger than any other). This term may also be generally used to describe any process in which small orbiting rocky bodies accumulate into larger bodies. Coagulation is normally considered to be the first stage of growth of bodies which ultimately accrete to form rocky planets.

See also

- [Planet Formation](#)
- [Protoplanetary Disk](#)

Coagulation, of Interstellar Dust Grains

Definition

Low-energy collisions of interstellar grains can result in the growth of the grains or grain aggregates, a process sometimes referred to as coagulation. The structure of the grains or aggregates presumably depends on the size and structure of the colliding particles, and possibly on the presence or absence of an icy grain mantle.

See also

- [Interstellar Dust](#)
- [Interstellar Ices](#)

Code

HUGUES BERSINI

IRIDIA, Université Libre de Bruxelles, Brussels, Belgium

Keywords

ASCII code, genetic code, programs, semaphore, Turing machine

Definition

At first and most basically, a code defines a mapping between one type of information and another. For instance, the ASCII code in computer science is the binary translation of our alphabet, mapping for instance the lowercase character “a” onto “1100001” and making possible for computers to store, treat, and exploit information expressed in words. “Code” is one of those terms that testify to the strong intellectual connection and mutual conceptual enrichment that, since Turing, Von Neumann, and the former systemic and cybernetic schools, has always existed between biology and computer science. Interestingly enough, the different meanings of this term in computer science is mirrored by a progressive semantic enrichment also of its use in biology.

Overview

The most celebrated biological code is without doubt the “genetic” one which maps triplets of four possible ► [nucleotides](#) (“A,” “T,” “G,” “C”) onto one of the 20 ► [amino acids](#) found in the ► [proteins](#) of living organisms. For instance, the triplet “AAT” is mapped onto the “Leucine” amino acid. Although the ► [genetic code](#) is not as arbitrary as the ASCII one, still a mapping table is really what defines the coding in both cases.

There is an extended, more sophisticated definition of “code” in computer science, such as when a programmer is writing a “code” to be executed by his computer. The mapping is not anymore between one type of representation and another, but pieces of the code serve as a index to executable processes, such as when a traffic light turns red requiring the driver to stop his car. An essential part of elementary instructions in computers is indeed expressed according to a specific code (like “add” or “load”), making both the central process unit and the memory participate in the execution of a whole process (such as adding numbers or copying information from one zone of the computer to another). The ambiguity recognized by many biologists in the meaning of “► [gene](#)” can be considered in the light of these basic and extended meanings. As a matter of fact,

a gene can be seen not only as coding for the associated protein, but more and more in a richer manner, as indexing a whole and sophisticated biological process that might even execute differently according to the surrounding environment (rendering the distinction between innate and acquired characteristics much more subtle and interesting). When Richard Dawkins evolves his biomorphs (Dawkins 1996 [1986]), as described in his book “The Blind Watchmaker,” the sophistication of the obtained creatures is not so much a reflection of the genetic code used by him, but rather appears as an outcome of the recursive program simply parameterized by this code. The genes boil down to a simple parameterization of a very sophisticated process responsible for the major part of the resulting complexity. A mapping is still in place, but the action/process/object mapped by the gene (such as the action/process/object mapped by a software instruction in a program) is far from static. It turns out to be a very rich one-to-many mapping, from one gene to many potential dynamical processes, the latter being capable to behave in a very sophisticated manner and very sensitively to the surrounding environment. In the most complex cases, these dynamic processes can even interfere back on the genes, requiring then to include the temporal dimension in the definition of this mapping.

See also

- [Artificial Life](#)
- [Genetic Code](#)

References and Further Reading

Dawkins R (1996 [1986]) *The blind watchmaker*. WW Norton, New York. ISBN 0-393-31570-3

Codon

Definition

A codon is each of the non-overlapping nucleotide triplets in the coding sequence of an mRNA, which specifies an amino acid, following the equivalences of the ► [genetic code](#).

See also

- [Anticodon](#)
- [Genetic Code](#)
- [Ribosome](#)
- [RNA](#)
- [Translation](#)
- [Wobble Hypothesis \(Genetics\)](#)

Codon Table

- ▶ [Genetic Code](#)

Coenzyme

Synonyms

[Cofactor](#)

Definition

Coenzyme is any organic, low molecular mass, freely dissociable factor, which is essential for the activity of an enzyme. For example, some dehydrogenases require NAD^+ as electron carrier and some reductases use NADPH.

See also

- ▶ [NADH](#), [NADPH](#)

Cofactor

Definition

Cofactor is a non-protein (organic or inorganic) factor necessary for the activity of an [enzyme](#). This factor can be firmly bound to the enzyme (i.e., prosthetic group, e.g., [cytochromes](#)) or freely dissociable (i.e., [coenzyme](#), e.g., NAD(P)H).

See also

- ▶ [Coenzyme](#)
- ▶ [Cytochromes](#)
- ▶ [Enzyme](#)
- ▶ [NADH](#), [NADPH](#)

Coleman–Sagan Equation

Definition

The Coleman Sagan equation is used for establishing the probability of contaminating another planetary body by Earth microorganisms, and was first published by M. Coleman and C. Sagan in 1965.

This formula can be written as $P_c = N_0 R P_S P_I P_R P_g$.

In [▶ planetary protection](#), the formulation is often used by determining the initial number of microorganisms (N_0) that could be present on or in a spacecraft, and multiplying this number by an appropriately-selected set of factors representing the probability this number could be reduced. The first reduction in proportion (R) is depending on various parameters, including conditions to which the spacecraft is exposed both before and after launch. Then, while present on the spacecraft, the microorganisms have to reach the surface of the planet. The value P_I describes the probability of the spacecraft to hit the planet. This value is ranging from 10^{-5} for a satellite up to one for a landing probe. The probability for a microbe to be released (P_R) in the environment while the spacecraft is on the ground is generally set to one in case of crash landing. The probability of growth (P_g) in the particular extraterrestrial environment is also included in the calculation, but for targets with liquid water is assumed to be one. The “probability of contamination” is taken to be equivalent to the fractional number of organisms (e.g., 1×10^{-4}) that could be present on a spacecraft after various reduction factors are included.

See also

- ▶ [Bioburden](#)
- ▶ [Microorganism](#)
- ▶ [Planetary Protection](#)

References and Further Reading

Sagan C, Coleman S (1965) Spacecraft sterilization standards and contamination of Mars. *Astron Aeron* 3(5):1–22

Collapse, Gravitational

Synonyms

[Star formation](#)

Definition

The rapid contraction of a fluid mass because of the mutual gravitational attraction of its component particles is called gravitational collapse. If the forces supporting the object are weak, then its internal elements freely fall toward one another, leading to a highly condensed final configuration. As a consequence of the inverse-square nature of the gravitational force, the duration of collapse (known as the [▶ free-fall time](#)) depends mainly on the object’s initial density. In practice, only the very large masses found in astronomical bodies are susceptible to

this process. Examples are dense cores within molecular clouds, which collapse to form stars, and the interiors of massive stars, prior to supernova explosion.

See also

- ▶ [Fragmentation \(Interstellar Clouds\)](#)
- ▶ [Free-Fall Time](#)
- ▶ [Protostars](#)
- ▶ [Protostellar Envelope](#)

Collection en Orbite de Matériel Extra Terrestre

- ▶ [COMET \(Experiment\)](#)

Collisional Rate

- ▶ [Langevin Rate Coefficient](#)

Colonization (Biological)

SILVANO ONOFRI

Department of Ecology and Sustainable Economic Development, University of Tuscia, Viterbo, Italy

Synonyms

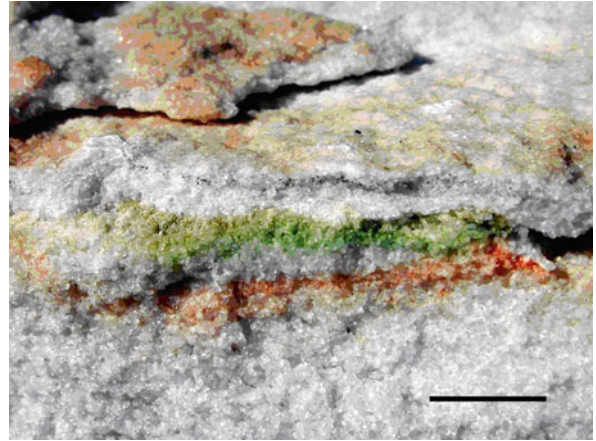
[Settlement](#)

Keywords

Archaea, dormant state, ecological niche, eukarya, extremotolerance, habitat, microbial community, origin of life, panspermia

Definition

Colonization is the occupation of a ▶ [habitat](#) or territory by a biological community or of an ecological niche by a single population of a species. Biological colonization relates to all species, from microbes – including bacteria, archaea, and ▶ [fungi](#) – to more complex organisms, like plants and animals. The term also applies to the occupation of new territories, including planets, by the human species. Biological colonization is a dynamic process that



Colonization (Biological). Figure 1 Cryptoendolithic (hidden within rock) microbial community colonizing sandstone, McMurdo Dry Valleys, continental Antarctica (bar 1 cm) Copyright © 2009 Laura Zucconi (permission obtained)

begins when unoccupied habitats, territories, or niches become available, or when organisms acquire the ability to survive and reproduce under environmental conditions of new niches, by a process of adaptation (Fig. 1).

Overview

The colonization of new habitats involves a succession of biological communities that can be studied and, to some extent, predicted. In many cases, the biological colonization of new habitats and territories begins with microorganisms, which has particular relevance to astrobiology. All known life forms are based on ▶ [carbon](#) chemistry and are related to the availability of ▶ [water](#). Organisms are able to colonize all environments that fall within the limits of habitability, i.e., conditions of low (Kappen et al. 1996) to high temperatures (up to 121°C, Kashefi and Lovley 2003), low water availability (Billi and Potts 2002), extreme acidity (Amaral Zettler et al. 2002) or alkalinity, high pressure, salinity (Oren 2000, Pikuta and Hoover 2007), and radiation (Billi et al. 2000). We find life, primarily microbial, in hot springs on the ocean floor, within the crust to depths over 3,000 m (Cockell 2003), in deserts (Friedmann 1982) and on the highest mountains, in the Arctic and Antarctic ▶ [permafrost](#) (Rivkina et al. 2000), high in the stratosphere, in salt crystals, in acidic (up to pH 0 or negative) to very basic waters, and in sites contaminated by nuclear radiation (Figs. 2 and 3).

The limits of metabolically active life define the habitability of celestial bodies. Biological colonization is thought to be possible wherever water could be available, such as in the permafrost of ▶ [Mars](#) or on ▶ [Europa](#)

Jupiter's moon. The notion of biological colonization beyond Earth leads to speculation about the transfer of life from one celestial body to another. Today, we know that the conditions suitable for the origin of life could have existed on Mars and perhaps on other planets. Many organisms are capable of surviving in a dormant state in conditions far more prohibitive than those suitable for active metabolism. Some organisms, e.g. bacteria (Horneck et al. 1994), microfungi (Onofri et al. 2008) and lichens (Sancho et al. 2007) have been shown to

withstand space vacuum, temperatures, and radiation. Thus, they are valuable model organisms for studying possible extraterrestrial life. Bacterial spores within rocks are able to withstand the shock of an ► [asteroid](#) impact and could therefore have been ejected from the parent planet and could also have survived the landing process. Life could thus have been transferred from one planet to another (► [lithopanspermia](#)), beginning the biological colonization of new territories (Horneck and Baumstark-Khan 2002) (Figs. 4 and 5).



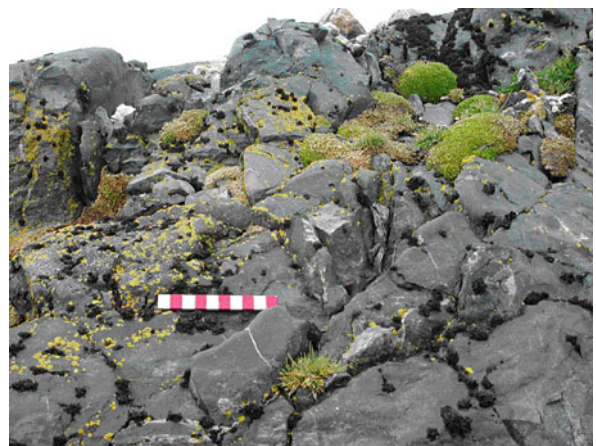
Colonization (Biological). Figure 2 A "lichen's grass" (*Usnea antarctica*) in King George Island, Antarctica (bar 10 cm). Copyright © 2001 Silvano Onofri



Colonization (Biological). Figure 4 A higher plant (*Colobanthus quitensis*) colonizing soil in King George Island, Antarctica (bar 10 cm). Copyright © 2001 Silvano Onofri



Colonization (Biological). Figure 3 Mosses colonizing rocks in King George Island, Antarctica (bar 10 cm). Copyright © 2001 Silvano Onofri



Colonization (Biological). Figure 5 Lichens (*Umbilicaria* and *Xanthoria*) and higher plants (*Colobanthus quitensis* and *Deschampsia antarctica*) colonizing rocks in King George Island, Antarctica (bar 10 cm). Copyright © 2001 Silvano Onofri



See also

- ▶ [Antarctica](#)
- ▶ [Asteroid](#)
- ▶ [BIOPAN](#)
- ▶ [Black Smoker](#)
- ▶ [Carbon](#)
- ▶ [Deep-sea Microbiology](#)
- ▶ [Deep-subsurface Microbiology](#)
- ▶ [Epilithic](#)
- ▶ [Europa](#)
- ▶ [Expose](#)
- ▶ [Extreme Environment](#)
- ▶ [Fungi](#)
- ▶ [Habitable Zone](#)
- ▶ [Habitat](#)
- ▶ [Lithopanspermia](#)
- ▶ [Mars](#)
- ▶ [Meteorites](#)
- ▶ [Panspermia](#)
- ▶ [Permafrost](#)
- ▶ [Rock](#)
- ▶ [Space Environment](#)
- ▶ [Space Vacuum Effects](#)
- ▶ [Spallation Zone](#)
- ▶ [Spore](#)
- ▶ [UV Radiation \(Biological Effects\)](#)
- ▶ [Water](#)

References and Further Reading

- Amaral Zettler LA, Gomez F, Zettler E, Keenan BG, Amils R, Sogin ML (2002) Eukaryotic diversity in Spain's River of Fire. *Nature* 417:137
- Billi D, Friedmann EI, Hofer KG, Grilli Caiola M, Ocampo Friedmann R (2000) Ionizing-radiation resistance in the desiccation-tolerant cyanobacterium *Chroococcidiopsis*. *Appl Environ Microbiol* 66: 1489–1492
- Billi D, Potts M (2002) Life and death of dried prokaryotes. *Res Microbiol* 153:7–12
- Cockell C (2003) Impossible extinction. Cambridge University Press, Cambridge
- Friedmann EI (1982) Endolithic microorganisms in the Antarctic cold desert. *Science* 215:1045–1053
- Horneck G, Baumstark-Khan C (eds) (2002) *Astrobiology – the quest for the conditions of life*. Springer, Berlin
- Horneck G, Bückler H, Reitz G (1994) Long-term survival of bacterial spores in space. *Adv Space Res* 14:41–45
- Kashefi K, Lovley DR (2003) Extending the upper temperature limit for life. *Science* 301:934
- Kappen L, Schroeter B, Scheidegger C, Sommerkorn M, Hestmark G (1996) Cold resistance and metabolic activity of lichens below 0°C. *Adv Space Res* 12:119–128
- Onofri S, Barreca D, Selbmann L, Isola D, Rabbow E, Horneck G, de Vera JPP, Hattori J, Zucconi L (2008) Resistance of Antarctic black fungi e cryptoendolithic communities to simulated space and Mars conditions. *Stud Mycol* 61:99–109

- Oren A (2000) Diversity of halophilic microorganisms: environments, phylogeny, physiology, and applications. *Jour Ind Microbiol Biotechnol* 28:56–63
- Pikuta EV, Hoover RB (2007) Microbial extremophiles at the limits of life. *Crit Rev Microbiol* 33:183–209
- Rivkina EM, Friedmann EI, McKay CP, Gilichinsky DA (2000) Metabolic activity of permafrost bacteria below the freezing point. *Appl Environ Microbiol* 66:3230–3233
- Sancho LG, de la Torre R, Horneck G, Ascaso C, de los Rios A, Pintado A, Wierzbos J, Schuster M (2007) Lichens survive in space: Results from the 2005 LICHENS experiment. *Astrobiol* 7:443–454

Color-Magnitude Diagram

- ▶ [Hertzsprung–Russell Diagram](#)

Color Excess

Definition

The color excess is the difference between the observed color index of a star and the intrinsic color index predicted from its spectral type. It is a quantity that is always positive and that gives a measure of the absorption of starlight by the intervening ▶ [interstellar medium](#). The apparent ▶ [reddening](#) of the starlight comes from a stronger absorption in the blue than in the red by dust particles. Generally, it's the excess of the [B-V] color index of the ▶ [Johnson](#) photometric system which is used: it is denoted E_{B-V} .

See also

- ▶ [Color Index](#)
- ▶ [Dust Grain](#)
- ▶ [Interstellar Medium](#)
- ▶ [Magnitude](#)
- ▶ [Reddening, Interstellar](#)

Color Index

Definition

A color index is the difference between the ▶ [magnitude](#) of a star measured at one standard wavelength and the magnitude at another, albeit longer, standard wavelength: this

is a quantitative measure of a star's color. A positive color index indicates a star redder (generally cooler) than an A0 star, such as Vega, and a negative one, a bluer (hotter) star.

See also

- ▶ [Color Excess](#)
- ▶ [Magnitude](#)

Column Density

Definition

The column density between two points in a medium is the projected number density of a given species (H-atom, dust particles) contained in a cylinder whose length is the distance between the two points. The unit is m^{-2} . When applied to the interstellar matter lying between an object and the Earth, it's a quantity proportional to the opacity, with the approximate relation: $A_v = 5 \cdot 10^{-26} N(H)$, where $N(H)$ is the column density or projected number of H atoms per square meter, and A_v is the visual extinction.

See also

- ▶ [Extinction, Interstellar or Atmospheric](#)

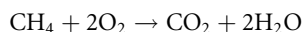
Coma

- ▶ [Comet](#)

Combustion

Definition

In chemistry, combustion is the complete or incomplete oxidation of a fuel by oxygen or other oxidants to give oxidized carbon species, such as CO (for incomplete combustion) and CO_2 (for complete combustion), and water, and the concomitant production of heat:



Respiration is an example of a biological combustion reaction.

See also

- ▶ [Oxidation](#)
- ▶ [Respiration](#)

Comet

JACQUES CROVISIER

LESIA - Bâtiment ISO (n°17), Observatoire de Paris, Meudon, France

Synonyms

Chury

Keywords

Small body

Definition

A comet is a small body, formed in the outer region of the Solar System, generally on a highly eccentric orbit, and containing a large fraction of volatiles. When coming close to the Sun, vaporization of the ices causes the development of spectacular cometary phenomena: the coma, and the dust and ion tails.

History

Comets are among the most remarkable sky phenomena for both the layman and the scientist (Fig. 1, Table 1). For a long time, their unexpected apparitions and their unknown nature induced both fascination and fear. Nowadays, they are considered as natural laboratories meeting extreme physical conditions and as key objects for understanding the history of the Solar System.

The historical background of comets is reviewed in the books by Yeomans (1991) and Schechner Genuth (1997). Important milestones for the science of comets were:



Comet. Figure1 Comet C/2006 P1 (McNaught) over the Pacific. This comet became spectacular as it passed perihelion at 0.17 AU from the Sun on 12 January 2007. © Sebastian Deiries (ESO)

**Comet. Table 1** A selection of well-known comets

(a)	(b)	(c)	(d)	(e)	(f)	(g)	(h)
C/1577 V1	1577 I		27 Oct. 1577	0.178	1.0		First parallax measurement
C/1680 V1 "Kirch's comet"	1680		18 Dec. 1680	0.0062	1.000		Sungrazer
C/1729 P1 "Sarabat's comet"	1729		16 Jun. 1829	4.05	1.0		Intrinsically very bright
C/1743 X1 "Chézeaux's comet"	1744		1 Mar. 1744	0.222	1.0		
D/1770 L1 Lexell	1770 I		14 Aug. 1770	0.67	0.786	5.6	Approached Earth at 0.015 AU
C/1811 F1 Great comet	1811 I		12 Sep. 1811	1.04	0.995		
C/1819 N1 Great comet	1819 II		28 Jun. 1819	0.342	1.0		First polarization observation
C/1843 D1 Great March comet	1843 I		27 Feb. 1843	0.0055	0.999	513	Sungrazer
C/1858 L1 Donati	1858 VI		30 Sep. 1858	0.578	0.996	2000	
C/1861 J1 Great comet	1861 II		12 Jun. 1861	0.82	0.985	409	
C/1864 N1 Tempel	1864 II		16 Aug. 1864	0.91	0.996		First spectral observations
C/1868 L1 Winnecke	1868 II		26 Jun. 1868	0.58	1.0		
C/1874 H1 Coggia	1874 III	1874c	9 Jul. 1874	0.68	0.998		
C/1881 K1 Great comet	1881 III	1881b	16 Jun. 1881	0.73	0.996		
C/1882 R1 Great September comet	1882 II	1882b	17 Sep. 1882	0.00775	0.9999	759	Sungrazer
C/1887 B1 Great southern comet	1887 I	1887a	11 Jan. 1887	0.0048	1.0		Sungrazer
C/1901 G1 Great comet	1901 I	1901a	24 Apr. 1901	0.245	1.0		
C/1907 L2 Daniel	1907 IV	1907d	4 Oct. 1907	0.512	0.999		
C/1908 R1 Morehouse	1908 III	1908c	26 Dec. 1908	0.945	1.0007		
C/1910 A1 Great January comet	1910 I	1910a	17 Jan. 1910	0.129	0.9999		
C/1911 O1 Brooks	1911 V	1911c	28 Oct. 1911	0.49	0.997		
C/1927 X1 Skjellerup-Maristany	1927 IX	1927k	18 Dec. 1927	0.176	0.9998		
C/1940 R2 Cunningham	1941 I	1940c	16 Jan. 1941	0.368	1.0005		
C/1947 X1 Southern comet	1947 XII	1947n	2 Dec. 1947	0.110	0.9995		
C/1948 V1 Eclipse comet	1948 XI	1948l	27 Oct. 1948	0.135	0.99994		
C/1956 R1 Arend-Roland	1957 III	1956h	8 Apr. 1957	0.316	1.0002		
C/1957 P1 Mrkos	1957 V	1957d	1 Jul. 1957	0.355	0.9994		
C/1969 Y1 Burnham	1960 II	1959k	29 Mar. 1960	0.355	0.9994		
C/1961 R1 Humason	1962 VIII	1961e	10 Dec. 1962	2.13	0.990		
C/1965 S1 Ikeya-Seki	1965 VIII	1965f	21 Oct. 1965	0.00779	0.99992		Sungrazer
C/1969 Y1 Bennett	1970 II	1969i	20 Mar. 1970	0.538	0.996		
C/1973 E1 Kohoutek	1973 XII	1973f	28 Dec. 1973	0.142	1.000		International obs. campaign
C/1975 V1 West	1976 VI	1975n	25 Feb. 1976	0.197	1.000		
C/1980 E1 Bowell	1982 I	1980b	12 Mar. 1982	3.364	1.057		Active far from the Sun
C/1983 J1 Sugano-Saigusa-Fujikawa	1983 V	1983e	1 Apr. 1983	0.471	1.000		Approached Earth at 0.063 AU
C/1983 H1 IRAS-Araki-Alcock	1983 VII	1983d	21 May 1983	0.991	0.990		Approached Earth at 0.031 AU
C/1983 O1 Cernis	1983 XII	1983l	21 Jul. 1983	3.33	1.002		Active at more than 20 AU
C/1986 P1 Wilson	1987 VII	1986l	20 Apr. 1987	1.200	1.0003		

Comet. Table 1 (Continued)

(a)	(b)	(c)	(d)	(e)	(f)	(g)	(h)
C/1989 X1 Austin	1990 V	1989c1	10 Apr. 1990	0.350	1.0002		
C/1990 K1 Levy	1990 XX	1990c	24 Oct. 1990	0.939	1.0004		
D/1993 F2 Shoemaker-Levy	91994X	1993e					Crashed on Jupiter
C/1996 B2 Hyakutake			1 May 1996	0.230	0.999	8 9000.	Approached Earth at 0.10 AU
C/1995 O1 Hale-Bopp			1 Apr. 1997	0.914	0.995	2400.	Extensive observ. campaign
C/1999 S4 LINEAR			26 Jul. 2000	0.765	0.9994		Nucleus broke at perihelion
C/2001 A2 LINEAR			24 May 2001	0.779	0.9993		Successive nucleus breakings
C/2002 T7 LINEAR			23 Apr. 2004	0.615	1.0006		
C/2001 Q4 NEAT			15 May 2004	0.962	1.0006		
C/2004 Q2 Machholz			24 Jan. 2005	1.205	0.9995		
C/2006 P1 McNaught			12 Jan. 2007	0.171	1.0000		Reached mv = -5 at perihelion
Some numbered short-period comets							
(a)	(d)	(e)	(f)	(g)	(h)		
1P/Halley	9 Feb. 1986	0.587	0.967	76.0	Target of several space missions		
2P/Encke	9 Sep. 2000	0.340	0.847	3.30	Comet of shortest period		
3D/Biela	23 Sep. 1852	0.861	0.756	6.62	Split comet now lost		
9P/Tempel 1	5 July 2005	1.505	0.518	5.51	Target of Deep Impact mission		
17P/Holmes	4 May 2007	2.053	0.432	6.88	Huge outburst in October 2007		
19P/Borrelly	14 Sep. 2001	1.358	0.624	6.86	Target of Deep Space 1 mission		
21P/Giacobini-Zinner	5 Sep. 1985	1.028	0.708	6.59	Target of ICE space mission		
26P/Grigg-Skjellerup	22 July 1992	0.995	0.664	5.10	Target of Giotto extended mission		
29P/Schwassmann-Wachmann 1	10 July 2004	5.724	0.044	14.7	Nearly circular Orbit		
55P/Tempel-Tuttle	28 Feb. 1998	0.977	0.906	33.2	Assoc./Leonid meteor stream		
67P/Churyumov-Gerasimenko	28 Feb. 2009	1.246	0.640	6.45	Target of Rosetta mission		
73P/Schwassmann-Wachmann 3	7 June 2006	0.939	0.693	5.36	Split comet		
81P/Wild 2	25 Sep. 2003	1.590	0.539	6.40	target of Stardust mission		
95P/Chiron	14 Feb. 1996	8.454	0.383	50.7	Centaur, also listed as asteroid		
103P/Hartley 2	28 Oct. 2010	1.059	0.695	6.47	Target of EPOXI mission		
109P/Swift-Tuttle	12 Dec. 1992	0.958	0.964	133.3	Assoc./Perseid meteor stream		
133P/Elst-Pizarro	29 June 2007	2.642	0.164	5.61	Main-belt comet		

(a) Official IAU designation

(b) Old style designation before 1995

(c) Provisional designation before 1995

(d) Date of perihelion

(e) Perihelion distance [AU]

(f) Eccentricity

(g) Period (years)

(h) Remarks



- The understanding that comets are not atmospheric phenomena, which was demonstrated by Tycho Brahe (1546–1601) and his colleagues who measured the parallax of the comet of 1577
- The determination of cometary orbits with the works of Isaac Newton (1644–1727) and Edmond Halley (1656–1742)
- The knowledge of the comet phenomenon; formation and development of both the coma and the tails (end of the eighteenth and nineteenth centuries)
- The determination of the composition of comets with the emergence of spectroscopy (end of the nineteenth century) and the opening of new spectral domains (end of the twentieth century)
- The active exploration of comets with flyby and encounter space missions nowadays

Cometary science is the topic of several books and reviews, such as those of Festou et al. (1993a, b, 2004) and Krishna Swamy (2010).

Overview

Names of Comets

The nomenclature system for comets has changed several times. The Central Bureau for Astronomical Telegrams (CBAT) of the International Astronomical Union (IAU) is in charge of attributing names to comets. A registration code is given according to the order of discovery. It consists of “C/” followed by the year of discovery, then by a letter corresponding to the half-month of the discovery, then by an order numeral. In addition, the name of the discoverer (or of the first two discoverers) is traditionally associated. Thus, C/1995 O1 (Hale-Bopp) is the first comet discovered in the second half of July 1995, by Alan Hale and Thomas Bopp. Short-period comets with a period <200 years are registered “P/” instead of “C/”. Those that have been observed at several returns are given subsequently a number: 1P/Halley, 2P/Encke... See <http://www.cfa.harvard.edu/iau/lists/CometResolution.html> for more details, exceptions, and oddities.

One should be careful to comply with these IAU rules to avoid ambiguities. In particular, using only the discover(s) name(s), as is often the case in popular articles and even in some professional papers, should be discouraged (some discoverers were very prolific).

Cometary Orbits, Cometary Families, and Cometary Reservoirs

There are up to now more than 3,708 cometary apparitions for which secure orbits could be determined listed in

the Catalog of Cometary Orbits (Marsden, Williams 2008). As of December 2010, 245 comets have been observed at multiple returns and are now “numbered” short-period comets.

Some comets have slightly hyperbolic orbits. As far as this could be investigated, they just recently underwent gravitational perturbations with a planet (Jupiter in most of the cases) which changed their orbit from elliptic to hyperbolic. The apparition of a genuine interstellar comet, expelled from an extrasolar system, is not ruled out, but we are still awaiting for such an event.

The inspection of the Catalog of Cometary Orbits shows that there are two main families of comets (e.g., Morbidelli 2008):

- Short-period comets with low inclination over the ecliptic. Most of them have orbital periods close to 6 or 12 years. Their orbital evolution is governed by strong gravitational interaction with Jupiter. They are named “ecliptic comets” or “Jupiter-family comets.”
- Comets with random inclination over the ecliptic. They may have a long orbital period (“new” comets with a nearly parabolic comet) or a short period (such as Halley’s comet). They are named “nearly isotropic comets.” To explain the continuing supply of new comets, the existence of a distant, spherical reservoir of comets was postulated (► [Oort Cloud](#)). Thus these comets are alternatively named “Oort-cloud comets.”

Nearly isotropic comets are not believed to have formed in the Oort cloud, but in the traditional Solar System. They were subsequently ejected to the Oort cloud following gravitational interaction with giant planets. In turn, ecliptic comets could have formed in the trans-Neptunian region, among the ► [Kuiper Belt](#). They subsequently evolved to shorter period orbits, preserving their low inclination.

Also related to comets are ► [Centaurs](#), which are intermediate objects between Kuiper-belt objects and main-belt asteroids. Some of them, like Chiron (which is registered both as asteroid (2060) Chiron and comet 95P/Chiron), show cometary activity.

“Main-belt comets” are main-belt asteroids which show a low level of cometary activity. They are also known as “activated asteroids.” About half a dozen such objects (133P/Elst-Pizarro...) have been recently identified.

“Sun-grazing comets” pass within a few solar-radii from the Sun and are generally only detectable at that moment. More than 1,500 objects have been registered as sun-grazing comets from observations with space coronagraphs, such as SOHO. Most of these bodies are meter-size objects that do not survive after perihelion.

The Nature of Comets and Basic Cometary Processes

We now know that comet nuclei are solid icy conglomerates and that the sublimation of ices in comet nuclei is the motor of cometary activity, following the popular model of the “dirty snowball” of Fred Whipple (1906–2004). Comet nuclei are kilometer-size low-density porous and fragile bodies (see Lamy et al. 2004; Weissman et al. 2004 and the ► [Comet Nucleus](#) entry).

Water ice sublimates in the vacuum at temperatures greater than about 150 K. For cometary nuclei, this occurs at distances smaller than about 4 AU from the Sun; this results in the development of a cometary atmosphere: the gaseous coma. The gravity of the comet nucleus is too small to retain this atmosphere, which expands with a velocity ranging from 0.5 to a few km/s, depending on the distance to the Sun and the gas production rate. Thus, the gas density drops rapidly with increasing distance from the nucleus and the flow becomes collision free. The inner collisional region has a size of a few hundred to a few thousand kilometers, depending on the comet outgassing. As in laboratory molecular flows, the temperature drops rapidly: temperatures in the range 10–100 K are typically observed.

The production rate of water at a distance of about 1 AU from the Sun is typically 10^{28} molecules per second (300 kg/s) for small short-period comets, such as 9P/Tempel 1 or 67P/Churyumov-Gerasimenko, both the targets of space missions. It was 10^{30} molecules s^{-1} (30 t/s) for 1P/Halley, and as large as 10^{31} molecules s^{-1} (300 t/s) for the giant comet C/1995 O1 (Hale-Bopp).

Comets can still be active at distances larger than 4 AU from the Sun, where water sublimation is inefficient. This situation requires the sublimation of more volatile species, such as CO or CH₄, that are responsible for the cometary activity. Indeed, the production of carbon monoxide was observed in comet Hale-Bopp at distances as far as 14 AU.

The dominant chemical process in cometary atmospheres is the progressive molecular photolysis by the solar UV radiation. The lifetime of the water molecule at 1 AU from the Sun is about 1 day, but it may be significantly shorter for complex, organic molecules. Two-body reactions are inefficient because molecules spend only a short time in the collision region where temperature is low, and where the fraction of reactive ions and radicals is still low.

The radiation mechanisms for molecules, radicals, atoms, and ions are ► [fluorescence](#) of their electronic and vibrational bands excited by solar radiation, and thermal emission of rotational lines. Prompt (non-

fluorescence) emission from radicals and atoms, following their creation in an excited state as a result of photolysis, may also occur.

Cometary grains are dragged from the nucleus by gas. Their initial velocity is much smaller than that of the gas and depends on the grain size. The biggest (“boulders”) cannot escape the nucleus, which contributes to the formation of a regolith. Dust grains are repelled by the Sun, forming the sometimes spectacular dust tail, following the kinematic model first proposed by Bessel (1784–1846) and Bredichin (1831–1904). The physical process at work – the solar radiation pressure – was later explained by Svante Arrhenius (1859–1927). The biggest dust grains migrate along the cometary orbit where they form cometary trails that were first imaged by the infrared satellites IRAS and ISO. When the Earth encounters such a cometary trail, a meteor shower may be observed (the link between comets and meteor streams was first established for the case of the Perseid meteors and comet 109P/Swift-Tuttle).

Cometary ions in the coma are accelerated through magnetohydrodynamic interaction with the solar wind to velocities of several hundred km s^{-1} . They form a thin straight tail, easily distinguishable from the broad, curved dust tail. This tail is mainly composed of CO⁺ and H₂O⁺ ions. It is remarkable that this interaction was proposed by Ludwig Biermann (1907–1986) and modeled by Hannes Alfvén (1908–1995) before the solar wind was actually observed by space probes.

Atoms and molecules that undergo fluorescence excited by the Sun are also accelerated away from the Sun. The process is especially efficient for the resonant D lines of sodium at 589 nm. A neutral sodium tail results, which was peculiarly conspicuous in comet Hale-Bopp (Cremonese et al. 1997). The same process is responsible for a significant distortion of the large hydrogen coma.

Space Missions to Comets

A table listing past and current space missions to comets is given in the ► [Comet Nucleus](#) entry. The main steps of cometary exploration were (Keller et al. 2004):

- The ► [VEGA](#) and ► [Giotto missions](#) which flew by 1P/Halley in March 1986 revealed the reality of a solid comet nucleus.
- The ► [Stardust](#) mission which flew through the coma of 81P/Wild 2 on 2 January, 2004, sampled cometary grains and returned them to Earth for analysis on 15 January, 2006.
- The ► [Deep Impact](#) mission, an active experiment, sent an impactor to the nucleus of 9P/Tempel 1 on 4 July, 2005. The plume which developed after the



impact was observed from the spacecraft and from the Earth. The same spacecraft, in a mission renamed EPOXI, explored 103P/Hartley 3 on 4 November 2010.

- The ► **Rosetta mission** (Schulz et al. 2009) will encounter 67P/Churyumov-Gerasimenko in 2014–2015. An orbiter will stay in the comet vicinity for months, witnessing the development of cometary activity. A lander will make in situ analyses of the nucleus material.

An inescapable further step will be to return to Earth a sample directly taken from a comet nucleus. Such missions are currently under study, but are not yet firmly scheduled.

Space missions are not yet versatile enough to go to unexpected comets. Short-period comets, which have predicted returns, are presently the only practicable targets. Flybys at low velocity and rendezvous are only possible for ecliptic (Jupiter-family) comets, due to energy limitations. Up to now, the only comet not belonging to the Jupiter family that was explored was 1P/Halley; this was done with a very high flyby velocity (about 70 km/s).

Although in situ cometary explorations are invaluable, they were (and will probably be for a long time) restricted to a very small number of targets. Thus, a study of the comet diversity, which needs a statistical approach, can only be achieved with remote-sensing long-term observing programs.

Composition of Comets: Ices and Volatiles

For a long time, the chemical study of comets was restricted to visible spectroscopy. Radicals, atoms, and ions, such as CN, CH, C₂, C₃, NH, NH₂, OH, CO⁺ . . . (Feldman et al. 2004), were observed. It was proposed in the mid-twentieth century by Karl Wurm (1899–1975) and Pol Swings (1906–1983) that these unstable species were “daughter molecules” coming from the photodestruction or photoionization by the solar UV radiation of volatile stable molecules, the “► parent molecules,” released from the sublimation of nucleus ices. Proposed parents were H₂O, NH₃, CH₄, CO, CO₂, HCN... that could not be directly identified by the techniques available at that time.

Confirmation came with the advent of radio, infrared, and UV spectroscopy as well as in situ mass spectroscopy. We now have a confident knowledge of the main constituents of cometary ices (Bockelée-Morvan et al. 2004; Crovisier 2004; Crovisier et al. 2004; Fig. 2; Table 2). The main components are water (about 80% by number), followed by carbon monoxide and dioxide. Then come methanol, ammonia, methane and other hydrocarbons (C₂H₂, C₂H₆), hydrogen sulfide, and hydrogen cyanide.

About 15 other minor constituents were identified in small amounts, but they can only be observed in the most productive comets. For instance, the relatively complex organic molecules formic acid (HCOOH), methyl formate (HCOOCH₃), acetaldehyde (CH₃CHO), and ethylene glycol (CH₂OHCHOH) have been identified by their radio lines only in C/1995 O1 (Hale-Bopp).

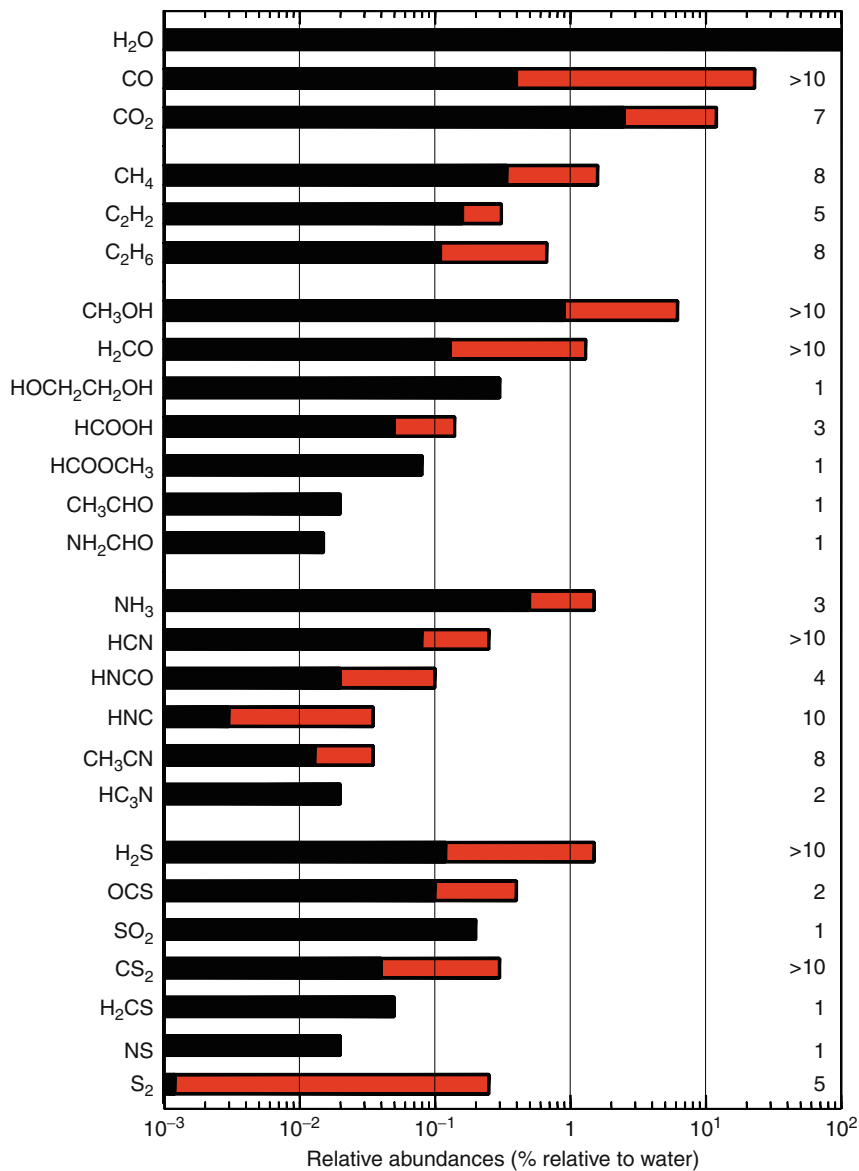
Indeed, the relationship between comets and spectroscopy is exemplary and dates back from the beginning of astrophysics in the second half of nineteenth century. Many molecular species were observed in comets before they could be studied in the laboratory.

Mass spectroscopic measurements were performed in situ on 1P/Halley with Giotto (Altwegg et al. 1999, and references therein). However, their interpretation was hampered by the limited mass resolution and the need for detailed chemical modeling to deduce neutral abundances from the mass spectra. This problem of mass ambiguity will be resolved with the equipment of the Rosetta orbiter. Also, the Rosetta lander will directly investigate the nucleus material, with mass spectroscopy and gas chromatography.

The Stardust mission returned samples from comet 81P/Wild 2. The collecting technique which was used (cometary grains were trapped by entering an aerogel substrate with a velocity of 6 km/s) could not preserve volatiles and favored refractory material. However, a careful analysis revealed the presence of methylamine (CH₃NH₂), ethylamine (CH₃CH₂NH₂), and possibly glycine (NH₂CH₂COOH) in the returned aerogel that could be of cometary origin (Elsila et al. 2009). These species could result from the degradation of carbonaceous cometary grains, rather than from the sublimation of nucleus ices.

Many features detected in cometary spectra at all wavelengths are still unidentified, suggesting that new cometary species are still to be identified. This requires further theoretical and laboratory spectroscopic studies.

Comets show a large diversity in their chemical composition (Fig. 2). It is important to assess whether this diversity is correlated with different sites of formation or to different evolutions of these bodies. Indeed, from the observations of daughter species, A’Hearn et al. (1995) have identified a class of carbon-poor comets, for which the C₂ radical is depleted. It appears that these carbon-poor comets are mostly present among Jupiter-family comets. However, how this carbon depletion could be related to the abundance of *bona fide* parent molecules is still unclear. Clues from infrared and radio spectroscopy are yet inconclusive, perhaps because the sample of investigated comets at these wavelengths is still sparse (DiSanti and Mumma 2008; Crovisier et al. 2009).



Comet. Figure 2 Relative production rates of cometary volatiles and their comet-to-comet variations. These rates are believed to trace the relative abundances in cometary ices. The red part of each bar indicates the range of variation from comet to comet. The number of comets in which the species was detected is indicated on the right (Adapted from Bockelée-Morvan et al. 2004)

Composition of Comets: Dust and (Semi) Refractories

Knowledge of the composition of cometary dust stems from infrared spectroscopy (with ground-based telescopes and the ISO and Spitzer space observatories) and from the samples collected in the coma of the Jupiter-family comet 81P/Wild 2 by the Stardust mission, providing ground-truth for the remote-sensing investigations (Hanner and

Zolensky 2010). Additional information comes from the analysis of interplanetary dust particles (IDPs), collected in the upper Earth's atmosphere, which could be of cometary origin. The analysis of the material excavated in the Jupiter-family comet 9P/Tempel 1 by the Deep Impact experiment revealed an inner-nucleus composition similar to that observed in more active, Oort-cloud comets, such as 1P/Halley or C/1995 O1 (Hale-Bopp).

Comet. Table 2 The relative composition of volatiles observed in comet C/1995 O1 (Hale-Bopp), normalized to water (From Bockelée-Morvan et al. 2005, with updates)

Water	H ₂ O	100	
Carbon monoxide	CO	12–23	(a)
Carbon dioxide	CO ₂	6	
Methane	CH ₄	1.5	
Acetylene	C ₂ H ₂	0.1–0.3	
Ethane	C ₂ H ₆	0.6	
Methanol	CH ₃ OH	2.4	
Formaldehyde	H ₂ CO	1.1	(a)
Formic acid	HCOOH	0.09	
Methyl formate	HCOOCH ₃	0.08	
Acetaldehyde	CH ₃ CHO	0.02	
Ethylene glycol	CH ₂ OHCH ₂ OH	0.25	
Formamide	NH ₂ CHO	0.015	
Ammonia	NH ₃	0.7	
Hydrogen cyanide	HCN	0.25	
Isocyanic acid	HNCO	0.10	
Hydrogen isocyanide	HNC	0.04	(a)
Methyl cyanide	CH ₃ CN	0.02	
Cyanoacetylene	HC ₃ N	0.02	
Hydrogen sulfide	H ₂ S	1.5	
Carbonyl sulfide	OCS	0.4	(a)
Sulfur dioxide	SO ₂	0.2	
Carbon disulfide	CS ₂	0.2	(b)
Thioformaldehyde	H ₂ CS	0.05	
NS radical	NS	0.02	(c)
Hydrogen peroxide	H ₂ O ₂	<0.03	
Propyne	CH ₃ CCH	<0.045	
Ketene	CH ₂ CO	<0.032	
Ethanol	C ₂ H ₅ OH	<0.10	
Dimethyl ether	CH ₃ OCH ₃	<0.45	
Glycol aldehyde	CH ₂ OHCHO	<0.07	
Acetic acid	CH ₃ COOH	<0.06	
Glycine I	NH ₂ CH ₂ COOH	<0.15	
Cyanodiacetylene	HC ₅ N	<0.003	
Ethyl cyanide	C ₂ H ₅ CN	<0.01	
Methanimine	CH ₂ NH	<0.032	
Cyanamide	NH ₂ CN	<0.004	
Methyl mercaptan	CH ₃ SH	<0.05	

(a) With possibly an additional distributed source in the coma

(b) From the observation of the CS radical

(c) Of unknown origin

Data derived from radio or infrared observations of comet Hale-Bopp made at heliocentric distances of about 1 AU.

Cometary dust appears to be heterogeneous, with silicates in both the amorphous (glassy) and crystalline forms, Fe and Ni sulfides and other minerals in minor amounts. The presence of carbonates and phyllosilicates is subject to debate. Cometary silicates, which constitute the most abundant part of the refractory grains, show a large diversity, comprising forsterite (Mg_2SiO_4), enstatite (MgSiO_3), olivines, and pyroxenes with a wide range in Mg/Fe. Among the 81P/Wild 2 samples were found highly refractory calcium aluminum-rich inclusions (CAI) and fragments of chondrules, as is usually found in primitive meteorites.

A significant fraction of cometary dust is in the form of carbonaceous grains (also known as “CHON particles”), first found in the space exploration of comet Halley. They could be a potential source of molecules, alternative to the sublimation of volatiles from nucleus ices. They have been invoked to explain the distributed sources of H_2CO , CO, OCS, HNC, CN... through photo- or, more likely, thermal degradation (Cottin and Fray 2008). Polyoxymethylene $(\text{H}_2\text{CO})_n$ (POM), hexamethylenetetramine $\text{C}_6\text{H}_{12}\text{N}_4$ (HMT), HCN polymers $(\text{HCN})_n$, and carbon suboxide polymers $(\text{C}_3\text{O}_2)_n$ have been proposed as cometary analogs, and their degradation was studied in the laboratory. It is likely, however, that the real cometary carbonaceous grains have a more complex composition than these analogs, similar to the insoluble organic matter found in the matrix of some ► **carbonaceous chondrites**.

Polycyclic aromatic hydrocarbon molecules (PAHs), which are ubiquitous in the interstellar medium, are also expected to be present in comets (see the review by Li 2009, and references therein). The identification of cometary PAHs from remote sensing, using near-ultraviolet or infrared spectroscopy (from features near 3.4, 6, 8, and 12 μm), is subject to debate. More compelling evidence of their presence comes from mass spectroscopy of the Stardust samples.

Icy grains released from the nucleus could be a significant source of gaseous material. At short heliocentric distances, such grains have short lifetimes and their outgassing is difficult to distinguish from the nucleus outgassing with ground-based observations.

Isotopic Ratios

Isotopic ratios, and especially the D/H ratio, are important for investigating the circulation of matter in the Universe and in the Solar System (Robert et al. 2000). The D/H ratio is a key parameter for understanding the origin of water on Earth. Up to now, D/H has only been measured in a limited number of comets, which are all Oort-cloud comets (Jehin et al. 2009; Fig. 3). These D/H values cluster

around $3 \cdot 10^{-4}$, which is about 12-times higher than the protosolar D/H value, but significantly below the D/H ratio in some molecular species in dense interstellar ► **molecular clouds**. In Earth's oceans, the D/H is $1.5 \cdot 10^{-4}$. However, before reaching a firm conclusion on the contribution of cometary infalls to terrestrial water, we need a more complete view of the D/H ratio for the whole cometary population, especially for Jupiter-family comets.

Formation and Evolution of Cometary Matter

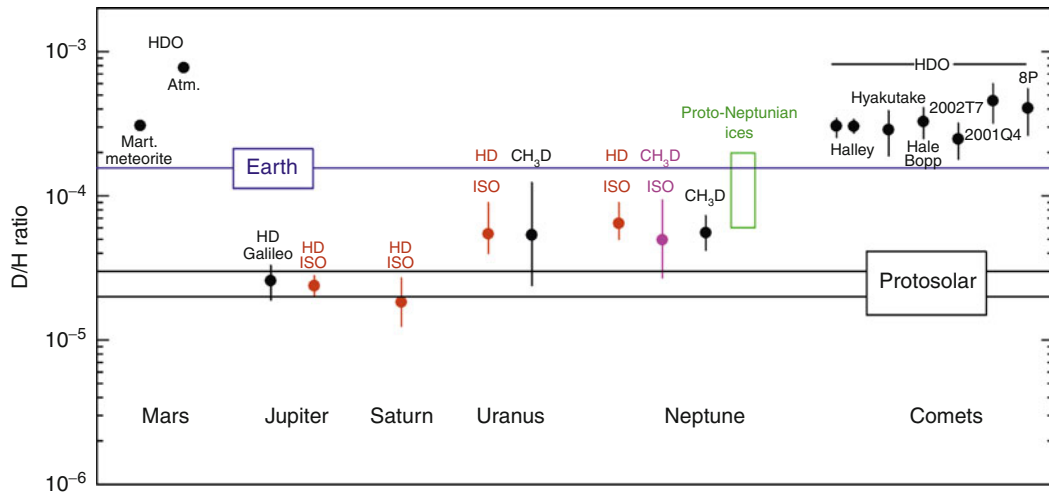
The composition of cometary volatiles is strikingly similar to that of some interstellar molecular clouds (Table 3), especially of hot molecular cores. This indicates that interstellar molecules in these clouds could come from the evaporation of comet-like ices. This could also suggest, as was advocated by Mayo Greenberg (1922–2001), that cometary material comes from the direct agglomeration of unprocessed interstellar grains. However, this is hardly tenable for cometary ices now, in view of our current understanding of the early solar system history. The similarity between interstellar and cometary matter would rather be due to a similarity of the physicochemical processes occurring in dense interstellar clouds and in the early solar nebula.

Observations, and especially the results from the Stardust mission, have shown that cometary matter includes ices as well as crystalline and amorphous silicates, originating from the cold and hot regions of the solar nebula. This points to an important turbulent mixing of the nebula. Thus, cometary silicates differ from interstellar silicates which are always in the amorphous state. Cometary refractory grains could have both an interstellar and a nebular origin (Wooden 2008).

Comets and the Origin of Life

The possible role of comets as a vector for ► **panspermia** was advocated in several papers, especially by Hoyle and Wickramasinghe (e.g., 1981). The objections raised to this hypothesis are the hostile radiation environment and the easy destruction of organic material following impact on Earth.

Could liquid water exist in comets, favoring the development of life in these bodies? As was studied in detail by Podolak and Prialnik (2006), a significant pressure together with a heating source are needed for this to be possible. The latter could be provided internally by ^{26}Al radioactivity or by amorphous-crystalline water ice transition. However, this would only be imaginable inside huge cometary nuclei (>100 km), or large KBOs.



Comet. Figure 3 D/H ratios in the Solar System. The D/H value is presently measured in six comets, all originating from the Oort cloud; it is not yet measured in any Jupiter-family, short-period comet from the Kuiper belt. All values are about twice the Earth oceans value (From Hartogh et al. 2009)

Comet. Table 3 The relative compositions of interstellar and cometary ices (From Despois and Cottin 2005)

Species	Interstellar ices high-mass YSO (a)	Interstellar ices low-mass YSO (b)	Cometary volatiles (c)
H ₂ O	100	100	100
CO	9–16	6–25	1.7–23
CO ₂	14–20	15–22	6
CH ₄	2	<1.6	0.6
C ₂ H ₆	<0.4	–	0.6
CH ₃ OH	5–22	<4	0.9–6.2
H ₂ CO	1.7–7	–	0.13–1.3
HCOOH	0.4–3	–	0.09
NH ₃	13–15	<9	0.7
X-CN	1–3	<0.4	0.08–0.25
OCS, XCS	0.05–0.3	<0.08	0.4

(a) High-mass Young Stellar Object such as W33A and N753S;

(b) Low-mass Young Stellar Object such as Elias 16 and Elias 26 (a category to which the protosun belonged);

(c) From Table 1 and Fig. 2.

The hypothesized delivery of organic molecules to the Earth by the infall of small solar system bodies was prompted by the discovery of carbonaceous matter in meteorites in the nineteenth century. The role of comets was pointed out by Chamberlin and Chamberlin (1908) and by Oró (1961). The important content of prebiotic molecules in cometary matter, which is now confirmed, brings a renewed interest in comets for elucidating the origin of life on Earth (Despois and Cottin 2005; Thomas et al. 2006).

See also

- ▶ Carbonaceous Chondrite
- ▶ Centaurs (Asteroids)
- ▶ Comet (Nucleus)
- ▶ Deep Impact
- ▶ Fluorescence
- ▶ Giotto Spacecraft
- ▶ Kuiper Belt
- ▶ Meteorites



- ▶ [Molecular Cloud](#)
- ▶ [Oort Cloud](#)
- ▶ [Panspermia](#)
- ▶ [Parent Molecule \(in Comet\)](#)
- ▶ [Rosetta \(Spacecraft\)](#)
- ▶ [Stardust Mission](#)
- ▶ [Vega 1 and 2 Spacecraft](#)

References and Further Reading

- A'Hearn MF, Millis RL, Schleicher DG, Osip DJ, Birch PV (1995) The ensemble properties of comets: results from narrowband photometry of 85 comets, 1976D1992. *Icarus* 118:223–270
- Altwegg K, Balsiger H, Geiss J (1999) Composition of the volatile material in Halley's comet from in situ measurements. *Space Sci Rev* 90:3–18
- Barucci MA, Boehnhardt H, Cruikshank DP, Morbidelli A (2008) The solar system beyond Neptune. The University of Arizona Press, Tucson
- Bockelée-Morvan D, Crovisier J, Mumma MJ, Weaver HA (2004) The composition of cometary volatiles. In: Festou MC, Keller HU, Weaver H (eds) *Comets II*. The University of Arizona Press, Tucson, pp 391–423
- Chamberlin TC, Chamberlin RT (1908) Early terrestrial conditions that may have favored organic synthesis. *Science* 28:897–910
- Cottin H, Fray N (2008) Distributed sources in comets. *Space Sci Rev* 138:179–197
- Cremonese G, Boehnhardt H, Crovisier J, Rauer H, Fitzsimmons A, Fulle M, Licandro J, Pollacco D, Tozzi GP, West RM (1997) Neutral sodium from comet Hale-Bopp a third type of tail. *Astrophys J* 490: L199–L202
- Crovisier J (2004) The molecular complexity of comets. In: Ehrenfreund et al (eds) *Astrobiology: future perspectives*. Kluwer, Dordrecht, pp 179–203
- Crovisier J, Bockelée-Morvan D, Colom P, Biver N, Despois D, Lis DC (2004) The composition of ices in comet C/1995 O1 (Hale-Bopp) from radio spectroscopy, further results and upper limits on undetected species. *Astron Astrophys* 418:1141–1157
- Crovisier J, Biver N, Bockelée-Morvan D, Boissier J, Colom P, Lis DC (2009) The chemical diversity of comets. *Earth Moon Planet* 105:267–262
- Despois D, Cottin H (2005) Comets: potential sources of prebiotic molecules for the early earth. In: Gargaud M, Barbier B, Martin H, Reisse J (eds) *Astrobiology*. Springer, Berlin/Heidelberg, pp 289–352
- DiSanti MA, Mumma MJ (2008) Reservoirs for comets: compositional differences based on infrared observations. *Space Sci Rev* 138:127–145
- Elsila JE, Glavin DP, Dworkin JP (2009) Cometary glycine detected in samples returned by Stardust. *Meteor Planet Sci* 44:1323–1330
- Feldman PD, Cochran AL, Combi MR (2004) Spectroscopic investigations of fragment species in the coma. In: Festou MC, Keller HU, Weaver H (eds) *Comets II*. The University of Arizona Press, Tucson, pp 425–447
- Festou MC, Rickman H, West RM (1993a) Comets. I. Concepts and Observations. *Astron Astrophys Rev* 4:363–447
- Festou MC, Rickman H, West RM (1993b) Comets. II. Models, evolution, origin and outlook. *Astron Astrophys Rev* 5:37–163
- Festou MC, Keller HU, Weaver H (2004) *Comets II*. The University of Arizona Press, Tucson
- Hanner MS, Zolensky ME (2010). The mineralogy of cometary dust. In: Henning T (ed) *Astromineralogy* (2nd edn). Springer Lecture Notes in Physics, Berlin/Heidelberg, pp 203–232
- Hartogh P et al (2009) Water and related chemistry in the Solar System. A guaranteed time key program for Herschel. *Planet Space Sci* 57:1596–1606
- Hoyle F, Wickramasinghe NC (1981) Comets – a vehicle for panspermia. In: Ponnampereuma C (ed) *Comets and the origin of life*. Reidel, Dordrecht, pp 227–239
- Jehin E, Manfroid J, Hutsemékers D, Arpigny C, Zucconi J-M (2009) Isotopic ratios in comets: status and perspectives. *Earth Moon Planet* 105:167–180
- Keller HU, Britt D, Buratti BJ, Thomas N (2004) In situ observations of cometary nuclei. In: Festou MC, Keller HU, Weaver H (eds) *Comets II*. The University of Arizona Press, Tucson, pp 211–222
- Krishna Swamy KS (2010) *Physics of comets*, 3rd edn. World Scientific, Singapore
- Lamy PL, Toth I, Fernandez YR, Weaver HA (2004) The sizes, shapes, albedos, and colors of cometary nuclei. In: Festou MC, Keller HU, Weaver H (eds) *Comets II*. The University of Arizona Press, Tucson, pp 223–264
- Li A (2009) PAHs in comets: an overview. In: Käufel HU, Sterken C (eds) *Deep Impact as a World Observatory Event*. Springer, Berlin/Heidelberg, pp 161–175
- Marsden BG, Williams GV (2008) *Catalogue of cometary orbits 2008*, 17th edn. IAU Minor Planet Center/Central Bureau for Astronomical Telegrams, Cambridge
- Morbidelli A (2008). Comets and their reservoirs: current dynamics and primordial evolution. In: Jewitt D, Morbidelli A, Rauer H (eds) *Saas-Fee Advanced Course 35 (Trans-Neptunian objects and comets)*. Springer, New York, pp 79–164
- Oró J (1961) Comets and the formation of biochemical compounds on the primitive earth. *Nature* 190:389–390
- Podolak M, Prialnik D (2006) The conditions for liquid water in cometary nuclei. In: Thomas PJ, Hicks RD, Chyba CF, McKay CP (eds) *Comets and the origin and evolution of life*, 2nd edn. Springer, New York, pp 303–314
- Robert F, Gautier D, Dubrulle N (2000) The solar system D/H ratio: observations and theories. *Space Sci Rev* 92:201–224
- Schechner Genuth S (1997) *Comets, popular culture and the birth of modern cosmology*. Princeton University Press, Princeton
- Schulz R, Alexander C, Boehnhardt H, Glassmeier K-H (2009) *ROSETTA*, ESA's mission to the origin of the solar system. Springer, New York
- Thomas PJ, Hicks RD, Chyba CF, McKay CP (2006) *Comets and the origin and evolution of life*, 2nd edn. Springer, Berlin/Heidelberg
- Weissman PR, Asphaug E, Lowry SC (2004) Structure and density of cometary nuclei. In: Festou MC, Keller HU, Weaver H (eds) *Comets II*. The University of Arizona Press, Tucson, pp 337–357
- Wooden DH (2008) Cometary refractory grains: interstellar and nebular sources. *Space Sci Rev* 138:75–108
- Yeomans DK (1991) *Comets. A chronological history of observation, science, myth, and folklore*. Wiley Science Editions, New York

COMET (Experiment)

Synonyms

Collection en orbite de matériel extra terrestre; ESEF

Definition

The experiment “COMET” flew actually three times on board Soviet then Russian space stations. These experiments placed in 1985 (COMET-1), 1995 (European Space Exposure facility), and 1999 (COMET-99) outside the stations aimed to collect interplanetary dust. This material is composed of grains with a size distribution dominated by particles in the micron range. Very long collection times are required to collect some grains with a reasonable size (10 μm or more). For instance, the experiment, Orbital Debris Collection Experiment (ODCE) sponsored by ► [NASA](#), was flown outside the MIR space station and collected for 18 months starting in March 1996 (Fig. 1).

Alternatively, during the crossing by the Earth of meteor streams, where the fluency can be enhanced by more than one order of magnitude, short collection times can be performed. Such collections were the aim of the COMET experiments and specially for COMET-99 performed outside the MIR station during the CMES sponsored Perseus mission. It targeted more specifically the collection of grains from the swarm of Leonids originated from the Temple-Tuttle comet.

The various collectors made of ultrapure metallic foil or aerogel, a transparent silicon dioxide material of very low density ($\sim 0.06 \text{ g/cm}^3$) came back to Earth by the end of the mission. On the metallic collectors, the incident particles sublime upon impact, leaving a crater, on the rims of which remnants of the particles can be found. The aerogel collectors are designed to avoid destroying the particles while impacting the surface. Penetrating inside the aerogel, they slow down and are trapped with little alteration. The metallic collectors



COMET (Experiment). Figure 1 The Comet hardware before being placed outside the MIR space station (Photo RKA/CNES)

show a very high density of large craters, due to particles larger than 20 μm attributed to the Leonid Swarm. Chemical identification was possible in one case, the EDS spectrum showing identification of Mg, Si, Ca, and Fe.

Optical scanning of the aerogel collectors locates grains as small as a few microns and reveals their penetration track. In one of the two aerogel collectors of COMET-99, two populations of the grains, with a mean diameter around 5 μm , have been found, with penetration tracks in two main directions. A dozen of these grains have been extracted.

The experience gained during these experiments was used preparing for the ► [Stardust mission](#).

References and Further Reading

Borg J (2002) Extraterrestrial samples from low Earth orbits: techniques for their collection and analysis. *Planet Space Sci* 50(9):889–894

Comet (Nucleus)

JACQUES CROVISIER

LESIA - Bâtiment ISO (n°17), Observatoire de Paris, Meudon, France

Keywords

Small body

Definition

A cometary nucleus is the small-size (typically a few kilometers in diameter) solid body in the head of a comet whose activity provides the source of the comet’s appearance.

Overview

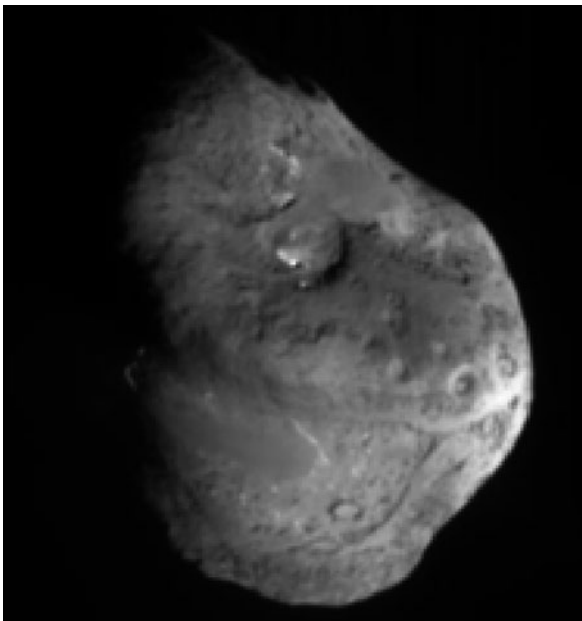
With typical sizes, from about 1 km to about 50 km (as for the giant comet C/1995 O1 (Hale-Bopp)), cometary nuclei are too small to be imaged by Earth-based telescopes. This can only be done with space probes that encounter or flyby these objects at small distances. This has been possible up to now only for a restricted number of objects (Table 1). These observations confirmed that cometary nuclei are really solid bodies (Fig. 1).

The unresolved comet nucleus can be observed when the comet is far from the Sun and inactive, or when the instrumental resolution allows us to separate the nucleus emission from that of the dust coma. It is then possible to evaluate the nucleus size and to investigate its rotation, using the same methods as those used for asteroids (Lamy et al. 2005). Radar studies are also possible for the nucleus of comets coming close to the Earth.

Comet (Nucleus). Table 1 Space missions which were able (or are on their way) to image cometary nuclei

Mission	Space agency	Launch date	Target	Encounter date	(a)	(b)
VEGA 1	IKI	15 Dec. 1984	1P/Halley	6 Mar. 1986 (flyby)	8,890 km	79 km/s
VEGA 2	IKI	21 Dec. 1984	1P/Halley	9 Mar. 1986 (flyby)	8,030 km	77 km/s
Giotto	ESA	2 Jul. 1985	1P/Halley	14 Mar. 1986 (flyby)	596 km	68 km/s
Deep Space 1	NASA	24 Oct. 1998	19P/Borrelly	22 Sep. 2001 (flyby)	2,170 km	17 km/s
Stardust	NASA	7 Feb. 1999	81P/Wild 2	2 Jan. 2004 (flyby)	237 km	6 km/s
Rosetta	ESA	2 Mar. 2004	67P/CG	2014–2015 (orb./land.)		
Deep Impact	NASA	12 Jan. 2005	9P/Tempel 1	4 Jul. 2005 (flyby/impact)		
			103P/Hartley 2	4 Nov. 2010 (flyby)		

For flybys are listed (a) the closest distance to the target and (b) the relative velocity. 67P/CG: Churyumov-Gerasimenko



Comet (Nucleus). Figure 1 The nucleus of 9P/Tempel 1 as seen by the Deep Impact probe. The nucleus average diameter is 6 km. © NASA/JPL-Caltech/UMD

Cometary nuclei are very dark, with ► [albedos](#) in the range 0.02–0.06, which makes them the darkest objects of the Solar System. Rotation periods range from a few hours to a few days. Some nuclei seem to be in an excited state of rotation (e.g., they are tumbling rather than rotating around a fixed axis).

The density of comet nuclei is still waiting for confident measurement. This will be done when it will be

possible to observe and measure the trajectory perturbation of a space probe in the small gravity field of a cometary nucleus. Indirect evaluations were performed using the effect of non-gravitational forces, caused by nucleus outgassing, on cometary orbits (Weissman et al. 2005). They all point to small densities in the range 0.5–1.2 g cm⁻³, suggesting that the nuclei could be porous bodies.

Comet nuclei are frequently observed to split, showing that they are bodies with weak tensile strength, such as rubble piles.

See the ► [Comets](#) entry for a discussion of composition and other details on comet nuclei.

See also

- [Albedo](#)
- [Comet](#)
- [Deep Impact](#)
- [Giotto Spacecraft](#)
- [Rosetta \(Spacecraft\)](#)
- [Stardust Mission](#)
- [Vega 1 and 2 Spacecraft](#)

References and Further Reading

- Boehnhardt H (2005) Split comets. In: Festou MC, Keller HU, Weaver H (eds) *Comets II*. The University of Arizona Press, Tucson, pp 301–316
- Festou MC, Keller HU, Weaver H (2004) *Comets II*. The University of Arizona Press, Tucson
- Keller HU, Britt D, Buratti BJ, Thomas N (2005) In situ observations of cometary nuclei. In: Festou MC, Keller HU, Weaver H (eds) *Comets II*. The University of Arizona Press, Tucson, pp 211–222
- Lamy PL, Toth I, Fernandez YR, Weaver HA (2005) The sizes, shapes, albedos, and colors of cometary nuclei. In: Festou MC, Keller HU, Weaver H (eds) *Comets II*. The University of Arizona Press, Tucson, pp 223–264

Samarasinha NH, Mueller BEA, Belton MJS, Jorda L (2005) Rotation of cometary nuclei. In: Festou MC, Keller HU, Weaver H (eds) *Comets II*. The University of Arizona Press, Tucson, pp 281–299

Weissman PR, Asphaug E, Lowry SC (2005) Structure and density of cometary nuclei. In: Festou MC, Keller HU, Weaver H (eds) *Comets II*. The University of Arizona Press, Tucson, pp 337–357

60 passages since its first discovery, comet Encke is a weak object that has lost most of its gas and dust.

See also

► [Comet](#)

Comet, Churyumov-Gerasimenko

Definition

Comet 67P/Churyumov-Gerasimenko is the target of the ESA ROSETTA spacecraft. ► [ROSETTA](#) will reach the comet in August 2014, and should deliver on the nucleus a lander called ► [PHILAE](#) in November 2014 after a global mapping of the surface in order to choose the best landing site. The comet was discovered by Klim Ivanovich Churyumov and Svetlana Ivanovna Gerasimenko in September 1969. Its current orbital period is 6.5 years, with an aphelion at 5.7 AU and a perihelion at 1.3 AU. Observations of the nucleus with the Hubble Space Telescope have shown that it has a fairly elongated shape (5×3 km), and that it rotates in about 12 h. It has been calculated that before 1840, the comet perihelion was about 4 AU, and that successive dynamical interactions with Jupiter progressively shifted it to its current position.

Comet Churyumov-Gerasimenko will be the first cometary nucleus so closely scrutinized by a spacecraft and on which an automated module will land.

See also

- [Comet \(Nucleus\)](#)
- [Philae Missions](#)
- [Rosetta \(Spacecraft\)](#)

Comet Encke

Definition

► [Comet](#) 2 P/Encke was named after Johannes Encke who, in 1821, calculated its orbit on the basis of previous measurements made by Pons in 1818. He predicted its return in 1821 with an accuracy of 1 day. In 1823, he identified that comet Encke already appeared in 1786, 1795, and 1805. Comet Encke was thus the second known periodic comet. Its period (3.3 years) is the shortest reported until today. Its perihelion is 0.33 AU. After over

Comet Giacobini-Zinner

Definition

► [Comet](#) 21 P/Giacobini-Zinner, discovered independently by Michel Giacobini in 1900 and Ernst Zinner in 1913, is a Jupiter-family comet with a period of 6.6 years; its perihelion is at 1.0 AU and its aphelion is at 6.0 AU. In September 1985, the comet was visited by the spacecraft ISEE 3, renamed International Cometary Explorer (ICE), which flew by the comet at a distance of 7,800 km. The spacecraft detected a shock front when the ionized cometary species came in contact with the solar wind. Six months before the encounter of comet Halley by five spacecraft, 21 P/Giacobini-Zinner was the first comet to be investigated by a space mission.

See also

► [Comet](#)

Comet Hale-Bopp

THERESE ENCRENAZ

LESIA, Observatoire de Paris, Meudon, France

Keywords

Comet

Definition

Comet C/1995 O1 (Hale-Bopp) was discovered simultaneously by Alan Hale and Thomas Bopp on July 23, 1995, at 7.1 AU from the Sun. It was soon realized that the comet, 100 times brighter than Halley at the same heliocentric distance, was abnormally big. Its 2,400-year period brought it to perihelion on April 1, 1997, at a distance of 0.91 AU from the Sun. It was a naked-eye object for over 2 months. As all long-period ► [comets](#), comet Hale-Bopp is an ► [Oort cloud](#) comet, one of the greatest of the twentieth century. Thanks to its early discovery and

its exceptional size, comet Hale–Bopp is among the few objects which have allowed a major achievement in our understanding of cometary physics.

Overview

A large international observing campaign was devoted to the comet in 1996 and 1997, using ground-based and space observatories at all wavelengths, from the X-ray to the radio range. Visible cameras (in particular aboard the Hubble Space Telescope) were used to determine the coma structure and the nucleus size and rotation. Parent molecules were mostly studied from infrared, millimeter, and submillimeter spectroscopy, including space observations from the Earth-orbiting Infrared Space Observatory (ISO).

With a diameter of 40–80 km, the nucleus of comet Hale–Bopp is the largest cometary nucleus ever measured. Its rotation period, determined from the evolution of the jets, is 11.4 h, a typical value for cometary nuclei. In addition to the dust and plasma tails usually visible on comets, a thin sodium tail, observed in the visible range, was detected for the first time (Fig. 1).

Many parent molecules were detected through infrared and millimeter spectroscopy. In addition to previously detected species (H_2O , CO, CO_2 , CH_3OH , H_2CO , HCN, H_2S , NH_3 , HNC, CH_3CN , HNC, and OCS), new molecules were found in the radio range: HCOOH , CH_3CHO , HCOOCH_3 , NH_2CHO , HC_3N , H_2CS , SO, SO_2 , and NS. The detection of HDO in the submillimetre range, in complement with the estimate of H_2O inferred from the radio monitoring, led to the determination of D/H. As for comets Halley and Hyakutake, the D/H was found to be 3×10^{-4} , i.e., twice its value in the terrestrial oceans; this result is important as it leads to the conclusion that only a minor fraction of water on Earth probably has



Comet Hale–Bopp. Figure 1 Comet Hale–Bopp, observed from Earth during its 1997 passage (© M. Jourdain de Muizon, 1997)

a cometary origin. Ground-based observations in the near-infrared range led to the detection of H_2O , CO, CH_4 , C_2H_2 , C_2H_6 , OCS, NH_3 , as well as several radicals.

Another important result is the determination of the nature of the cometary dust, inferred from ISO measurements. In addition to already known silicates signatures, the spectrum of Hale–Bopp, recorded over the whole infrared range, exhibited specific signatures which were attributed to forsterite, a magnesium-rich olivine (Mg_2SiO_4). This spectrum is remarkably similar to those of dust disks surrounding young or evolved stars, which show a close similarity between interstellar and cometary dust.

See also

- ▶ Comet
- ▶ Oort Cloud

Comet Halley

THERESE ENCRENAZ

LESIA, Observatoire de Paris, Meudon, France

Keywords

Comet

Definition

Known since antiquity, Comet Halley is probably the most famous comet in the world. With its 76-year period, it is the only bright comet whose trajectory is predictable enough for space exploration to be planned in advance. It is also the comet which allowed the astronomer Edmund Halley to demonstrate the nature and the periodic appearance of these objects: in 1705, on the basis of previous observations, he predicted the comet's return in 1758. The comet's apparition was actually observed in December 1758, 16 years after Halley's death. The apparition of comet Halley was decisive in confirming Newton's laws of universal gravitation.

Overview

Early apparitions of comet Halley go back to antiquity. Its 1,066 apparition was recorded in the Bayeux tapestry showing King Harold's fear shortly before the Hasting battle and the victory of William the Conqueror. In 1301, the famous Italian painter Giotto di Bondone

represented the comet as the Bethlehem star in his fresco “Adoration of the Magi” in Padua.

The 1835 comet Halley apparition led to the first observations of physical phenomena such as gas and dust ejection in form of jets and fans around the nucleus, represented, in particular, in Bessel’s drawings. His “fountain model” gave the first interpretation of the motion of cometary material ejected sunwards and being repelled away from the Sun. This was the first confirmation of Laplace’s predictions, in 1803, about a frozen nucleus. The next apparition, 1910, was especially favorable in terms of geometrical configuration: photographs and spectra of the comet were recorded, showing emissions from several radicals and ions. At that time, secondary products (coming from the photolysis and ionization of parent molecules), observed in the visible range, were much better known than the parent molecules themselves which are better probed at infrared and millimeter wavelengths. In 1950, on the basis of the H and OH production rates, the astronomer Fred Whipple proposed his “dirty snowball model,” which predicted that the ► [comets](#) are mainly composed of water ice together with minor amounts of dust.

The next apparition, in 1986, was not favorable in terms of geometry: with respect to the Earth, the comet was behind the Sun at the time of perihelion, on February 9, 1986. Ground-based monitoring was thus much more difficult than at the time of the 1910 apparition and the images of the comet were much less spectacular; best observations were performed when the geocentric distance of the comet was minimum in November 1985 and in April 1986. In spite of the poor observational conditions, the development of new technologies, both for ground-based and space exploration, allowed astronomers to get the best scientific return from this event. The apparition was prepared long in advance by an impressive worldwide observing campaign, including five spacecraft- and ground-based observations at all wavelengths, from the UV to the radio range, coordinated by the “International Halley Watch.” The five space missions included the European ► [Giotto mission](#), launched by ESA; the two ► [Vega](#) missions led by the Soviet Union; and two Japanese spacecraft, Suisei and Sakigake. For the first time, images of the nucleus were obtained; in-situ measurements of the cometary gas and dust were recorded; from space and ground-based experiments, parent molecules were actually detected, thanks to the development of infrared spectrometers and millimeter heterodyne spectroscopy.

Comet Halley was recovered in October 1982, at a heliocentric distance of 11 AU, with an angular distance

of only 9 arcsec of its predicted position. The observation was made at Mount Palomar Observatory (California, USA) and its recovery illustrated the growing success of CCD cameras in astronomy.

The Nucleus

The first images of a cometary nucleus were those of Comet Halley, taken by the Giotto spacecraft in 1986. They were surprising at least on two aspects: the nucleus had an elongated shape, with dimensions of $15 \times 8 \times 7$ km in size, and its mean albedo was very low (0.04). The nucleus surface was mostly covered with dark material, probably due to a carbonaceous deposit, with a surface temperature as high as 300 K; water vapor, together with dust, was outgassed through a few discrete active areas, at temperatures of about 200–220 K ([Fig. 1](#)).

The presence of carbonaceous material at the surface of the nucleus was also inferred by another discovery. The mass spectrometers of the Giotto and Vega spacecraft detected unexpected abundances of light elements (H, C, N, O), especially in complex hydrocarbon grains. This result was independently derived from the analysis of the



Comet Halley. Figure 1 The nucleus of comet Halley, as observed by the camera of the European Giotto mission on March 13, 1986, as the spacecraft flew over the comet at a distance of 500 km. Active areas showing jets of water and dust appear on the left side of the object. The dimensions of the nucleus are $15 \times 8 \times 7$ km. © ESA

near-infrared spectrum of Halley recorded by Vega, which revealed a broad emission attributed to both saturated and unsaturated hydrocarbons. Such spectral signatures have been observed under other circumstances in interstellar spectra and also in laboratory spectra of ice mixtures irradiated by solar UV or high-energy particles.

Long-period ground-based photometric monitoring has been used to determine the rotation period of Halley's nucleus. A two-component model has been favored with a slow precession (with a period of at least 7 days) and a 2-day rotation period.

The Coma

As a first result, Whipple's "dirty snowball model" was confirmed. Water, identified by its near-infrared vibration bands, was unambiguously detected, both from the Kuiper Airborne Observatory and from the Vega IKS spectrometer. Its relative water content, in number of atoms, was found to be close to 80%. In addition to water and hydrocarbons, other molecules were detected by IKS aboard Vega: CO₂, H₂CO, and CO were also detected in the UV range. Hydrogen cyanide HCN was detected from the first time in a comet from ground-based millimeter heterodyne spectroscopy. Some molecules are outgassed from the nucleus, but also from the grains of the halo. It is the case of CO and H₂CO which have been detected in the cometary grains. Another interesting result was the detection, by the UV spectrometer of Vega, of some polycyclic aromatic hydrocarbons (PAHs), especially naphthalene C₁₀H₈ and phenanthrene C₁₄H₁₀, in the close vicinity of the nucleus. Similar species have been also identified in interstellar spectra. It is striking to note that all parent molecules found in comet Halley have been also detected in the interstellar medium. These results strongly suggest a close link between interstellar and cometary matter.

Radio observations of the OH radical at wavelength of 18 cm have been used to monitor the water production of the comet as a function of its heliocentric distance.

An important parameter measured by mass spectroscopy was the D/H ratio inferred from HDO/H₂O in the coma. This ratio is diagnostic of the early conditions of the comet's formation: at low temperatures, the D/H ratio is enriched in ices as a result of ion–molecule and molecule–molecule reactions. D/H in comet Halley was found to be 3×10^{-4} , i.e., twice its value in the terrestrial oceans. This value was later confirmed by two measurements on other comets (Corvisier 2001; Newburn et al. 1999), which led to the same results. In all cases, the relatively high D/H ratio indicates that water on Earth cannot have come entirely from comets.

Origin and Fate of Comet Halley

As shown by its retrograde orbit, comet Halley is most likely a captured object from the Oort cloud. The Oort cloud already existed when the giant planets accreted; it was the reservoir from where many planetesimals were ejected by gravity perturbations due to these massive bodies. This explains why, after so many apparitions, comet Halley is still an active body: its long period allowed it to keep a significant fraction of its icy reservoir. At each perihelion passage, the surface of comet Halley is eroded and loses about 1 m depth of ice and dust. In the future, the icy content of comet Halley will slowly decrease.

See also

- ▶ Comet
- ▶ Comet (Nucleus)
- ▶ Daughter Molecule (in Comet)
- ▶ Giotto Spacecraft
- ▶ Parent Molecule (in Comet)
- ▶ Vega 1 and 2 Spacecraft

References and Further Reading

- Crovisier J (2001) Comet Hale-Bopp. In: Encyclopedia of astronomy and astrophysics. Institute of Physics Publishing, Bristol, pp 414–416
- Newburn RL, Rahe J, Neugebauer M (1999) Comets in the post-Halley Era. Kluwer Academic Press, Dordrecht

Comet Hyakutake

Definition

Comet C/1996 B2 Hyakutake was discovered in January 1996 and it approached the Earth in March 1996 at a distance of only 0.10 AU. It passed perihelion in May 1996 at a distance of 0.23 AU. It is a long-period comet (about 9,000 years) which presumably comes from the ▶ [Oort cloud](#). A campaign of astronomical observations was set up, taking advantage of its proximity to Earth. The comet nucleus is 2–3 km in diameter and its rotation period is 6.3 h. Many parent molecules were detected from infrared and millimeter ground-based spectroscopy (H₂O, CO, CO₂, CH₃OH, H₂CO, HCN, and H₂S).

See also

- ▶ Comet
- ▶ Oort Cloud

Comet Shoemaker-Levy 9

THERESE ENCRENAZ

LESIA, Observatoire de Paris, Meudon, France

Keywords

Comets

Definition

Comet Shoemaker-Levy 9 (SL9) was discovered in March 1993 by Eugene and Carolyn Shoemaker and by David Levy. At that time, it appeared as a trail of about 20 fragments. The study of their trajectories showed that it was a Jupiter-family comet which was disrupted by tidal forces at its previous closest (perijove) passage, in July 1992. It was soon predicted that the fragments would collide with ► [Jupiter](#) at its next closest passage, in July 1994 ([Fig. 1](#)).

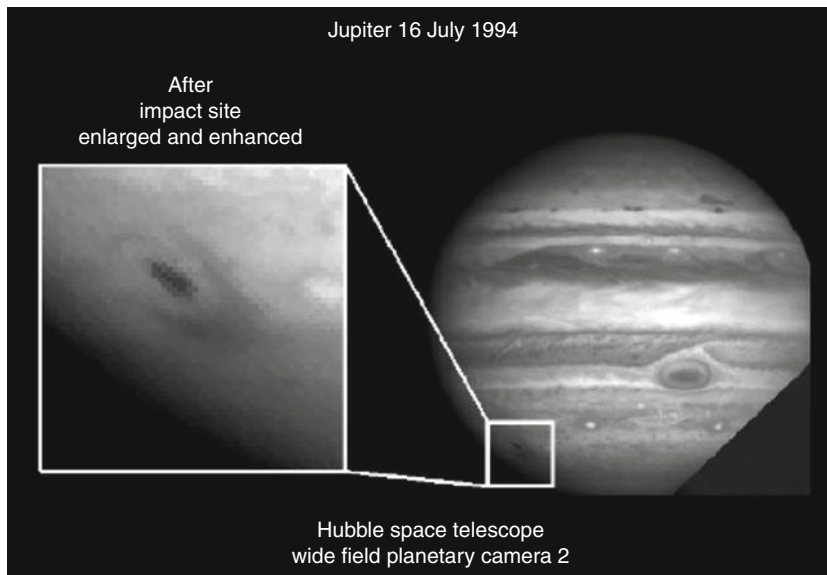
Overview

A collision of a comet with Jupiter is very rare: according to dynamical models, it could be expected only once every few centuries. Actually, a similar event was reported by Cassini at the end of the seventeenth century. As a consequence, at the time of the SL9 collision, a huge international campaign took place in order to monitor the event using all possible ground-based and space means,

covering the whole spectral range, from the X-ray to the radio range. Among the spacecraft were the Galileo spacecraft (en route to Jupiter for an approach in 1995), the Hubble Space Observatory (HST), the International Ultraviolet Explorer (IUE), and the X-ray satellite ROSAT. Among the objectives were: the determination of the impact altitude, the temperature elevation and decay, the monitoring of the impact craters, the search for new molecules formed by shock chemistry.

The fragments of SL9 entered the Jovian atmosphere at a latitude of 44S. Between July 16 and July 22, 1994, the impacts spread along the 44S parallel as the planet was rotating; the collisional events took place a few minutes within the predicted impact times. As seen from Earth, the impacts took place just behind the limb and came to direct view only about 10 min later. Galileo, still at a distance of 1.6 AU from Jupiter, was the only observatory which could see the whole event in direct view.

The successive events were recorded with three types of data: lightcurves, images, and spectra. Lightcurves, recorded at different wavelengths, allowed to determine the temperature evolution and gave an estimate of the energy budget. Images, taken from Galileo, the HST and ground-based telescopes, recorded the meteor entry (Galileo), the ejecta trajectories (limb images from the HST), and the crater evolution (HST and ground-based telescopes). Spectra, recorded in the UV (IUE, HST), the visible, infrared, and radio range, have detected new species and monitored their evolution.



Comet Shoemaker-Levy 9. Figure 1 Image of the comet Shoemaker-Levy 9 before its impact with Jupiter. © NASA

Temporal Sequence of the Impacts

The collisions of each individual fragments were remarkably similar, although of different intensities, depending on the impactor size. In all cases, the lightcurves showed a sequence of three phases:

- The entry phase was observed as a flash by the camera and the photometer of the Galileo spacecraft.
- The explosion phase occurred one minute later; it corresponded to the explosion of the impactor within the atmosphere and to the ascent of a fireball; HST images taken at Jupiter's limb showed ejecta up to an altitude of 3,000 km for all fragments (the smaller exploding at a higher altitude than the larger ones). The fireball increased adiabatically from 15 km, 10 s after the impact, to 100 km after 40 s. Explosions took place at a pressure level ranging between 0.1 and 1 bar. For the largest impacts, the temperature was over 10,000 K at the early beginning, and decreased to 2,000 K after about 15 s.
- The “splash phase” was studied from the lightcurves, the images, and the evolution of the spectra. In particular, the monitoring of methane emissions in the near-infrared range showed a decrease of the temperature from 1,000 K at $t = 10$ min to 600 K at $t = 25$ min. HST images showed the formation of dark craters surrounded by crescent-shaped areas resulting from infalling ejecta, indicating the formation of dust, possibly including carbonaceous and silicate material (Fig. 2).

New Molecules

Several new species have been detected in the stratosphere of Jupiter during the splash phase:

- The most abundant was CO, detected both in the infrared and in the millimeter range. In particular,

infrared spectra of CO showed a high excitation temperature of a few thousand K at the beginning of the splash phase.

- Water was detected in the near-infrared by the NIMS instrument aboard Galileo and by the Kuiper Airborne Observatory, with an excitation temperature of 1,000 K.
- Sulfur species were identified by the UV spectrometer of the HST: S₂, CS₂, CS, and possibly H₂S.
- From mid-infrared spectra (10–13 μm), NH₃, HCN, and C₂H₄ were identified.
- Ground-based millimeter heterodyne spectroscopy allowed the detection and long-term monitoring of CO, CS, OCS, and HCN.

The relative abundances of the newly formed species are indicated in Table 1.

Long-term Evolution of Impact Phenomena

The new molecules formed by shock chemistry had very contrasted lifetimes. Water was the first molecule to disappear after a few hours. Still, the water brought by the SL9 collision is believed to be at least partly responsible for the traces of stratospheric water discovered in 1997 by the Infrared Space Observatory, and later observed by other submillimeter satellites. OCS, NH₃, and S₂ were detected during a few weeks. CO and CS₂ were observed during several months, and HCS and CN were detectable over several years. The observed lifetimes were found to be in good overall agreement with the predictions inferred from photochemical models.

The dust observed in the impact craters could be monitored during the weeks and months following the collision. The clouds first extended in longitude as an effect of Jupiter's fast rotation and, after a couple of weeks, formed a continuous band at latitude 44S.



Comet Shoemaker-Levy 9. Figure 2 One of the first impact sites of the SL9 collision as observed by the HST. All impacts occurred at latitude 44S. The enlargement on the left side shows the crescent-shaped structure surrounding the main impact crater. © NASA



Comet Shoemaker-Levy 9. Table 1 New molecules formed in Jupiter atmosphere by shock chemistry

Molecule	Observations	Molecular mass in SL9 impact (g)	Elemental mass in SL9 impact	Elemental mass in a 10^{15} g fragment (comet)
H ₂ O	IR, (radio)	$>2 \times 10^{12}$	$>1.5 \times 10^{14}$ [O]	5×10^{14} [O]
CO	(IR), radio	2.5×10^{14}	"	"
NH ₃	(UV), IR	1×10^{13}	1×10^{13} [N]	2×10^{13} [N]
HCN	IR, radio	6×10^{11}		
S ₂	UV	1.5×10^{12}		
CS ₂	UV	1.5×10^{11}		
CS	(UV), radio	5×10^{11}	5×10^{12} [S]	4×10^{13} [S]
H ₂ S	UV	Marginal		
OCS	Radio	3×10^{12}	1×10^{14} [C]	2×10^{14} [C]
PH ₃	IR	3×10^{11} [P]	1×10^{12} [P]	
Silicate	IR	6×10^{12}	8×10^{13} [Si]	1×10^{14} [Si]
			4×10^{13} [Mg]	4×10^{13} [Mg]

During about a year, the clouds extended in latitude between 20S and 80S. Aerosols, first formed in the stratosphere, moved downward, contributing to the atmospheric profile cooling, to reach tropospheric levels after about a year.

Magnetospheric Effects

The Jovian magnetosphere was also affected by the collision. The synchrotron radiation, monitored at centimeter wavelengths, showed an enhancement of a few tens of percent during the week of impacts. The emission was mostly observed at localized longitudes, between 100° and 240°, showing evidence for a new population of excited electrons. This region correlates with the side where the magnetic field lines crossing the radiation belts, intercept the disk of Jupiter around latitude 44S.

Auroral phenomena were also recorded, in some cases, prior to the impacts, implying a strong heating of the upper stratosphere, in particular UV emissions of H and H₂ and H₃⁺ infrared. Often, auroral emissions were detected at the location of the northern counterparts of the impact sites, corresponding to the footprints of the connecting magnetic field lines: X-rays emissions were recorded by the ROSAT satellite at the time of two impacts; UV emissions were observed by the HST and H₃⁺ near-IR emissions were detected from the Earth ground.

About the SL9 Comet

All astrometric measurements performed before and during the collision were used to retrieve the best orbital fits

ever obtained for a comet. The progenitor of comet SL9 has been captured by Jupiter nearly in the year 1930. Before its capture, the comet's orbit was probably within Jupiter's orbit, with a low eccentricity and a low inclination.

From the disruption of the comets' nucleus in 1992, its tensile strength was inferred. The very low value, 100 Pa, is consistent with a fluffy aggregate of sub-micron particles. Models of the swarm elongation are consistent with a progenitor of 1.5 km in size, with a density of 0.5 g/cm³. These numbers are consistent with the estimates inferred for the impactors on the basis of the impact dynamical models. The comets' activity was measured in 1993 and 1994 before the impact. Very low dust production rates were estimated (1–5 kg/s for the different impacts). No gaseous activity was detected; an upper limit of 10²⁷ mol/s was retrieved for the OH production rate.

Information about the comet's composition was obtained from visible spectra taken during some impacts that showed a variety of atomic lines (Fe, K, Ca, H, Na, Mg, Mn, Cr, and for the first time, Li). UV spectra taken by the HST also showed atomic and ionic transitions: H, He, S, Si, Mg⁺, Fe⁺, Si⁺, Al⁺. All these species, absent from Jupiter's spectrum, belong to the impactor; they are frequently observed in the spectra of sun-grazing [comets](#).

The composition of SL9 is difficult to retrieve from the new molecules formed during the impacts because they result of recombination of products a part of them possibly having (at least partly) a planetary origin. Still, the



oxygen and sulfur-bearing molecules, absent from Jupiter's stratosphere, can be used to infer the O and S content of the impactor. The inferred O/S is consistent with cometary values. The carbon content of the impactor cannot be inferred as the new molecules may have been formed from Jovian methane. Assuming that all the nitrogen of the new molecules is coming from the impactor, the inferred N/O ratio is consistent with a cometary origin. The Si/O ratio inferred from the silicate signature at 10 μm is also in agreement with cometary values. In conclusion, several facts support a cometary rather than asteroidal origin for the impactor: the small size, the weak but real level of activity, the low density, the very low tensile strength, the chemical composition, and the presence of silicates. Comet SL9 was actually a very small and very common Jupiter-family comet.

In summary, the collision of comet SL9 with Jupiter has not allowed astronomers to fully understand the nature and the composition of the comet; however, it provided a real-time observation of the response of a planetary atmosphere to a large meteoritic impact.

See also

- ▶ [Comet](#)
- ▶ [Jupiter](#)

References and Further Reading

- Encrenaz T (2001) Shoemaker-Levy-Jupiter collision. In: Murdin P (ed) *Encyclopedia of astronomy and astrophysics*. IoP Publishing, Bristol, pp 2413–2420
- Noll KS, Weaver HA, Feldman PD (eds) (1996) *The collision of comet Shoemaker-Levy and Jupiter*. Cambridge, Cambridge University Press
- Spencer, K. R. and Mitton, J. (eds), *The Great Comet Crash*, Cambridge, Cambridge University Press, 1995
- West RM, Bohnhardt H (eds) (1995) *Proc European Workshop on the SL9-Jupiter Collision*, no. 52, Garching, ESO

Comet Shower

Definition

A comet shower is a short-lived burst in the flux of comets entering the inner Solar System from the ▶ [Oort cloud](#). Comet showers are thought to be triggered primarily by relatively close passages of nearby stars with the Solar System. Comet showers are not considered an impact threat on Earth.

See also

- ▶ [Oort Cloud](#)

Comet Tempel 1

Definition

▶ [Comet 9P/Tempel 1](#) was discovered in 1867 at the Observatoire de Marseille by the astronomer Ernst Wilhelm Tempel. Its orbit, very close to the ecliptic, has a period of 5.5 years around the Sun, and lies between the orbits of Mars and Jupiter. The diameter of the comet is 6.5 km and its rotation period is 41 h. Comet Tempel 1 has been explored in detail by the NASA probe Deep Impact which sent an impactor at its surface on July 4, 2005. The impact led to the formation of a 30-m large crater and the massive ejection of dust, water, and HCN.

See also

- ▶ [Comet](#)

Comet Wild 2

Definition

▶ [Comet 81 P/Wild](#), also named Wild 2, was discovered in 1978. After a passage close to Jupiter in 1974, its orbit moved toward the inner solar system, with a high ellipticity and a short period (6.4 years). Its perihelion is close to 1 AU. In January 2004, comet Wild 2 was approached by the ▶ [Stardust](#) spacecraft which collected cometary grains from its tail and brought them back to Earth in 2006. This cometary matter included material originate from different regions of the solar system. Comet Wild 2 is the only comet for which samples have been brought back to Earth and analyzed.

See also

- ▶ [Comet](#)
- ▶ [Stardust Mission](#)

Comets, History of

STÉPHANE LE GARS

Centre François Viète, Université de Nantes, Nantes, BP, France

Keywords

Astronomy, comets, gravitation, Halley, history, meteorites, Oort, physics

Abstract

Located between the Earth and the Moon for Aristotle, divine anger signs in the Middle Ages, from the fifteenth century comets started to be studied more systematically, in particular by measuring their distance from the Earth. With reference to Newton's works, the cause of their movements is ascribed primarily ("nongravitational forces", the jet effect due to asymmetric outgassing, are important for precise determination of orbits) to gravitation. In the nineteenth century, new techniques, such as spectroscopy, opened the way to their chemical and physical analysis.

History

Since ancient times, ► [comets](#) have raised questions and polemics. Visual observations of comets date back to the eleventh century BCE, when Chinese chronicles related a cometary apparition to war between two kings. There are many references in classical literature, including Pliny's report of a comet during the battle of Salamis (480 BCE). During the Middle Ages in Europe, comets were seen as portents, of the Norman conquest of England in 1066 in the Bayeux tapestry, and of the birth of Jesus as depicted by Giotto in 1304. The New World also linked comets and important events, including that observed by the Aztec emperor Moctezuma, prior to the conquest of Mexico by Cortez. If the Chaldean considered them as planets, some Greek philosophers such as Aristotle situated them in the area between the Earth and the Moon. From the fifteenth century, comets were being studied more systematically. Their movements were described through the constellations, an interest is taken in their tail's orientation with regard to the Sun, and an estimation of their parallax puts them definitely beyond the Moon.

It is since the universal gravitation law, proposed by Newton in 1687 in his *Philosophiae Naturalis Principia Mathematica*, that the astronomer Edmund Halley identified the 1682 comet with those of 1607 and 1531, and predicted its return for 1759: at this moment, it was proved that those celestial bodies were bound, like planets, by gravitation, describing on the other hand elliptical (in that case they are periodical), parabolic, or hyperbolic orbits about the Sun. Then, in the nineteenth century, attention turned to the origin and the composition of those heavenly bodies. Analysis of the spectrum and polarization of light permitted astronomers at this time to identify in the comet's coma (atmosphere; from the Latin word for "hair") and tail both dust and atoms and small molecules (typically photodissociation products).

It is only in 1950 that the American astronomer Fred Whipple described the comets as "dirty snowballs," speculating that their nucleus is essentially constituted of watered ice mixed with carbonic ice, silicates, and organic compounds. It is also in 1950 that Dutch astronomer Jan Oort calculated that long-period comets came from a gigantic spherical reservoir, containing thousands of millions of those little bodies, and located them at 1 or 2 light years from the Sun. Starting with the return of Comet Halley in 1986, radio and infrared astronomers have identified many molecular constituents of comets by observing their emission at millimeter wavelengths. In 2006, the Stardust space probe brought back to Earth dust from the Wild-2 comet, out of which analysis led to new knowledge on the solar system.

See also

- [Comets](#)
- [Kuiper Belt](#)
- [Oort Cloud](#)

References and Further Reading

- Acker A (2005) *Astronomie astrophysique. Introduction*. Dunod, Paris
- Bosler J (1928) *Cours d'Astronomie. III Astrophysique*. Librairie scientifique Hermann et Cie, Paris
- Durán D *Historia de las Indias de Nueva España y Islas de Tierra Firme, Fondos de la Biblioteca Nacional (Spain)*
- Flammarion C (1880) *Astronomie populaire*. C. Marpon et E. Flammarion, Paris
- Henarejos P (1999) *Comètes*. In: *Dictionnaire de l'Astronomie, Encyclopaedia Universalis et Albin Michel*, Paris, pp 164–175
- Millochau G (1910) *De la Terre aux astres*. Librairie Delagrave, Paris
- Olson R, Pasachoff J (1987) *New information on comet P/Halley as depicted by Giotto di Bondone and other Western artists*. *Astron Astrophys* 187:1–11
- Yeomans D (1991) *Comets: a chronological history of observation, science, myth, and folklore*. New York, Wiley

Comisión Nacional de Actividades Espaciales

- [CONAE \(Argentina\)](#)

Committee on Space Research

- [COSPAR](#)

Common Ancestor

Synonyms

Concestor; Most recent common ancestor; MRCA

Definition

A common ancestor is the ancestral biological entity (i.e., a species or a molecular ► [sequence](#)) from which a group of different biological entities have evolved. One of the main ideas of Charles Darwin in *The Origin* (1859) is that species are related by common ancestry (i.e., have evolved by divergence from a common ancestral species). As a result of evolution by divergence from a common ancestor, the ► [phylogenetic](#) relationships among species or DNA/protein sequences can be described using a tree-like structure. The concept is also applied to define the Most Recent Common Ancestor (MRCA) of a group of individuals in a population.

See also

- [Cenancestor](#)
- [Darwin's Conception of Origins of Life](#)
- [Endosymbiosis](#)
- [Evolution \(Biological\)](#)
- [Homology](#)
- [Last Universal Common Ancestor](#)
- [Phylogenetic Tree](#)
- [Phylogeny](#)
- [Sequence](#)

Community Genome

- [Metagenome](#)

Compatible Solute

JOSEFA ANTÓN

Departamento de Fisiología, Genética y Microbiología,
Universidad de Alicante, Alicante, Spain

Synonyms

Osmolyte

Keywords

Haloadaptation, halophile, halotolerant

Definition

A compatible solute is a substance compatible with the cellular metabolism that accumulates in the cytoplasm to balance external osmotic pressure. This accumulation can be due either to transport from the medium or to de novo synthesis and helps maintaining turgor pressure, cell volume, and concentration of electrolytes, all needed for cell viability and proliferation.

Overview

Microorganisms cope with osmotic stress (due to high salt, freezing, and/or desiccation) by using two different types of strategies. *Archaea* of the order *Halobacteriales*, anaerobic *Bacteria* belonging to the order *Haloanaerobiales*, and some members of the *Bacteroidetes* (i.e., *Salinibacter ruber*) accumulate high concentrations of inorganic ions (mostly potassium) in the cytoplasm. This is known as the “salt-in” strategy and requires the adaptation of the entire intracellular machinery in order to function in this highly saline environment. The second strategy relies on intracellular accumulation, either by uptake or de novo synthesis, of low-molecular-weight organic compatible solutes (also called osmolytes) to balance the external osmotic pressure. The accumulation of such solutes is very widespread in nature since the cytoplasm of most organisms do not tolerate salt. In addition, this is a very versatile strategy that allows for rapid response to changing environments since organisms can regulate their intracellular concentration according to the surrounding salinity.

Compatible solutes are small organic molecules that act as osmoprotectants thanks to their ability to stabilize cellular proteins, providing an hydration shell and stabilizing their tertiary structures without interfering in cell metabolism (this is why they are called “compatible”). Indeed, compatible solutes not only provide protection from osmotic stress but some can also act as thermostabilizers, a property that has been exploited for biotechnological purposes.

There is a wide range of compatible solutes, but they can be classified into a few chemical categories (Empadinhas and da Costa 2008) such as amino acids and derivatives (including ectoines and hydroxyectoines), sugars and derivatives, phosphodiesteres, and polyols. Some of them, such as glycine betaine, are universal compatible solutes, while others are restricted to a specific group of microorganisms. For a detailed description of the chemical nature and occurrence of organic compatible solutes within halophilic and halotolerant organisms, see Roberts (2005).

See also

- ▶ [Halophile](#)
- ▶ [Halotolerance](#)

References and Further Reading

- Empadinhas N, da Costa MS (2008) Osmoadaptation mechanisms in prokaryotes: distribution of compatible solutes. *Int Microbiol* 11:151–161
- Roberts MF (2005) Organic compatible solutes of halotolerant and halophilic microorganisms. *Saline Syst* 1:5

Complex Organic Molecules**Definition**

The term “complex organic molecules” is used differently in astronomy and chemistry. In astronomy, complex organic molecules are molecules with multiple carbon atoms such as benzene and acetic acid. These molecules have been detected in interstellar space with radio telescopes. In chemistry, “complex organic molecules” refer to polymer-like molecules such as ▶ [proteins](#). Proteins are typical complex organic polymers with well-defined three-dimensional shapes, composed of 20 kinds of amino acids. Given the immense possible variety of these polymers, they are indeed “complex.” During chemical evolution, other types of complex organic compounds can be formed. For example, HCN polymerizes to give polymers of complex undefined structure. A gas mixture of methane and nitrogen also yields complex organic compounds upon UV irradiation or exposure to an electric discharge. These are sometimes referred to as ▶ [tholins](#), and they can be formed abiotically in the atmosphere of ▶ [Titan](#) (the largest satellite of Saturn).

See also

- ▶ [HCN Polymer](#)
- ▶ [Insoluble Organic Matter](#)
- ▶ [Protein](#)
- ▶ [Radio Astronomy](#)
- ▶ [Tholins](#)
- ▶ [Titan](#)

Complex Organic Product

- ▶ [Tholins](#)

Complex Organisms

- ▶ [Multicellular Organisms](#)

Complexity

CARLOS GERSHENSON

Instituto de Investigaciones en Matemáticas Aplicadas y en Sistemas, Universidad Nacional Autónoma de México, DF, Mexico

Keywords

Complex systems, computation, information, interactions, non-reductionism, scientific paradigm

Definition

There is no single definition of complexity (Edmonds 1999; Gershenson 2008; Mitchell 2009), as it acquires different meanings in different contexts. A general notion is the amount of information required to describe a phenomenon (Prokopenko et al. 2009) (note that this depends on the scale (Bar-Yam 2004) and context in which the description is made, e.g., an organism requires more information to be described at a molecular scale than at a population scale), but it can also be understood as the length of the shortest program required to compute that description, as the time required to compute that description, as the minimal model to statistically describe a phenomenon, etc.

Overview

The study of complexity and complex systems is so broad and encompasses so many disciplines that it is difficult to define. There are different definitions suitable for different contexts and purposes. Etymologically, complexity comes from the Latin *plexus*, which means interwoven. A complex system is one in which elements interact in such a way that it is difficult to separate their behavior. In other words, if one element affects the state of another element, the dynamics of the system cannot be *reduced* to the states of the elements, since interactions are relevant for the future state of the system. Examples of complex systems include a ▶ [cell](#), a brain, a city, the Internet, a market, a crowd, an ▶ [ecosystem](#), a ▶ [biosphere](#), and an atmosphere. A cell is composed of molecules, but the behavior of a cell cannot be reduced to that of molecules.

Their interactions generate constraints and information that is not present in molecules and determine the behavior of the cell.

Some approaches to complexity do not focus on its systemic aspect, but more on its probabilistic or algorithmic aspect. These are related with information theory, e.g., how probable is a string of bits, how long is the shortest algorithm that produces a string of bits, what is the shortest time it can take an algorithm to produce a string of bits, or how compressible is a string of bits. Intuitively, in most of these descriptions, complexity represents a balance between order (stability) and chaos (variability) (Kauffman 1993).

Since complexity can be found in almost any field, some people question its usefulness, while others defend it as a novel scientific paradigm that complements the traditional reductionist approach (Gershenson and Heylighen 2005; Morin 2006).

Basic Methodology

There have been many methods developed within the study of complexity that have proven to be very useful, since they are able to take into account the interactions of the elements of a complex system. Tools include agent-based modeling, networks, ► [cellular automata](#), ► [genetic algorithms](#), and swarm intelligence.

Most of complexity research is based on computer simulations. On the one hand, complex models tend to involve large numbers of elements and/or interactions, which are difficult to handle without computer aid. On the other hand, interactions generate novel and relevant information that is not present in initial or boundary conditions. This makes it difficult to know a priori a final state of a system without computing all of its transitions, i.e., predictability is limited. A model has to “run” before something definitive can be said about it. Cellular automata provide a clear example of this. Thus, an equation-based approach is in many cases insufficient to explore the properties of a model.

There are many concepts that are related to the study of complexity, such as nonlinearity, self-organization, adaptation, chaos, and ► [emergence](#).

Key Research Findings

The scientific study of complexity has increased the understanding of phenomena in many different fields. Common examples include models of collective behavior, complex networks (molecular, metabolic, genetic, neural, trophic, ecologic, social, economic, organizational, political, geographical), nonlinear dynamics, evolution, and distributed

systems. Theoretically, complexity has also provided several concepts, formalisms, and tools.

The main difference of complexity-related and traditional techniques is that complexity can easily include millions of variables into consideration, e.g., with cellular automata, multi-agent systems, or networks. This is difficult to achieve with, e.g., differential equations, which are more suitable for contexts where there are few variables considered and the state space or phase space does not change, i.e., is stationary. The tools of complexity are suitable for studying nonstationary spaces, i.e., those that change with time.

Applications

The scientific study of complexity and complex systems has found applications in physical, chemical, biological, computational/informational, social, economic, engineering, and other fields. In many cases, the concepts, tools, and methods of complexity have been applied to specific problems, e.g., self-assembly, pattern formation, adaptive control, protein folding, ecological studies, robotics, evolution, etc. In other cases, the study of complexity per se has also attracted broad attention.

Complexity formalisms allow the study of phenomena at different scales and to relate them under the same framework. This is useful when multiple scales (spatial, temporal, functional, dynamical) interact within a system, since the same language can be used to relate the scales. This is not feasible with a reductionist approach.

Future Directions

Some have speculated that complexity is a fad and it will lose its popularity, following the steps of similar movements: cybernetics, catastrophe theory, and chaos theory. Nevertheless, complexity has been studied (under this name) since the 1980s, and everything indicates that the interest in it is growing. The concepts and methods that have been developed within the study of complexity and complex systems are permeating into all disciplines. Maybe people will not use the term complexity, but this is not relevant. Complexity is helping shape a shift in the scientific worldview, from reductionist to “interactionist.” This is relevant, since this shift is allowing us to expand the frontiers of our knowledge.

See also

- [Artificial Life](#)
- [Cellular Automata](#)
- [Emergence of Life](#)
- [Genetic Algorithms](#)
- [Scale Free Networks](#)

References and Further Reading

- Bar-Yam Y (1997) Dynamics of complex systems. Studies in nonlinearity. Westview, Boulder
- Bar-Yam Y (2004) Multiscale variety in complex systems. *Complexity* 9(4):37–45
- Edmonds B (1999) Syntactic measures of complexity. Doctoral Thesis, University of Manchester, Manchester
- Gershenson C (ed) (2008) Complexity: 5 questions. Automatic Press/VIP, Copenhagen, Denmark, ISBN:8792130135
- Gershenson C, Heylighen F (2005) How can we think the complex? In: Richardson K (ed) Managing organizational complexity: philosophy, theory and application. Information Age, Greenwich, Chapter 3
- Holland JH (1995) Hidden order: how adaptation builds Complexity. Helix Books/Addison-Wesley, Reading
- Kauffman SA (1993) The origins of order. Oxford University Press, Oxford
- Meyers RA (ed) (2009) Encyclopedia of complexity and systems science. Springer, New York
- Mitchell M (2009) Complexity: a guided tour. Oxford University Press, Oxford
- Morin E (2006) Restricted complexity, general complexity. In: Gershenson C, Aerts D, Edmonds B (eds) Philosophy and complexity, worldviews, science and Us. World Scientific, Singapore
- Prokopenko M, Boschetti F, Ryan A (2009) An information-theoretic primer on complexity, self-organisation and emergence. *Complexity* 15(1):11–28

Computational Biology

- [Bioinformatics](#)

CONAE (Argentina)

Synonyms

[Comisión Nacional de Actividades Espaciales](#)

Definition

The “Comisión Nacional de Actividades Espaciales” (CONAE) is the space agency for Argentina. Argentina’s first activities in the space field date back to 1961, when the National Commission for Space Research (Comisión Nacional de Investigaciones Espaciales, CNIE) was first established within the Argentine Air Forces area. With other local and international organizations, CNIE carried out, by means of rockets and stratospheric balloons, the first southern hemisphere scientific atmospheric studies, which included wind measuring and assessment of neutral atmosphere dynamics using the alkaline clouds technique. Together with the Argentine Institute of Aeronautics and Space Research, CNIE designed and constructed a family of one- and two-stage sounding rockets.

In 1991, the Argentine Government decrees the creation of this National Commission for Space Activities as a civil organization. Since 1996; this specialized agency accomplishes its mission governed by the Ministry of Foreign Affairs.

CONAE is involved, in particular, in use of space data for telemedicine, tele-epidemiology, and use of space infrastructure for health emergencies during disaster management.

Concentration Gradients

DAVID DEAMER

Department of Biomolecular Engineering, University of California, Santa Cruz, CA, USA

Keywords

Membrane potential, semipermeable membrane, stored energy

Definition

Concentration is a measure of the amount of solute in a solvent, typically expressed in units of moles per liter. A 1.0 molar solution (abbreviated 1.0 M) contains one mole of a solute in one liter of total volume. A concentration gradient exists when a higher concentration of a solute is separated from a lower concentration, by a semipermeable membrane.

Overview

Concentration gradients of solutes are common in living cells and are essential sources of energy for all forms of life. Concentration gradients are generated and maintained across biological membranes by ion pump enzymes that transport ionic solutes such as sodium, potassium, hydrogen ions, and calcium across the membrane. Energy is required to produce a gradient, so the gradient is a form of stored energy. An important example is the sodium and potassium ion gradient across most cell membranes, which produces the resting potential and action potentials of excitable membranes like those of neurons. Hydrogen ion gradients are generated by the electron transport systems embedded in membranes, either as a pH gradient or a ► [membrane potential](#). For instance, a gradient equivalent to 210 mv or 3.5 pH units (~1000-fold gradient) is the source of energy driving ATP synthesis in mitochondria, chloroplasts, and bacterial membranes. Although

concentration gradients are essential to life today, it is uncertain what role they may have played in the origin of life. Early membranes were likely to be relatively permeable to solute ions, so that primitive cells would be unable to use gradients as an energy source.

See also

- ▶ [Membrane Potential](#)

Concestor

- ▶ [Common Ancestor](#)

Condensate Layer

- ▶ [Clouds](#)

Condensation Sequence

AVI M. MANDELL

NASA Goddard Space Flight Center, Greenbelt, MD, USA

Keywords

Cosmochemistry, solar nebula

Definition

In planetary science the condensation sequence refers to the order in which chemical compounds transition from gas to solid phase in a protoplanetary nebula, based on the condensation temperature of each compound. The condensation sequence is important because the temperature of a protoplanetary nebula varies radially and temporally, and the chemical composition and mass of any bodies formed at a particular place and time will be defined by the materials that can condense at the local temperature.

Overview

Condensation is defined as the process by which chemical materials change phase from the gaseous or liquid phase to the solid phase. Chemical condensation occurs within a narrow range of temperature specific to each individual

chemical compound (a few tens of degrees), defined by the abundance of the elements in the nebular gas and the molecular structure and composition of the solid compound. Effective condensation temperatures depend on the local environment (i.e., pressure), and can be lowered by including catalytic reactions (i.e., grain growth reactions). A “condensation sequence” orders a specific list of chemical compounds of interest by their condensation temperatures, in order to determine which materials will condense in a medium of a specific temperature.

The Solar System is thought to have formed from a rotating disk of gas and dust called the “▶ [solar nebula](#)” (this is true for other planetary systems as well; we call these disks “▶ [protoplanetary disks](#)”). The temperature of the solar nebula varied both radially (from the inner regions of the disk to the outer regions) and vertically (from the midplane to the surface) due to heating from the Sun and viscous heating at the midplane. The temperature in different parts of the solar nebula also changed over time as the disk material was depleted due to accretion and ▶ [photoevaporation](#). The material condensing out of the gaseous solar nebula into grains and larger bodies would therefore be a function of both location and of age, resulting in a changing chemical composition of bodies over space and time in the nebula. A typical condensation sequence of the nebular gas starts with refractory oxides and silicates (1700–1400 K), followed by the iron and nickel which will eventually segregate into planetary cores and the silicates of their future mantle and crust (1350–1150 K). Alkali elements and sulfide-loving (chalcophile) elements such as Cu, Zn, Pb follow, and finally volatile elements such as S, C, N, and H₂O join between 600 and 100K. The temperature at which condensation came to a halt for the material of a planetary body, therefore, defines its depletion in volatiles, amongst them water.

One of the most interesting consequences of the condensation sequence is therefore the proposed existence of a “▶ [snow line](#)” in the solar nebula. The snow line is defined as the radial location in the solar nebula beyond which the local temperature of the nebula drops below the condensation temperature of water. Bodies formed beyond this boundary would contain solid water, while bodies inside this boundary would be relatively water-poor. In fact, Earth is thought to have formed inside the snow line; hence the concept of “water delivery”.

See also

- ▶ [Feeding Zone](#)
- ▶ [Photoevaporation](#)
- ▶ [Protoplanetary Disk](#)

- ▶ [Snow Line](#)
- ▶ [Solar Nebula](#)
- ▶ [Water, Delivery to Earth](#)

Condensation Temperature

Definition

The condensation temperature is that at which a given gas-phase constituent condenses into a liquid. This temperature depends on the physical and chemical state of the system.

Conjugation

Definition

In microbiology, conjugation is the process by which two individuals of the same – or even different – species exchange their ▶ [genetic](#) material during a temporary union. Among ▶ [bacteria](#), conjugation is a widespread mechanism that allows the transmission of one conjugative ▶ [plasmid](#) from one cell, called “donor,” to another, the “recipient,” through the physical contact between them. Conjugative plasmids carry genes that promote bacterial conjugation, and are frequently involved in ▶ [lateral gene transfer](#) – also called horizontal gene transfer, HGT – between individuals of different species. For example, antibiotic resistance or the ability to metabolize a new organic molecule can be transmitted by conjugation among microorganisms. In the majority of bacteria, conjugation is not a standard mode of reproduction as it is the case in sexual organisms. In turn, in certain ▶ [protists](#) such as paramecia, although they usually reproduce asexually by fission, conjugation is a sexual process of reproduction between individuals of opposite mating types. Conjugation is also used as a genetic engineering technique in the lab.

See also

- ▶ [Bacteria](#)
- ▶ [Domain \(Taxonomy\)](#)
- ▶ [Genetics](#)
- ▶ [Lateral Gene Transfer](#)
- ▶ [Plasmid](#)
- ▶ [Protists](#)
- ▶ [Transformation](#)

Contamination, Probability

Definition

For purposes of ▶ [planetary protection](#), the probability of contamination is determined, using a formulation of the ▶ [Coleman–Sagan equation](#) that an Earth-originating organism might grow and propagate in another planetary environment.

See also

- ▶ [Coleman–Sagan Equation](#)

Continental Crust

Definition

Continental crust is that portion of the Earth’s crust composed mainly of low-density siliceous (granitoid) rock. It occupies about one-third of the total crust and underlies most of dry land. Its thickness varies from ≤ 10 km in rifts to up to 80 km beneath mountain belts. Dominant constituents are granitic rocks and their metamorphic equivalents (gneiss) and metasedimentary or metavolcanic sequences. Continental crust forms in subduction zones and contains a large proportion of the Earth’s budget of incompatible trace elements and heat-producing elements. The presence of continental crust is a signature of ▶ [plate tectonics](#) that distinguishes the ▶ [Earth](#) from other planets.

See also

- ▶ [Crust](#)
- ▶ [Earth](#)
- ▶ [Granite](#)
- ▶ [Plate Tectonics](#)

Continental Lithosphere

- ▶ [Continents](#)

Continental Plate

- ▶ [Continents](#)
- ▶ [Lithospheric Plate](#)

Continental Tectosphere

► [Continents](#)

Continents

BALZ SAMUEL KAMBER

Department of Earth Sciences, Laurentian University,
Sudbury, ON, Canada

Synonyms

[Continental lithosphere](#); [Continental plate](#); [Continental tectosphere](#)

Keywords

Buoyancy, gravity anomaly, mechanical strength, mountain belt, plate motion, radioactive heat, sedimentary basin, subcontinental lithospheric mantle, subduction

Definition

On a planet with ► [plate tectonics](#), continents are the topographic expression of emergent, buoyant, strong, and cool plates, contrasting with thinner and hotter oceanic plates covered by water. A thinner crust and a much thicker subcontinental ► [mantle](#) form the continental ► [lithosphere](#) that moves as a coherent unit. Together they have the capacity to withstand destructive convective forces for billions of years. The uppermost crust is enriched in many trace elements, including the sources of radioactive heat. Where continents collide with other plates, their edges thicken to form mountain belts, which eventually erode to fill sedimentary basins.

Overview

From a geological perspective, large expanses of land – continents – are an expression of the greater buoyancy of continental plates compared to oceanic plates. Continental plates consist of an upper layer, the ► [continental crust](#), which on Earth is typically 35 km thick, and a lower layer, called the subcontinental lithospheric mantle, which on Earth can reach as deep as 250 km. The density of both layers is lower than typical convecting upper mantle, resulting in a negative gravity anomaly over continents (Barrell 1914).

► [Radiogenic isotopes](#) demonstrate that the two layers are formed contemporaneously during subduction of oceanic plates (e.g., Nägler et al. 1997). At depth, where subducted ► [oceanic crust](#) experiences ► [metamorphism](#), hydrous fluids are released into the mantle, allowing a partial melt to form, which preferentially consumes the denser mantle minerals and also incorporates many chemical elements that are not favored by mantle minerals. This leaves behind a less dense residue that is depleted in many trace elements, amongst others, in the radioactive heat producers. Such subcontinental lithospheric mantle acts as a buoyant, strong, cool protective root for continental crust (Jordan 1978). The melt itself rises to the ► [Moho](#) (the boundary between the Earth's crust and mantle) and differentiates into the continental crust, which is also buoyant and chemically very different from the bulk planet (Taylor and McLennan 1985). The buildup of radioactive heat in the crust leads to chemical stratification, typically culminating in an event of widespread granite emplacement (cratonization) after which the new crust achieves full mechanical stability (Sandiford and McLaren 2002).

On Earth, continents have an average age of ca. 2.2 billion years and the oldest continental fragments are 3.8 billion years old. Such antiquity is testimony to the thermal and mechanical stability of continents (de Wit et al. 1992). The familiar concept of continents surrounded by ocean basins may only be valid on planets whose interiors cool via the plate tectonic process. Furthermore, as a result of relative plate motion, the continental plates (which cannot be destroyed by subduction processes) can thicken and deform along their edges, leading to the formation of mountain belts. Continents on young planets with higher crustal heat production have lesser mechanical strength and topography, whereas mid-aged planets, like Earth, have continents supporting rapid vertical movement. Amalgamation of several continental plates produces ► [super continents](#), whose breakup is typically triggered by thermal erosion of the subcontinental lithospheric mantle by heat upwellings from the deeper mantle (► [mantle plumes](#); McKenzie and Bickle 1988). Large sedimentary basins that accommodate the erosion products of mountain belts express the thinning of the continental lithosphere.

See also

- [Continental Crust](#)
- [Greenstone Belts](#)
- [Heat Flow \(Planetary\)](#)

- ▶ [Lithosphere](#)
- ▶ [Mantle](#)
- ▶ [Mantle Plume \(Planetary\)](#)
- ▶ [Metamorphism](#)
- ▶ [Moho](#)
- ▶ [Oceanic Crust](#)
- ▶ [Plate Tectonics](#)
- ▶ [Plate, Lithospheric](#)
- ▶ [Radioactive Heating](#)
- ▶ [Radiogenic Isotopes](#)

References and Further Reading

- Barrell J (1914) The strength of the Earth's crust. *J Geol* 22:425–433
- de Wit M, Roering C, Hart JR, Armstrong RA, de Ronde CEJ, Green RWE, Tredoux M, Peberdy EP, Hart RA (1992) Formation of an Archaean continent. *Nature* 357:553–562
- Jordan TH (1978) Composition and development of the continental tectosphere. *Nature* 274:544–548
- McKenzie D, Bickle MJ (1988) The volume and composition of melt generated by extension of the lithosphere. *J Petrol* 29: 625–679
- Nägler TF, Kramers JD, Kamber BS, Frei R, Prendergast MDA (1997) Growth of subcontinental lithospheric mantle beneath Zimbabwe started ≥ 3.8 Ga: A Re-Os study on chromites. *Geology* 25:983–986
- Rudnick RL (1995) Making continental crust. *Nature* 378:571–577
- Sandiford M, McLaren S (2002) Tectonic feedback and the ordering of heat producing elements within the continental lithosphere. *Earth Planet Sci Lett* 204:133–150
- Taylor SR, McLennan SM (1985) The continental crust: its composition and evolution. *Geoscience Texts*, Blackwell, Oxford

Continuum

Definition

A continuum is the smooth, continuously varying portion of a radiation ▶ [spectrum](#), with no spectral features such as atomic or molecular lines or bands. It may be produced by different processes: radiative recombination of electrons previously in free states, two-photon decays of metastable levels, thermal ▶ [bremsstrahlung](#), ▶ [black body](#) radiation, or synchrotron emission.

See also

- ▶ [Background](#)
- ▶ [Blackbody](#)
- ▶ [Bremsstrahlung Radiation](#)
- ▶ [Radiative Processes](#)
- ▶ [Electromagnetic Spectrum](#)

Convection, Stellar

STEVEN STAHLER

Department of Astronomy, University of California, Berkeley, CA, USA

Definition

Convection is the transport of heat by turbulent motion of gas. Within stars, this thermal energy is supplied either by nuclear fusion or bulk gravitational contraction. The luminosity of the Sun is carried outward by convection in the outer third of its radius. The shifting pattern of granulation visible on the solar surface represents rising and falling gas cells in the convection zone. The upwelling of gas in this zone, together with the Sun's rotation, amplifies and maintains the solar magnetic field. When the Sun was a ▶ [pre-main-sequence star](#), its relatively high surface cooling drove convection throughout its interior.

Overview

Stars generate energy by nuclear fusion or gravitational contraction. This energy is transported through the interior, eventually streaming outward as radiation from the surface. The transport occurs either through the diffusion of radiation or convection. In the Sun, whose luminosity stems entirely from fusion, convection operates in the outer third of the radius. This zone is a remnant from the Sun's pre-main-sequence epoch, when it was entirely convective.

Convection occurs through upwelling of gas cells. The hot cells are buoyant and rise toward the surface, expanding and releasing energy by radiation. The cooled cell, now denser, falls back down, where it is reheated by the star's energy source. The cycle then repeats itself in a circulating pattern of motion. Convection only occurs if the specific entropy (entropy per unit mass) of the gas declines toward the surface. In regions where the entropy rises, fluid cells can rise temporarily, but then quickly fall back down and thereafter oscillate. Net energy transport in such regions occurs through radiative diffusion.

The specific entropy inside a star falls if the object is either heated from below or cooled from above. The first mechanism operates in ▶ [main-sequence](#) stars, where hydrogen fusion generates energy in the central region. The second mechanism operates in pre-main-sequence stars. These stars have such large radii that surface cooling alone drives convection throughout the interior.

The upwelling of convective eddies in the Sun is visible directly in the ever-changing pattern of granulation near the surface. It is a combination of this upward motion and the Sun's internal rotation that creates the star's magnetic field. This field, in turn, channels the solar wind, and provides a braking mechanism for the star's rotation. This general idea is confirmed by observations of other main-sequence stars. Those with outer convection zones rotate much more slowly than stars lacking them.

The rise and fall of cells, while it has an overall order, is also a somewhat chaotic process. In this regard, convection is similar to other forms of fluid turbulence, all of which are difficult to treat in a quantitative manner. The most successful approach is *mixing-length theory*. Models of stellar interiors that use mixing-length theory accurately reproduce the chief properties of main-sequence stars, including the depth of the convection zone itself.

See also

- ▶ [Main Sequence](#)
- ▶ [Pre-Main-Sequence Star](#)
- ▶ [Protostars](#)
- ▶ [Stellar Winds](#)
- ▶ [T Tauri Star](#)

References and Further Reading

Foukal PV (2004) Solar astrophysics. Wiley-VCH, Weinheim
 Shore SN (2003) The tapestry of modern astrophysics. Wiley, New York

Convergent Margin

- ▶ [Subduction](#)

Cool Early Earth

NICHOLAS ARNDT
 Maison des Géosciences LGCA, Université Joseph Fourier,
 Grenoble, St-Martin d'Hères, France

Synonyms

[Early earth](#)

Definition

The term “Cool Early Earth” refers to the new vision of the ▶ [Hadean](#)-early Archean Earth characterized by much more temperate surface conditions than believed before. The term was coined by the American geochemist John Valley in 2002. A popular image of the early Earth is indeed of a planet covered by hot magma. This image is at the origin of the term Hadean (from the Greek God of the underworld, *Hades*) for the first eon. The fractionated oxygen isotopic compositions of 4.4 to 4.3 Ga old ▶ [Jack Hills](#) zircons indicate, however, that during long intervals in the Hadean, the surface temperatures were low. It is possible therefore that liquid water was present at the surface of the Hadean Earth and more clement surface conditions prevailed.

Overview

The chemical composition of the 4.4 to 4.3 Ga Jack Hills zircons implies that they crystallized from granitic magma. To form the granite in turn necessitates that water was transported into the mantle, perhaps by subduction of hydrated oceanic crust. The implication is that oceans were present at the surface and that ▶ [plate tectonics](#) operated in the interior. The presence of oceans allows speculation that life was present at that time. Sedimentary rocks and ▶ [pillow lavas](#) in 3.8 Ga old sequences from the ▶ [Isua Supracrustal Belt](#) (West Greenland) provide evidence of liquid water and temperate conditions early in the Archean.

It is commonly accepted that the ▶ [Sun](#) was less luminous in the first part of Earth history, 25–30% less than today during the Hadean and early Archean. This should have resulted in extremely cold conditions at the surface of the Earth and other telluric planets. The probable explanation of hotter temperate conditions is the presence in the atmosphere of a high proportion of greenhouse gases such as CO₂ and methane, and some sort of internal regulation that maintained their concentrations at the levels needed to preserve clement conditions at the surface (the so-called ▶ [Faint Young Sun Paradox](#)).

See also

- ▶ [Archea](#)
- ▶ [Earth's Atmosphere, Origin and Evolution of](#)
- ▶ [Earth, Formation and Early Evolution](#)
- ▶ [Faint Young Sun Paradox](#)
- ▶ [Hadean](#)
- ▶ [Isua Supracrustal Belt](#)
- ▶ [Jack Hills \(Yilgarn, Western Australia\)](#)
- ▶ [Oceans, Origin of](#)
- ▶ [Water, Delivery to Earth](#)

Coonterunah Subgroup, Australia

Definition

The Coonterunah Subgroup is one of the oldest well-preserved supracrustal sequences known on Earth. Located in the ► [Pilbara craton](#), Western Australia, the sequence has a 5-km stratigraphic thickness and is 75 km in length. It consists mainly of tholeiitic and minor ► [komatiitic basalt](#), some felsic lava with intercalated carbonate, and ► [chert](#) beds. It is 3.52 Ga old and its metamorphic grade is only mid-greenschist to lower amphibolite facies. It contains sedimentary carbonate and ► [kerogen](#) that may represent some of the oldest ► [traces of life](#) on Earth.

See also

- [Basalt](#)
- [Chert](#)
- [Kerogen](#)
- [Komatiite](#)
- [Mafic and Felsic](#)
- [Pilbara Craton](#)
- [Archean Traces of Life](#)

Coordinate, Systems

FRANÇOIS MIGNARD

CNRS, Observatoire de la Côte d'Azur, University of the Nice Sophia-Antipolis, Nice, France

Synonyms

[Reference frame](#)

Keywords

Astrometry, declination, fundamental astronomy, hipparcos, ICRF, ICRS, right-ascension, VLBI

Definition

An astronomical coordinate system is a set of three orthogonal directions, an origin, and a choice of mathematical coordinates within this system, with respect to which the position and motion of celestial bodies are referred.

Overview

Motion and position are not absolute concepts and must be described with respect to some reference. In astronomy

this is a reference frame, that is to say the realization of a set of axes with the means to assign coordinates to an object. Since these axes are not given a priori on the celestial sphere, one must use existing celestial bodies or directions to define the coordinate system. In this context, it is important to draw attention to the difference between a reference system and a reference frame. A reference system is the set of prescriptions stating how a celestial coordinate system is to be formed. It defines the origin and fundamental planes (or axes) of the coordinate system, together with the constants and models necessary to fully define the system. A reference frame consists of a set of identifiable points on the sky, together with their coordinates, which serves as the practical realization of a reference system.

A system of axis is determined by the choice of an origin and of three mutually orthogonal directions labeled by the unit vectors e_1 , e_2 , and e_3 . With the underlying assumptions of absolute Euclidean space, the orientation of the system does not change when translated between two origins, meaning that the choice of the origin and directions are independent of each other. The commonest origins are the location of the observer (topocentric frame), the center of the Earth (geocentric frame), the barycentre of the solar system (barycentric frame), and the center of the Galaxy (the galactic frame). The center of a planet or a satellite can be used as well for specific purposes. The set of three directions is constructed by selecting the polar direction e_3 , or equivalently by selecting a fundamental plane going through the origin, and a direction e_1 in this plane for the x -axis. A point M is then represented by the Cartesian coordinates in this frame or by spherical coordinates. The latter are more convenient to represent directions on the celestial sphere and are widely used in observational astronomy or to construct stellar catalogues and ephemerides of low accuracy. Cartesian coordinates are preferred to model motions in the solar system and to produce accurate ephemerides with position and velocity vectors. The choice of the fundamental directions is dictated by the necessity to make them accessible to observation, so that the system is materialized in space. This leads to the following usual systems, appearing in most astronomical work.

- The horizon coordinate system uses the observer's local vertical as a fundamental direction, or equivalently the local horizon as a fundamental plane. This is a physical definition that can be accessed with a plumb line or a spirit level. The pole overhead is the zenith, and the one diametrically opposite is the nadir. The two angles that specify the spherical coordinates are

the azimuth angle (A) and the altitude (h). The azimuth is measured in the horizontal plane from one of the two points of intersection of the celestial meridian with the horizon. The altitude is the angular height of a point with respect to the horizon, counted positively above the horizon, and negatively below. Instead of altitude h , its complement measured from the zenith, the zenith distance z , is also frequently used.

- In the equatorial coordinate system, the primary direction is defined by the Earth's spin axis, giving the ► [celestial equator](#) (the projection on the sky of the Earth's equator) as fundamental plane. The reference point on the celestial equator is the vernal equinox, the direction on the celestial sphere at which the Sun, in its yearly path around the celestial sphere, crosses the equatorial plane moving from south to north. The ► [declination](#) (δ) of a body is its angular distance north or south of the equator and the ► [right ascension](#) (α) is its angular distance measured eastward along the equator from the equinox. Because both the celestial equator and the ► [ecliptic](#) are moving (precession of the equinoxes), the coordinate systems that they define must be specified at a particular date. In contrast, the ICRF (International Celestial Reference Frame) has fixed directions determined by the positions of a set of extragalactic sources observed in radio interferometry, with an origin at the barycentre of the solar system. However, these axes correspond closely to what would conventionally be described as the equator and equinox of J2000.0 and therefore to the equatorial system at this epoch. For application with accuracy requirement less than 0.1 arcsec, the distinctions between ICRS and the conventional definition are not significant. The subset of the single stars of the Hipparcos Catalogue is a secondary realization at optical wavelengths and is designated as the HCRF (Hipparcos Celestial Reference Frame).
- Of less importance are the ecliptic system, using the mean orbital plane of the Sun as fundamental plane with origin at the vernal equinox, and the Galactic coordinate system defined by arbitrarily assigning equatorial coordinates for the pole and the origin in the Galactic equator, nominally close to the galactic center. In the ICRF, the galactic pole is near $\alpha_p = 192.75^\circ$, $\delta_p = 27.13^\circ$ and the Galactic center is located at about $\alpha_p = 266.40^\circ$, $\delta_p = -28.93^\circ$.

See also

- [Astrometry](#)
- [Celestial Equator](#)

- [Declination](#)
- [Ecliptic](#)
- [Right Ascension](#)

References and Further Reading

- Green RM (1985) Spherical astronomy. Cambridge University Press, Cambridge
- Kovalevsky J, Seidelman PK (2004) Fundamentals of astrometry. Cambridge University Press, Cambridge
- Léna P, Rouan D, Lebrun F, Mignard F, Pelat D (2008) L'observation en astrophysique, Chap. 4. EDP Sciences, (coll. Savoirs actuels – Astrophysique)

Core Accretion (Model for Giant Planet Formation)

Definition

Core accretion is part of the current paradigm for giant planet formation. The core accretion model proposes that ► [giant planets](#) form from the bottom-up: small bodies continually collide to form larger ones, eventually reaching the stage of protoplanetary cores, which are essentially large planetary embryos that form in the giant planet region. Cores that reach masses of a few Earth masses begin to accrete gas from the ► [protoplanetary disk](#), slowly at first, and then at a runaway rate when the gaseous envelope's mass becomes comparable to the core mass. Cores, therefore, represent the “seeds” of gas giant and ice giant planets in this model. The core accretion model contrasts with the disk instability model—the model that proposes that giant planets form from the top-down via gravitational collapse.

See also

- [Atmosphere, Primitive Envelope](#)
- [Giant Planets](#)
- [Planet Formation](#)
- [Protoplanetary Disk](#)
- [Runaway Gas Accretion](#)

References and Further Reading

- Lissauer JJ, Stevenson DJ (2007) Formation of giant planets. In: Reipurth B, Jewitt D, Keil K (eds) Protostars and Planets V. University of Arizona Press, Tucson, pp 591–606, 951 pp
- Pollack JB, Hubickyj O, Bodenheimer P, Lissauer JJ, Podolak M, Greenzweig Y (1996) Formation of the giant planets by concurrent accretion of solids and gas. *Icarus* 124:62–85

Core, Planetary

TILMAN SPOHN

German Aerospace Center (DLR), Institute of Planetary Research, Berlin, Germany

Synonyms

[Planetary core](#)

Keywords

Planets, satellites

Definition

The core is the central spherical region of a [planet](#). In a [terrestrial planet](#) it consists of an iron-rich alloy. In a [satellite](#) the core may be composed of a mixture of iron, [silicates](#), and ice depending on the degree to which the satellite interior is differentiated (see [differentiation, Planetary](#)). In a [giant planet](#), the core is made of a similar mixture of iron, [rock](#), and ice albeit at much larger pressures and temperatures.

Overview

The interiors of planets and satellites are differentiated to varying degrees with the heaviest materials at the center. The degree of differentiation in solid planets and satellites depends on their thermal histories since differentiation requires at least partial melting at some early epoch. Cosmochemical models of the planets and satellites – taking their composition to be Chondritic – suggest the existence of cores and provides estimates of their sizes and masses. An iron-rich core has been proven beyond doubt for the [Earth](#) by the inversion of seismic and gravity data. The Earth's core is composed of a Fe–Ni alloy but also contains a small fraction (<10%) of a lighter element such as Si, O, or S and is layered with a liquid outer core and a solid inner core. (See Rabinowicz et al. (2007) for reviews on the interior structure of the Earth and Olsen and Schubert (2007) for reviews on the Earth's core dynamics.) It is widely agreed that the inner core is the result of core freezing and that it grows as the planet cools. It is also widely agreed that the energy liberated upon core freezing powers the generation of its [magnetic field](#) through a [dynamo](#). [Mars](#)' core is inferred from gravity data and the chemistry of the [SNC meteorites](#) (Sohl and Schubert 2007 for a review). Its density, chemistry, and the absence of a present-day magnetic field suggest that the core is completely liquid (Schubert and Spohn 1990). The cores of [Venus](#) and [Mercury](#) are constrained by

the average densities of these planets and cosmochemistry. Venus is thought to have a core approximately as large as the Earth's. The large average density of Mercury suggests that the core is unusually large with a radius of about 0.8 planetary radii, or about 1,800 km. Recent re-analysis of Apollo seismic data by Weber et al. (2010) suggests that the Moon has a solid inner core with a radius of 240 ± 10 km surrounded by a fluid, iron-rich outer core of 330 ± 20 km. The interpretation of the data suggests a partially molten zone in the rock mantle above the core of 480 ± 15 km. A solid mantle and a crust complete the lunar interior structure. The gravity fields measured at the Galilean satellites of [Jupiter](#) suggest that [Io](#), [Europa](#), and [Ganymede](#) have iron-rich cores (e.g., Schubert et al. 2004). This is particularly true for Ganymede for which the magnetic field suggests a liquid iron-rich core with possibly a solid inner core. [Callisto](#) and [Titan](#) (Iess et al. 2010), as the data suggest, are incompletely differentiated and likely have large cores composed of ice, silicates, and possibly iron or iron oxides. The gravity fields of Jupiter and [Saturn](#) suggest cores consisting of ice, silicates, and iron but their masses and, in particular, their radii are uncertain (Guillot and Gautier 2007 for a review). Estimates range from a few to about 10 Earth masses. Uranus and [Neptune](#) may have similar cores but interpretations of the gravity field suggest that the layering in the interiors of the latter two planets is less pronounced than in Jupiter and Saturn. Rather, density and composition change with depth more gradually (Podolak et al. 1995).

See also

- [Callisto](#)
- [Differentiation \(Planetary\)](#)
- [Dynamo \(Planetary\)](#)
- [Earth](#)
- [Europa](#)
- [Ganymede](#)
- [Giant Planets](#)
- [Io](#)
- [Jupiter](#)
- [Magnetic Field](#)
- [Mars](#)
- [Mercury](#)
- [Neptune](#)
- [Planet](#)
- [Rock](#)
- [Satellite or Moon](#)
- [Saturn](#)
- [Silicate Minerals](#)
- [SNC Meteorites](#)

- ▶ [Terrestrial Planet](#)
- ▶ [Titan](#)
- ▶ [Uranus](#)
- ▶ [Venus](#)

References and Further Reading

- Guillot T, Gautier D (2007) Giant Planets. In: Spohn T, Schubert G (eds) *Treatise on geophysics*, vol 10. Elsevier, Amsterdam, pp 439–464
- Iess L, Rappaport NJ, Jacobson RA, Racioppa P, Stevenson DJ, Tortora P, Armstrong JW, Asmar S (2010) Gravity field, shape, and moment of inertia of Titan. *Science* 12:1367–1369
- Olsen P, Schubert G (eds) (2007) Core dynamics. *Treatise on geophysics*, vol 8, Elsevier, Amsterdam, pp 1–358
- Podolak M, Weizman A, Marley M (1995) Comparative models of uranus and neptune. *Planet Space Sci* 43:1517–1522
- Rabinowicz B, Dziewonski A, Schubert G (eds) (2007) Seismology and the structure of the earth. *Treatise on Geophysics*, vol 1, Elsevier, Amsterdam, 858 pp
- Schubert G, Spohn T (1990) Thermal history of Mars and the sulphur content of its core. *J Geophys Res* 95:14095–14104
- Schubert G, Armstrong JD, Spohn T, McKinnon WB (2004) Interior composition, structure, and dynamics of the Galilean Satellites. In: Bagenal F, Dowling TE, McKinnon WB (eds) *Jupiter. The planet, satellites, and magnetosphere*. Cambridge University Press, Cambridge, pp 281–306
- Sohl F, Schubert G (2007) Interior structure, composition and mineralogy of the terrestrial planets. In: Spohn T, Schubert G (eds) *Treatise on geophysics*, vol 10. Elsevier, Amsterdam, pp 27–68
- Weber RC evol (2010) Seismic detection of the lunar core. *Science* 331:309. doi:10.1126/science.1109375

Corona Discharge

Definition

A corona discharge is a positive or negative electrical discharge created by the ionization of a gas surrounding a conductor, for example, a mineral surface, which occurs when the strength of the electric field exceeds a certain threshold value. A charged [plasma](#) is created around the surface generating ions, which dissipate their charge to proximal areas of lower potential, or recombine to form neutral molecules. If the ionized region continues to grow instead of quenching, a momentary spark, or a continuous arc may result. A neutral atom or molecule of the medium, in a region of strong electric field may be ionized, for example, by the absorption of a photon, to create a positive ion and a free electron. The electric field around the surface may then separate these charged particles and prevent their recombination. As a result of the acceleration of the electrons, further electron/positive-ion pairs may be created when they collide with other neutral atoms. These then undergo the same processes creating a cascade of electrons.

Such energetic processes may have contributed to prebiotic synthesis, providing electrical energy similar to the electric discharge used in Miller–Urey type experiments. Corona discharges are estimated by some to discharge some three times the energy of lightning strikes on the present Earth, and this ratio may have been similar on the primitive Earth.

See also

- ▶ [Miller, Stanley](#)
- ▶ [Plasma](#)

Corona, Coronae

Definition

Coronae are volcano-tectonic landforms only seen on the planet [Venus](#). They are oval to circular features typically 100–300 km in diameter. A few of the coronae are even larger. They have a circular or nearly circular, tectonically deformed annulus, which usually stands a few hundred meters above the surrounding plains. The area inside the annulus is typically lower than the surrounding plains and has been flooded with plains-forming volcanic lava. Aprons of young lobate (tongue-shaped) volcanic flows are seen radiating from many coronae. At the center of some coronae one finds the corona core, an elevated and tectonically deformed area.

See also

- ▶ [Venus](#)

Coronagraphy

DANIEL ROUAN

LESIA, Observatoire de Paris, CNRS, UPMC, Université Paris-Diderot, Meudon, France

Definition

Coronagraphy designates the group of optical techniques that aims at suppressing or reducing the halo of light that surrounds the image of a star, in order to detect faint structures like a circumstellar disk or companions, especially exoplanets. Invented in 1930 by the French astronomer Bernard Lyot ([Fig. 1](#)) to study the sun's corona, the extremely faint emission from the region around the sun,



Coronagraphy. Figure 1 Bernard Lyot, a French astronomer who invented the coronagraph, an optical instrument whose original purpose was to study the faint extended emission around the Sun, the so-called corona

at times other than during a solar eclipse, the coronagraph is at its simplest an occulting disk in the focal plane of a telescope combined with a mask in front of the entrance aperture that blocks the image of the solar disk and reduces by a large factor the stray light. Since then, the term has been kept and designates now any optical system able to block as much as possible the glare of a star to allow detection of companions or disk structures in its immediate vicinity.

Overview

The ability to directly image an extrasolar planet – that is, to separate the light emitted or reflected by the surface or atmosphere of a planet from that of the star it orbits – offers the greatest prospect for characterizing these objects. Direct [▶ imaging](#) gives the possibility of determining the colors and spectra of planets, in a way independent of their orbital inclination. This information allows astronomers to distinguish between gas giants, ice giants, and earth-like planets under a variety of circumstances such as distance from the star, age, etc. Direct imaging offers the possibility to not only study the

surfaces of these planets but also their atmosphere, cloud systems, etc. Finally, direct imaging may also become the successful means for establishing the habitability of an exoplanet.

Directly imaging extrasolar planets requires (a) angular resolution sufficient to spatially separate the planet from its central star and, (b) the means to suppress the diffracted light from the central star such that the planet's brightness becomes comparable to or greater than the residual diffracted star light.

Concerning the first point, at optical wavelengths a conventional telescope of several meters diameter is in principle sufficient to spatially resolve a planet on an orbit comparable to those observed in our solar system, around nearby stars.

As regards the second requirement, this is precisely the role of a coronagraph – to block the starlight using optical elements within the telescope.

The main challenge of using an optical coronagraph for exoplanet imaging is the star–planet brightness contrast ratio. For an Earth-sized planet orbiting a star similar to our Sun, it is about 10^{10} to 1 in the visible. Any successful starlight suppression technique must reduce this contrast ratio by a huge factor and must do so at a very small angle, typically equal to $\theta = 2-5 \lambda/D$, where λ is the wavelength of observation and D is the diameter of the telescope ([▶ Diffraction](#)). An important parameter is thus the smallest star–planet angular separation at which this suppression level is achieved to avoid the need for primary mirror diameter larger than, say, 10 m.

There are other challenges albeit a little less stringent.

- The optical bandwidth of the light suppression technique – that is, the range of wavelengths over which the required light suppression can be maintained – should be as large as possible to enable either broadband photometry ($\Delta\lambda/\lambda = 10\%$) or the spectroscopic study of possible exoplanet atmospheric features at various different wavelengths.
- Imperfections in the telescope mirrors and coatings cause *speckles* in the image, that is, small spots of light extra intensity, after the coronagraphic mask; their intensity and variability can easily be high enough to obscure the extremely faint exoplanet image. It is possible to reduce these speckles using deformable mirrors ([▶ Adaptive Optics](#)), controlled thanks to smart algorithms, or to code them in order to recognize them from the planet image.
- Finally, the weak signal from an extrasolar planet requires substantial integration times (many hours) during which it is essential that the residual stellar

leakage be kept extremely stable, which is especially challenging on the ground, considering atmospheric as well as thermal fluctuations. This stresses the need to conduct research of Earth-sized exoplanets from space, but, even then, drifts and vibrations in the telescope cause varying stellar “speckles” that can limit the ultimate sensitivity for planet detection.

Under the pressure of the *planet hunters*, coronagraphy is an area that has shown enormous progress in the past decade as presented below, with a flourishing of very new concepts and technical breakthroughs. Ground-based instruments are already capable of direct detection of exoplanets in the most favorable cases, and a first generation of coronagraphic instruments installed on the largest telescopes (8–10 m diameter) will soon extend by a large factor the population of directly detected exoplanets. It is rather likely that within another decade or so, a coronagraphic space mission will be able to obtain the first images of planets that are analogs to our Earth.

Basic Methodology

A star observed with a perfect telescope in space, thus unaffected by the aberrations of the Earth’s atmosphere, will produce an image still surrounded by a halo of light diffracted from the edges of the telescope aperture. Known as the Airy pattern, this halo, which is structured with concentric rings of decreasing intensity (see Fig. 2), is many orders of magnitude brighter than any extrasolar



Coronagraphy. Figure 2 The airy pattern is the appearance that the image of a star made by a perfect telescope in space would present. Because of the phenomenon of diffraction, it is not an extremely sharp spot but rather a central core surrounded by characteristic rings. The larger the diameter of the telescope and the smaller the wavelength, the sharper the diameter of the core

planet image that would be superimposed on it. Suppressing this halo is the role of a coronagraph.

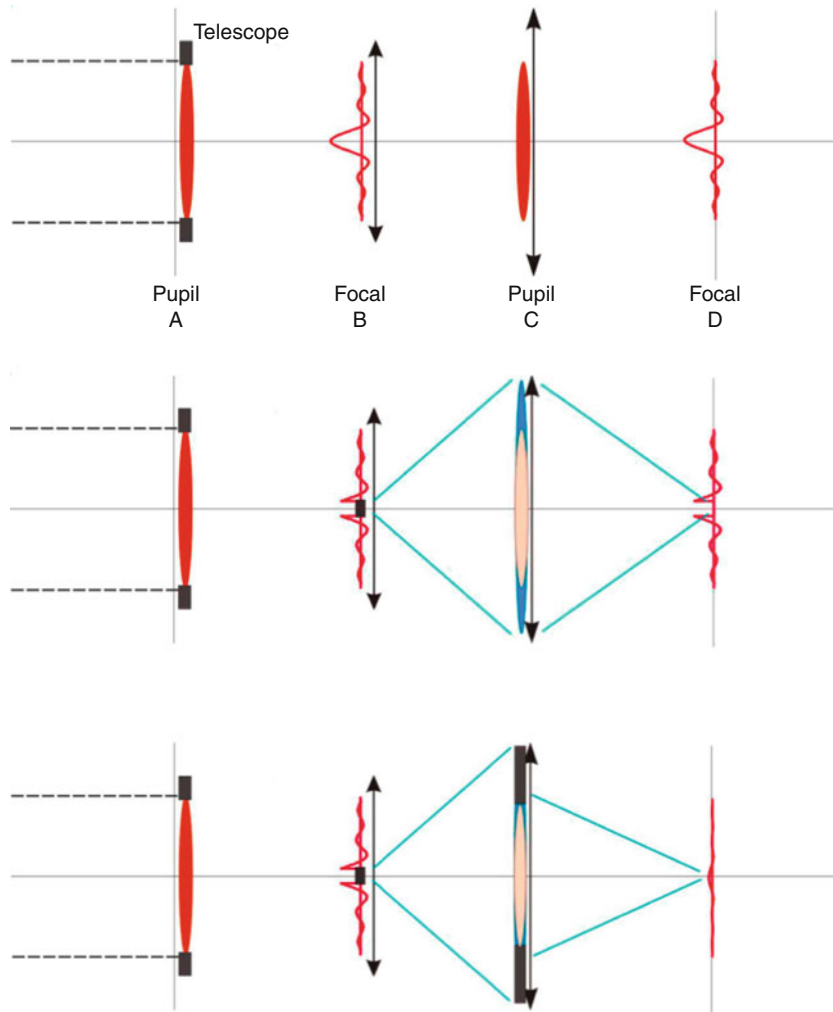
The Basic Lyot’s Coronagraph

The main finding of Bernard Lyot (Lyot 1939) is that blocking the light with an opaque mask in the focal plane that follows the contour of the bright object (the Sun’s surface in his case) is not sufficient at all, because light diffracted by the edge of the mask will spread far beyond the limits of the beam defined by geometric optics and finally will be able to refocus. This is illustrated in Fig. 3 (top and mid panels): the first mask in the focal plane blocks the core of the starlight, but leaves residual diffracted light in the reimaged pupil (blue beam). Lyot realized that if a mask with a central circular hole slightly smaller than the pupil image was installed, then it would block the essential part of this diffracted light as shown on the bottom panel of Fig. 3.

The New Coronagraphic Concepts

Over the past decade, coronagraphic concepts have proliferated far beyond Lyot’s basic vision into a vast family of devices that can be broken down into various broad categories: amplitude or phase mask coronagraphs, interferometric coronagraphs, pupil apodization. A fifth family is the external occulter. Each one offers pros and cons that can be measured by a few key parameters. Four of those parameters are especially important:

- The Inner Working Angle (IWA) is the angle of separation from the star below which the flux from the planet is rapidly attenuated and/or beyond which the flux from a resolved star rapidly increases. Currently, the most mature concepts feature an IWA of $\sim 4\lambda/D$, and it is suggested that an IWA of $\sim 2\lambda/D$ is achievable.
- The planet throughput, that is, the fraction of the planet’s light that reaches the detector. Current throughputs of 8–30% are measured, but claims that a throughput of 80% or higher are reachable are made. In addition, several coronagraphs produce stellar halo suppression within only a fraction of the entire field of view, for instance a sector or a ring, sometimes referred to as the “discovery space.”
- The sensitivity of the coronagraph to wavefront errors such as image position and focus. These defects arise due to drift and misalignment, even very small ones and their effects can hide or mimic a planetary signature.
- The chromaticity of the coronagraph, that is, its ability to suppress starlight across a broad wavelength range, thus allowing a lower total integration time. Typical useful bandwidth is $\Delta\lambda/\lambda \sim 20\%$ or less.



Coronagraphy. Figure 3 The principle of the Lyot's coronagraph. *Top*: optical scheme of an imaging system with relay optics. The image of a point-like object at infinity (star) is formed by a telescope (A) at its focal plane (B); a lens at this location forms the image of the telescope aperture in another plane (C) where a third lens re-images the star in plane D. The intensity of the light distribution is represented by the curve which is a cut of the image. *Middle*: An opaque mask is put at the focal plane and blocks a large part of the light; however, because of diffraction by the edges of the mask, a fraction of the light is spread beyond the geometrical beam and produces a significant intensity in the focal plane. *Bottom*: a ring mask placed in the pupil plane is efficient to block most of this spurious light

A thorough study on how each coronagraph design behaves with respect to those key parameters was done by Guyon et al. (2006).

Improvement on the Lyot Concept with Amplitude Masks

Those concepts evolved from Lyot's original solar coronagraph, using a mask at an image of the star, and another mask at a later image of the entrance aperture. It can be shown that, in this basic form, Lyot's

concept cannot reach the rejection required for planet detection by several orders of magnitude. An important variant of this concept is the band-limited coronagraph (Kuchner and Traub 2002), where the focal plane mask features a carefully tailored transmission profile confining the residual diffracted light to a well-defined region of the pupil plane. This type of coronagraph has produced excellent laboratory results with a measured contrast of 6×10^{-10} , albeit only in monochromatic light.

Another Lyot variant is the Apodized-Pupil Lyot Coronagraph (APLC), which modifies the entrance pupil with a dedicated transmission mask (Soummer 2004). Laboratory demonstrations to date have achieved contrast levels in the 10^{-6} range. One advantage is that it may be easily adapted to conventional telescopes with central obstruction, such as those used in the next generation of ground-based coronagraph projects.

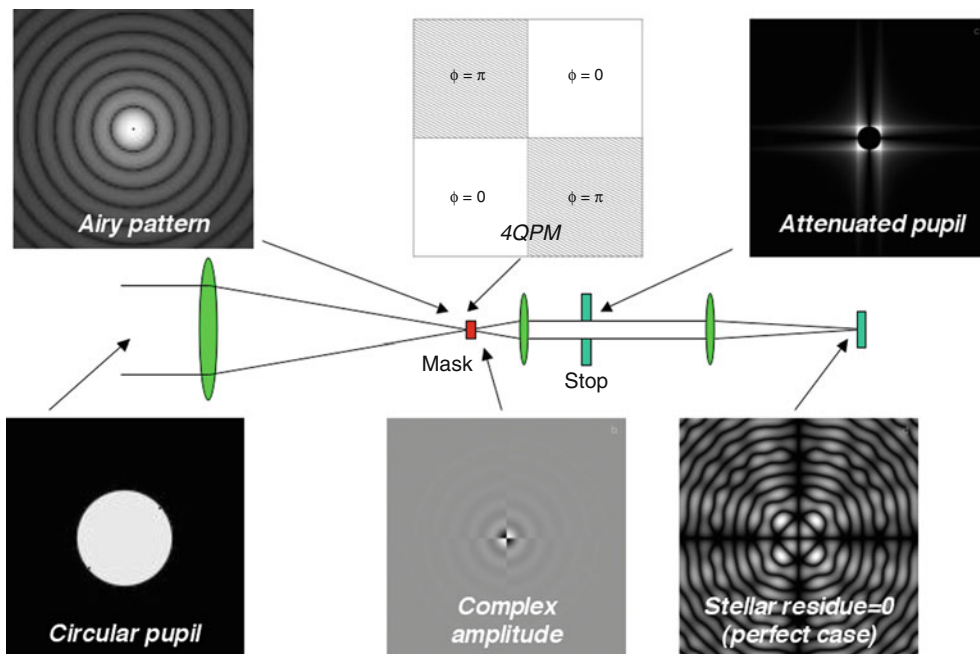
Phase-Based Lyot Coronagraphs

A similar approach to the Lyot concept is to induce a phase shift rather than an amplitude variation in the focal plane; destructive interference is then produced for on-axis starlight at the pupil level. In the first proposed idea (Roddier and Roddier 1997), the opaque spot of Lyot was simply replaced by a transparent spot of a proper size. The best-known example of this concept remains the 4-Quadrant Phase-Mask (4QPM) coronagraph (Rouan et al. 2000), which focuses the starlight onto a mask that shifts light passing through half the focal plane by half a wavelength (see Fig. 4). Such coronagraphs have near-ideal theoretical performance with high throughput and an IWA of $1 \lambda/D$. However, they are also sensitive to star position in the focal plane with respect to the center (angle θ), with performance degrading rapidly with tip/tilt errors. One variant

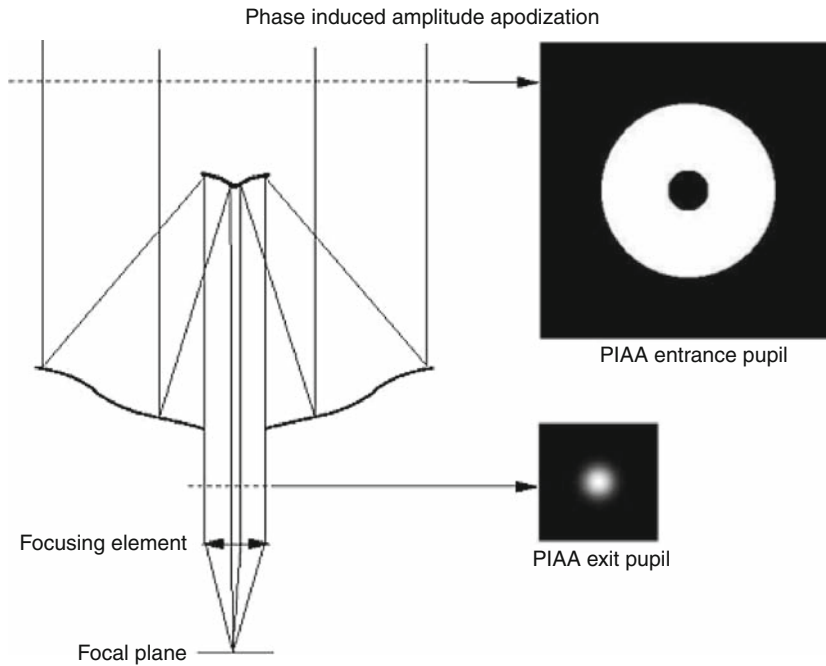
(Rouan et al. 2007) that allows improving on this sensitivity is the 8-quadrant phase mask, where the canceling function is proportional to θ^4 rather than θ^2 . There exist several solutions to manufacture them for broadband light: one uses polarization properties of uniaxial crystals, another is based on the stacking of several 4QPM with rejection performance increasing exponentially with the number of devices. A recently proposed variant of the 4QPM is the Optical Vortex Coronagraph (Foo et al. 2005), which uses a spiral-staircase phase mask. They are more robust against degradation due to the star's position.

Pupil Apodization

Using the Fresnel principle, it can be shown that the diffraction pattern at the focus of a telescope – that is, the actual distribution of intensity in the image of a point source at infinity, such as a star – is directly related to the shape of the entrance aperture. More precisely, this intensity is given by a mathematical transformation of the aperture, called the Fourier transform. The sharp edges of a conventional telescope result in the Fourier ringing that produces the well-known Airy pattern. Conceptually, the simplest coronagraph would entail a modification of the telescope aperture so it lacks these sharp edges. Called apodization, this modification can be achieved by tapering



Coronagraphy. Figure 4 Schematics describing the principle of the four-quadrant phase-mask coronagraph and the distribution of the amplitude of the light at the various planes of the optical system



Coronagraphy. Figure 5 The principle of the phase-induced-amplitude-apodization coronagraph that produces apodization by modifying the light intensity within the beam

the telescope transmission through a gray mask that falls gradually to zero transmission at the edges. These masks trade throughput for inner working angle, with a typical mask designed for an IWA of $4 \lambda/D$ having a transmission of 8%. However, manufacturing such a mask with graded attenuation is extremely difficult. Significant effort has been invested in binary approximations to these apodization functions, using sharp-edged metal masks that suppress diffraction over only part of the field of view (Kasdin et al. 2003). Referred to as “shaped pupils,” these masks, which can include micron-sized features, must be carefully fabricated but are feasibly produced with current manufacturing techniques. These masks operate in a complex trade space of inner working angle, throughput, and discovery space. These designs are inherently achromatic, and may be attractive for characterization of planets with known positions, where they can be optimized for throughput over a narrow region of the focal plane. Shaped-pupil masks have been demonstrated in the laboratory at the 2×10^{-9} contrast level, even in broadband light.

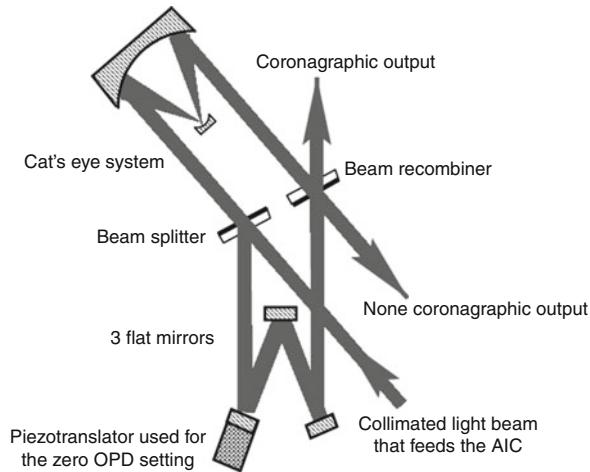
An alternative approach to performing apodization is to modify the phase of the light to modulate the intensity in the pupil plane. The Phase-Induced-Amplitude-Apodization Coronagraph (Guyon 2003) of O. Guyon is

based on this approach, using highly aspheric mirrors to redistribute the uniform beam of light into a tapered profile (see Fig. 5). The off-axis planet image is highly distorted, but this effect can be compensated. Contrary to classical apodization, no light collected by the entrance pupil is lost and the inner working angle can be as small as $2\text{--}3 \lambda/D$ for a throughput of 80% or more. However, this requires optical surfaces very difficult to manufacture, located in various conjugate planes.

Interferometric Coronagraph

The nulling coronagraph is a coronagraph based on a nulling interferometer, as opposed to more familiar designs of an apodized aperture telescope and Lyot coronagraph. This family uses concepts of interferometry and aims at producing destructive interference between two beams. The Achromatic Interferometric Coronagraph (AIC) was the first of this type to be proposed, by Gay and Rabbia as early as 1997, and has been refined since then (Rabbia et al. 2007). It is basically a Michelson–Fourier interferometer modified by inserting on one arm an achromatic π phase shift and a pupil rotation by 180° (see Fig. 6). The smart idea is to produce the π phase shift by crossing of a focus, thus making it perfectly achromatic. The collimated beam from the

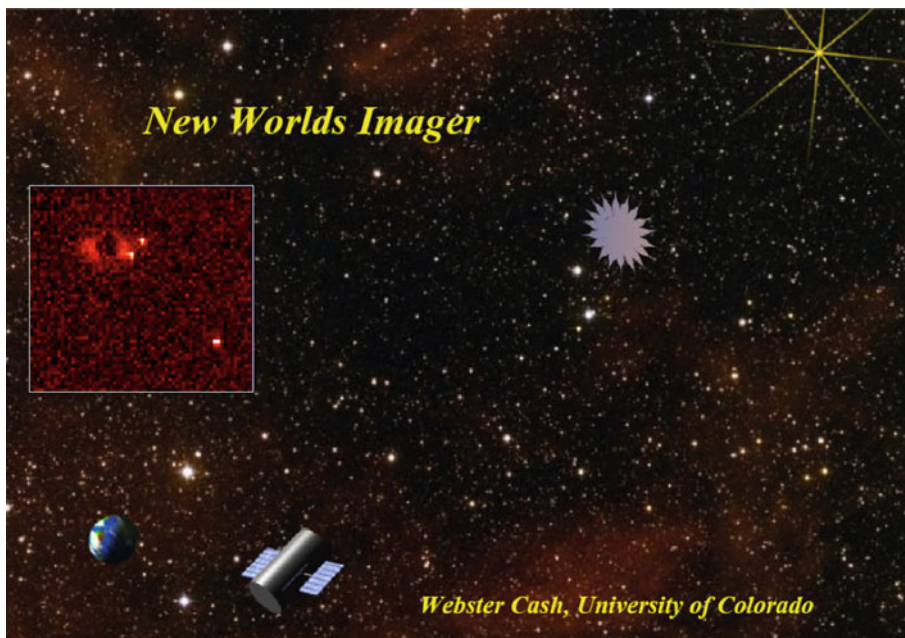
telescope is split into two sub-beams forming the two interferometric arms, one where the focus-crossing occurs. The beams are recombined afterward. Other designs have been proposed, such as the nulling coronagraph of M. Shao (Shao 2007).



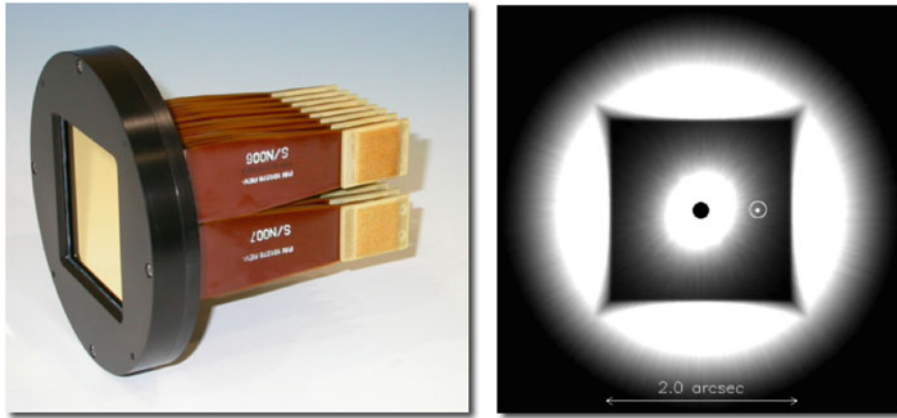
Coronagraphy. Figure 6 The principle of the achromatic interferometric coronagraph (AIC) based on destructive interference between two beams, one having suffered the crossing of a focus

External Occulter Coronagraphs

This type of coronagraph belongs to a peculiar family, since it relies on optical systems separated by several ten thousand kilometers! In 1960, Lyman Spitzer proposed the combination of a telescope and a starshade in space for discovery of planets. The concept implied enormous distances and starshade dimensions. With recent studies (Cash 2006), the inter-spacecraft separation has been reduced and the level of suppression improved by using petal shapes that would permit operation using a shade with a nominal diameter of 40 m at a telescope–starshade separation of 40,000 km (see Fig. 7). The telescope can be an ordinary space telescope, and its diameter is determined mainly by the requirement to detect faint planets. It has inherently achromatic properties, a strong advantage. However, operation remains the main drawback, since pointing from one star to another requires that the starshade travel several thousand kilometers. To accomplish this within a few weeks demands large starshade velocities and accelerations and thus a substantial power. However, the engineering effort recently done led to some mission scenarios that yield satisfactory efficiency with one occulter, and much better with two occulters. The deployment of the large starshade and the propulsion required for many stellar observations remain major technology issues to be addressed.



Coronagraphy. Figure 7 An artist view of the “New Worlds Imager” project based on a large deployable external occulter at a distance of 40,000 km from a conventional space telescope. The insert shows a simulated image of the solar system as it would be detected



Coronagraphy. Figure 8 A deformable mirror with many actuators (left) can provide a fair correction of the residual defects in the wavefront, producing an image with a characteristic “dark hole” central region (right)

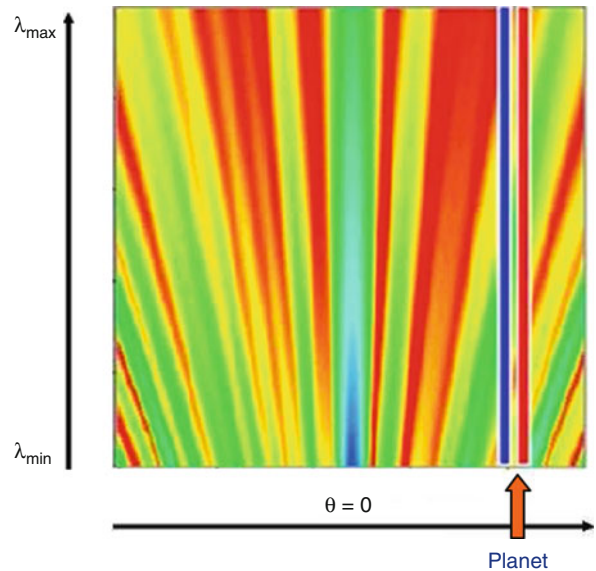
Future Directions

Wavefront Control

A problem common to all internal coronagraphs is wavefront accuracy and stability. Wavefront errors produced by imperfections in the telescope mirrors and coatings cause speckles in the image after the coronagraph masks have suppressed most of the starlight. The intensity and variability of these speckles can easily make the faint exoplanet image indiscernible. Achieving Airy rings suppression sufficiently to allow detection of Earth-sized planets would require wavefront phase errors of less than an angstrom (10^{-10} m) – well beyond current polishing capabilities for telescope-sized mirrors. However, use of a smaller deformable mirror in the optical train allows irregularities in the wavefront to be corrected by feedback, up to a spatial frequency set by the deformable mirror’s actuator spacing (Bordé and Traub 2007). With state-of-the-art deformable mirrors, this allows a large fraction of low- and mid-spatial-frequency errors to be removed from the wavefront, producing an image with a characteristic “dark hole” central region (see Fig. 8). It can be shown that with two deformable mirrors, both phase and amplitude defects can be corrected, for an even better improvement.

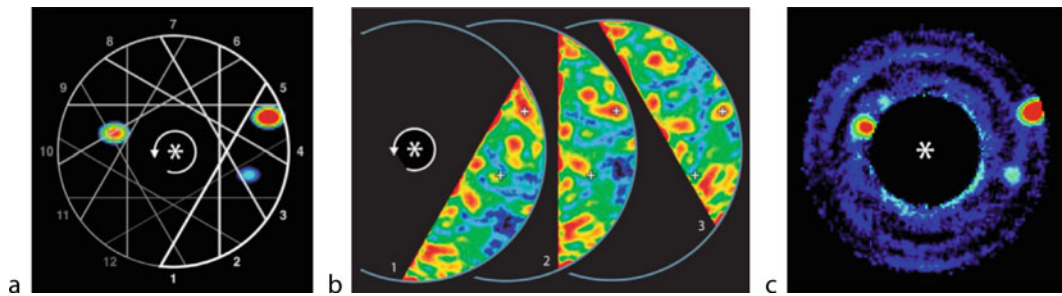
Calibration of Residual Speckles

The field image is small, a few arcsec in diameter, but an average flux of 10^{-10} times the star flux implies that there could be several hundred speckles as bright as an Earth-like planet. Only one of those speckles is a planet. One technique to identify it makes use of the coherence of starlight, that is, light from the star is coherent (i.e., will interfere coherently) with speckles whose origin is



Coronagraphy. Figure 9 Integral field spectroscopy produces spectra of all points in an image: most of the light that remains after coronagraphy is due to speckles whose size changes with wavelength (λ is along the vertical axis), while a planet would be of about a constant size with wavelength

scattered starlight, but will not interfere with light in the focal plane that comes from the planet (or dust) orbiting the star. Because of the interferences, the intensity distribution of the stellar flux features fringes that striate the speckles. The fringes can be detected by a proper processing, such as a Fourier transform of the image.



Coronagraphy. Figure 10 Rotational differential imaging. The telescope is rotated around the line of sight and images are taken at each angle. The optical defects that rotate with the telescope can be subtracted

This is, for instance, the principle of the self-coherent camera proposed by Baudoz et al. (Galicher and Baudoz 2007).

Differential Coronagraphy

Even with the best correction of the wavefront, there will still remain some defects and it becomes clear that a good way of correcting them is to subtract a similar image that presents the same defects, for instance of another star or the same star, but where presumably no planet image would be present. Several concepts have been proposed in that spirit and several of them have been tested on the sky: spectral differential imaging, rotational differential imaging, polarization differential imaging.

In spectral differential imaging (Racine et al. 1999), two images of the star are taken at two close wavelengths, carefully chosen so that the planet would have a different contrast, for instance within and outside a spectral feature characteristic of some expected compound in its atmosphere (e.g., methane). In another version (Sparks and Ford 2002), one produces the spectra of all the pixels in the image, with a so-called integral field spectrograph, and looks for differences in behavior between speckles, whose size changes with wavelength, and a planetary image whose size is constant, as illustrated on Fig. 9.

Rotational differential imaging (Marois et al. 2006) requires that the telescope be rotated around its axis several times, an image being taken at each position: the optical defects will rotate as well, in sky coordinates, while the planet image would remain stable. Figure 10 illustrates this technique.

Finally, in polarization differential imaging, one makes the reasonable guess that the light from the planet is significantly polarized, while the starlight is not: images taken in different polarization states could reveal the planet after subtraction.

Combining All Techniques

The challenge to beat a contrast of 10^{10} is so difficult that it becomes more and more evident that the good strategy cannot be to rely on one technique alone, but to combine many of them.

The coming years, or decades, will probably show that the winning instrument, the one that will pick up the first image of a cousin of our Earth, will have included together an efficient coronagraph combining pupil and image plane masks, a super-polished telescope with no central obstruction, one or two deformable mirrors, several differential imaging techniques, and of course will have been operated in space.

See also

- ▶ Adaptive Optics
- ▶ Diffraction
- ▶ Direct-Imaging, Planets
- ▶ Exoplanet, Detection and Characterization
- ▶ Exoplanets, Discovery
- ▶ Imaging

References and Further Reading

- Bordé P, Traub W (2007) Speckle noise reduction techniques for high-dynamic range imaging. *CR Phys* 8:349
- Cash W (2006) Detection of Earth-like planets around nearby stars using a petal-shaped occulter. *Nature* 442:51
- Foo G, Palacios DM, Swartzlander GA (2005) Optical vortex coronagraph. *Opt Lett* 30:3308–3310
- Galicher R, Baudoz P (2007) Expected performance of a self-coherent camera. *CR Phys* 8:333
- Guyon O (2003) Phase-induced amplitude apodization of telescope pupils for extrasolar terrestrial planet imaging. *Astron Astrophys* 404:379
- Guyon O, Pluzhnik EA, Kuchner MJ, Collins B, Ridgway ST (2006) Theoretical Limits on Extrasolar Terrestrial Planet Detection with Coronagraphs. *Astrophys J Suppl Ser* 167:81

- Kasdin NJ, Vanderbei RJ, Spergel DN, Littman MG (2003) Extrasolar planet finding via optimal apodized pupil and shaped-pupil coronagraphs. *Astrophys J* 582:1147–1161
- Kuchner M, Traub W (2002) A coronagraph with a band-limited mask for finding terrestrial planets. *Astrophys J* 570:900–908
- Liot B (1939) The study of the solar corona and prominences without eclipses (George Darwin lecture, 1939). *Mon Not R Astron Soc* 99:580
- Marois C, Lafrenière D, Doyon R, Macintosh B, Nadeau D (2006) Angular differential imaging: a powerful high-contrast imaging technique. *Astrophys J* 641:556–564
- Rabbia Y, Gay J, Rivet J-P (2007) The achromatic interfero coronagraph. *CR Phys* 8:385
- Racine R, Walker GAH, Nadeau D, Doyon R, Marois C (1999) Speckle noise and the detection of faint companions. *Publ Astron Soc Pac* 111:587–594
- Roddier F, Roddier C (1997) Stellar coronagraph with phase mask. *Publ Astron Soc Pac* 109:815–820
- Rouan D, Riaud P, Boccaletti A, Clénet Y, Labeyrie A (2000) The four-quadrant phase-mask coronagraph I. Principle. *Publ Astron Soc Pac* 112:1479–1486
- Rouan D, Baudrand J, Boccaletti A, Baudoz P, Mawet D, Riaud P (2007) The four quadrant phase mask coronagraph and its avatars. *CR Phys* 8
- Shao M (2007) Calibration of residual speckle in a nulling coronagraph. *CR Phys* 8:340
- Soummer R (2004) Apodized pupil Lyot coronagraphs for arbitrary telescope apertures. *Astrophys J* 618:161–164
- Sparks WB, Ford HC (2002) *Astrophys J* 578:543

OCA, with significant contributions from Austria, Belgium, Brazil, ESA, Germany, and Spain.

Basic Methodology

Stars, acted on by gravity, pressure and Coriolis forces, behave as oscillators with many specific modes. These oscillations are detectable through tiny variations in the stellar luminosity, and their analysis provides important parameters on the stars' internal structure.

When an exoplanet travels between its host star and us, it induces a weak drop of the star's luminosity (a mini-eclipse). The detection of this periodic **transit** in the star's light curve, together with its careful analysis, reveal the existence of the exoplanet and provide important characteristics such as its radius, its orbit parameters, and the rotation period of the star.

CoRoT's wide field of view enables it to monitor the flux from thousands of stars for uninterrupted period of several months, in order to detect and measure the tiny variations in this flux, either for stellar activity measurements or for exoplanets' transit detection. The satellite carries a 27 cm, 2 mirrors off-axis visible telescope focusing the stars' light on a focal unit hosting the 4 frame transfer CCD matrices of $2,048 \times 4,096$ pixels (Baglin et al. 2007; Auvergne et al. 2009). The detectors, whose temperature is regulated at -40°C , have a high quantum efficiency in the visible wavelengths. On top of this instrument a baffle reduces the parasitic stray light down to a few photons/second/pixel (Fig. 1).

1. Since a failure in March 2009, only two CCD matrices are left operating.

Key Research Findings

Asteroseismology

In December 2010, about 130 stars had been observed for uninterrupted durations of about 150 days in most cases. A few highlights of the results already achieved by CoRoT are presented here.

Solar-Like Pulsation, Granulation, and Convective Core

CoRoT measured solar-like oscillations and granulation in stars hotter than the Sun (Michel et al. 2008). The modes' widths (inversely proportional to the lifetime of the modes) have been found to be noticeably larger than those in the Sun, and larger than expected. In terms of stellar structure, the first seismic interpretations of the measured eigen-frequencies address the crucial question of the extension of the mixing beyond the stellar

CoRoT Satellite

OLIVIER LA MARLE

Centre National d'Etudes Spatiales DSP/EU,
Paris Cedex 01, France

Keywords

Asteroseismology, CoRoT, exoplanet, transit

Definition

The CoRoT mission is a satellite for the study of the stellar structure through asteroseismology and for the detection of transiting **exoplanets**.

Overview

CoRoT (for Convection, Rotation and Planetary Transits) is the first space mission designed for the study of the stellar physics through **asteroseismology** and for the search for exoplanets with the method of transits. It was launched on December 27, 2006, from Baïkonour, and should be operated at least until March 2013. CoRoT was developed and is operated by the French space agency **CNES** and French laboratories LESIA, LAM, IAS, and



CoRoT Satellite. Figure 1 The CoRoT satellite during its integration onto the Soyouz launcher

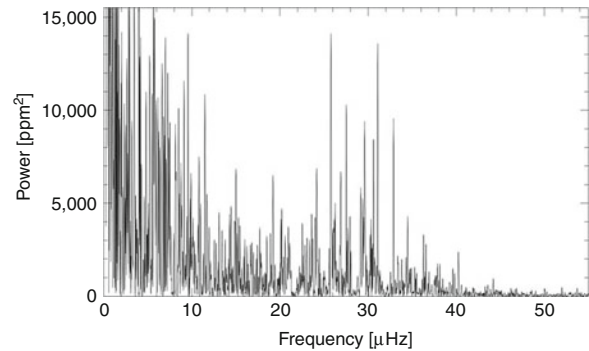
convective core. This key process is responsible for the present large uncertainty on stellar age determinations.

Red Giants and the Future of Our Sun

Toward the end of their lives, stars like the Sun expand and become ► [red giant](#) stars. Because of the turbulent convection in their outer layers, red giants stars are expected to exhibit solar-like oscillations, but in a much lower range of frequencies (10–100 μHz). CoRoT data allowed to measure clearly for the first time such oscillations in a large sample of red giants (Fig. 2).

In addition, unambiguous evidence of the excitation of both radial and nonradial modes was provided, previously an open question. CoRoT data also confirmed the existence of modes with lifetimes of the order of one month (De Ridder et al. 2009; Carrier et al. 2010).

The first theoretical modelling of this stellar evolution stage suggests that it would be possible to explain the observed oscillation spectra and their variety for different stages of the structure of stars along their expansion in the red giant phase. Indeed these red giants of different masses and ages are representative of all the successive generations of stars in the Galaxy.



CoRoT Satellite. Figure 2 Power spectrum of the CoRoT observations of the red giant HR 7349. Carrier et al. (2010) (Reproduced with permission © ESO)

New Type of Pulsators

CoRoT data led to the discovery of new types of pulsating stars. HD180872 is one of them. This star was known to belong to the Beta Cephei class of pulsators, young massive stars which are progenitors of SN-II type supernovae and thus mainly responsible for the enrichment of the Universe in carbon and oxygen. These stars classically show oscillation periods of the order of a few hours. In the lightcurve of HD180872, CoRoT data revealed, at very low amplitude, the existence of higher frequency modes, due to stochastic oscillation, very comparable to the ones observed in the Sun (Belkacem et al. 2009). This confirms the existence of a powerful convective zone and will allow the scaling of its energetics. This discovery opens new perspectives in the study of these objects where low frequency oscillations and high frequency ones could be used in a complementary way to probe the center and the outer layers of the star.

Search for Exoplanets

By December 2010 about 140,000 stars had been monitored by CoRoT. Fifteen exoplanets had been confirmed, and several other candidates were in the confirmation process (Fig. 3).

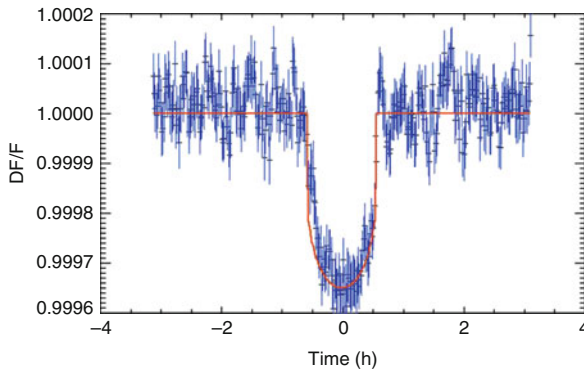
These discoveries widen the variety of the known exoplanets family (Table 1). CoRoT-3b, the heaviest and the densest one, lies at the frontier with ► [brown dwarfs](#) (Deleuil et al. 2008). On the opposite side, CoRoT-7b is the first telluric exoplanet which mass and radius are known (Léger et al. 2009; Queloz et al. 2009). It provides evidence for the existence of Earth cousins in orbit around Sun-like stars.

CoRoT-7b is phase-locked, that is to say that its orbital and rotational periods are equal (0.85 day, which is the shortest known orbital period for an exoplanet).



Therefore, it shows always the same face to its star (as the Moon does relatively to the Earth). This induces a very hot temperature (up to 2,600 K) on the dayside and a very cold one (down to 50 K) on the nightside.

CoRoT-9b is the first transiting temperate exoplanet. Indeed, the medium surface temperature of this Jupiter-like gaseous planet stands between -20°C and 150°C ,



CoRoT Satellite. Figure 3 CoRoT-7b light curve. The 0.03% dip in the star's flux during the planet's transit is clearly visible (© CoRoT)

depending on the models, and the temperature excursion between daytime and nighttime is probably low (Deeg et al. 2010). Its low eccentricity ensures a relatively low seasonal temperature variation. Further spectroscopic observations of its transits should open a new era in the study of exoplanets, allowing planetologists and biochemists to enter the game. Such complementary data might be acquired with the ► [VLT](#), with the ► [Hubble Space Telescope](#), and from the coming ► [James Webb Space Telescope \(JWST\)](#).

CoRoT also detected the secondary transit of exoplanets at the visible wavelength for the first time (Alonso et al. 2009a, b). This phenomenon occurs when the planet disappears behind its star, inducing a slight dip in the total flux received from the two of them. In the case of CoRoT-1b, for instance, this dip was only of 2/10,000. This allowed to measure the planet albedo (reflectivity), which turns to be of about 10% (compared to about 40% for the Earth).

Applications

CoRoT should let us make a giant step forward in our knowledge of stars' and the planets' birth, life, and death, and therefore bring a major contribution of our

CoRoT Satellite. Table 1 Characteristics of the first 15 planets discovered by CoRoT

Name	Period (day)	Mass (M_{Jupiter})	Radius (R_{Jupiter})	Density (g/cm^3)	Star type	Main features
CoRoT-1b	1.51	1.03	1.49	0.38	G0V	Metal poor host star – Secondary transit detected
CoRoT-2b	1.74	3.31	1.46	1.31	G7V	Active star – Secondary transit detected
CoRoT-3b	4.26	21.6	1.0	26.4	F3V	Brown dwarf or Super planet
CoRoT-4b	9.202	0.72	1.19	0.525	F9V	Synchronized system
CoRoT-5b	4.03	0.46	1.39	0.217	F9V	Very low density
CoRoT-6b	8.89	2.96	1.15	2.32	F9V	Metal poor host star
CoRoT-7b	0.85	0.014–0.019	0.157	4.23	G9V	First telluric exoplanet ($M=4.8 M_{\text{Earth}}$, $R=1.7 R_{\text{Earth}}$)
CoRoT-8b	6.12	0.22	0.57	1.6	K1V	Neptune-like exoplanet
CoRoT-9b	95.27	0.84	1.05	0.90	G3V	First temperature transiting exoplanet
CoRoT-10b	13.24	2.75	0.97	3.7	K1V	High eccentricity (0.53)
CoRoT-11b	2.99	2.33	1.43	0.99	F6V	High rotation rate of the star
CoRoT-12b	2.83	0.92	1.44	0.31		Very low density
CoRoT-13b	4.04	0.88	1.31	2.34	G0V	
CoRoT-14b	1.51	7.6	1.09	7.3	F9V	Very dense hot giant
CoRoT-15b	3.06	63.3	1.12	96	F7V	Very dense brown dwarf

knowledge of the Universe we live in. It also paves the way for the search for life in the universe: on one hand, it identifies planets for which detailed analysis with other techniques will be of particularly high interest. On the other hand, it eases the work of its successors, the US mission ► [Kepler](#) (Basri et al. 2005) and the future European mission ► [Plato](#) (Catala et al. 2010), by providing a great know-how on the transit method, in particular on the optimal strategy for data processing and on the ground follow-up. It also helps the delicate thinking of the astronomical community in the definition of the best strategy for the search for extraterrestrial life.

Future Directions

In stellar physics, CoRoT was a pioneer in establishing the richness of asteroseismology. The future will probably be devoted to the increase of the sample and of the variety of stars observed. CoRoT, Kepler, and later on Plato will be major contributors.

Several international scientific bodies have recently been brainstorming on the definition of a roadmap for the exoplanets and extraterrestrial life detection, in Europe (EP-RAT, Blue Dots initiative) or in the US (Decadal Survey). The Pathways conference in Barcelona in September 2009 proposed a three-step strategy:

1. Statistical study of planetary objects
2. Designate sources suitable for spectroscopic follow-up
3. Carry out spectroscopic characterization

The first and second steps would involve several methods such as transits, radial velocities, and microlensing. The ongoing Kepler mission and, on a larger scale, the future Plato mission intend to make a wide census and characterization of transiting planetary systems. GAIA and Euclid will also contribute. The spectroscopic characterization will require large ground telescopes, such as the ESO VLT, and/or space-based facilities such as the James Webb Space Telescope.

See also

- [Asteroseismology](#)
- [Atmosphere, Temperature Inversion](#)
- [Brown Dwarfs](#)
- [CNES](#)
- [Exoplanet, Detection and Characterization](#)
- [Exoplanets, Discovery](#)
- [Exoplanets, Modeling Giant Planets](#)
- [Habitability \(Effect of Eccentricity\)](#)
- [Habitable Zone, Effect of Tidal Locking](#)
- [Hot Jupiters](#)

- [Hot Neptunes](#)
- [James Webb Space Telescope](#)
- [Kepler Mission](#)
- [Microlensing Planets](#)
- [Planetary Migration](#)
- [Plato](#)
- [Radial Velocity](#)
- [Red Giant](#)
- [Secondary Eclipse](#)
- [Spectroscopy](#)
- [Stellar Pulsation](#)
- [Stellar Rotation](#)
- [Super-Earths](#)
- [Transit](#)
- [Transiting Planets](#)
- [VLT](#)

References and Further Reading

- Alonso R, Guillot T, Mazeh T et al (2009a) The secondary eclipse of the transiting exoplanet CoRoT-2b. *Astron Astrophys* 501:23–26
- Alonso R, Alapini A, Aigrain S et al (2009b) The secondary eclipse of CoRoT-1b. *Astron Astrophys* 506:331–336
- Auvergne M, Bodin P, Boissard L et al (2009) The CoRoT satellite on flight: description and performances. *Astron Astrophys* 506: 411–424
- Baglin A et al (2007) The CoRoT mission and its scientific objectives. *AIP Conf Proc* 895:201–209
- Basri G, Borucki WJ, Koch D (2005) The Kepler mission: a wide-field transit search for terrestrial planets. *New Astron Rev* 49(7–9 [SPECIAL ISSUE]):478–485
- Belkacem K, Samadi R, Goupil MJ et al (2009) Solar-like oscillations in a massive star. *Science* 324(5934):1540–1542
- Carrier F, De Ridder J, Baudin F et al (2010) Non-radial oscillations in the red giant HR 7349 measured by CoRoT. *Astron Astrophys* 509:A73
- Catala C, Arentoft T, Fridlund M et al (2010) PLATO: Planetary transits and oscillations of stars – the exoplanetary system explorer. *ASP Conference Series* 430:260–265
- De Ridder J, Barban C, Baudin F et al (2009) Non-radial oscillation modes with long lifetimes in giant stars. *Nature* 459:398–400
- Deeg HJ, Moutou C, Erikson A et al (2010) A transiting giant planet with a temperature between 250 K and 430 K. *Nature* 464:384–387
- Doleuil M, Deeg H, Alonso R et al (2008) Transiting exoplanets from the CoRoT space mission-VI. CoRoT-Exo-3b: the first secure inhabitant of the Brown-dwarf desert. *Astron Astrophys* 491(3): 889–897
- Léger A, Rouan D, Schneider J et al (2009) Transiting exoplanets from the CoRoT space mission-VIII. CoRoT-7b: the first Super-Earth with measured radius. *Astron Astrophys* 506:287–302
- Michel E, Baglin A, Auvergne M, Catala C et al (2008) CoRoT measures solar-like oscillations and granulation in stars hotter than the Sun. *Science* 322(5901):558–560
- Queiroz D, Bouchy F, Moutou C et al (2009) The CoRoT-7 planetary system: two orbiting super-Earths. *Astron Astrophys* 506: 303–319

Corotation Torque

Definition

The corotation torque is that exerted on a planet's orbit by material (usually gas) co-orbiting with the planet. This has a very important effect on the orbital migration of planets of less than roughly 50 Earth masses that form in gaseous ► [protoplanetary disks](#). In fact, recent results suggest that very rapid, inward "type 1" migration – caused by tidal interaction between the disk and a planet – may in fact be slowed or even reversed in certain situations due to the corotation torque.

See also

- [Lindblad Resonance](#)
- [Planetary Migration](#)
- [Protoplanetary Disk](#)

Corrosion

- [Oxidation](#)

Cosmic Background Radiation

STÉPHANE LE GARS

Centre François Viète, Université de Nantes, Nantes, BP, France

Synonyms

[CMB](#); [Cosmic microwave background](#); [Radiation](#)

Keywords

Arno Penzias, astronomy, big bang, cosmic background radiation, cosmology, George Gamow, Georges Lemaître, history, nucleosynthesis, physics, Robert Wilson

Abstract

In 1965, Arno Penzias and Robert Wilson found evidence for an electromagnetic background noise at radio wavelengths coming from the whole universe. Although some previous measurements of the background had been made, this discovery made sense within the Big Bang

theoretical framework. The idea of a non-static expanding universe had been formulated by the Russian mathematician Alexander Friedman in the 1920s, and then independently by the Belgian physicist Georges Lemaître a few years later. Subsequently, Georges Gamow in the 1940s pointed out that a universe that was originally dense and hot would have produced radiation that, as it cooled off because of its expansion, would exist today as a fossil background noise.

History

In 1965, two American physicists, Arno Penzias and Robert Wilson, accidentally discovered electromagnetic background noise at 7.35 cm wavelength in the millimeter radio wave region. Penzias and Wilson were working for the Bell Telephone Laboratories on satellite communication improvement when they brought to light this homogeneous and isotropic radiation resulting from the universe as its whole; it was quickly read as fossil radiation from a universe that was originally dense and hot, and had cooled off because of its expansion to a 3.5 K temperature today. In 1978, Penzias and Wilson got the Nobel Prize for this discovery.

However, there had been some previous investigations in this general area. The French physicist Charles-Edouard Guillaume had calculated in 1896, by Abney's works and according to the black body's law that Stefan granted in 1879, that an isolated body in the space, only subdued to stars' radiation, would see its temperature increasing of nearly 5 K. In 1926, Sir Arthur Eddington shows that the real temperature of the space, due to star's radiance, is 3.18 K. But there was a lack of theoretical framework to give sense to theoretical calculations assuming some model of the universe. Indeed, Edwin Hubble proved in 1924, with detailed observations, that the universe is formed of myriads of galaxies. In 1929, he also discovered empirically that these galaxies all move away from one another. At the same time, the Belgian physicist Georges Lemaître's works interpreted the observational data in terms of relativity theory to show that the universe is expanding.

In the 1940s, the American astrophysicist George Gamow laid down the basis of nucleosynthesis, the formation of the chemical elements. According to Gamow, the chemical elements could have been made at a hot and dense period of the universe, in the bosom of an "original soup" that he named "ylem," and that represented an early stage of the Big Bang. In 1948, two Gamow's collaborators, Alpher and Hermann, developed Gamow's ideas and predicted the existence of

a diffuse radiation background with a 5 K temperature. Within this theoretical framework, this cosmic background radiation has become the experimental mainstay of the Big Bang theory, which includes the universal expansion and the nucleosynthesis of the lightest elements. The background radiation has recently been measured very accurately in 2001 and 2006, respectively, with satellites COBE and WMAP.

References and Further Reading

- Acker Agnès (2005) *Astronomie-Astrophysique-Introduction*. Paris, Dunod
- Assis AKY, Neves MCD (1995) The redshift revisited. *Astrophys Space Sci* 227:13–24
- Charles-Edouard G (1896) La température de l'espace. *La Nature* 24:234
- Dicke RH, Peebles PJE, Roll PG, Wilkinson DT (1965) Cosmic black-body radiation. *Astrophys J* 142:414–419
- Eddington AS (1926) *The internal constitution of the universe*, Cambridge University Press, Cambridge
- Marc L-R (2004) Cosmologie scientifique. *Rev Métaphys De Morale* 43:399–411
- Penzias AA, Wilson RW (1965) A measurement of excess antenna temperature at 4080 Mc/s. *Astrophys J* 142:419–421
- Wilson Robert (1978) The cosmic background radiation, Nobel Lecture, 8 décembre

Cosmic Dust

- [Interstellar Dust](#)

Cosmic Microwave Background

- [Cosmic Background Radiation](#)

Cosmic Ray Ionization Rate

Definition

The ► [cosmic ray ionization](#) rate is the rate at which H₂ molecules as well as atomic H and He are ionized by the flux of Galactic cosmic rays. This process is fundamental to driving the chemistry in dense interstellar clouds. Current estimates place the value in the range $1\text{--}40 \times 10^{-17} \text{ s}^{-1}$ with

the higher values being more appropriate for lower-density diffuse interstellar clouds.

See also

- [Diffuse Clouds](#)
- [Molecular Cloud](#)

Cosmic Rays (in the Galaxy)

NIKOS PRANTZOS¹, JUN-ICHI TAKAHASHI²

¹Institut d'Astrophysique de Paris, Paris, France

²NTT Microsystem Integration Laboratories, Atsugi, Kanagawa, Japan

Synonyms

[Galactic cosmic radiation](#); [Radiation](#)

Keywords

Electrons, energetic particles, galactic cosmic rays, nuclei

Definition

Galactic cosmic rays are high-energy (relativistic) electrons and nuclei, accelerated by supernova explosions and massive stellar winds and traveling through the Galaxy by scattering on fluctuations of interstellar magnetic fields, which render their flux isotropic.

Overview

The energy spectrum of Galactic cosmic rays (CR) covers the energy range from a few MeV/nucleon up to 10^{15} MeV/nucleon and is well approximated by a power-law $N(E) \propto E^\alpha$ of slope $\alpha = -2.7$ below 10^6 GeV/nucleon and $\alpha = -3$ above that. Below a few GeV/nucleon, the CR spectrum progressively flattens (with α even becoming positive) and its intensity varies, in a way that anti-correlates with solar activity (“solar modulation”); the solar wind prevents the lowest energy CR from entering the heliosphere. The total Galactic power of CR is estimated to 10^{41} erg/s, that is, about 10% of the total kinetic power of ► [supernovae](#) and stellar winds, which are thought to be the main CR accelerators. However, no Galactic accelerator can account for the highest energy CR (up to $\sim 10^{12}$ GeV), the origin of which remains unknown. The residence time of CR in the Galactic disk is $\sim 10^7$ years. The composition of CR nuclei is overall similar to the solar one: it consists of $\sim 87\%$ protons, 12% alpha nuclei (Helium atoms), and 1% heavier nuclei (in addition to the nucleonic component



~3% of the CR flux are high-energy electrons). The major uncertainties are at extremely high energies and for elements heavier than iron. There are several important differences: the metallicity (see ► [Metallicity](#)) of CR is ~10 times solar, with refractory elements (Fe-peak nuclei) relatively more enhanced than the volatiles; and the fragile Li, Be, and B nuclei are 10^6 times more abundant in CR than in the Sun. These features suggest that CR are accelerated from a mixture of interstellar gas and dust grains (where refractory elements are overabundant) and during their propagation in the Galaxy they spallate abundant CNO nuclei to produce Li, Be, and B.

From the standpoint of astrobiology, CR may play a crucial role, either as effective energy sources for synthesizing the precursors of terrestrial bio-organic compounds in interstellar media or as agents inducing mutations in living organisms and thereby promoting biological evolution. They may even be lethal in case of a nearby supernova.

See also

- [Biostack](#)
- [Cosmic Rays in the Heliosphere](#)
- [Evolution \(Biological\)](#)
- [HZE Particle](#)
- [Ionizing Radiation \(Biological Effects\)](#)
- [Mutation](#)
- [Nucleon](#)
- [Proton Irradiation](#)
- [Radiation Biology](#)
- [Radiochemistry](#)
- [Spallation Reactions](#)
- [Supernova](#)

References and Further Reading

Strong A, Moskalenko I, Ptuskin V (2007) Cosmic ray propagation and interactions in the Galaxy. *Annu Rev Nucl Part Sci* 57:285–327

Cosmic Rays in the Heliosphere

DON F. SMART

Air Force Research Laboratory (Emeritus), Bedford,
MA, USA

Keywords

Cosmic radiation, elemental composition, solar modulation

Definition

Cosmic rays are very energetic particles thought to pervade space. Within the solar system the cosmic ray flux is modulated by the solar activity cycle.

Overview

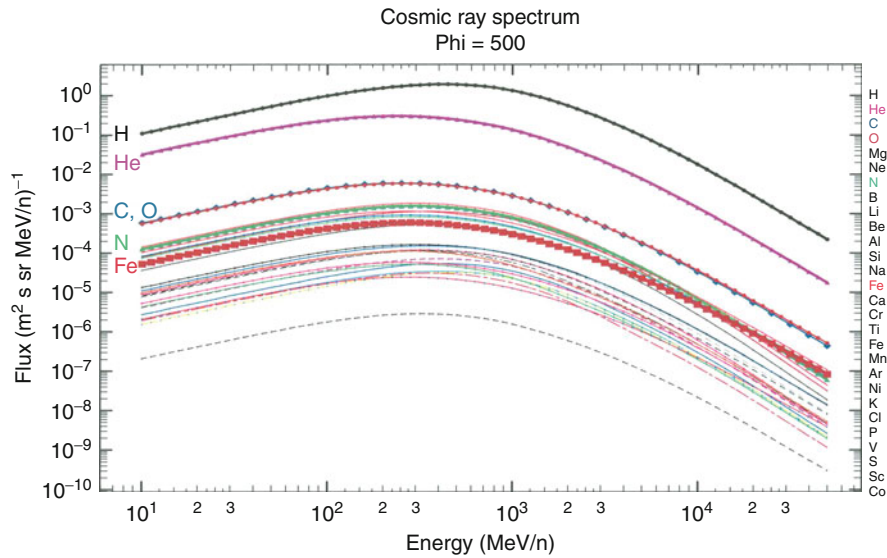
Cosmic radiation observed at the Earth consists of ~83% protons, 12 % alpha particles, 1% heavy nuclei with atomic number >2 , and ~3% electrons. The cosmic ray composition of the most common elements has been measured to a reasonable precision (see [Fig. 1](#)). The major uncertainties are at extremely high energies and for elements heavier than iron. The local interstellar spectrum (outside the heliosphere) is constant, but inside the heliosphere the spectrum and fluence of particles below ~10 GeV/nucleon are modified by solar activity with a phase that is the inverse of the solar sunspot cycle. The cosmic ray flux decreases with increasing energy and the proton flux is reduced by 50% at 1.5 GeV. The cosmic ray flux of the heavier nuclei is reduced by 50% at 0.9 GeV/nucleon. The maximum total isotropic flux in free space at 1 AU is ~3 particles $\text{cm}^{-2} \text{s}^{-1}$ during solar minimum conditions; during solar maximum conditions, the total cosmic ray flux is reduced by ~40%. The diffusion of the cosmic ray flux inwards through the turbulent interplanetary medium results in an average radial cosmic ray gradient of a few percent per AU. The cosmic radiation flux at Mars (1.5 AU) is only a few percent larger than at Earth.

The major factors modulating the cosmic radiation intensity include the solar wind speed, turbulence in the solar wind, and solar magnetic polarity. Cosmic ray modulation theory adequately models the flux at the Earth and at our most distant space probes. The modulation parameter, designated by the symbol Φ , is normally expressed in units called MV. The modulation parameter at 1 AU during solar minimum typically ranges between 400 and 500 MV; however, extreme solar activity can generate transient modulation levels in excess of 1600 MV (see [Fig. 2](#)).

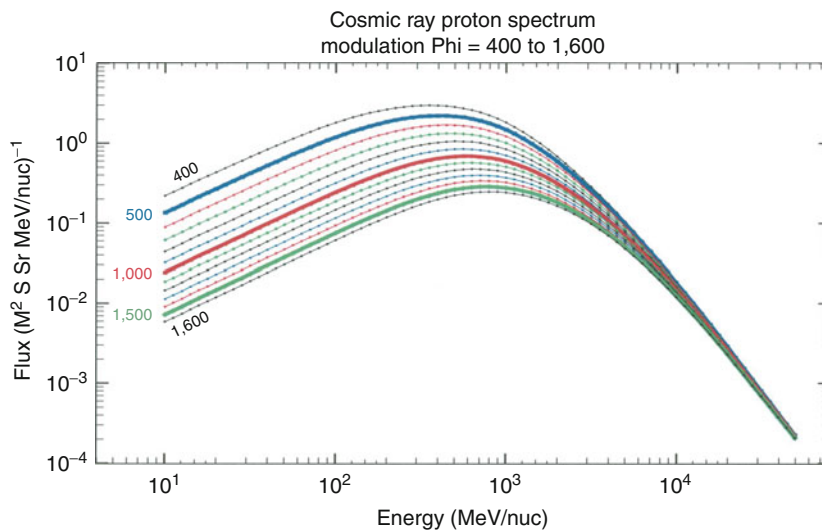
The particle flux below ~2 GeV/nucleon makes the most important contribution to radiation dose. Since the energy deposition in matter is proportional to the square of the atomic charge, the heavy elements are important for computing radiation dose.

References and Further Reading

Townsend LW, Badhwar GD, Blakely EA, Braby LA, Cucinotta FA, Curtis SB, Fry RJM, Land CE, Smart DF (2006) Information needed to make radiation protection recommendations for space missions beyond low-earth orbit. NCRP Report No. 153, National Council on Radiation Protection and Measurements, Bethesda



Cosmic Rays in the Heliosphere. Figure 1 A model of the modulated differential cosmic ray spectrum at 1 AU for the most abundant elements in the cosmic ray flux during average low solar activity conditions. The elements listed on the right side of the figure are in the order of their observed abundance. Original figure created by the author



Cosmic Rays in the Heliosphere. Figure 2 A model of the modulated differential cosmic ray proton spectrum at 1 AU for modulation conditions, ranging from near solar minimum to solar maximum. Original figure created by the author

Cosmic Spherules

Definition

Spherule comes from the Greek word “sphaira” for sphere. Cosmic spherules are solidified, rounded particles ranging from microscopic to millimeter size with distinct chemical

compositions indicating their extraterrestrial nature. Cosmic spherules are predominantly found in ocean floor deposits on Earth and are mainly produced by frictional heating, melting, and [ablation](#) of [meteoroids](#) upon atmospheric entry. Solidified impact-induced molten droplets of meteoroid and target materials are less abundant on Earth but would predominate on the exposed

surfaces of atmosphere-less bodies like the ► [Moon's](#) that were strongly gardened by impacting meteoroids in their early history.

See also

- [Ablation](#)
- [Meteoroid](#)
- [Moon, The](#)

Cosmochemistry

MATTHIEU GOUNELLE

Laboratoire de Minéralogie et Cosmochimie du Muséum (LMCM) MNHN USM 0205 - CNRS UMR 7202, Muséum National d'Histoire Naturelle, Paris, France

Synonyms

[Meteoritics](#)

Keywords

Accretion disk, ► [CAIs](#), chondrites, chondrules, proto-planetary disk

Definition

Cosmochemistry is the study of the formation and evolution of the Solar System and its individual components through the analysis of extraterrestrial samples in the laboratory.

History

The first mention of a meteorite in western literature concerns the prediction of the fall of a meteorite by Anaxagoras of Clazomenae in the year 467 BC. During Antiquity, ► [meteorites](#) were revered as gods in many places of the Mediterranean basin. During the Middle Ages, they were still considered with superstition and fear. Though more rational interest was paid to meteorites in the Renaissance, they still belonged to the reign of natural wonders. Interestingly, the Enlightenment era failed to identify the true provenance of meteorites, probably because analytical chemistry was yet to be developed.

Ernst Florens Chladni (1756–1827) can be seen as the founder of cosmochemistry. At a time when most scientists believed meteorites were mere stones from volcanoes or atmospheric condensations, he proposed in a provocative pamphlet published in 1794 that meteorites

were extraterrestrial objects. This bold proposition was harshly discussed for the next 10 years among the European scientific community. It was finally accepted in 1803 after the fall of a meteorite at l'Aigle in France and the publication of a detailed report by Jean-Baptiste Biot (1774–1862, [Fig. 1](#)). Being the first scientist to travel to the place of a meteorite fall, and helped by a beautiful literary style, Biot was able to convince his peers that stones fell from the sky.

At that time, many of the early cosmochemists such as Chladni, Laplace (1749–1827), or Biot thought meteorites came from the Moon. It is not until the mid-nineteenth century that scientists realized that most meteorites come from ► [asteroids](#), the first of which, Ceres, was discovered in 1801. After the recognition of the extraterrestrial nature of meteorites, the field of cosmochemistry blossomed. It started with the development of elaborate classification schemes (strikingly similar to the one used now) and



Cosmochemistry. **Figure 1** Jean-Baptiste Biot (1774–1862). After the fall of the L'Aigle meteorite in 1803 in France, he wrote a report which definitely established the extraterrestrial origin of meteorites

chemical analyses, which expanded on the pioneering studies of Lavoisier (1743–1794) and Howard (1774–1816). The identification of new minerals and of chondrules, a major component of the primitive meteorites unknown in terrestrial rocks, clearly set meteorites apart from terrestrial rocks.

Basic Methodology

Meteorites are studied using the same techniques as terrestrial rocks. The petrography (relative abundance and textural relationships between the different components and individual minerals) and mineralogy (structure and chemical composition of minerals) are made on rock sections (i.e., cut and polished) with a diversity of optical and electronic microscopes. Isotopic analyses are performed with a diversity of mass spectrometers. Secondary Ion Mass Spectrometers and Thermo Ionization and Inductively Coupled Plasma Mass Spectrometers are used for a wide range of rock-forming elements. While the former provide a very good spatial resolution (micron scale), the latter have reached precisions of the order of tens of ppm. Organic matter within meteorites is now studied in detail with techniques imported from the oil industry (► [Meteorite \(Murchison\)](#)).

Key Research Findings

Today, extraterrestrial samples can be collected directly from space thanks to sophisticated and expensive space missions, such as Stardust, which brought back cometary dust from the Wild 2 comet in January 2006. But these missions are still rare. Most cosmochemists focus their work on meteorites and micrometeorites that fall on Earth, a cheaper way to sample celestial bodies millions of kilometers away. Roughly 50 t of meteorites (size range 1 g–100 kg) and 7,000 t of micrometeorites (< mg) fall on the Earth's surface every year. In April 2010, the number of meteorites registered by the Meteoritical Society was 38,800.

Nowadays, cosmochemistry is a very active scientific discipline, which greatly benefits from its proximity with other fields, especially astrophysics, but also geology and material sciences. Thanks to the diversity of extraterrestrial samples (meteorites as well as lunar rocks and cometary dust brought back by space missions), to the wealth of techniques used and its fecund interaction with a large number of neighboring fields, it can address a diversity of fundamental scientific questions. The following point of view on cosmochemistry is complementary to that presented in the entry ► [meteorites](#); special emphasis will be given to important discoveries and open questions.

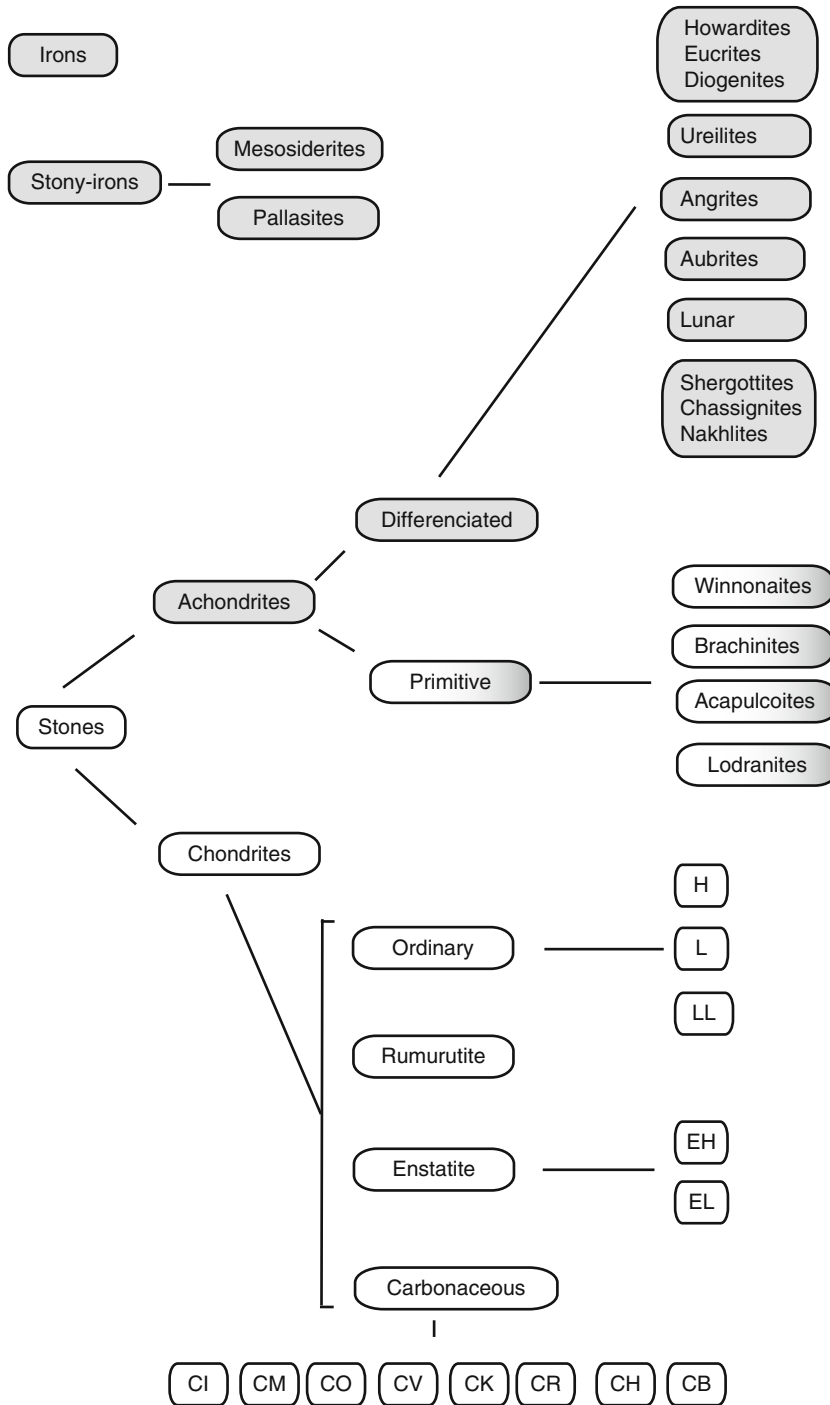
What Do Meteorites Look Like?

Meteorites are rocks made of minerals (and occasionally glasses). They can be distinguished from terrestrial rocks mainly by their fusion crust (► [Meteorite \(Allende\)](#)), i.e., a mm-thick veneer of glass produced during their entry at cosmic velocity (~10–20 km/s) into the Earth's atmosphere.

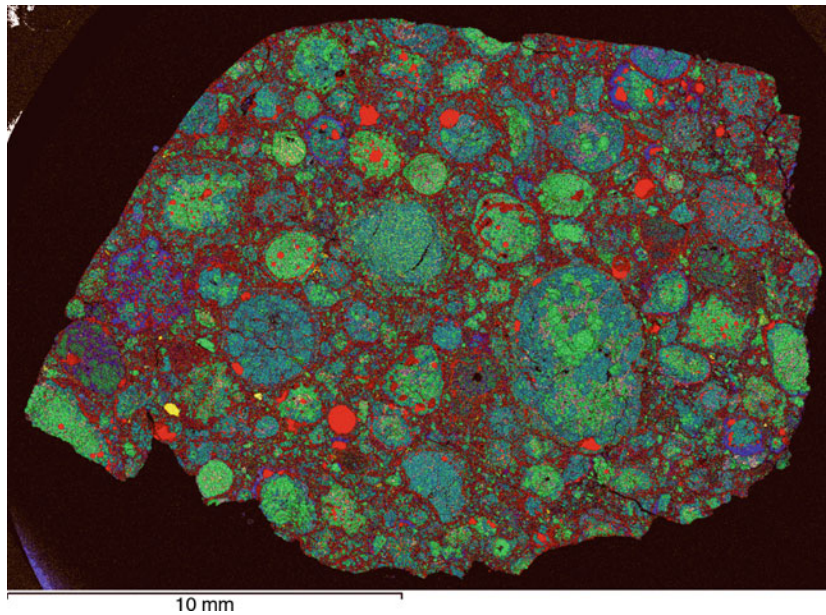
Though meteorites can be divided into 135 different classes, mineralogically there exist three main groups of meteorites (Fig. 2): stones (94% of the observed falls), stony-irons (1%), and irons (5%). Though some of them might have an impact origin, irons are believed to represent the cores of large, differentiated asteroids or planetesimals; and stony-iron meteorites are thought to be mixtures of core and mantle or core and crust material. Stony meteorites can be divided into chondrites and achondrites. The former are characterized by a large abundance of small mm-sized blobs known as chondrules (see below) that have a chemical composition similar to that of the Sun. Achondrites are magmatic rocks. They lack chondrules and have a strongly fractionated chemical composition relative to that of the Sun; they are believed to originate from the crust of planets and other smaller differentiated bodies.

Chondrites are made of Calcium-Aluminum-rich Inclusions (CAIs), chondrules, and matrix (Fig. 3). The relative abundance of these three components varies between chondrite groups. In most chondrites (except CIs), chondrules represent the dominant component. CAIs are an assemblage of calcium- and aluminum-oxides and -silicates (► [CAIs](#)). Some of them show evidence of melting. Chondrules are an assemblage of iron-magnesium silicates plus metal and sulfides. Chondrules usually show an igneous texture indicating they were at some point extensively melted in the solar protoplanetary disk. Matrix is made of fine-grained (<1 μm) iron-magnesium silicates, metal, and sulfides. In the case of carbonaceous chondrites, the matrix is rich in organic matter. For most chondrite groups, the matrix has been modified on the parent-asteroid due to secondary geological processes such as thermal metamorphism or hydrothermal alteration.

Achondrites, at first sight, look like terrestrial igneous rocks. They are made of mafic minerals such as olivine and pyroxene and an aluminum-rich silicate, plagioclase. If it were not for the fusion crust, they would be difficult to distinguish from terrestrial basalts, though detailed studies show they come from evolved bodies, which had a different geologic history than the Earth.



Cosmochemistry. Figure 2 Simplified classification of meteorites. *Gray boxes* indicate differentiated meteorites while *white boxes* indicate primitive meteorites. Primitive achondrites (shaded *gray*) are objects having the composition of chondrites and the texture of differentiated rocks



Cosmochemistry. Figure 3 Chemical composition of the chondrite GRO 03116. Red, green, blue, yellow, and white code, respectively, for iron, magnesium, silicon, calcium, and aluminum. One can appreciate the richness in reduced iron (red), the high abundance of chondrules (green-blue iron-magnesium silicate spheres) and the rarity of CAIs (in yellow-white). Picture courtesy of Anton Kearsley (NHM)

Where Do Meteorites Come from?

Most meteorites are chondrites. They are cosmic sediments whose components were made in the protoplanetary disk and cemented together via poorly characterized processes. Chondrites were not differentiated, i.e., metal and silicates were not segregated after melting. The larger a body is, the easier it is to melt, therefore the undifferentiated nature of chondrites indicates they originate from small celestial bodies, ► [asteroids](#) or ► [comets](#). The determination of the orbits of a few meteorites has confirmed that most chondrites come from asteroids, though some, such as CI chondrites, could come from comets (► [Meteorite \(Orgueil\)](#)). It is however not possible to pinpoint from which specific asteroid meteorites come from, except for one noticeable exception. The good match between the infrared spectrum of HED meteorites and the asteroid (4) Vesta suggests these meteorites come from that asteroid.

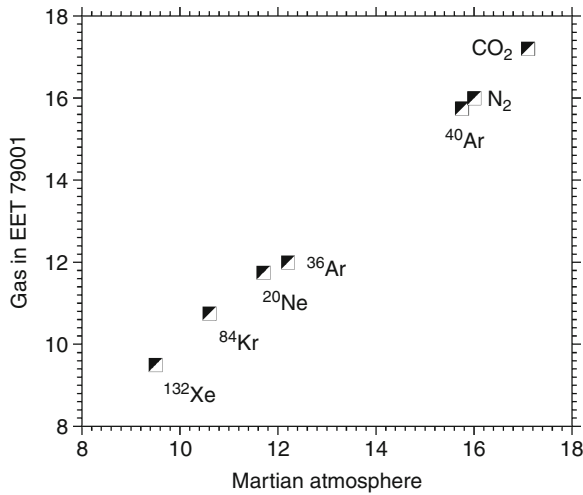
On the other hand, the compositional and mineralogical similarities of roughly 100 meteorites to lunar samples collected by the space missions Apollo and Luna establish that they come from the Moon. The same number of meteorites – forming the SNC (Shergottite-Nakhilite-Chassignite) group – come most likely from the

planet Mars. This was demonstrated by the excellent match in composition between gas bubbles trapped within meteorites from the SNC group and the Martian atmosphere composition measured by the Viking landers in 1976 (Fig. 4).

The origin of micrometeorites is still debated. Recent work suggests they come mostly from comets rather than from primitive asteroids. It is worth noticing that the precise origin of micrometeorites does not matter much, as the analysis of cometary samples returned by the Stardust mission has demonstrated that comets and primitive carbonaceous asteroids are similar in nature.

Dating Meteorites and Other Bodies: A Rough Sequence of Events

One of the major achievements of cosmochemistry has been to date extraterrestrial samples. In 1956, Claire Patterson proposed an age of 4.55 Ga for the Solar System and the Earth (see Age of the Earth). To accomplish this fundamental task, he used two long-lived radionuclides ^{235}U and ^{238}U which decay into ^{207}Pb and ^{206}Pb , with respective half-lives of 0.7 and 4.5 Gyr. The long-lived radioisotope ^{87}Sr ($T_{1/2} = 48$ Gyr) was also extensively used to date early Solar System processes during the

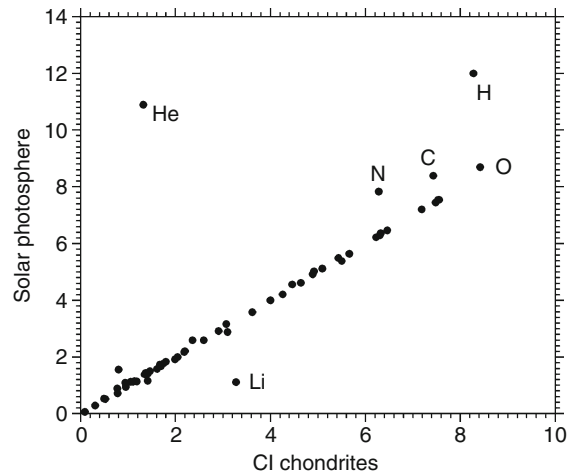


Cosmochemistry. Figure 4 Chemical composition of the gas trapped in the SNC (martian) meteorite EET 79001 compared to that of the Martian atmosphere determined by the Viking spacecraft in the 1970s. From Bogard et al. (1984)

1960s and 1970s, but is today too imprecise for the task (compared to other systems). Iodine-129 with half-life of 15.7 Myr was the first short-lived radionuclide whose past presence in a meteorite was unambiguously demonstrated. Many more were to follow (see below).

The use of chronometers, combined with astronomical observations, made it possible to date the sequence of events from the collapse of the portion of a molecular cloud to the Solar System in its present configuration. The lifetime of the molecular cloud precursor of our Solar System is not known, but molecular clouds usually live for a few million years before they get disrupted by the harsh effects (photoionization, powerful winds) of the stars to which they gave birth. The following stage, i.e., the gravitational collapse of a portion of the molecular cloud, takes some 100,000 years and can be seen as a transition phase during which, however, important gas-grain chemistry occurs. In the next stage, the proto-sun is surrounded by an accretion disk through which it is fed with matter. Because it is within the same disk that the components of chondrites, chondrites themselves, planetesimals (from 1 km up to 1,000 km), and large planetary embryos (1,000 km-sized bodies) formed, the accretion disk or Solar nebula is also called a protoplanetary disk.

CAIs most likely formed first in the protoplanetary disk 4,568 Ga ago, followed by chondrules which formed 1.5 Myr later. Accretion of chondrites from their components, and of planetesimals from chondrites occurred as soon as chondrules were formed. The disk was dissipated



Cosmochemistry. Figure 5 Chemical composition of the Sun's photosphere compared to that of the CI chondrites (shown on a logarithmic scale, normalized to silicon)

after a few million years, according to astronomical observations of other stellar systems. Embryos probably grew on that same million-year timescale.

Chemical and Isotopic Composition

CI chondrites have the same chemical composition as the Sun for all elements except for the most volatile ones, such as H, He, C, and N (Fig. 5). This discovery suggests that chondrites are extremely primitive rocks that sample the earliest phases of the protoplanetary disk. The relatively small chemical fractionation of other chondrites relative to CI chondrites is attributed to physical processing in the protoplanetary disk, either before or during chondrule formation.

The bulk isotopic and chemical composition of chondrites is the result of the chemical evolution of the Galaxy over the last 10 billion years. Interestingly enough, the isotopic composition of all but a few elements in Solar System bodies (chondrites, achondrites, Earth, Mars. . .) is remarkably identical in meteorites, lunar and terrestrial samples. This indicates that Solar System matter was well homogenized by high-temperature processes in the protoplanetary disk, possibly linked to chondrule formation.

A few solids escaped this processing and preserved their chemical and isotopic properties. These are called presolar grains. They were discovered in the matrix of chondrites in the late 1980s at the University of Chicago. They were isolated thanks to severe chemical treatments and recognized because of their isotopic composition,

radically different from that of Solar System matter. Presolar grains were made in the atmospheres of stars formed hundreds of million 's before our Solar System. Thanks to their study, stellar nucleosynthesis has become an experimental field.

The oxygen isotopic composition of meteoritic components, e.g., CAIs and chondrules, is an exception to the similarity discussed above, in that it varies a great deal. While chondrules have a composition roughly similar to that of the Earth, CAIs are enriched in ^{16}O by at least 4% relative to chondrules. The origin of that enrichment – known since 1973 – is not well understood. The most popular model – the self-shielding model – invokes photochemical processes either in the parent molecular cloud or in the protoplanetary disk (► [oxygen isotopes](#)).

Short-Lived Radionuclides

Short-lived radioisotopes (SRs) are radioactive elements with half-lives ranging from a few weeks to 100 Myr. Their presence in the nascent Solar System is inferred from excesses of their daughter isotopes in meteorite components, mostly in primitive components such as the CAIs. Some SRs were present in the protoplanetary disk at abundances significantly higher than the expected average contribution of the interstellar medium. These SRs therefore require a last-minute origin. They were either made within a star such as a supernova and injected into the nascent protoplanetary disk or produced within the disk itself via nuclear reactions between solar cosmic-rays and ambient dust. The origin of SRs is a hotly debated topic of cosmochemistry, as it has important consequences for our understanding of: (1) the early Solar System chronology, (2) planetesimal heating, and (3) the astrophysical context of our Solar System birth.

If SRs were homogeneously distributed in the Solar System, they can be used to define a chronology of Solar System events. Aluminum-26 ($T_{1/2} = 0.74$ Myr), ^{53}Mn ($T_{1/2} = 3.7$ Myr), and ^{182}Hf ($T_{1/2} = 9.0$ Myr) are especially useful as chronometers because their initial content is known in a diversity of objects. Ages based on SRs confirm the early formation of CAIs relative to chondrules and the rapid evolution of Solar System bodies. Dating of some iron meteorites indicate indeed that differentiation of large planetesimals or asteroids occurred contemporaneously with CAI formation.

Aluminum-26 and ^{60}Fe ($T_{1/2} = 2.6$ Myr) emit gamma-rays when they decay. They have been proposed as heat sources for planetesimals. The extent of heating and therefore the subsequent geological evolution depends on the initial content of these two SRs in the parent-body considered – and therefore on their initial content in the Solar

System – as well as on the timing of formation of the bodies considered. Current models indicate that ^{26}Al is a more efficient heat source than ^{60}Fe .

The presence of ^{60}Fe in the Solar System seems to indicate that the Sun was born in a second-generation molecular cloud enriched in radioactive elements by massive stars. At present, there is no satisfactory model accounting for the presence of ^{26}Al in our Solar System. It might result from an improbable sequence of events, in which case the Solar System would be special in having hosted ^{26}Al while it formed. In such a case, our Solar System might be unlike others in having evolved (differentiated) parent-bodies. Given that life, as we know it, is intimately linked to the geological history of our planet, it means that its development might result from a rare astrophysical event.

High-Temperature Processes in the Protoplanetary Disk

CAIs are very abundant in carbon-rich carbonaceous chondrites, while they are virtually absent from other chondrites. They are especially large and abundant in CV chondrites (► [Meteorite \(Allende\)](#)). They therefore represent on the whole a tiny fraction of chondritic matter. Understanding their formation is, however, important because they are the first solids to have formed in the protoplanetary disk. Their mineralogy is compatible with that of condensation from a gas of chondritic composition. Some of them show evidence of remelting and evaporation. It is widely believed that CAIs were formed close to the Sun (~ 0.1 AU), where temperatures in the disk were higher than 1,600 K. They were subsequently transported to asteroidal distances, where chondrites formed, either by turbulent diffusion or via magneto-hydrodynamic winds rooted at the disk inner boundary.

Chondrules are far more abundant than CAIs. They make up to 80% of ordinary chondrites in volume. As ordinary chondrites represent more than 80% of the meteorites, chondrules were probably the most abundant solids in the disk. Some authors estimate that there might have been between 10^{24} and 10^{25} g of chondrules produced in the asteroid belt. Understanding how they were made from precursor solids and disk gas is therefore a key task of cosmochemistry.

It is widely believed that chondrules were heated up to $\sim 2,000$ K on timescales of a few minutes and cooled relatively slowly (10–1,000 K/h) compared to a cooling controlled by free radiation into space. Because of these short timescales, one speaks of flash heating. Most chondrules have been flash-heated several times, suggesting that a repetitive process was responsible for high-temperature

processing. At present, the most popular mechanism for chondrules formation is the shockwave model, whereby a shockwave of speed ~ 10 km/s impacts dusty aggregates and heats them. The source of these shockwaves in the protoplanetary disk is not well identified. Gravitational instabilities, X-ray flares, and planetesimals supersonic motions have been proposed. All three models seem to face important difficulties.

Formation and Early Evolution of Telluric Planets

When the protoplanetary disk gas dissipated, we were left (in the inner Solar System) with a swarm of planetesimals and planetary embryos. It took roughly 100 Myr to collect these bodies into the terrestrial planets we know, such as the Earth. Growth occurred through random encounters of embryos. Though many embryos contributing to a given planet came from its neighborhood (the feeding zone), a significant number of embryos came from more distant regions.

Though accretion was mostly constructive, some impacts were also partly destructive. It is widely believed that the Moon was made when a planetary embryo, roughly the size of Mars, hit the proto-Earth. The Moon was built from that embryo, sometimes called Theia, and the Earth's mantle. Thanks to the Hf-W isotopic system, it is possible to constrain that catastrophic event which gave birth to our satellite. Latest measurements suggest it occurred 62_{-10}^{+90} Ma after Solar System formation, taken as the CAI formation.

It is worth noting that dynamical studies demonstrated that the presence of the Moon stabilized the Earth's obliquity. Were the Moon absent, the Earth's obliquity would vary chaotically and Earth's climate would have been far less stable than it has been. This singular, hazardous, event might therefore have played an important role in the development of life as we know it.

While planets were forming, they developed a magma ocean and iron cores appeared. Measurements based on the Hf-W isotopic system demonstrated that the Martian core formation was completed 10 Myr after the start of the Solar System. At present there is no undisputed estimate for the age of the Earth's core.

The origin of the terrestrial atmosphere is an unsolved problem. It is a combination of delivery of volatile compounds from extraterrestrial matter and of a primordial, solar-type atmosphere trapped in the Earth's mantle and subsequently degassed. The excess of ^{129}Xe (daughter isotope of ^{129}I) in the Earth's mantle compared to the Earth's atmosphere indicates that the degassing occurred early, possibly during the first 150 Myr.

The origin of terrestrial oceans has long been debated. Because they have a hydrogen isotopic composition different from that of Earth water, long-period comets such as comet Halley probably did not contribute significantly to the water budget. Jupiter-Family Comets and dark, water-rich asteroids are the best candidates. Their D/H ratio – measured in carbonaceous chondrites – is compatible with that of the terrestrial oceans. These celestial bodies might also have delivered organic matter which might have provided precursors to life chemistry. The timing of Earth's water delivery relative to the formation of the Moon is debated, though it seems pretty secure to state that water was delivered during the first 150 Myr.

At that point, all bodies were formed, and the architecture of the Solar System was only to be significantly changed once, during the Late Heavy Bombardment (LHB) 3.8 Ga ago. At that epoch, after 0.8 Gyr of slow migration, the giant planets Jupiter and Saturn crossed a resonance and destabilized a disk of planetesimals, which were sent to the inner Solar System. Many of the large craters seen today on the Moon date from that time. It is actually thanks to the return of the Moon rocks and their detailed study that the LHB was identified. If there was any life present on Earth at that time, it may have been severely affected. Some other authors proposed that these impacts could have, on the other hand, stimulated life.

Future Directions

It is a challenging task to foresee the development of a scientific discipline whose future depends on the advancement of techniques, on the emergence of individuals, and on the general policy adopted by a few prosperous countries which might not remain so indefinitely. Some progress will be made on the – already populous – data collection front. That should serve to solve pending key questions such as the homogeneity of short-lived radionuclides, or the locus and timing of organosynthesis. Instrumental developments should also help to revisit dogma that is rarely disputed, such as the flash heating model of chondrule formation for which evidence is thin.

Laboratory experiments trying to reproduce key processes of the early Solar System should also be developed. Condensation and evaporation experiments will illuminate the complex relationships between gas and solids within the protoplanetary disk, and establish chemical as well as isotopic modifications induced by these fundamental processes.

An almost virgin direction of research is the study of the mechanical property of meteorites. Very little is known, for example, on their tensile strength which is

key to our understanding of planetary accretion and evolution. Such measurements are desperately needed in the light of several space missions.

It is striking that, while a great deal is made of deuterium (^2H) and ^{15}N excesses in organic matter, the processes that gave rise to them are still debated. Developments on the modelling front is highly needed.

Cosmochemistry will certainly benefit from increased interaction with astrophysics. Observations of star-forming regions can be seen as a proxy of the environment of our Solar System formation. Thanks to space telescopes such as ► [Herschel](#), or ground-based interferometers, such as ► [ALMA](#), our understanding of accretion disks will be bettered, enabling us to “see” closer to the central star, in regions where precursors of planets similar to the Earth might form. Theoretical astrophysics should be a daily companion of cosmochemists, and one could dream of a world in which most, if not all, data collected are interpreted within a theoretical framework.

One exigency could represent a horizon for cosmochemistry: that of holding things together. Too many disparate interpretations coexist without being really coherent one with the other. Though some patches of the jigsaw puzzle have been thoroughly assembled, and though the global vision is probably correct, many of the data collected find no explanation within our current knowledge. In that respect, astrophysics will, as always, teach us humility. Though there is no reason for our Solar System to be special, there are many possible outcomes of star and planetary formation. Ours is one among billions in the Galaxy.

See also

- [ALMA](#)
- [Asteroid](#)
- [CAIs](#)
- [Comet](#)
- [Geochronology](#)
- [HERSCHEL](#)
- [Meteorite \(Allende\)](#)
- [Meteorite \(Murchison\)](#)
- [Meteorite \(Orgueil\)](#)
- [Oxygen Isotopes](#)

References and Further Reading

- Adams FC (2010) The Birth Environment of the Solar System. *ARAA* 48:47–85
- Bernatowicz TJ, Fraundorf G, Ming T, Anders E, Wopenka B, Zinner E, Fraundorf P (1987) Evidence for interstellar SiC in the Murray carbonaceous chondrite. *Nature* 330:728–730

- Bogard DD, Nyquist L et al (1984) Noble gas contents of shergottites and implications for the Martian origin of SNC meteorites. *GCA* 48:1723–1739
- Brownlee DE et al (2006) Comet 81P/wild 2 under a microscope. *Science* 314:1711–1716
- Clayton RN, Grossman L et al (1973) A component of primitive nuclear composition in carbonaceous meteorites. *Science* 182:485–488
- Clayton DD, Nittler LR (2004) Astrophysics with presolar stardust. *Annu Rev Astron Astr* 42:39–78
- Engrand C, Maurette M (1998) Carbonaceous micrometeorites from Antarctica. *Meteorit Planet Sci* 33:565–580
- Gomes R, Levison HF, Tsiganis K, Morbidelli A (2005) Origin of the cataclysmic late heavy bombardment period of the terrestrial planets. *Nature* 435:466–469
- Krot AN, Scott ERD et al (2005) Chondrites and the protoplanetary disk. *ASP Conference Series*, San Francisco
- Lauretta DS, McSween HY Jr (2008) *Meteorites and early solar system 2*. Arizona University Press, Tucson
- Lee T, Papanatassiou DA et al (1976) Demonstration of ^{26}Mg excess in Allende and evidence for ^{26}Al . *Geophys Res Lett* 3:109–112
- Lodders K (2003) Solar system abundances and condensation temperatures of the elements. *Astrophys J* 591:1220–1247
- McCall GJH, Bowden AJ, Howarth RJ (2006) *The history of meteoritics and key meteorite collections: fireballs, finds and falls*. Geological Society Special Publications, London
- Papike JJ (1998) *Planetary materials*. Mineralogical Society of America, Washington
- Patterson C (1956) Age of meteorites and the earth. *Geochim Cosmochim Acta* 10:230–237
- Shu FH, Shang H, Lee T (1996) Toward an astrophysical theory of chondrites. *Science* 271:1545–1552

Cosmogony

Definition

A cosmogony is any theory about the origin of the universe and/or the objects it contains. Most cultures developed their own cosmogony. In astronomy, the term usually refers to theories of formation of the Solar System.

COSPAR

Synonyms

[Committee on space research](#)

Definition

After the USSR launched its first Earth Satellite in 1957 and thereby opened the space age, the International Council of Scientific Unions (ICSU), now the International Council for Science, it established its Committee on Space Research (COSPAR) during an international meeting in London in 1958.

COSPAR's objectives are to promote on an international-level scientific research in space, with emphasis on the exchange of results, information and opinions, and to provide a forum open to all scientists. These objectives are achieved through the organization of Scientific Assemblies, publications, and other means. COSPAR's first Space Science Symposium was organized in Nice in January 1960. Now general assemblies are organized every other year.

In its first years of existence COSPAR, played an important role as an open bridge between East and West for cooperation in space. When this role became less prominent with the decline in rivalry between the two blocs, COSPAR, as an interdisciplinary scientific organization, focused its objectives on the progress of all kinds of research carried out with the use of space means (including balloons).

These activities are divided in "commissions" and inside the commission F is dedicated to Life sciences and subcommission F3 is devoted to astrobiology.

COSPAR has also concerned itself with questions of biological contamination and spaceflight while exploring the solar system. This proceeds from Article IX of the Treaty on Principles Governing the Activities of States in the Exploration and Use of Outer Space, Including the Moon and Other Celestial Bodies (also known as the UN Space Treaty of 1967). COSPAR, based on work of a dedicated planetary protection panel, proposes and maintains a planetary protection policy for the reference of spacefaring nations.

See also

- ▶ [Outer Space Treaty](#)
- ▶ [Planetary Protection](#)

Covalent Bonds

Definition

Covalent bonds are molecular bonds formed via the sharing of electrons according to Lewis rules to form closed electron shells of two, four, or six electrons (for single, double, or triple bonds, respectively). They are differentiated from ionic and ▶ [weak bonds](#) by the amount of energy required to break them; typically on the order of 150–1000 kJ/mole (~1.5–10 eV/mole), depending on the species. Covalent bonds tend to form between atoms of similar electronegativity. Covalent bonds formed between atoms of dissimilar electronegativity (i.e., C-Cl) will be polar, with a greater amount of the electron density centered around the more electronegative nucleus.

See also

- ▶ [Hydrogen Bond](#)
- ▶ [Weak Bonds](#)

Crater Chain

- ▶ [Catena, Catenae](#)

Crater, Impact

ROLAND J. WAGNER

German Aerospace Center (DLR), Institute of Planetary Research, Berlin, Germany

Keywords

Asteroid, collision, comet, impact, micrometeorite, surface

Definition

An impact crater is a mostly circular or elliptical elongate depression, generally with a raised rim, which is created by the impact of a minor body on the solid surface of a ▶ [planet](#) or ▶ [satellite](#). Impact craters range from the size of microcraters seen only microscopically on surfaces of ▶ [rock samples](#) (e.g., rocks from the lunar surface) to large craters and ▶ [impact basins](#) several hundreds or thousands of kilometers across. Impacts into the atmospheres of the large gaseous planets in the outer ▶ [Solar System](#) can produce transitory circular or semicircular features resembling craters, as has been observed on ▶ [Jupiter](#) after the impact of ▶ [Comet Shoemaker/Levy-9](#).

Overview

Impact craters on solid surfaces of planets and satellites are created by hypervelocity collisions with smaller bodies. These bodies, termed *impactors* or *projectiles*, range in size from ▶ [micrometeorites](#) to large bolides up to tens or hundreds of kilometers in diameter, which form impact basins several hundreds or thousands of kilometers across (Pike 1980; Melosh 1989). Candidate impactors are (1) ▶ [asteroids](#) from the ▶ [main belt](#) (MBA) or from other asteroid families, for example, Near-Earth asteroids (NEA) (Neukum et al. 2001; Strom et al. 2005), (2) ▶ [comets](#), including ▶ [ecliptic](#) or short-period comets (EC, orbital period < 200 years) derived from the ▶ [Kuiper belt](#), and nearly isotropic or long-period comets

(NIC, orbital period > 200 years) from the ► [Oort cloud](#) (Zahnle et al. 2003), (3) bodies or debris in planetocentric orbits (Neukum 1985; Chapman and McKinnon 1986), and (4) remnants of planetary accretion (planetesimals) (Wetherill 1975).

The number or frequency of craters on a surface per unit area records its age: the higher the crater frequency, the higher the age of the surface due to the longer exposure time to the incoming impactor flux. This relationship can be used as an important tool in planetary chronology.

Morphology and sizes of impact craters reflect impact conditions, projectile properties, target properties, and changes of target properties with time (Schenk et al. 2004). The smallest craters identified in camera images are simple craters, characterized by a bowl-shaped, parabolic crater morphology (e.g., Melosh 1989). With increasing diameter, crater forms become more complex. The simple-to-complex transition diameter approximately scales with the inverse of the gravity acceleration, except for icy surfaces as on ► [Mars](#) (ice in the regolith) and the icy satellites in the ► [Outer Solar System](#) (Chapman and McKinnon 1986; Melosh 1989; Schenk et al. 2004). Features observed in complex craters include (Pike 1980; Chapman and McKinnon 1986; Melosh 1989; Schenk et al. 2004) (a) flat crater floors (b) terraces at crater wall interiors, (c) central peaks, or (d) peak rings. On icy satellites, complex crater forms include (e) central pits (also observed on Mars [e.g., Barlow 2009]), (f) central domes, or (g) bright, almost flat circular areas termed *palimpsests* (► [Faculae](#)) devoid of prominent topographic features such as crater rims.

The largest impact structures are ► [impact basins](#), which exhibit two or even more rings (ridges or graben) and are termed multi-ring basins (e.g., Spudis 1993).

See also

- [Asteroid](#)
- [Asteroid Belt, Main](#)
- [Catena, Catenae](#)
- [Chronology, Cratering and Stratigraphy](#)
- [Comet](#)
- [Comet Shoemaker-Levy 9](#)
- [Ecliptic](#)
- [Facula, Faculae](#)
- [Impact Basin](#)
- [Jupiter](#)
- [Kuiper Belt](#)
- [Mars](#)
- [Micrometeorites](#)
- [Oort Cloud](#)
- [Planet](#)

- [Planet Formation](#)
- [Planetesimals](#)
- [Rock](#)
- [Satellite or Moon](#)
- [Solar System Formation \(Chronology\)](#)

References and Further Reading

- Barlow NG (2009) Martian central pit craters: summary of northern hemisphere results. Lunar and Planetary Science Conference 40th, abstr. 1915 [CD-Rom]
- Chapman CR, McKinnon WB (1986) Cratering of planetary satellites. In: Burns JA, Matthews MS (eds) *Satellites*. University of Arizona Press, Tucson, pp 492–580
- Melosh HJ (1989) *Impact cratering: a geologic process*. Oxford monographs on Geology & Geophysics, vol 11. Oxford University Press, New York, p 245
- Neukum G (1985) Cratering records of the satellites of Jupiter and Saturn. *Adv Space Sci* 5:107–116
- Neukum G, Ivanov BA, Hartmann WK (2001) Cratering records in the inner solar system in relation to the lunar reference system. In: Hartmann WK, Geiss J, Kallenbach R (eds) *Chronology and evolution of Mars*. Kluwer, Dordrecht, pp 53–86
- Pike RJ (1980) Control of crater morphology by gravity and target type: Mars, Earth, Moon. *Proceedings of the Lunar and Planetary Science Conference 11th*, Houston, pp 2159–2189
- Schenk PM, Chapman CR, Zahnle K, Moore JM (2004) Ages and interiors: the cratering record of the Galilean satellites. In: Bagenal F, Dowling T, McKinnon W (eds) *Jupiter – the planet, satellites and magnetosphere*. Cambridge University Press, Cambridge, pp 427–456
- Spudis PD (1993) *The geology of impact basins: the moon and other planets*. Cambridge University Press, Cambridge, 263 pp
- Strom RG, Malhotra R, Takashi I, Yoshida F, Kring DA (2005) The origin of planetary impactors in the inner Solar System. *Science* 309:1847–1850
- Wetherill GW (1975) Late heavy bombardment of the moon and the terrestrial planets. *Proceedings of the Lunar and Planetary Science Conference 6th*, Houston, pp 1539–1561
- Zahnle K, Schenk P, Levison H, Dones L (2003) Cratering rates in the outer Solar System. *Icarus* 163:263–289

Cratering Chronology

- [Chronology, Cratering and Stratigraphy](#)

Craton

Definition

A *craton* is an old and stable part of the continental ► [lithosphere](#). The crustal part typically is composed of granitoids and high-grade, strongly deformed metamorphic rocks, and less metamorphosed metavolcanic

and metasedimentary segments (► [greenstone belts](#)). The crustal portion is thicker than normal continental crust (40 km) and is underlain by a deep (up to several hundred km) root of low-density depleted lithospheric mantle. Cratons formed through orogenesis (mountain-building processes) and accretion of crustal fragments during the Archean when mantle and crustal temperatures were higher than those of today. When covered by younger sedimentary basins, they are referred to as platforms.

See also

- [Archea](#)
- [Continental Crust](#)
- [Crust](#)
- [Granite](#)
- [Greenstone Belts](#)
- [Lithosphere](#)
- [Shield](#)

Crenarchaeota

Definition

Crenarchaeota is one of the four phyla of ► [Archaea](#). Crenarchaeota comprises both hyperthermophilic and cold-dwelling prokaryotes. The hyperthermophilic species of Crenarchaeota tend to cluster closely together and occupy short branches on the 16S rRNA gene phylogenetic tree. These organisms are considered good models for early Archaea. In contrast, cold-dwelling Crenarchaeota have been identified only as community samples of 16S ribosomal RNA in the ocean. Phylogenetically, these are a more rapidly evolving species. Most hyperthermophilic Crenarchaeota have been isolated from geothermal heated soils, waters containing elemental sulfur and sulfides, or hydrothermal vents. Among the hyperthermophilic Crenarchaeota, we can find members of the Sulfolobales, Thermoproteales and Desulfurococcales orders. One species of *Sulfolobus*, *S. acidocaldarius*, was the first hyperthermophilic Archaea discovered. It was isolated by Thomas Brock and colleagues in ► [Yellowstone National Park](#), U.S.A. in 1970. Special mention should be given to *Pyrodictum fumarii* that can grow at 113°C.

See also

- [Acidophile](#)
- [Archea](#)
- [Deep-Sea Microbiology](#)

- [Hyperthermophile](#)
- [Phylogeny](#)
- [Sulfur Cycle](#)
- [Yellowstone National Park, Natural Analogue Site](#)

Crossing Over

- [Recombination](#)

Crust

Definition

The crust is the outer rocky layer of the Earth. It is also refers to the outer rocky layer of telluric planets or moons. The Earth's crust has a relatively low density and floats on the underlying mantle. ► [oceanic crust](#), which covers about two thirds of the Earth's surface, is 6–9 km thick and composed mainly of basalt. ► [continental crust](#) is thicker – about 10-km thick in rifted portions, >80 km thick beneath active mountain belts, averaging about 30 km. Continental crust is composed mainly of granitic and metamorphic rocks. Oceanic crust forms at spreading centers and is never older than 200 Ma. Continental crust has formed continuously throughout Earth's history, from 3.8 or even 4.3 Ga. Mars and probably Venus have basaltic crusts. The lunar crust is basaltic in maria and composed of ► [anorthositic](#) breccia in lunar highlands.

See also

- [Anorthosite](#)
- [Continental Crust](#)
- [Craton](#)
- [Crust](#)
- [Kreep](#)
- [Moon, The](#)
- [Oceanic Crust](#)
- [Plate Tectonics](#)

Crustal Deformation

- [Archean Tectonics](#)

Cryocooler

- ▶ [Cryostat](#)

Cryophile

- ▶ [Psychrophile](#)

Cryosphere

Definition

The *cryosphere* is that part of the Earth and other planets in which temperatures are low and water is solid. On Earth, it constitutes the polar ice caps and pack ice, mountain glaciers, cold deserts, and regions of permafrost. During the times of global ▶ [glaciation](#) in the Proterozoic – the “▶ [Snowball Earth](#)” periods – the cryosphere encompassed almost all the planet, as is the case at the present time for icy moons such as ▶ [Europa](#).

See also

- ▶ [Europa](#)
- ▶ [Glaciation](#)
- ▶ [Snowball Earth](#)

Cryostat

Synonyms

[Cryocooler](#); [Dewar flask](#)

Definition

A cryostat is an apparatus used to maintain very low (“cryogenic” ~100 K) temperatures. It typically consists of two vessels, one mounted inside of the other. The inner vessel contains the cold sample (cryogen) mounted inside an evacuated outer vessel. The vessels are held together by a material with low-thermal conductivity. The vacuum in the outer vessel serves as a thermal insulator. The two vessels are separated by a radiation shield to prevent heat transfer. The radiation shield is cooled by a cryocooler.

In medicine, a cryostat is a device to cut histological slides, consisting of a microtome (ultra-thin slicer) in a freezer.

Cryovolcanism

Definition

Cryovolcanism is a volcanic phenomenon that occurs in extremely low temperature environments. There, instead of molten silicates, cryovolcanoes erupt liquid water, methane, ammonia, or sulfur dioxide onto the icy surface of a body. It has been observed on several satellites in the outer solar system. In particular, active cryovolcanism has been discovered on ▶ [Enceladus](#), a satellite of Saturn. Traces of cryovolcanism are also found on ▶ [Titan](#) and on Neptune’s satellite ▶ [Triton](#). Cryovolcanism generally erupts water (H₂O), methane (CH₄), and ammonia (NH₃). Cryovolcanism could also be present on other satellites of the giant planets and on ▶ [trans-Neptunian objects](#).

See also

- ▶ [Enceladus](#)
- ▶ [Titan](#)
- ▶ [Trans-Neptunian Object](#)
- ▶ [Triton](#)

Cryptoendolithic

Definition

Cryptoendolithic refers to one of the three subclasses in which “▶ [Endolithic](#)” microorganisms are classified. Cryptoendolithic microorganisms are those able to colonize the empty spaces or pores inside a rock with the connotation of being hidden. This connotation is important to astrobiology as these protected environments inside rocks are putative habitable niches where life could be sustained in very adverse conditions or space environments. Cryptoendolithic microorganisms can survive on inorganic metabolites from the surroundings, thus these microbes are mainly lithotrophs. Depending on the physicochemical properties of the mineral structure of the rock, it can provide protection against damaging radiation. Some reported examples have been described in

basaltic rocks from Antarctica where low temperatures are very restrictive for life, or from high altitude environments with high radiation doses.

See also

- ▶ [Chemolithotroph](#)
- ▶ [Endolithic](#)

CS

- ▶ [Carbon Monosulfide](#)

CSA

Synonyms

[Canadian Space Agency](#)

Definition

The Canadian Space Agency was established in 1989 and is committed to lead the development and application of space knowledge for the benefit of Canadians and humanity. Canada began space activities at the early stage of the space era, through an agreement with the US National Aeronautic and Space Administration (▶ [NASA](#)) to build and launch satellites to study the upper atmosphere. For several years from 1958, Canada operated jointly with the USA, the Fort Churchill base in Manitoba, to launch sounding rockets. In 1969, the federal government created Telesat Canada to build and exploit Canadian communication satellites. The government also set up a Department of Communications that immediately took over from the Communications Research Centre and the Interdepartmental Committee on Space. In 1974, NASA awarded Canada the responsibility of designing, developing, and building the Shuttle Remote Manipulator System (SRMS) for the Space Shuttle. This agreement resulted in Canadarm, the shuttle's 15-m robotic arm and led to the flight, in 1984, of the first Canadian Astronaut (Marc Garneau). In 1979, Canada became an associate member of the European Space Agency (▶ [ESA](#)) and in 1985, Canada accepted to participate in the ▶ [International Space Station programme](#). Canadian scientists are cooperating worldwide in manned space flight, space sciences, and exploration of the Solar System. For astrobiology, Canada offers also several sites that could be studied or used as Martian analogues.

Canada is pursuing a strategy to develop its expertise in remote sensing, space robotics, and space telecommunication.

In 2010, the CSA is employing around 700 full-time equivalents.

Culture Media

- ▶ [Macronutrient](#)

Curiosity

- ▶ [Mars Science Laboratory](#)

Cuvier's Conception of Origins of Life

History

The French naturalist Georges Cuvier (1769–1832) was one of the most important comparative anatomists and paleontologists of the beginning of the nineteenth century. Concerning history of life, Cuvier claimed a form of fixism explaining changes of species during geological time. He imagined several disasters during which certain species would disappear and after which new species would come from other places. During the first part of the nineteenth century, his proposal had a very significant place in biology and paleontology.

See also

- ▶ [Darwin's Conception of Origins of Life](#)
- ▶ [Lamarck's Conception of Origins of Life](#)

Cyanamide

Synonyms

[Amidocyanogen](#); [Carbamonitrile](#); [Carbimide](#);
[Carbodiimide](#); [Cyanamine](#); [N-Cyanoamine](#);
[Cyanogenamide](#); [Cyanogen nitride](#); H_2NCN ; [Hydrogen cyanamide](#)

Definition

A simple compound (H_2NCN) formed by the irradiation of cyanide. Cyanamide has been detected in the interstellar medium, and has been shown to be an effective condensation agent for both peptides and nucleotides. Reaction of cyanamide with water yields urea:



Reaction with ammonia gives guanidine:



Reaction with amines, such as amino acids, gives *N*-carbamoylamino acids and hydantoins.

See also

► [Hydantoin](#)

4-Cyano-1,3-Butadiynyl

Synonyms

C_5N ; [Cyanobutadiynyl radical](#)

Definition

The C_5N ► [radical](#) is found in both the envelopes of evolved carbon stars and in cold, dark interstellar ► [molecular clouds](#) (typically those that have not been heated by star formation). It is an intermediary in the chemistry of the ► [cyanopolyynes](#) and related molecules (Guelin et al. 1998). The rotational transitions of the cyanobutadiynyl radical are observed by radio astronomers at millimeter wavelengths. The anion of this species C_5N^- has also been found in space (Cernicharo et al. 2008).

See also

► [Cyanopolyynes](#)
 ► [Molecular Cloud](#)
 ► [Radical](#)
 ► [Stellar Evolution](#)

References and Further Reading

Cernicharo J, Guélin M, Agúndez M, McCarthy MC, Thaddeus P (2008) Detection of C_5N^- and vibrationally excited C_6H in IRC +10216. *Astrophys J* 688:L83–L86

Guelin M, Neiningen N, Cernicharo J (1998) Astronomical detection of the cyanobutadiynyl radical C_5N . *Astron Astrophys* 335:L1–L4

Cyano Radical

► [Cyanogen Radical](#)

Cyanoacetylene

Synonyms

[CAA](#)

Definition

Cyanoacetylene, HC_3N ($\text{H}-\text{C}\equiv\text{C}-\text{C}\equiv\text{N}$), is an organic molecule that is the simplest cyanopolyne ($\text{H}(-\text{C}\equiv\text{C})_n-\text{C}\equiv\text{N}$). It was one of the first molecules detected in space using radioastronomical techniques (Turner 1971). It is also an important component of ► [Titan's atmosphere](#) (Kunde et al. 1981), where it is found in the gas phase in the upper atmosphere and in ice form in the lower stratosphere (see, e.g., Anderson et al. 2010). It is a trace constituent in cometary atmospheres (comae). Cyanoacetylene has been proposed as a prebiotic reagent for the formation of pyrimidine bases, nucleosides, and nucleotides (Sanchez and Orgel 1970; Powner et al. 2009).

See also

► [Titan](#)

References and Further Reading

Anderson CM, Samuelson RE, Bjoraker GL, Achterberg RK (2010) Particle size and abundance of HC_3N ice in Titan's lower stratosphere at high northern latitudes. *Icarus* 207:914

Kunde VG, Aikin AC, Hanel RA, Jennings DE, Maguire WC, Samuelson RE (1981) C_4H_2 , HC_3N and C_2N_2 in Titan's atmosphere. *Nature* 292:686

Powner MW, Gerland B, Sutherland JD (2009) Synthesis of activated pyrimidine ribonucleotides in prebiotically plausible conditions. *Nature* 459:239

Sanchez RA, Orgel LE (1970) Studies in prebiotic synthesis. V. Synthesis and photoanomerization of pyrimidine nucleosides. *J Mol Biol* 47:531

Turner BE (1971) Detection of interstellar cyanoacetylene. *Astrophys J* 163:L35

Cyanamine

► [Cyanamide](#)

Cyanobacteria

JOSEF ELSTER^{1,2}, JANA KVÍDEROVÁ¹

¹Institute of Botany, Academy of Sciences of the Czech Republic, Třeboň, Czech Republic

²University of South Bohemia, České Budějovice, Czech Republic

Synonyms

Blue-green algae; Blue-green bacteria; Cyanophyceae

Keywords

Antarctic, carbon and nitrogen cycles, desiccation, endosymbiosis, extremophiles, freeze-melt stress, halophily, irradiance, limits of survival, oxygenic photosynthesis, psychrophily, thermophily, ultraviolet radiation

Definition

► **Cyanobacteria** are photosynthetic ► **bacteria** that use ► **water** as reducing power to release O₂. They evolved early in Earth history. As bacterial primary producers, cyanobacteria occupy a privileged position among organisms due to their role in the carbon and nitrogen cycles. They are widely adapted to different extreme environments and play an important role, especially in cold polar and alpine environments, because of their tolerance of a wide temperature range, ► **desiccation**, freeze-melt and salinity stress.

Overview

Cyanobacteria are oxygenic photosynthetic prokaryotes responsible for the transformation of a reduced atmosphere to an oxidized one. The oxygen produced by this photosynthetic group of bacteria drove life to adapt to the newly formed aerobic environments, resulting in the evolution of novel physiologies, biochemistries and morphologies. In addition, cyanobacteria, as the photosynthetic partner in the primary endosymbiotic event, introduced photoautotrophy to eukaryotes. The geopaleological record indicates that cyanobacterial ► **photosynthesis** took place early in our planet's history. As primary producers, cyanobacteria occupy a privileged position among organisms because of their role in carbon and nitrogen (N-fixers) cycles (Whitton and Potts 2000; Knoll 2008; Swingle et al. 2008).

In comparison with other groups of bacteria, cyanobacteria exhibit an unusually wide range of morphologies. Traditional taxonomic cyanobacterial classification

is based on morphology and development, recognizing five principal groups: Group I – *Chroococcales* – solitary and colonial unicellular forms; Group II – *Pleurocapsales* – unicellular to pseudo-filamentous, with cells capable of multiple as well as binary fission; Group III – *Oscillatoriales* – filamentous forms with ► **cell** differentiation; Group IV – *Nostocales* – filamentous with cell differentiation to produce akinetes and heterocysts; and finally Group V – *Stigonematales* – with cell differentiation and complex multicellular organization (Komárek and Anagnostidis 1998, 2005). Results of the application of recent molecular techniques (e.g., sequence of the 16 S rRNA gene), support some but not all these groups. Features like cell differentiation or multiple fissions are supported by molecular analyses, whereas unicellular forms and simple filaments do not generate monophyletic groups. It has been possible to reconstruct an evolutionary history of the cyanobacterial groups, establishing a framework for resolving how their metabolic and phenotypic diversity came about (Six et al. 2007).

Probably due to their evolutionary antiquity, cyanobacteria are widely adapted to all extremes related to changes in geological time (Elster et al. 2001). Tolerance of low-oxygen conditions is still widespread among cyanobacteria and free sulfide is tolerated by some strains. In addition, some cyanobacterial strains can use H₂S as a hydrogen donor. They also tolerate high doses of ultraviolet B and C radiation. All these features have been especially important in the early evolution of cyanobacteria.

Many cyanobacteria can develop in extreme environments, at extremely high (geothermal springs) and low (Antarctic, Arctic, alpine areas, permafrost) temperatures, in hypersaline (halophiles) and alkaline (alkaliphiles) habitats, under high radiation conditions, desiccation, and toxicity stress, etc. A brief survey follows the occurrence of cyanobacteria in different extreme environments.

Thermophilic Cyanobacteria

Results of recent molecular biological studies provide new information about cyanobacteria that inhabit high-temperature habitats. A number of earlier reports proposed that thermophilic cyanobacteria had branched out at the beginning of their evolution. However, recent studies have brought arguments for a later emergence of thermophilic cyanobacteria. The present analyses (Ward and Castenholz 2000) strongly confirm two distinct thermophilic lineages. Geothermal springs can be considered as isolated islands and therefore an ideal site for the origin and evolution of endemic species. Some species of

Thermosynechococcus spp. are clearly restricted in geographical distribution, although other thermophilic cyanobacteria, such as *Mastigocladus laminosum* and *Cyanothece minervae*, appear to be cosmopolitan.

Cyanobacteria occupying geothermal springs are not observed below ► pH 4, and their diversity is quite restricted at pH below 6. Temperature, in combination with availability of nitrogen and the presence of free sulfide determines the cyanobacterial species composition, because sulfide is an efficient inhibitor of oxygenic photosynthesis. The detected upper-temperature limit for cyanobacteria (*Synechococcus lividus*) and for global photosynthesis is presently 73–74°C.

Cyanobacteria Under Low Temperature, Desiccation, and Salinity Stress

Cyanobacteria, frequently considered warm water organisms, play an important role in the carbon and nitrogen cycling in cold polar and alpine environments. The ecophysiological features that predetermine their dominance in these environments include: slow growth rate over a wide temperature range, tolerance to desiccation, freeze-melt and salinity stress, and a variety of photoacclimation strategies to both high and low solar irradiance. In cold environments, where invertebrate grazing pressure is limited, the large standing stocks of cyanobacterial biomass are the result of its gradual accumulation over many seasons (Vincent 2000).

Most polar and alpine cyanobacterial species tested up to now are rather more psychrotolerant than psychrophilic. Polar cyanobacteria have long doubling times in comparison with psychrophilic eukaryotic ► algae and heterotrophic bacteria.

Diverse evidence indicates that the unsaturation of ► membrane lipids correlates with low-temperature sensitivity, although this is not the only factor that regulates low-temperature resistance in cyanobacteria. The unsaturation apparently protects the photosystem II complex from low-temperature photoinhibition.

Cyanobacteria have several strategies to minimize osmotic and mechanical stresses. They are able to produce mucopolysaccharides (exopolymeric substances), which slow down the flow of liquid water during freeze up and thaw (Vincent 2000). Cyanobacteria also respond to these stresses by producing compatible solutes. Large disaccharide sugars, such as trehalose, sucrose, and glucosylglycerol, are typical compatible solutes in water-stressed cyanobacteria (Reed et al. 1984). The extreme tolerance of cyanobacteria to desiccation is exemplified by their ability to tolerate very low water potential. *Chroococcus* and

Chroococciopsis can both fix CO₂ at remarkably low water potentials.

Cyanobacteria are an important component of hypersaline ecosystems. Compatible solutes are especially vital for cyanobacterial survival in saline desert evaporate soils when they are under the combined stress of desiccation and hypersaline conditions (Oren 2000). In these habitats, glycine betaine is the most common compatible solute. A wide range of species belonging to different taxonomical groups has been reported to thrive at high salt concentrations (e.g., *Microcoleus chthonoplastes*, *Oscillatoria limnetica*, *Synechocystis* spp.).

Light and UV Radiation

Under natural conditions, cyanobacteria experience light conditions that fluctuate rapidly, frequently reaching suboptimal levels for photosynthesis. Both the intensity and quality of the irradiance can vary dramatically during the day and amongst habitats. In desert terrestrial environments, irradiance may be very bright and cause photoinhibition or damage to the reaction centers of PSII (photooxidative bleaching). Cyanobacteria can modify the protein composition of PSII at high irradiance, making the PSII reaction centers less susceptible to photoinhibition. Rapid light intensity or quality fluctuations result in rapid photoacclimation processes, such as state transition that can modify the photosynthetic apparatus within minutes. These short-term modifications usually do not need protein synthesis. For example, during the state transitions, the phycobilin antennae migrate between the photosystems to optimize the distribution of incoming radiant ► energy (Bhaya et al. 2000).

In addition, many cyanobacteria are exposed to environmental conditions where continuous ultraviolet radiation (UVR) plays an important role. UVR can lead to direct photochemical damage and degradation of cellular components, or to indirect effects produced by reactive oxygen species. Cyanobacteria possess four lines of defense against UVR (Vincent 2000): (1) They can avoid UVR injuries by selection of ► habitat (move to deeper water, live beneath rock surface, or deep within microbial mats); (2) production of umbrella compounds that filter UVR, such as the black or dark pigment Scytonemin (absorbance at ca 390 nm) and mycosporine-like amino acids (absorbance at 310–360 nm); (3) production of carotenoids (canthaxanthin, myxoxanthophyll, and related compounds), which protect the cells from the oxidative stress caused by the UVR; (4) further protection against long-term effects of UVR exposure due to the ability to identify

and repair the photochemical damage to DNA or the photosynthetic apparatus (Vincent 2000).

Key Research Findings

Some extreme environments on Earth are used as field analogues of extraterrestrial conditions, allowing the limits of survival of various ► [microorganisms](#) including photosynthetic cyanobacteria to be determined. Since cyanobacteria dominate in the polar regions, they can serve as model organisms for evaluation of survival at low temperatures and other stress factors common to the polar ► [environment](#). In the most extreme Antarctic conditions, cyanobacteria play a determining role in (1) desert communities, including soil crust, ► [epilithic](#), and ► [endolithic](#) species of cold polar deserts, e.g., in Dry Valleys in the Antarctic, where the conditions resemble the ► [Mars](#) surface (Friedmann 1982), and (2) benthos of permanently frozen lakes, e.g., Lakes Hoare and Fryxell, in the Antarctic, which represent another environment that could occur on Mars (de Pablo et al. 2008). The conditions of permanently ice-covered lakes and seas could also be relevant for ► [Europa](#); however, cyanobacteria are not common components of polar seas.

Simulation of conditions on other planets or during interplanetary transport is another approach to the estimation of limits of survival. *Chroococcidiopsis* sp. is able to survive in Mars-like conditions when it is covered by at least 1 mm of Mars soil analogue that reduces the incoming ► [UV radiation](#). Due to its resistance, this cyanobacterium was proposed as a pioneer microorganism for Mars terraforming (Friedmann and Ocampo-Friedmann 1995). The resistance of the ► [halotolerant](#) *Synechococcus* to space conditions was evaluated during the BIOPAN-3 mission and the effect of space radiation on primary producers, including cyanobacteria, as part of the EXPOSE-R mission launched on 2008 (Rabbow et al. 2009).

Future Directions

As mentioned, cyanobacteria represent the earliest organisms capable of oxygenic photosynthesis. Together with other non-oxygenic photoautotrophs, such as sulfur bacteria, they provide insight into the origin and evolution of photosynthetic processes and data for the estimation of their possible modifications on planets orbiting stars of different spectral classes (Xiong and Bauer 2002).

See also

- [Adaptation](#)
- [Antarctica](#)

- [Bacteria](#)
- [Biofilm](#)
- [Carbon Cycle \(Biological\)](#)
- [Chlorophylls](#)
- [Chloroplast](#)
- [Cryptoendolithic](#)
- [Colonization \(Biological\)](#)
- [Cryosphere](#)
- [Desiccation](#)
- [Earth's Atmosphere, Origin and Evolution of](#)
- [Endolithic](#)
- [Endosymbiosis](#)
- [Epilithic](#)
- [Extreme Environment](#)
- [Extremophiles](#)
- [Fossil](#)
- [Halophile](#)
- [Halotolerance](#)
- [Mars Terrestrial Analogues](#)
- [Membrane](#)
- [Mesophile](#)
- [Microbial Mats](#)
- [Microfossils](#)
- [Nitrogen Cycle \(Biological\)](#)
- [Nitrogen Fixation](#)
- [Osmolite](#)
- [pH](#)
- [Photosynthesis](#)
- [Phototroph](#)
- [Phylogeny](#)
- [Psychrophile](#)
- [Stromatolites](#)
- [Thermophile](#)
- [UV Radiation](#)
- [Water](#)

References and Further Reading

- Bhaya D, Schwarz R, Grossman AR (2000) Molecular responses to environmental stress. In: Whitton BA, Potts M (eds) The ecology of cyanobacteria; their diversity in time and space. Kluwer Academic Publishers, Dordrecht, London/Boston, pp 397–442
- de Pablo MA, Pacifici A, Komatsu G (2008) A possible small frozen lake in Utopia Planitia, Mars. In: 39th lunar and planetary science conference, (lunar and planetary science XXXIX), League City, Texas, p 1057
- Elster J, Seckbach J, Vincent WF, Lhotský O (eds) (2001) Algae and extreme environments; ecology and physiology. Nova Hedwigia, Berlin, Stuttgart, p 602
- Friedmann EI (1982) Endolithic microorganisms in Antarctic cold desert. Science 215:1045–1053
- Friedmann EI, Ocampo-Friedmann R (1995) A primitive cyanobacterium as pioneer microorganism for terraforming Mars. Adv Space Res 15:143–246

- Knoll AH (2008) Cyanobacteria and earth history. In: Herrero A, Flores E (eds) *The cyanobacteria: molecular biology, genomics and evolution*. Caister Academic, Norfolk, UK, pp 1–19
- Komárek J, Anagnostidis K (1998) Cyanoprokaryota 1. Teil: chroococcales. In: Ettl H, Gärtner G, Heynig H, Mollenhauer D (eds) *Süßwasserflora von mitteleuropa 19/1*. Gustav Fisher, Jena, Stuttgart/Lübeck, Ulm, p 548
- Komárek J, Anagnostidis K (2005) Cyanoprokaryota 2. Teil: oscillatoriales. In: Ettl H, Gärtner G, Heynig H, Mollenhauer D (eds) *Süßwasserflora von mitteleuropa 19/2*. Gustav Fisher, Jena, Stuttgart/Lübeck, Ulm, p 759
- Oren A (2000) Salts and brines. In: Whitton BA, Potts M (eds) *The ecology of cyanobacteria; their diversity in time and space*. Kluwer Academic Publishers, Dordrecht, London/Boston, pp 281–306
- Rabbow E, Horneck G, Rettberg P, Schott J-U, Panitz C, L'Afflito A, von Heise-Rotenburg R, Willnecker R, Baglioni P, Hatton J, Dettmann J, Demets R, Reitz (2009) EXPOSE, an astrobiological exposure facility on the international space station. *Orig Life Evol Bios* 39:581–598
- Reed RH, Richardson DL, Warr SRC, Stewart WDP (1984) Carbohydrate accumulation and osmotic stress in cyanobacteria. *J Gen Microbiol* 130:1–4
- Six Ch, Thomas J-C, Garczarek L, Ostrowski M, Dufresne A, Blot N, Scanlan DJ, Partensky F (2007) Diversity and evolution of phycobilisomes in marine *scheuchococcus* spp.: a comparative genomic study. *Genome Biol* 8:259
- Swingley WD, Blankenship RE, Jason R (2008) Insights into cyanobacterial evolution from comparative genomics. In: Herrero A, Flores E (eds) *The cyanobacteria: molecular biology, genomics and evolution*. Caister Academic, Norfolk, UK, pp 21–43
- Vincent WF (2000) Cyanobacterial dominance in polar regions. In: Whitton BA, Potts M (eds) *The ecology of cyanobacteria; their diversity in time and space*. Kluwer Academic Publishers, Dordrecht, London/Boston, pp 321–340
- Ward DM, Castenholz RW (2000) Cyanobacteria in geothermal habitats. In: Whitton BA, Potts M (eds) *The ecology of cyanobacteria; their diversity in time and space*. Kluwer Academic Publishers, Dordrecht, London/Boston, pp 37–59
- Whitton BA, Potts M (2000) Introduction to the cyanobacteria. In: Whitton BA, Potts M (eds) *The ecology of cyanobacteria; their diversity in time and space*. Kluwer Academic Publishers, Dordrecht, London/Boston, pp 1–11
- Xiong J, Bauer CE (2002) Complex evolution of photosynthesis. *Annu Rev Plant Biol* 53:503–521

Cyanobacteria, Diversity and Evolution of

LUCAS J. STAL
Department of Marine Microbiology, Netherlands
Institute of Ecology NIOO-KNAW,
Yerseke, The Netherlands

Synonyms

Blue-green algae; Oxygenic phototrophic bacteria; Oxyphotobacteria

Keywords

Carbon dioxide fixation, chloroplast, cyanobacteria, diversity, evolution, heterocysts, nitrogen fixation, oxygenic photosynthesis, photosynthesis

Definition

Cyanobacteria are oxygenic phototrophic microorganisms. They belong to the ► **Bacteria** domain of life and have a plant-type ► **photosynthetic** apparatus. They possess two photosystems, PS-I and PS-II, which are connected in series and their reaction centers usually contain *chlorophyll a*. Water is used as the electron donor and is split into electrons and oxygen by PS-II. The electrons are transported through an electron transport chain through PS-I and eventually reduce electron carriers. These are mainly used for the fixation of carbon dioxide through the reductive pentose phosphate pathway. Their main light-harvesting pigments are the blue and red colored phycobiliproteins.

Overview

Cyanobacteria are a monophyletic but highly diverse group of microorganisms (Rippka et al. 1979). Although they are often called “blue-green algae,” they belong to the domain Bacteria and they lack a nucleus or other cell organelles (Stanier and Cohen-Bazire 1977). The confusion with algae, which belong to the domain Eukarya, is understandable since cyanobacteria possess a plant-type photosynthetic system, with two photosystems, PS-I and PS-II, connected in series. Cyanobacteria use water as the electron donor, which by its splitting results in the evolution of oxygen, and their reaction centers normally contain the plant pigment *chlorophyll a*. Cyanobacteria fix CO₂ through the reductive pentose phosphate pathway (Calvin cycle) with ribulose-1,5-bisphosphate carboxylase/oxygenase (RubisCO) as the CO₂-fixing enzyme. This pathway is also common among other autotrophic Bacteria. Cyanobacteria occur in almost any illuminated environment of earth, including those characterized by extreme conditions, perhaps with the exception of acidic environments.

It is now well established that the eukaryotic plant cell evolved through an endosymbiotic event during which a cell engulfed a cyanobacterium, which subsequently evolved to become a chloroplast, the photosynthetic factory of plant cells (Raven and Allen 2003). The 16 S rRNA genes of the chloroplast cluster phylogenetically with the cyanobacteria. Modern cyanobacteria enter into a large variety of symbioses with microalgae and plants, often providing their hosts with fixed nitrogen (Rai et al. 2000).

Cyanobacteria invented oxygenic photosynthesis and were therefore responsible for the oxygenation of the Earth's atmosphere (Knoll 2003). The first big oxygen event occurred 2.5 billion years ago when the oxygen concentration reached 10% of its present value. Besides this rise in the oxygen level of the atmosphere there is other evidence for the presence of cyanobacteria at that time. There are microfossils that resemble modern cyanobacteria since 2.1 Ga and there are molecular fossils such as methylhopanoids that are considered to have originated from them since 2.7–2.5 Ga. Moreover, phylogenetic evidence also points to the presence of cyanobacteria at that time (Sanchez-Baracaldo et al. 2005). Other studies have suggested an even earlier origin of cyanobacteria of up to almost 3.5 billion years. This goes back to the earliest evidence of life on Earth. This evidence was based on microfossils interpreted to possess similarity to modern cyanobacteria and stable isotope data suggestive of CO₂ fixation by autotrophic organisms. It goes without saying that other organisms could have been responsible for these signatures. However, there is no doubt that cyanobacteria must have evolved long before free oxygen appeared in the atmosphere. It must have taken a long time until the oxygen evolved by the cyanobacteria had oxidized the massive reducing crust and the euphotic layer of the ocean. Thus, it is likely that the origin of cyanobacteria occurred early in the evolution of life on Earth, earlier than 2.5 Ga.

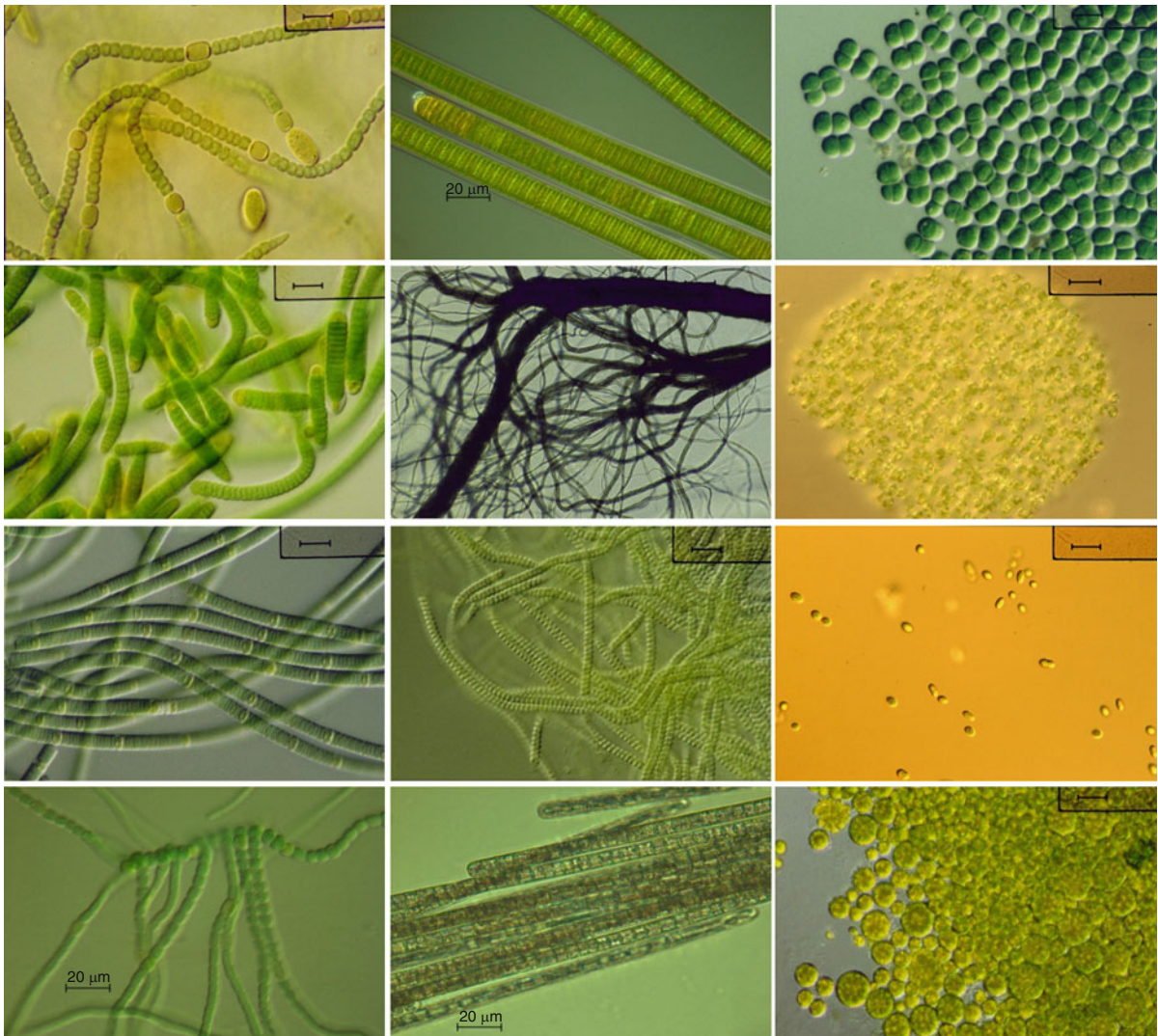
Obviously, an oxygenic phototrophic organism with two photosystems did not evolve at once (Olson and Blankenship 2004). There is no doubt that the predecessor of the cyanobacteria was an anoxygenic phototrophic organism with one photosystem. However, such organism might have been morphologically indistinguishable from modern cyanobacteria. Some modern cyanobacteria are capable of anoxygenic PS-I dependent photosynthesis using sulfide as the electron donor.

Although monophyletic, cyanobacteria exhibit an amazing diversity. They differ 2 orders of magnitude in size from the smallest cyanobacteria measuring ~0.5 µm to the biggest of ~50 µm and from unicellular forms to filamentous species of which the trichomes can be as long as 10 mm. Cyanobacteria are also quite unique since they are among the very few organisms outside the Eukarya that display true cell differentiation. Moreover, the growth of populations of Cyanobacteria may be macroscopic in the form of well-defined structured aggregates.

Cyanobacteria are divided into 5 large divisions that are supported by the phylogeny of the 16 S rRNA gene (Fig. 1). Divisions 1 and 2 are unicellular. Cyanobacteria of division 1 may divide in one, two, or three planes,

resulting in typical morphologies of the aggregates. Division 2 is composed of cyanobacteria that divide by multiple fissions and produce small daughter cells, called bacocytes. Although considered unicellular, several representatives form more or less regular aggregates or colonies, often surrounded with a structured sheath. Division 3 comprises all filamentous cyanobacteria with solely undifferentiated cells. Also these cyanobacteria may form various forms of more or less structured sheathed colonies and bundles. Divisions 4 and 5 comprise filamentous cyanobacteria that show true cell differentiation. Under nitrogen starvation some cells in the filaments differentiate into heterocysts (also called by the more appropriate but less common name heterocytes). Heterocysts have only photosystem I and therefore do not evolve oxygen and do not fix CO₂. For carbon and reducing equivalents they depend on the neighboring cells. Heterocysts are the site of N₂ fixation in these organisms. The special thick glycolipid cell envelope represents a gas diffusion barrier, limiting the flux of oxygen into the cell, thereby providing an anaerobic environment for the oxygen-sensitive nitrogenase. Many heterocystous cyanobacteria also produce akinetes (Adams and Duggan 1999). These are differentiated cells that have also been termed incorrectly “spores” and serve to enhance survival of the organism under unfavorable conditions. Akinetes are drought and radiation resistant but are not heat resistant like bacterial endospores. Akinetes contain ample amounts of storage compounds, such as glycogen (carbon and energy storage) and cyanophycin (nitrogen storage). Akinetes germinate and form hormogonia, another form of differentiation. Hormogonia may also differentiate from vegetative cells when the organism is exposed to environmental stress. Hormogonia are short, motile trichomes with cells smaller than those of the mature organism and do not possess heterocysts. They serve as a dispersion mechanism for the organism and are also important for entering into symbiotic relationships. The main difference between the Divisions 4 and 5 is that the latter shows true branching. This occurs when a cell divides in more than one plane and distinguishes it from apparent branching that may occur in both divisions. Heterocystous cyanobacteria also may form colonies and aggregates.

Cyanobacteria are phototrophs and therefore possess photopigments. The great variety of photopigments of cyanobacteria gives these organisms a plethora of colors and allows them to adapt to a variety of light conditions. The main pigment in the photosynthetic reaction centers is the plant-type chlorophyll *a*. The main light-harvesting pigments are the phycobiliproteins. These pigments are organized in phycobilisomes that are connected to the



Cyanobacteria, Diversity and Evolution of. **Figure 1** Diversity of Cyanobacteria and examples from each of the 5 divisions. *Left column:* heterocystous cyanobacteria. Top three belong to division 4: *Anabaena* sp. with heterocysts (lighter cells) and akinetes (very large cells); *Calothrix* sp. with terminal heterocysts; *Nodularia* sp. with intercalary heterocysts. *Bottom:* *Fischerella* sp. with true branching (division 5). *Middle column:* non-heterocystous filamentous cyanobacteria (division 3). *From top to bottom:* *Lyngbya* sp., *Phormidium* sp., *Spirulina* sp., and *Trichodesmium* sp. *Right column:* unicellular cyanobacteria. Top three belong to division 1. *Gloeocapsa* sp., the colony forming *Microcystis* sp. and the tiny *Crocosphaera* sp. *Bottom:* *Dermocarpa* sp. with baeocytes (division 2)

photosynthetic thylakoid membranes (Adir 2005). All phycobilisomes contain allophycocyanin. In addition, phycocyanin (blue) or phycoerythrin (orange to red) or both may be present, rendering the organism a blue-green, orange, red, or brown color. Phycoerythrocyanin is another phycobiliprotein with a reddish color that has a rather limited distribution and occurs only in some heterocystous cyanobacteria. Phycoerythrin comes in two

forms, namely with the chromophore phycoerythrobilin (PEB) (red) and phycourobilin (PUB) (orange). Both chromophores can be bound to phycoerythrin in various ratios. Some cyanobacteria are capable of complementary chromatic adaptation (Mullineaux 2001). Depending on the wavelength of light, the amounts of phycocyanin and phycoerythrin will vary, turning cells blue-green in red light and red in green light. Another form of more subtle

chromatic adaptation occurs when organisms vary the ratio of PEB:PUB as a response to the prevailing underwater light conditions (Everroad et al. 2006).

Prochloron and *Prochlorothrix* are cyanobacteria that lack phycobiliproteins and contain chlorophylls a and b. The oceanic picoplanktonic cyanobacterium *Prochlorococcus* contains the divinyl derivatives of chlorophyll a and b, which are specific for this genus (Scanlan et al. 2009). Some strains contain small amounts of phycoerythrin, but phycobilisomes are lacking and this pigment does not serve as a light-harvesting pigment in *Prochlorococcus*. Another unusual cyanobacterium is represented by the genus *Acaryochloris* which contains chlorophyll d instead of chlorophyll a and is an adaptation to the specific light conditions in its natural environment.

Cyanobacteria utilize a variety of nitrogen sources (Herrero et al. 2001). Many but not all cyanobacteria are capable of fixing atmospheric dinitrogen (N_2). Nitrogenase, the enzyme complex that reduces N_2 to NH_3 , is inactivated by oxygen (Bergman et al. 1997). Therefore, the occurrence of N_2 fixation in the oxygenic cyanobacteria is paradoxical. N_2 -fixing cyanobacteria have evolved mechanisms to ensure an anoxic intracellular environment for nitrogenase. Many cyanobacteria are capable of fixing N_2 only under anaerobic and anoxygenic conditions, a strategy that can be termed avoidance (of oxygen) (Gallon 1992). The most advanced strategy is the differentiation of heterocysts (see above). These cells contain nitrogenase and the strategy is a temporal separation of oxygenic photosynthesis (in the vegetative cells) and N_2 fixation (in the heterocysts). Many non-heterocystous N_2 -fixing cyanobacteria (filamentous as well as unicellular) exhibit a temporal separation of both incompatible processes by confining the fixation of N_2 to the night (Sherman et al. 1998). The oceanic non-heterocystous species *Trichodesmium* is an enigma as it fixes N_2 exclusively during the daytime. It is hypothesized that this organism employs a combination of spatial and temporal separation of N_2 fixation and oxygenic photosynthesis, i.e., that nitrogenase activity is confined to temporary non-oxygenic photosynthetic cells which have also been termed “diazocytes.”

Cyanobacteria possess a remarkably versatile, flexible, and reactive metabolism. In addition to the typical cyanobacterial metabolisms mentioned above, some cyanobacteria exhibit also efficient anaerobic metabolism. For instance, they can perform anoxygenic photosystem I-dependent photosynthesis during which sulfide is used as the electron donor. Some species do this in concert with oxygenic photosynthesis while others rely only on anoxygenic photosynthesis and CO_2 fixation.

Cyanobacteria obviously possess dark metabolism in order to survive and cope with the natural day and night cycle. Under aerobic conditions, the glycogen reserve is respired through the oxidative pentose phosphate cycle (the reverse of the Calvin Cycle of CO_2 fixation) using oxygen as the electron acceptor. Under anaerobic conditions some cyanobacteria are capable of fermenting glycogen via a variety of different pathways and when available they can use elemental sulfur as electron acceptor (Stal and Moezelaar 1997). In order to tune all these processes to the natural day night cycle, cyanobacteria are the only Bacteria with a circadian clock, which occurs otherwise only within the Eukarya (Golden 2003).

See also

- ▶ Archean Traces of Life
- ▶ Bacteria
- ▶ Belcher Group, Microfossils
- ▶ Great Oxygenation Event
- ▶ Microfossils
- ▶ Oxygenation of the Earth's Atmosphere
- ▶ Photosynthesis
- ▶ Stromatolites

References and Further Reading

- Adams DG, Duggan PS (1999) Heterocyst and akinete differentiation in cyanobacteria. *New Phytol* 144:3–33
- Adir N (2005) Elucidation of the molecular structures of components of the phycobilisome: reconstructing a giant. *Photosynth Res* 85:15–32
- Bergman B, Gallon JR, Rai AN, Stal LJ (1997) N_2 fixation by non-heterocystous cyanobacteria. *FEMS Microbiol Rev* 19:139–185
- Everroad C, Six C, Partensky F, Thomas J-C, Holtzendorff J, Wood AM (2006) Biochemical bases of type IV chromatic adaptation in marine *Synechococcus* spp. *J Bacteriol* 188:3345–3356
- Gallon JR (1992) Reconciling the incompatible: N_2 fixation and O_2 . *New Phytol* 122:571–609
- Golden SS (2003) Timekeeping in bacteria: the cyanobacterial circadian clock. *Curr Opin Microbiol* 6:535–540
- Herrero A, Muro-Pastor AM, Flores E (2001) Nitrogen control in cyanobacteria. *J Bacteriol* 183:411–425
- Knoll AH (2003) The geological consequences of evolution. *Geobiology* 1:3–14
- Mullineaux CW (2001) How do cyanobacteria sense and respond to light? *Mol Microbiol* 41:965–971
- Olson JM, Blankenship RE (2004) Thinking about the evolution of photosynthesis. *Photosynth Res* 80:373–386
- Rai AN, Söderbäck E, Bergman B (2000) Cyanobacterium-plant symbioses. *New Phytol* 147:449–481
- Raven JA, Allen JF (2003) Genomics and chloroplasts evolution: what did cyanobacteria do for plants? *Genome Biol* 4:209
- Rippka R, Deruelles J, Waterbury JB, Herdman M, Stanier RY (1979) Generic assignments strain histories and properties of pure cultures of cyanobacteria. *J Gen Microbiol* 111:1–61
- Sánchez-Baracaldo P, Hayes PK, Blank CE (2005) Morphological and habitat evolution in the Cyanobacteria using a compartmentalization approach. *Geobiology* 3:145–165

- Scanlan DJ, Ostrowski M, Mazard S, Dufresne A, Garczarek L, Hess WR, Post AF, Hagemann M, Paulsen I, Partensky F (2009) Ecological genomics of marine picocyanobacteria. *Microbiol Mol Biol Rev* 73:249–299
- Sherman LA, Meunier P, Colón-López MS (1998) Diurnal rhythms in metabolism: a day in the life of a unicellular, diazotrophic cyanobacterium. *Photosynth Res* 58:25–42
- Stal LJ, Moezelaar R (1997) Fermentation in cyanobacteria. *FEMS Microbiol Rev* 21:179–211
- Stanier RY, Cohen-Bazire G (1977) Phototrophic prokaryotes: the cyanobacteria. *Annu Rev Microbiol* 31:225–274

Cyanobacterial Mats

- ▶ [Microbial Mats](#)

Cyanobutadiynyl Radical

- ▶ [4-Cyano-1,3-Butadiynyl](#)

Cyanoethane

- ▶ [Ethyl Cyanide](#)
- ▶ [Vinyl Cyanide](#)

Cyanoethynyl Radical

Synonyms

[C₃N]

Definition

The four atom ▶ [radical](#) C₃N is found in the gas phase in both interstellar ▶ [molecular clouds](#) and in the expanding envelopes of evolved carbon-rich stars. It is an intermediary in the chemistry of the ▶ [cyanopolyynes](#) and related radicals.

History

The presence of C₃N in the envelope of the carbon star IRC + 10216 was announced from the pattern of detected emission lines at millimeter wavelengths by Guelin and Thaddeus (1977), before the frequencies of these transitions had been measured in the laboratory. Friberg et al. (1980) stated that the chain of logic leading to this deduction was “worthy of Hercule Poirot (Christie 1945).”

This identification is a particularly good example of the ability of heterodyne (high frequency resolution) astronomical measurements to contribute to fundamental molecular physics.

See also

- ▶ [Cyanopolyynes](#)
- ▶ [Molecular Cloud](#)
- ▶ [Radical](#)
- ▶ [Stellar Evolution](#)

References and Further Reading

- Christie A (1945) Sparkling cyanide. Collins, London
- Friberg P, Hjalmarson Å, Irvine WM (1980) Interstellar C₃N: detection in taurus dark clouds. *Astrophys J* 241:L99–L103
- Guelin M, Thaddeus P (1977) Tentative detection of the C₃N radical. *Astrophys J* 212:L81–L85

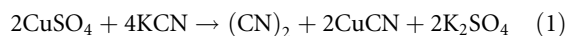
Cyanogen

Synonyms

[Carbon nitride](#); [Dicyan](#); [Dicyanogen](#); [Nitriloacetonitrile](#); [Oxalic acid dinitrile](#); [Oxalonitrile](#); [Oxalyl cyanide](#)

Definition

Cyanogen is a compound of formula (CN)₂. It is a colorless gas at standard temperature and pressure. A cyanogen molecule consists of two CN groups bonded together at their carbon atoms (N≡C–C≡N). Cyanogen is the anhydride of oxamide. It can be generated from cyanide compounds and solutions of metal salts (such as copper(II) sulfate).



It is also formed when ▶ [nitrogen](#) and ▶ [acetylene](#) are acted upon by an electrical discharge.

It is implicated as a possible phosphorylating agent for nucleosides and a possible precursor to cyanates and ureas.

See also

- ▶ [Electric Discharge](#)
- ▶ [Hydrogen Cyanide](#)

Cyanogen Nitride

- ▶ [Cyanamide](#)

Cyanogen Radical

Synonyms

CN; Cyano radical

Definition

The diatomic radical CN, containing carbon and nitrogen, is widely observed in the ► [interstellar medium](#) of the Milky Way and external galaxies. It plays an important role in interstellar chemistry, being an intermediate in the production and destruction of such important species as HCN and HNC. The CN radical is also prominent in the visible wavelength spectra of cometary comae (atmospheres), where it is presumably a photodissociation product of molecules such as HCN that are sublimated from the icy nucleus. Note that the molecule C_2N_2 is also referred to as the cyanogen radical. A chemical compound that contains the CN functional group (carbon triple-bonded with nitrogen) is called a cyanide, while an organic compound with this CN group is called a nitrile.

History

Unlike most interstellar molecules, which were discovered by radio astronomical observations, CN was first identified at ultraviolet wavelengths in 1940, and it was one of the first known interstellar molecular species. The fundamental rotational line was observed radio astronomically in 1970.

See also

- [Comet](#)
- [Hydrogen Cyanide](#)
- [Hydrogen Isocyanide](#)
- [Interstellar Medium](#)

References and Further Reading

- Crovisier J, Encrenaz T (2000) *Comet Science: the study of remnants from the birth of the solar system*. Cambridge University Press, Cambridge
- McKellar A (1940) Evidence for the Molecular Origin of Some Hitherto Unidentified Interstellar Lines. *Publ Astron Soc Pacific* 52:187–192

Cyanogenamide

- [Cyanamide](#)

Cyanomethane

- [Acetonitrile](#)

Cyanomethylamine

- [Aminoacetonitrile](#)

Cyanophyceae

- [Cyanobacteria](#)

Cyanopolyynes

Definition

Cyanopolyynes are long carbon-chain molecules found in many astrochemical sources. Whereas polyynes are organic compounds with alternating single and triple bonds, the simplest being ► [diacetylene](#) ($HC\equiv C-C\equiv CH$), cyanopolyynes are end-capped by the cyano group ($-CN$). Examples are $HC\equiv C-C\equiv C-CN$ and $HC\equiv C-C\equiv C-C\equiv C-CN$.

See also

- [Diacetylene](#)

Cyclic Replicator Equation

- [Hypercycle](#)

Cyclohexa-1,3,5-triene

- [Benzene](#)



Cyclopropenylidene

Synonyms

[C₃H₂, c-C₃H₂]

Definition

This 3-carbon ring molecule C₃H₂ is classified chemically as a ► [carbene](#) and is highly reactive in the laboratory. It was the first cyclic molecular species detected in the molecular clouds. Immediately following its identification at short radio wavelengths, it was discovered to be nearly ubiquitous in the interstellar medium (Matthews and Irvine 1985), and it has subsequently also been found in the envelope of evolved carbon-rich stars. The linear isomer of C₃H₂ is also detected in molecular clouds, but its abundance is typically an order of magnitude lower than that of the cyclic isomer (Cernicharo et al. 1991). In diffuse clouds, the abundance ratio between the linear and the cyclic isomers increases by a factor 10 with respect to that observed in dense molecular clouds (Cernicharo et al. 1999). Both 13-carbon and deuterated isotopic forms of C₃H₂ have been detected astronomically.

History

The laboratory measurement of the frequencies of several C₃H₂ rotational transitions by Thaddeus et al. (1985) proved the identification of emission lines that they had earlier observed astronomically.

See also

- [Carbenes](#)
- [Deuterium](#)
- [Isomer](#)
- [Molecular Cloud](#)
- [Stellar Evolution](#)

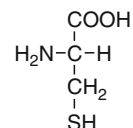
References and Further Reading

- Cernicharo J, Cox P, Fosse' D, Gusten R (1999) Detection of linear C₃H₂ in absorption toward continuum sources. *Astron Astrophys* 351: 341–346
- Cernicharo J, Gottlieb CA, Guelin M, Killian TC, Paubert G, Thaddeus P, Vrtilek JM (1991) Astronomical detection of linear H₂CCC. *Astrophys J* 368:L39–L42
- Matthews HE, Irvine WM (1985) The hydrocarbon ring C₃H₂ is ubiquitous in the galaxy. *Astrophys J* 298:L61–L64
- Thaddeus P, Vrtilek JM, Gottlieb CA (1985) Laboratory and astronomical identification of cyclopropenylidene, C₃H₂. *Astrophys J* 299: L63–L66

Cysteine

Definition

Cysteine is one of the 20 protein ► [amino acid](#), whose structure is shown in [Fig. 1](#). Its three-letter symbol and



Cysteine. [Figure 1](#) Chemical structure of cysteine

one-letter symbol is Cys and C, respectively. Among the protein amino acids, only cysteine and methionine contains a sulfur atom in their structures. The side chain of cysteine contains a thiol (-SH) group, which often works in the active site of enzymes. In protein molecules, two cysteine residues often make a disulphide bond, which is essential in folding the ► [proteins](#) and stabilizing their structure. When proteins are acid hydrolyzed for amino acid analysis, cysteine is easily dimerized to give ► [cystine](#). Cysteine has been produced in a variety of prebiotic experiments from reducing gas mixtures, but has not been detected in carbonaceous chondrites, possibly due to its instability.

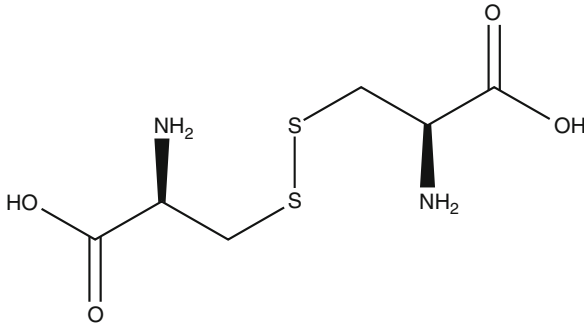
See also

- [Amino Acid](#)
- [Cystine](#)
- [Proteins](#)

Cystine

Definition

Cystine is a dimeric ► [amino acid](#) formed by the oxidative condensation of two ► [cysteine](#) molecules. Cysteine, one of the 20 ► [protein](#) amino acids, has a ► [thiol](#) (-SH) group. In aqueous solution, two cysteine molecules are readily oxidized to form a ► [disulfide bond](#) (-S-S-). Thus, cystine rather than cysteine is usually determined when the amino-acid composition of protein hydrolysates is analyzed. It can be easily reduced to give two cysteine



Cystine. Figure 1 Chemical structure of cystine

molecules by addition of thiols. In protein molecules, two cysteine residues make intramolecular disulfide bonds, which stabilize protein tertiary structure.

See also

- ▶ [Amino Acid](#)
- ▶ [Cysteine](#)
- ▶ [Disulfide Bond](#)
- ▶ [Protein](#)
- ▶ [Thiol](#)

Cytochromes

Definition

Cytochromes are a class of electron-transferring metalloproteins containing a heme as prosthetic group, and that participate in many different respiratory and photosynthetic ▶ [electron transport](#) chains, usually as membrane-bound electron carriers. The function of cytochromes as electron carriers involves the alternate ▶ [oxidation](#) and ▶ [reduction](#) of the iron ion present in the heme group, one electron each time (i.e., between the reduced ferrous state and the oxidized ferric state), and with a standard ▶ [redox potential](#) between -100 and $+500$ mV. The cytochromes are classified on the basis of their characteristic, redox-sensitive, visible absorbance spectra.

See also

- ▶ [Electron carrier](#)
- ▶ [Electron transport](#)
- ▶ [Oxidation](#)

- ▶ [Photosynthesis](#)
- ▶ [Redox potential](#)
- ▶ [Reduction](#)
- ▶ [Respiration](#)

Cytoplasm

Definition

Cytoplasm is the internal space of a ▶ [cell](#) containing all soluble chemical components and, in the case of eukaryotic cells, the organelles (▶ [nucleus](#) mitochondria, plastids, microbodies, etc.), the cytoskeleton, and the endomembrane system (endoplasmic reticulum, Golgi apparatus, etc.). The fluid, non-particulate fraction of the cytoplasm is known as cytosol.

See also

- ▶ [Cell](#)
- ▶ [Cell Membrane](#)
- ▶ [Nucleus](#)

Cytoplasmic Membrane

- ▶ [Cell Membrane](#)

Cytosine

Definition

Cytosine (C) is one of the four heterocyclic nitrogenous bases found in DNA (A, T, C, and G) and RNA (A, U, C, and G). It is a pyrimidine with two functional group substituents: an amine at the C⁴ position and a keto group at the C² position. When cytosine is combined with ribose via a glycosidic linkage between its N¹ nitrogen and the C¹ position of the sugar, it forms a nucleoside called cytidine; removal of the 2'-OH group of this molecule results in the formation of 2'-deoxycytidine also known as deoxycytidine. In Watson-Crick base pairing in nucleic acids, these derivatives form three hydrogen bonds with guanine.

Cytosine and its derivatives hydrolyze fairly rapidly under physiological conditions to give ► [uracil](#) via deamination, with a half-life of approximately 73 years at 37°C at pH 7. In biological systems this relatively rapid loss of structural genetic information is corrected by DNA repair enzymes.

Cytosine has been synthesized under simulated prebiotic conditions from cyanoacetaldehyde and urea, as well as from ► [cyanoacetylene](#) and cyanate. It can also be

derived from the deamination of 2, 4-diaminopyrimidine, itself derived from the condensation of guanidine with cyanoacetaldehyde.

See also

- [Cyanoacetylene](#)
- [Pyrimidine Base](#)
- [Uracil \(Ura\)](#)

